Thèse n° 8434

Towards an in vitro cardiac model: 3D environment, co-culture, alignment, and mechanical stimulation impact on cell behavior

Présentée le 14 avril 2021

Faculté des sciences et techniques de l'ingénieur
Laboratoire de microsystèmes 4
Programme doctoral en microsystèmes et microélectronique

pour l'obtention du grade de Docteur ès Sciences

par

Fatemeh NAVAEE

Acceptée sur proposition du jury

Prof. J. Brugger, président du jury
Prof. Ph. Renaud, Prof. T. M. Braschler, directeurs de thèse
Prof. M. Jaconi Dévaud , rapporteuse
Dr G. Weder, rapporteur
Prof. M. Gijs, rapporteur

École polytechnique fédérale de Lausanne

2021

To my lovely family

Acknowledgements

Firstly, I would like to express my sincere gratitude to my advisors Prof. Philippe Renaud, and Prof. Thomas Braschler for the continuous support of my Ph.D. study and related research, for their patience, motivation, and immense knowledge. Philippe, thank you very much for giving me the opportunity to work at LMIS4 laboratory at EPFL. Your guidance helped me in all the time of research and writing of this thesis. I would not have been able to complete the work presented in this thesis without the excellent supervision and support given by you. During all this time, you made me understood the meaning of research, collaborate in a team and critical thinking, and how patience and hard working are the foundations to do a good job. I remember the time that I was really down in my life and you told me "I want to give the Ph.D. diploma to a happy person! Your side project is to take care of yourself!". I am deeply grateful for having such a person in my side, not just as a supervisor, but like a father who cares about her daughter. Thomas, your enthusiasm, kindness, commitment, and faith in my abilities have been extremely helpful and motivating to pursue my research work under the best conditions. You are, and will be my great role model in my scientific life. I would like to thank you for your passion, the friendly atmosphere you provided in your lab, the courage to try all the possible solution, your advices and all the discussions we had. For all of these reasons, I am deeply grateful to you.

Besides my advisors, I would like to thank my thesis committee: I greatly appreciate my thesis jury members Prof. Jürgen Brugger (jury president), Prof. Marisa Jaconi (external examiner), Dr. Gilles Weder (external examiner) and Prof. Martinus Gijs (internal examiner), for taking their precious time to evaluate my thesis, their insightful comments and encouragement, but also for the questions which incented me to widen my research from various perspectives. Thank you again for participating my private defense and for your constructive feedback on my work and the valuable advices for the continuous work on this project.

I would like to thank Prof. Stephan Rohr, and specially Mrs. Regula Fluckiger, our collaborators from University of Bern, who played an important role in our research for providing neonatal cardiac cells unconditionally during my PhD study.

I would like to express my sincerest gratitude to Dr. Arnaud Bertsch for all his helps during the Ph.D. journey and to face the difficulties encountered during this time. I will be always impressed by his golden heart. I would like to acknowledge Harald van Lintel, Karin Juillerat, Sylvie Clavel, Christine Vuichoud and Lucie Auberson for their help on all the tasks that needs to be done in order for the laboratory, scholarship and the doctoral school to work smoothly, also for their patience and kindness from the first days of my arrival in Switzerland. Here I would also like to acknowledge the financial support of Swiss government excellence scholarship for helping and providing the funding for my Ph.D. studies.

A big thanks to the bioimaging and optics platform and especially to Romain and Luigi for his help on confocal microscopes. The histology facility and the center of micro-nano technology (CMi) provided outstanding services and I am extremely grateful to their staff members for their help and effort to make this facility a great environment to work in.

My sincere thanks also go to Dr. Daniel Smart, Dr. Omar Alijevic, and Dr. Damian McHugh, who provided me an opportunity to join their team as intern, and who gave access to the laboratory and research facilities at Philip Morris International company. I am also grateful to the all PMI friends for providing a great atmosphere for me, especially in tough COVID-19 situation.

It was a great pleasure for me to share the office with David, Faye, Clarisse, Jiande, and Daniel. We all had great discussions and you all made my time in BM 3.118 colorful and amazing. Daniel, thank you very much for all your kindness and I am pretty sure our collaboration will be continued at CSEM. Jiande, I had so many great moments with you in the office and I really appreciate your pure emotions. I would also like to acknowledge every old and new member of the LMIS4 group: Margaux for being always there in my worst moments of life. It was wonderful to pass time with you! Jonathan for being so friendly and helpful, Stefano for being the energy bomb. Mahya is another very important person to me during my Ph.D. life. Thanks for all your encouragement! Benoît, Nicolas, David, Clementine, Ludovic, Tugba, Amelie, Patrick, Martina, Giullme, Joan, Thamani, Miguel, Albert, Lucas, Sébastien, Elodie, George, Marc, Nadya: it was great sharing laboratory with all of you during last few years.

I would like to thank all my colleagues at MicroNiche lab at University of Geneva for their great support and friendly environment. Aleksandra, Joe, Fabian, David, Laurent, Neil, Kevin, I learnt a lot from you including the scientific side from the group meetings and the active attitude for daily life.

During my PhD, I also assisted several master students. From these experiences, I learnt how to teach and communicate with students. I would like to thank the master students, Sara, Niloufar, and Emmanuelle, for your contribution to this work. Niloufar, we passed fabulous time together and have so many good memories, not just in research, but also, in all the aspects of life! You are really like my little sister and I am always proud of you!

Elahe is one of the main reasons that I did not feel lonely from the very first moments of my life in Switzerland. She did not even know me, but she behaved in such a way that I felt I have a great sister here and can rely on her for everything! I believe no word can express my great gratitude! I am always impressed by your golden heart and kindness.

Special thanks go to my lovely friends in Lausanne and Tehran who support me during these years: specifically I would like to thank Roza, Behshid, Sara, Morteza Toupchi, Mehrnaz, Soheil, Sogol, Amir, Saba, Amirhossein, Homa, Amir sheikhha, Mohsen, Reza, Vahid, Mohamad, Aida, Parima, Fereshte, Hossein, Sadegh, Shayan, Armita, Abolfazl, Bahar, Ehsan, Atena, Morteza, Ahmad, Bahare, Fatemeh,

Farnaz, Eli, Mahdie, Yasi, Foruq, Vahide, and all the other friends with whom I shared many pleasant moments. You were always here to hang out and supporting each other. For all those precious moments that we spend together, I thank you.

Special thanks go to Ali Saeidi for all of his friendship from the very beginning of my life in Switzerland. Many thanks for being the support system of my scientific and personal life! I just wanted to mention how much I appreciate your positive influence on my life.

I would like to say a big “thank you” to Zhaleh, my flat mate, the best friend, and the kindest sister! I would say “best friends are like diamonds, precious and rare”, and you my dear are the most sparkling gem of them all, and I was, am, and will be the luckiest person for having you in my life! Thank you for your great friendship. Thank you for always being there for me when I just needed someone to listen, when I needed to cry on your shoulder. We had so much fun together during these years! Sometimes I just wonder what I would have done without you! It doesn’t matter where we are physically in this world. I know you have a piece of my heart with you.

I want to express my deepest gratitude for Ali Pahlevan. Countless times, you have proved that friendship goes beyond words and encompasses actions. You have been the most amazing friend anybody could dream of. your support, joy of living, positiveness, and kindness have been always priceless and I couldn’t be happier than with you. You have filled my life with pleasure and amusement and had spread so many colors around it, I wish to walk along you till the last moment of my life.

There is no bond stronger than family. Last but not the least, I would like to thank my family, my parents, Mansoureh and Ahmad, and my brother, Ali, who have provided me through moral and emotional support in my life. I do not have the words to tell you how truly fortunate I feel to have you in my life. I know it must not be easy to open your heart like you have and accept my decisions, and so I thank you all the more for doing so. If I could choose anybody at all to be in my corner, backing me up, through all the difficulties of life, it would be my family a hundred times over. I love you.

Lausanne, September 2020 Fatemeh Navaee

Abstract

Our aim is to develop a 3D model unit of cardiac muscle: an *in-vitro* analog of the *trabeculae carneae* found *in vivo*. As a base hydrogel matrix for cardiomyocyte culture in 3D, we develop a blend of decellularized extracellular matrix (dECM) and fibrin. This blend contains essential components of cardiac ECM, provides rapid, cell-friendly coagulation, and closely matches the mechanical properties of native myocardium. Co-culture of the H9c2 model cell line with fibroblast cells in this hydrogel showed enhancement in attachment, spreading, and cardiogenic differentiation of H9c2 cells. This is ascribed primarily to the collagen content of the dECM. Calcium imaging and analysis of beating motion of primary rat neonatal cardiomyocytes cultured in the 3D hydrogel showed specific improvement in recovery, frequency, synchronicity and beating rates compared to a series of common hydrogel controls, including collagen-fibrin composites. This establishes the dECM-fibrin hydrogel as an optimal base matrix for cardiac tissue culture and engineering.

The *trabeculae carneae* are cardiac muscle fibers at the inner surface of the ventricles. They are an accessible representation of the tiniest building blocks of the cardiac tissue because of their dimensions and cellular orientation. Molding cell-seeded dECM-fibrin hydrogel in microfabricated grooves, we fabricated *in vitro* analogs of the *trabeculae carneae*. In these 3D structures, propagation of cell alignment due to the corner contact guidance successfully addresses the challenge of 3D cell orientation. The effect provides alignment 250-300 µm from the corners, enabling full 3D orientation in 350 µm by 350 µm square section microgrooves. The cell-laden hydrogel can be detached from the PDMS surface while maintaining cell alignment. The alignment enhanced the functionality of rat neonatal cardiomyocytes beating by maintaining the contractility of the cells for longer time compared to the random distribution of the cells in the hydrogel.

Mechanical forces play key roles in the development and cardiac tissue morphogenesis. Relatively well-known in 2D cultures, knowledge about mechanical effects in 3D is scarcer. We investigate the combined effect of topography and mechanical stimulation on 3D cardiac cell culture. For application of cyclic stretch, we designed and fabricated a user-friendly mechanical stimulator. In 2D cultures, the cells orient perpendicularly to the direction of applied cyclic stretch in agreement with known strain-avoidance mechanisms. In 3D, the cells react to combined topography and mechanical stimulation by adopting an orientation around 45°. This reflects integration of the conflicting stimuli of alignment along the grooves but perpendicular to the stretch direction. Off-axis alignment may be a novel mechanism for maintenance of helicoidal fiber alignment in the heart. As anticipated, mechanical stimulation also improved the maturation and functionality of the neonatal cardiac cells.

Overall, we provide a novel biomaterial for 3D cardiac cell culture and find an effective, yet simple approach to encourage 3D cell alignment. Adding mechanical stretching enhances the maturation and

functionality of the bioengineered tissue *in vitro*, and provides the possibility of off-axis alignment reminiscent of the helicoidal fiber arrangement in the heart. Our *trabeculae carneae* unit model therefore provides an enhanced 3D environment for investigating cell fate and tissue functionality.

Keywords

dECM-fibrin hydrogel; Neonatal cardiomyocyte culture; H9c2 cell differentiation; Beating synchrony; 3D co-culture; Hydrogel patterning; Microfabrication; Mechanical stimulation; Cardiac tissue model, Heart torsion; Trabeculae carneae

Résumé

Le sujet de cette thèse est la constitution et l'optimisation d'une unité minimale de muscle cardiaque. Pour ceci, nous nous instruisons d'un élément de l'anatomie cardiaque : les trabécules carnés. Il s'agit de fibres musculaires cardiaques individualisées sur la surface interne des ventricules cardiaques. De par leur dimension, organisation spatiale et fonctionnement, ils inspirent notre modèle de culture cardiaque *in-vitro*.

En tant que premier pas, nous constituons et optimisons un hydrogel pour la culture de cardiomyocytes. Il s'agit d'un mélange de matrice extracellulaire décellularisée (dECM) cardiaque et de fibrine. La co-culture de la lignée modèle H9c2 et de fibroblastes dans cet hydrogel montre une amélioration de l'attachement et de la différenciation cardiogénique des cellules H9c2. Ceci est principalement dû au contenu en collagène du gel dECM. En revanche, la dECM cardiaque fournit un avantage spécifique dans la culture et fonction des cardiomyocytes primaires de rat : on observe effectivement une amélioration significative de la récupération, de la fréquence, et de la synchronicité des battements spontanés par rapport aux hydrogels témoins. L'hydrogel dECM-fibrine sera donc le constituant de base de notre modèle de trabécules carnées.

Pour atteindre une orientation physiologique localement parallèle des cardiomyocytes, nous avons coulé notre hydrogel ensemencé de cardiomyocytes dans des sillons d'un moule microfabriqué en silicone. Les cellules proches des arrêtes du moule se sont aligné sur les sillons par effet de guidage de contact connu. En sus, cet alignement s'est propagé de 250-300 µm dans l'hydrogel. Donc, avec des rainures de section carrée de 350 µm sur 350 µm, on peut atteindre un alignement complet en 3D des cardiomyocytes cultivés dans l'hydrogel. L'hydrogel chargé de cellules est suffisamment solide pour être détaché de la surface du moule tout en maintenant l'alignement des cellules. Nous avons pu démontrer une amélioration de la fonctionnalité des cardiomyocytes néonatals de rats de par cet alignement en 3D : les cellules alignées ont maintenu leur contractilité spontanée pendant des périodes étendues par rapport à des cellules ensemencées aléatoirement dans l'hydrogel.

Les forces mécaniques jouent un rôle clé dans le développement et la morphogenèse des tissus cardiaques. Nous avons étudié l'effet d'une stimulation mécanique cyclique en 3D. Les cellules cardiaques se sont orientées à angle droit par rapport à la direction de l'extension périodique appliquée, transposant les résultats connus en cultures 2D à notre système 3D. De manière intéressante, la combinaison de la stimulation mécanique en 3D avec la topographie des sillons aboutit à une orientation oblique proche de 45°. Les cellules semblent intégrer les effets compétitifs d'alignement le long des rainures et à angle droit par rapport l'étirement mécanique. Ces résultats constituent un germe d'explication mécanistique de l'alignement hélicoïdal des fibres musculaires dans le myocarde dans le cœur. La

stimulation mécanique a également amélioré la maturation et la fonctionnalité des cellules cardiaques néonatales.

Dans l'ensemble, nous avons pu découvrir un nouveau biomatériau et modèle pour la culture de cellules cardiaques alignées en 3D. L'ajout de l'étirement mécanique cyclique a permis d'améliorer la maturation et la fonctionnalité des trabécules carnés reconstitués, tout en fournissant un premier indice d'alignement hélicoïdal physiologique.

Mots-clés

dECM-fibrine hydrogel ; culture de cardiomyocytes néonatals ; différenciation des cellules H9c2 ; battements synchrones ; co-culture 3D ; modelage de l'hydrogel ; microfabrication ; stimulation mécanique ; modèle de tissu-sue cardiaque, torsion cardiaque ; trabécules carnées

Contents

List of Figures

List of Tables

Chapter 1 Introduction

1.1 Main hypothesis and synopsis

The main hypothesis of this thesis is that environmental cues can be used to improve the phenotype and function in cardiomyocytes. To investigate the main hypothesis, we focused on three environmental cues and investigate their impact on the functionality and phenotype of the cardiomyocytes. Therefore, the hypothesizes in chapter 2 to 4 are as follows:

Chapter 2: The extracellular matrix can improve the cardiac cell's identity and functionality.

Chapter 3: 3D surface topography and spatial geometry will determine the alignment and improve function of the cardiac cells in the hydrogel.

Chapter 4: Mechanical stimulation helps to improve alignment and functionality of cardiac cells in 3D hydrogel.

Regarding the mentioned hypothesizes, the introduction chapter reviews the cardiac structure, *in vitro* cardiac models, techniques to manipulate the cardiac tissue *in vitro* towards a more mature model, and the applications of cardiac tissue models.

1.2 Cardiovascular diseases and heart failure

Cardiovascular diseases, especially myocardial infarction, are the main cause of death all around the world [1]. Better understanding of the cardiovascular problems and the pathological behavior of cardiac cells in native tissue is crucial and provides wider insight for investigating the impact of different cues

on cardiac cells *in vitro*. In the case of heart ischemia, the partial or total blockage of coronary arteries leads to oxygen deficiency, cell injury and cell death at the final stage [2], [3],[4], [5]. Indeed, severe heart diseases, such as myocardium infarction, can have a dramatic impact on heart function such as permanent loss of cardiomyocytes, since the cardiomyocytes show fairly poor regenerative properties [6]. In such case, to repair the cardiac tissue after cardiomyocytes death, cardiac muscle might be progressively replaced by a fibrotic, non-elastic, and non-contractile scar tissue which does not match the same mechanical, electrical and biological properties compared to the rest of the heart tissue, thereby impairing the contractile functions of the organ [7]. In the long-term, the consequences of the infarction lead to ventricular remodeling in terms of the volume, shape and wall thickness, which can finally cause arrhythmia and heart failure [8].

As cardiovascular diseases are one of the leading causes of death worldwide, tremendous efforts were recently invested by different research teams in the implementation of new designs and engineering approaches to tackle this challenge. Current approaches for treating the diseased heart, include pharmacological approaches, surgical assistance, implantation of devices such as pacemakers and stents, intended to prevent the progression of the symptoms and provide a temporally solution before the total organ failure. However, they cannot regenerate the effected myocardium tissue. Cell-based therapies, such as cardiomyoplasty or grafts, are very promising forms of cardiac repair [9]. Unfortunately, the functionality of the different constructs is still far compared to the one of the native heart, and approaches focusing on cardiomyocytes differentiation still leads to cells displaying a rather immature phenotype, leading to clinical results with a very limited success [10], [11].

A curative approach for heart failure is heart transplantation [12], although it is applicable only under limited circumstances. It is a heavy surgical procedure, including long-term burden such as the need of immunosuppression for the remainder of the patients' lives, as well as lack of physiological innervation and ensuing limited performance [13]. Maybe most importantly, it is often not applicable in the time frame of cardiac deterioration, and even if, there is a dramatic shortage of immune-matching organ donors compared to the increasing demand for heart transplantation every year [12]. Therefore, finding strategies to overcome these limitations, improve the functionality and regeneration of the cardiac tissue, and enhance our knowledge of cardiac tissue by capturing the complex criteria of the in vivo environment is critical [14]. However, providing an ideal cardiac model *in vitro* which mimics the important criteria of the native tissue is a huge challenge in the field of tissue engineering [15].

There are several research groups who are working on developing a functional cardiac tissue model in 2D and 3D with different applications such as *in vitro* drug screening and discovery, disease modeling, and tissue engineering applications e.g. transplantation [16]–[18]. These models are a step towards reaching a precise model with similar responses as native tissue. Moreover, the cardiac models reduce the number of animal models that are currently used in drug screening as well as decrease the costly drug testing which may lead to failure at the end. These studies include the generation of 2D and 3D

structures using biomaterials and encouraging the maturation of the tissue by applying different stimuli such as 3D culturing, co-culturing, mechanical, electrical, and biochemical stimulations in different manners, and an overview will be given in the following sections.

1.3 Cardiac function and the structure of cardiac tissue

1.3.1 Cardiac anatomy and the cardiac cycle

Heart tissue consists of four chambers: left and right atrium, and left and right ventricle which are paired as the left heart and the right heart. There are two periods in heart function: diastole and systole. Cardiac relaxation and refilling with blood happen in diastole and a strong contraction and pumping of blood happen in systole. The performance of the heart from the ending of one beat to the beginning of the next one is called cardiac cycle. Each cardiac cycle in healthy heart takes around 0.8 seconds to

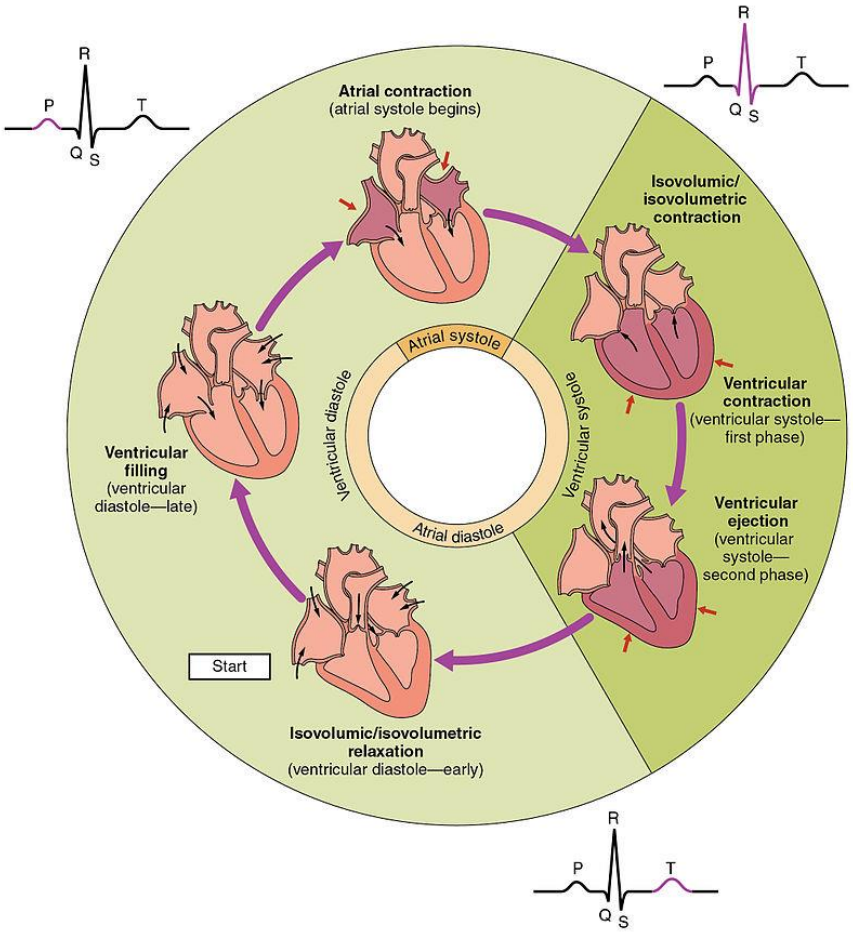

Figure 1-1 The cycle diagram depicts one heartbeat of the continuously repeating cardiac cycle, namely: ventricular diastole followed by ventricular systole, etc. while coordinating with atrial systole followed by atrial diastole, etc. The cycle also correlates to key electrocardiogram tracings: The T wave (which indicates ventricular diastole); the P wave (atrial systole); and the QRS 'spikes' complex (ventricular systole) all shown as color purple-in-black segments [19].

complete. The cycle starts with the early ventricular diastole, i.e., the heart relaxes and expands (isovolumic relaxation), following by the late ventricular diastole which is the filling step. At the end of this step, atria contract and pump blood to the ventricles (atrial systole). It follows by ventricular systole (at the same time of atrial diastole) which is the contraction of the ventricles, initiated with electrical signals from the sinoatrial node, and ejecting the blood to the lungs and different organs of the body.

The heart valves have a key role in cardiac cycle. The mitral and tricuspid valves open during the ventricular diastole (ventricle filling with blood). In ventricular systole phase, the back-pressure against these valves leads to the AV-valves closing. This pressure opens aortic and pulmonary valves which permits blood ejection to the organs. The heart cycle diagram is presented in figure 1-1.

1.3.2 Cardiac tissue structure

To investigate the impact of environmental cues on cardiac cells, one needs firstly to consider the structure and function of the cardiac tissue in its native environment. Understanding how cardiomyocytes mature and function is getting more and more crucial every day as success of future strategies, aiming to restore cardiac function in patients, highly depends on new methods to evaluate cardiomyocytes properties [20]. The myocardium tissue is composed of different cell types which are embedded in an extracellular matrix to form the tissue structure with defined function [21]. The extracellular matrix (ECM) of each tissue type is exclusive for that tissue and evolves during the development which leads to the differentiation and maturation of their specific cell lineage by providing sufficient mechanical, biophysical, electrical and biochemical cues [22]. Cardiac cells in heart tissue are located in a special extracellular matrix (ECM) which is composed of a variety of components including collagen I, collagen IV, elastin, glycosaminoglycans (GAGs), and proteoglycans [23]. GAGs have relatively low content in the tissue (2-5% by dry weight), however, they have a great influence on viscoelasticity and residual stress. GAGs can be also contribute in mechanosensing, although its mechanical interactions with collagen fibers are not fully understood [24]. This composition in addition to the different stimulation in cardiac tissue, encourage the cardiac cells to provide a dense, aligned, and highly connected tissue structure with defined functional properties [25]. Because of the density of the cardiac tissue and its dimensions, almost all the cells are surrounded by vascular network to provide enough nutrients for the cardiac cells [26]. There are also tiny structures of aligned cardiomyocytes at the surface of the myocardium wall which are called trabeculae carneae [27]. These structures are small in their size. Hence, they do not need internal vascularization, as the oxygen and nutrient can easily diffuse in them from the surrounding capillaries. These structures can be considered as the smallest building blocks of the native cardiac muscular tissue[28]. As such, they are highly interesting for research on cardiac tissue and pharmacology, due to the fact that it resembles the cardiac structure and is an accurate model for studying the

cardiac cells response to different stimuli [28], [29]. Figure 1-2 shows a schematic view of heart anatomy.

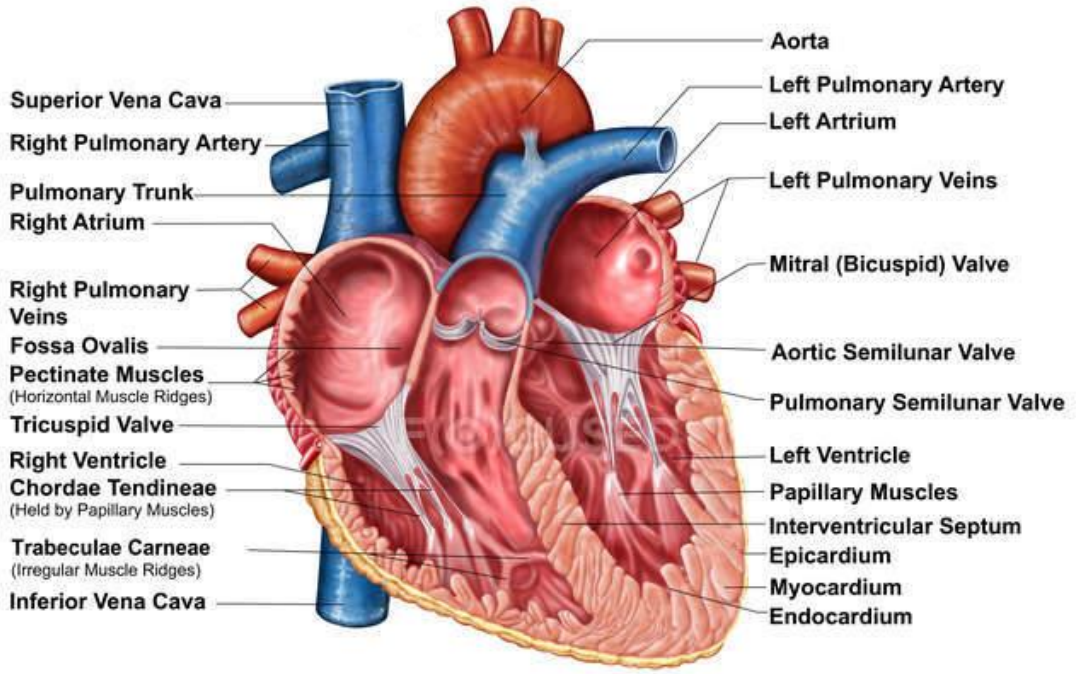

Figure 1-2 Heart sectional anatomy [30].

Different cell types are located in the myocardial tissue including cardiomyocytes, fibroblasts and endothelial cells [31]. Cardiomyocytes are rod-shaped cells (Figure 1-3) which are aligned in the direction of the myofibrils in the tissue [32]. This alignment of the cardiomyocytes gradually changes from endocardium to epicardium which form an overall helical rotation and anisotropic structure in the muscle that promote the contractility, electrical transmission, and heart function [33]. During myocardial development, replicating, smaller immature cardiomyocytes exit the cell cycle while increasing their size and fuse to each other to provide multinucleated cells which is one of the characteristics of mature cells. The adult cardiomyocytes are connected to each other by highly aligned and parallel intercalated discs which facilitate the functionality of cardiac tissue in terms of mechanical and electrical coupling, propagation, conductivity and contractility [34], [35], [36].

Although cardiomyocytes occupy around 75% of the volume of normal myocardial tissue, they count for only 30-40% of the total cell numbers. The rest, are non-cardiomyocyte cell, primarily fibroblasts and endothelial cells [37]. Fibroblasts surround the cardiomyocytes and play a key role in cardiac development, architecture, cell signaling, and function of the cardiac tissue through the gap junctions [38], [39]. Fibroblasts also secret collagen and ECM compounds reinforcing the mechanical stiffness of

the tissue [40], [41]. They preserve the ECM, distribute the force via ECM and cell-cell interactions and help the development of the endothelial cells. Fibroblasts can promote the release of cytokines and growth factors and improve the repair of injured site [42].

Due to the thickness of the myocardium and its metabolism, the vasculature and capillary networks are necessary to provide oxygen and nutrients for the cardiomyocytes. Endothelial cells are responsible for developing the network and ensure sufficient oxygen and nutrient supply for the cardiomyocytes [43], [44].

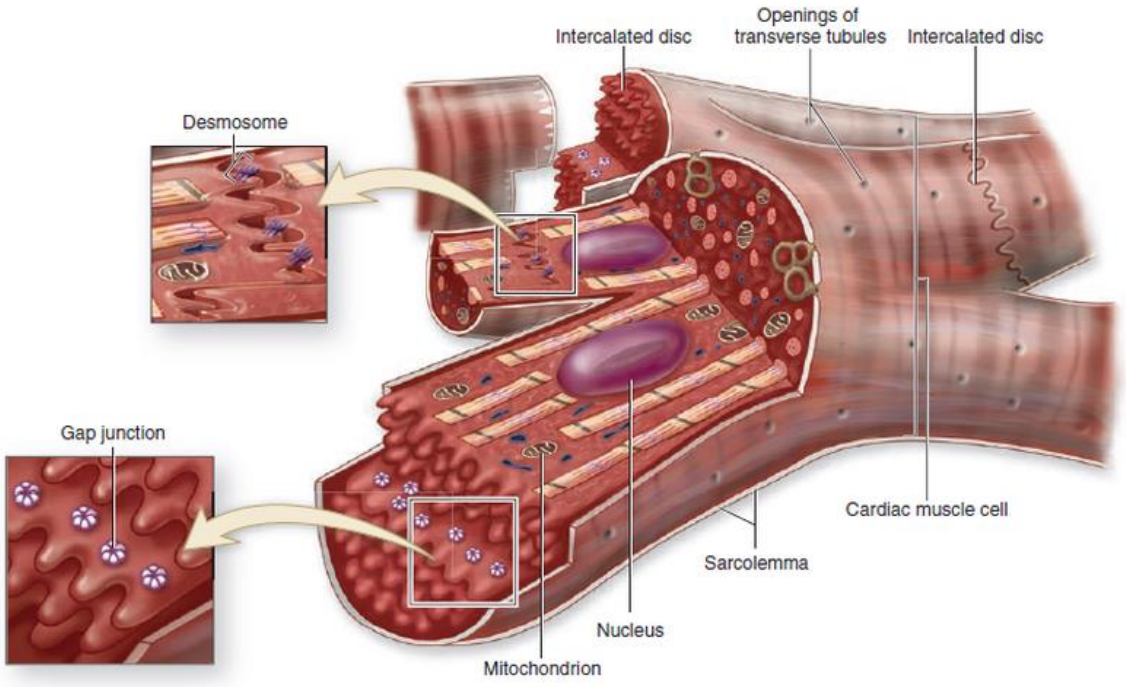

Figure 1-3 The diagram of cardiomyocytes connected by intercalated discs comprising desmosomes, gap junctions, and adherent junctions [45]

The major role of heart is to act as a pump to dispense blood to all body organs. The steady blood stream supplements them with all required nutrients, gases and waste removal. In order to perform its role at best, the heart relies on numerous electrical events which, in turn, determine at which rate and strength the heart needs to beat to ensure adequate supply of organs, depending on the activity. These electrical impulses originate from two main intrinsic conduction systems, namely the sinoatrial and the atrioventricular nodes. These nodes work autonomously from the nervous system, although to satisfy physiological needs, they are tightly regulated by vegetative (sympathetic and parasympathetic) nerves as well as circulating hormones (namely, adrenalin) [46]. Hence, these nodes are directly responsible for initiating the electrical activity that ultimately results in cardiac contraction [47]. Upon electrical

stimulation, a preprogrammed sequence involving sequential atrial and ventricular contraction ensues. This serves to pump the blood first from the atria to the ventricles, and then from the ventricles into the circulation – pulmonary for the right heart, general for the left [48]. This specific contraction pattern arises the timed propagation of the electrical excitation from the atria and propagating down to the apex, and then through the ventricular myocardium. Such programmed and synchronized movement is made possible thanks to the intrinsic structure of the cardiac electrical excitation system as well as the cardiac muscle [49]. Indeed, the myocardium, like skeletal muscular tissues, is organized in a striated way, due to the sarcomeric assembly of the tissue. The sarcomere is the basic unit of striated muscle tissue and is formed by an entangled meshwork of actin and myosin fibers, which slide upon one another to create cardiac contraction. Repeating sections of sarcomeres ultimately constitute cardiomyocytes, also called cardiac muscle cells. These cells are finally connected to each other through intercalated discs, a particular type of gap junctions, that link cardiac cells to efficiently and rapidly propagate action potentials to yield synchronized contraction of the myocardium [47].

The heart tissue has a complex structure due to the torsion. The torsion is a ventricular motion created by myofibers in the myocardium. During systole and diastole, the rotation direction from apex to base changes. This different rotation induces the torsion, which determines the oblique orientation of the myofibers. Hence, the subendocardial fibers are right-hand-oriented, whereas, the subepicardial fibers are left-hand- oriented [50]. As the heart torsion is directly related to the myofiber orientations, the orientation alteration may represent the malfunctionality of the heart [50], [51]. Several cardiovascular diseases are the result of twisting changes in heart tissue [50].

1.3.3 Quantitative cardiac tissue composition

The heart is composed of several different types of tissue, among them the flexible valves, the strongly fibrous annular plate, the self-depolarizing nodes as well as the proper myocardium. We are here most interested in the myocardial tissue, and particularly the ventricular myocardium. The ventricular myocardium consists of both cellular and extracellular elements, and knowledge of its composition is essential for the purpose of *in vitro* cardiac model construction (table 1-1).

Table 1-1 composition of the myocardial tissue.

Element	% mass	Reference
Cellular elements	Ca. 70%	[52]
Interstitium	Ca. 20%	[52]
Blood	Ca. 10%	[52]
ECM (part of interstitium)	Collagen: 0.4%	[53]

1.4 Cardiac models

As the main hypothesis of this work is enhancing the functionality and phenotype of the cardiac tissue model, it is necessary to review some of the developed cardiac models in this section. The fields of tissue engineering and regenerative medicine jointly aim at constructing biological substitutes to ultimately restore and maintain normal function in diseased or injured tissues [54]. However, recapitulating biological structures, even the simplest, is challenging. Indeed, tissue biology is strongly characterized by a highly heterogenous organization, composed of multiple different types of cells, as well as extracellular matrix components, that, altogether, contribute to a unique interplay and favor extensive cross-talk between the resident cell populations [55]. Therefore, engineered substitutes must mimic the native structure by spatially arranging in a specific architecture, which will, in turn, modulate their function to recapitulate the physiological one. Creating these complex tissue components requires new methods of combining cells, growth factors, and biomaterials in ways that facilitate tissue and organ morphogenesis.

Mimicking the myocardial tissue of the heart *in vitro* is challenging as several factors should be taken into account such as different cell-cell and cell-ECM communications, 3D organization, mechanical, electrical and biochemical cues. However, providing a reliable platform, which mimics the heart tissue is beneficial to reduce the number of animal testing as well as non-relevant 2D assessments [18]. To have such a reliable tissue model, various techniques, different requirements and limitations have to be considered. These considerations mostly depend on the final applications. Cardiac models originally emerged to fill the gap between drug development and clinical trials. At present, neither animal nor *in vitro* models fully replicate the physiology of human tissue. Animal models are typically affected by inter-species difference, while *in vitro* models are still overly simplified [17], [56]. Nevertheless, these models have expanded their domains of application to disease modeling, transplantation, and cell therapy. Therefore, improvements in *in vitro* cardiac models to better predicts the response and behavior of the human cells would be of substantial interest for both bioengineers and pharmacologists.

An ideal *in vitro* cardiac model should be able to mimic the real conditions of the cells in the native tissue, e.g. the orientation, 3D culture, co-culturing, etc. Although 2D *in vitro* models are informative, they cannot replicate a main parameter of the native heart which is its complex 3D structure. Hence, the results of 2D models can not directly be generalized to 3D and native tissue. One of the approaches for developing the 3D structure is that one uses the biomaterials for embedding the cells in 3D which provides the structure and controllable environment for cardiac tissue formation and regulation [57]. Several cardiac tissue engineering approaches exist. The main element in most of them is the biomaterial, either in combination with cells or alone, used for replicating the native tissue, fabricating the scaffold, providing 3D stable structure, and improving cell functionality. Further sophistication such as

adding different stimulation, regulatory signals and methods to improve the model's functionality can be considered to develop more tissue-like constructs in *in vitro* conditions [17].

In the upcoming sections, we provide deepened insight into research conducted on some of the aspects of 3D tissue models relevant to this thesis. Hence, we first review the biomaterials for cardiac tissue models. Then, we progress with some methods to manipulate the cells *in vitro*, and the key aspects of different cardiac models. Finally, the applications of these cardiac models will be discussed.

1.4.1 Biomaterials

As mentioned, cells in each tissue are located in the extracellular matrix, which at the chemical level comprises a hydrated and often crosslinked mix of proteins and carbohydrate moieties [58]. The extracellular matrix provides both structural support and biological cues in the form of growth factors and cell adhesion motives. Thus, generating an engineered tissue necessitates the use of biomaterials that

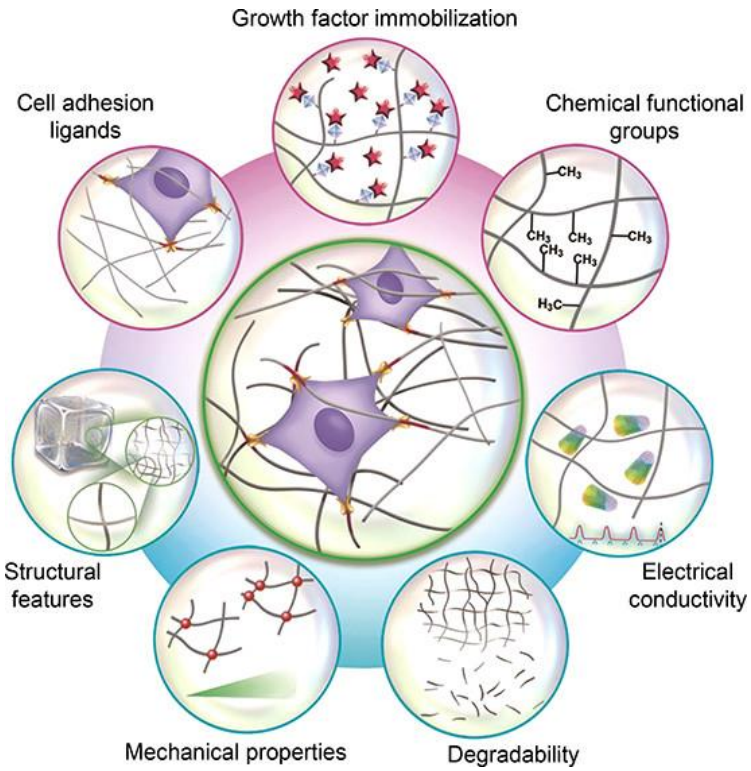

Figure 1-4 The elements that have to be considered in a biomaterial. Reprinted with permission from [59]. Copyright (2017) American Chemical Society.

meet the specific requirement of the tissue [60]. Some general aspects of a biomaterial are its biocompatibility, biodegradability, mechanical stiffness, porosity, and specifically for *in vitro* observation,

transparency. Moreover, for cardiac tissue applications some other criteria need to be considered such as the ability to orient the cells, improve their synchronicity, enhance the cell-cell interaction, vascularization, injectability, and transmission of the electrical and mechanical signals [42]. Figure 1-4 shows some of the main characteristics of biomaterials.

The biomaterials can be used in different forms such as solid porous scaffolds, sheets, 3D hydrogels, and injectable materials based on their applications [61]. In addition, they can originate from naturally-derived, synthetic, or the combination of both materials [62].

Table 1-2 Relevant estimates of the stress and strains encountered *in vivo.*

Physical quantity (all left-ventricular, adult, human)	**Value**	**Reference**
Myocardial elongation changes during cardiac cycle (ventricles)	20%. Passive during filling, active contraction during ejection	[63]
Minimum myocardial wall stress (beginning of diastole)	Ca. 3kPa	[63], Extrapolation from Fig. 3a
Myocardial wall stress after filling (end-diastolic)	6.2kPa	[64], Table 2
Myocardial peak wall stress during contraction (systolic)	33kPa	[64], Table 2

Among all of the biomaterial's properties, mechanical stiffness is critical for cardiac tissue models, due to the fact that the cardiac cells in native tissue are exposed to relatively large forces arising from the contractility and blood pumping function. Therefore, the relevant mechanical stiffness of the chosen biomaterial provides a special niche to support the development and functionality of the cells. This relevance becomes more critical when it applies to *in vivo* studies, in which the bioengineered tissue needs to integrate with the surrounding tissue of the heart. Relevant estimates of the stress and strains encountered *in vivo* are noted in Table 1-2. During diastole (ventricular filling), a relative wall extension of about 20% occurs due to passive stretching by filling of the ventricles with incoming blood. There is a concomitant increase in myocardial passive tension from about 3kPa to 6kPa [64]; with considerable inter-individual variation in both health and disease). Of note, under physiological conditions, the wall stress never drops to zero, the structures are therefore always pre-strained, a condition known to contribute to cardiac contractility through the Frank-Starling mechanism [65]. The passive increase of wall stress by about 3kPa for 20% elongation corresponds to an effective passive myocardial Young modulus

of about 15kPa for the left-ventricular myocardial wall. *Ex vivo* estimations by uniaxial compression yield similar results at similar strains, confirming the validity of the *ex vivo* analysis. The forces deployed by active contraction finally are much greater, stress values reaching over 30 kPa, and nearly the double in certain pathological conditions [64]. It is also noteworthy to mention that the mechanical stiffness of the native heart increases during the development from the embryonic state to the adult heart, which reflects in the maturation and functionality of the cells. *In vitro*, several studies have directly shown the impact of the mechanical stiffness of the cell environment on the maturation, function and organization of the cardiac cells [66]–[73].

Initially, scaffolds used in cell multiplication ex vivo. Technology development provides more interesting applications for scaffolds such as cell delivery, implantation, and *in vitro* studies[42]. One of the most frequently applied materials categories in tissue engineering are hydrogels of both natural or synthetic origin [74]. Hydrogels can support both mechanically and biologically cellular 3D structures and their properties can be manipulated to reach the desired characteristics [75]. In the following section, we discuss more the natural and synthetic hydrogels that have been used in cardiac tissue regeneration.

1.4.1.1 Natural hydrogels

The extracellular matrix of the heart is composed of various natural materials such as collagen and elastin. These biomaterials allow cell attachment, proliferation and differentiation *in vitro* and are widely used in tissue engineering approaches because of their intrinsic biocompatibility and, contrary to cells, relative lack of ability to provoke an immune response [14], [76]. The byproducts of biodegradation of these polymers are also not toxic [14]. Despite their great potential in cardiac tissue regeneration, the lack of sufficient mechanical properties and the batch-to-batch variation limits their use in this field.

Some natural hydrogels, particularly of animal origin, are bioactive and provide native adhesion sites that can recapitulate the *in vivo* environment signals responsible for cell differentiation into the desired tissue [77]. In addition to particular purified ECM components, decellularized, but not otherwise purified extracellular matrix (dECM) is increasingly used as a biomaterial [78]. Such decellularized extracellular matrix dECM has also been proposed as a biomaterial in cardiac tissue models, as it mimics the main architecture and composition of the heart tissue [79], [80]. In this thesis we use porcine cardiac dECM as a main hydrogel component for constituting 2D and 3D cardiomyocyte environments. We discuss the isolation of dECM, its processing and characterization in chapter 2. After decellularization, most of the cues, which at present are difficult to create synthetically, remain in the specific ECM and later interact with the seeded cells [81]. The presence of intact growth factors has been confirmed in ECM hydrogels, although in smaller quantities compared to native tissues or ECM scaffolds[78]. The formation of ECM hydrogel is mainly based on the self-assembly of collagen with the presence of

glycosaminoglycans, proteoglycans, and other ECM proteins [78]. This formation and intact cues make decellularized ECM hydrogel an excellent candidate for cell culture by providing cell signals and initiating the differentiation into specific lineages[81].

A hallmark study in the use of natural hydrogels for cardiac modelling and transplantation is the pioneering work by Zimmermann *et al*. [82]. They came up with a millimeter-scaled engineered heart tissue model from neonatal rat heart cells. For this, they suspended the cells in a mix of collagen and Matrigel (Engelbreth-Holm-Swarm tumor exudate) and provided the cells with the possibility to perform dynamic mechanical work against a specifically designed spring load. They further provided metabolic support by facilitating both metabolite entry into the cells with application of insulin and increased atmospheric oxygen to compensate for the long diffusion distances in their constructs. Their constructs were spontaneously beating, and upon implantation showed no delay in electrical signal conduction with native tissue upon implantation [82]. In light of clinical application and *in vitro* modelling, the use of Matrigel with its high inter-lot variability and tumor origin is nevertheless problematic.

Recent efforts have therefore been made to avoid the use of Matrigel. This is not trivial, since Matrigel consists of thousands of different molecules [83], varying in each lot, but of which many can have beneficial effects for cell survival and function. Collagen on its own having limited mechanical stiffness [84], in this respect, fibrin is an interesting option for cell-compatible hydrogel formation. Fibrin is indeed a cell-degradable biopolymer which has been found responsible for hemostasis and is produced from the enzymatic polymerization of fibrinogen monomers by the action of thrombin [85], [86]. Fibrin polymerization forms a mesh-like structure with a good mechanical stability [87]. Fibrin-based hydrogels have low inflammatory response and foreign body reaction [86]. Kong *et al*. [88] performed a comparison between Matrigel, collagen I, and fibrin to determine which of these substrates could support the indirect cardiac reprogramming process. The results of their study show that fibrin gel improves cell dedifferentiation and cardiac cell differentiation more efficiently than Matrigel and collagen I. They also observed that a higher concentration of fibrin gel increases the efficiency of cardiac reprogramming[88].

dECM conserves many cell adhesion motives and to some extent the growth factors natively present [89], [90], and so it emerges as natural candidate for physiologically meaningful and potentially clinically applicable cardiac modelling and tissue engineering. The combination with fibrin has been reported to be particularly successful by Williams [79], albeit it was found necessary to use transglutaminase cross-linking to achieve sufficient mechanical properties in this study, with ensuing cytotoxicity. Our aim here is to investigate whether the use of transglutaminase cannot be circumvented to achieve a fully cell-compatible hydrogel system, and also to better define whether there is an actual advantage of using the chemically ill-defined dECM over commercial, purified collagen I in fibrin composites or alone. This investigation is the object of chapter 2 of this thesis. Based on the results of this investigation, we use dECM-fibrin composites for the further geometrical alignment and mechanical stimulation experiments.

The use of neonatal cells greatly facilitates cardiac modelling experiments due to their high regenerative and survival potential [91], and thanks to a collaboration with Prof. Rohr, University of Bern, we use neonatal rat cardiomyocytes in this work as well. However, in light of reduction of animal experiments as well as potential clinical applicability, alternative cell sources are of interest. Induced pluripotent stem cells directed towards cardiac differentiation are an option: For example, in a study conducted to model dilated cardiomyopathy caused by a mutation in titin sarcomeric protein, Hinson et al. show that cardiac microtissues obtained from iPSC embedded in collagen are a powerful system for evaluating the pathogenicity of titin gene variants [92].

1.4.1.2 Synthetic hydrogels

The other source of biomaterials is synthetic polymers which have the ability to be modified and tailored, based on the application and the required properties, e.g. mechanical stiffness, topography, different physical and chemical properties, that are predictable and reproducible [14], [93]. However, their main problems are immune response, toxic byproducts after degradation, and complex synthesizing procedure [93]. Some of the mostly used biomaterials in cardiac 3D tissue engineering include polylactic acid (PLA), polyglycolic acid (PGA), polyurethane (PU), poly e-caprolactone (PCL), and polylactic glycolic acid (PLGA) [94]. Most of the synthetic biomaterials require a bioactivation step to make them appropriate for cell support [95].

Figure 1-5 represents some examples of cardiac models based on synthetic biomaterials. Orlova et al. used electrospun polymethylglutarimide (PMGI) nanofibrous meshes to control the architecture of the engineered cardiac tissue (Figure 1-5A, [96]). In this study, permeability and nutrient penetration was limited as it mainly relied on the porosity in this case. Moreover, the degradation of the material was not assessed at all in this study, which may constitute an important step further. Ghasemi-Mobarakeh *et al*. used blend of collagen, gelatin and poly-caprolactone to create highly aligned nanofiber constructs via rotary jet spinning (RJS) and electrospinning [97] (Figure 1-5B).

With such approach, the authors obtained that the highly anisotropic RJS fibers were able to support optimal cellular alignment, maturation and self-organization for a polymer/protein ratio of 75/25. The ratio of 50/50 used in their previous studies had shown less aligned cells and increased biodegradation rates [98]. In another example of synthetic material-based models, Zhen *et al*. studied contractility malfunctions in a highly defined scaffold structure which was fabricated by two-photon initiated polymerization (TPIP) (figure 1-5C) [99]. However, the obtained scaffold displayed significantly lowered contraction forces compared to a native adult heart and, thus, can hardly be considered as a physiological *in vitro* model. Ma *et al*. used 3D printing technology to fabricate force gauge arrays from a synthetic photosensitive polymer based on poly ethylene glycol diacrylate (PEGDA) (figure 1-5D) [100]. The

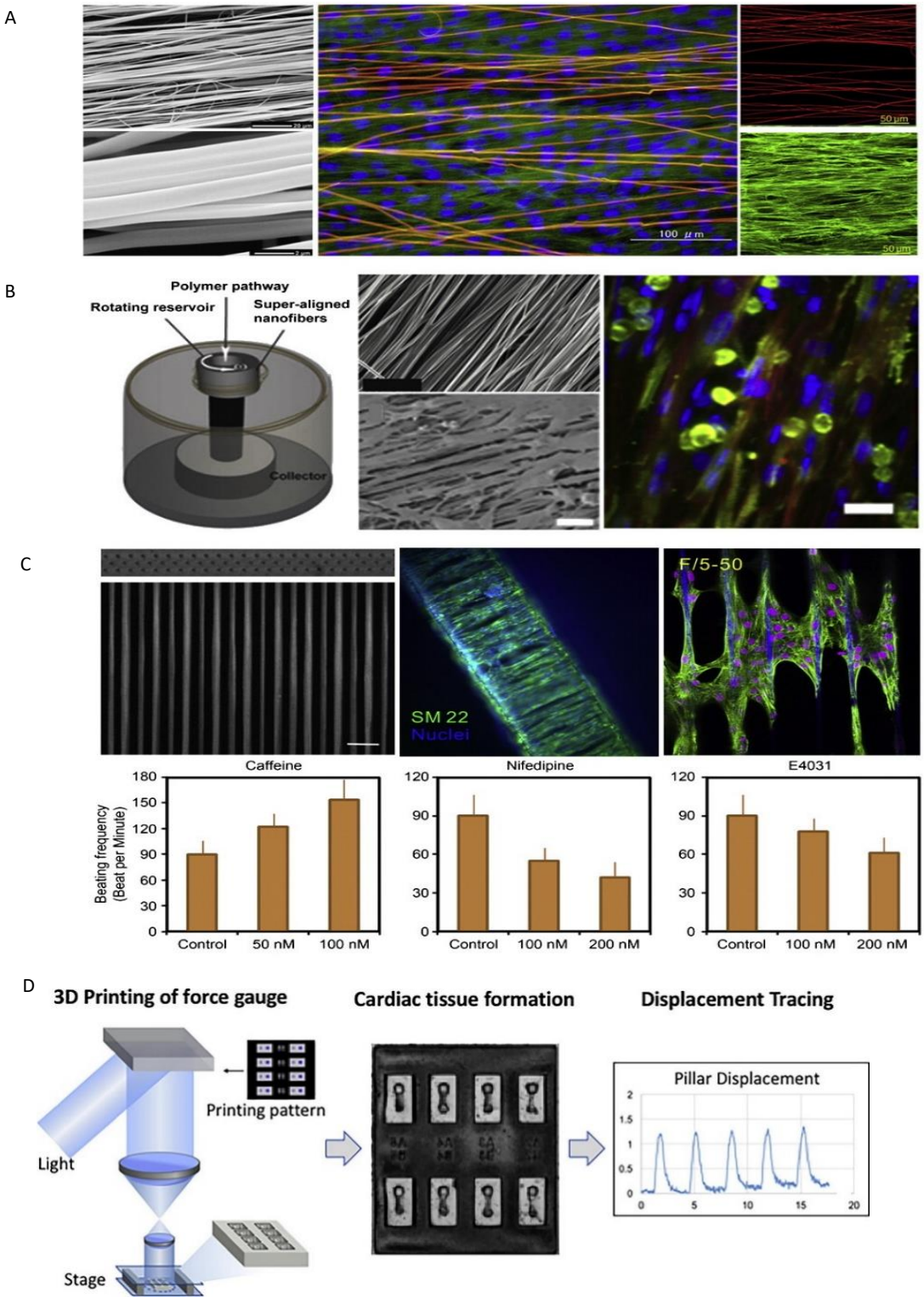

Figure 1-5 Some of the examples of cardiac models based on synthetic hydrogels. A. Electrospun nanofiber scaffolds were made for creating the continuous anisotropic cardiac tissue [94]. B. Aligned nanofiber scaffolds made by rotary jet spinning promoted better sarcomere formation in CMs [95]. C. High-defined filamentous scaffolds made by two-photon initiated polymerization were used to create an aligned hiPSC-CMs-based cardiac model for drug screening [97]. D. 3D printing technology to fabricate force gauge arrays from a synthetic photosensitive polymer based on poly ethylene glycol diacrylate (PEGDA) [98]. Reprint with permission from [17]. Copyright © 2015 Elsevier B.V.

results of this study are promising for high throughput applications. Hu *et al*. developed a micropat-

terned biodegradable, electroactive film based on poly (glycerol sebacate)-co-aniline trimer (PGSAT) which promoted the alignment and elongation of H9c2 cells [101].

As the biomaterials have different origins and properties, finding a single material to cover all the requirements of cardiac tissue engineering is challenging. Hence, hybrid materials containing two or more biomaterials to meet different criteria were developed and studied in several groups. In this thesis, we also use a mixture of dECM and fibrin to cover the most important criteria of the cardiac tissue in *in vitro* condition.

1.4.2 Regulatory signals

To improve the functionality and identity of the cardiac cells in a cardiac model, one should consider the environmental cues and the regulatory signals to compensate them. The cardiac cells in native 3D tissue undergo a variety of stimulations, which regulate both the development of the heart and its physiological pumping function [102]. Tissue engineering approaches are trying to mimic these stimulations for improving the tissue maturity by modifying the microenvironment of the cells *in vitro*. In order to create a bioengineered cardiac tissue, some criteria should be met. Fig. 1-6 compiles the main known microenvironment influences on cardiomyocytes [103]. From this, one can deduce a list of criteria for cardiac *in vitro* models:

- The **matrix** of cell culturing needs to allow basic adhesion and should favor correct differentiation and function; it should not by cytotoxic.
- Culture should be in **3D** to mimic the native conditions, yet nutrient and oxygen access should be physiological.
- Cells should be **aligned** for proper force transmission and adopt proper 3D organization in cardiomyocyte bundles.
- **Mechanical** stimulation and stiffness parameters should match physiological parameters to enhance cell functionality and maturation [104], throughout the desired culture time.
- **Electrical** stimulation should occur at physiological rate and synchronicity, preferentially by means of self-depolarizing cells mimicking the cardiac sino-atrial and atrio-ventricular nodes.
- The cellular composition should reflect the native composition, implying **co-culture** with non-cardiomyocyte cells.
- Ideally, the culture system would be **chemically defined** for reproducibility, yet provide the entire set of biochemical signals encountered *in vivo*.

- Ideally, the system could be used for **specific applications** such as high throughput screening or implantation

Some of these parameters have been mentioned in figure 1-6. In the following section, we discuss more in detail most relevant cues to our subject, including the chemical and topographical patterning, mechanical stimulation, co-culture, and 3D cell culture.

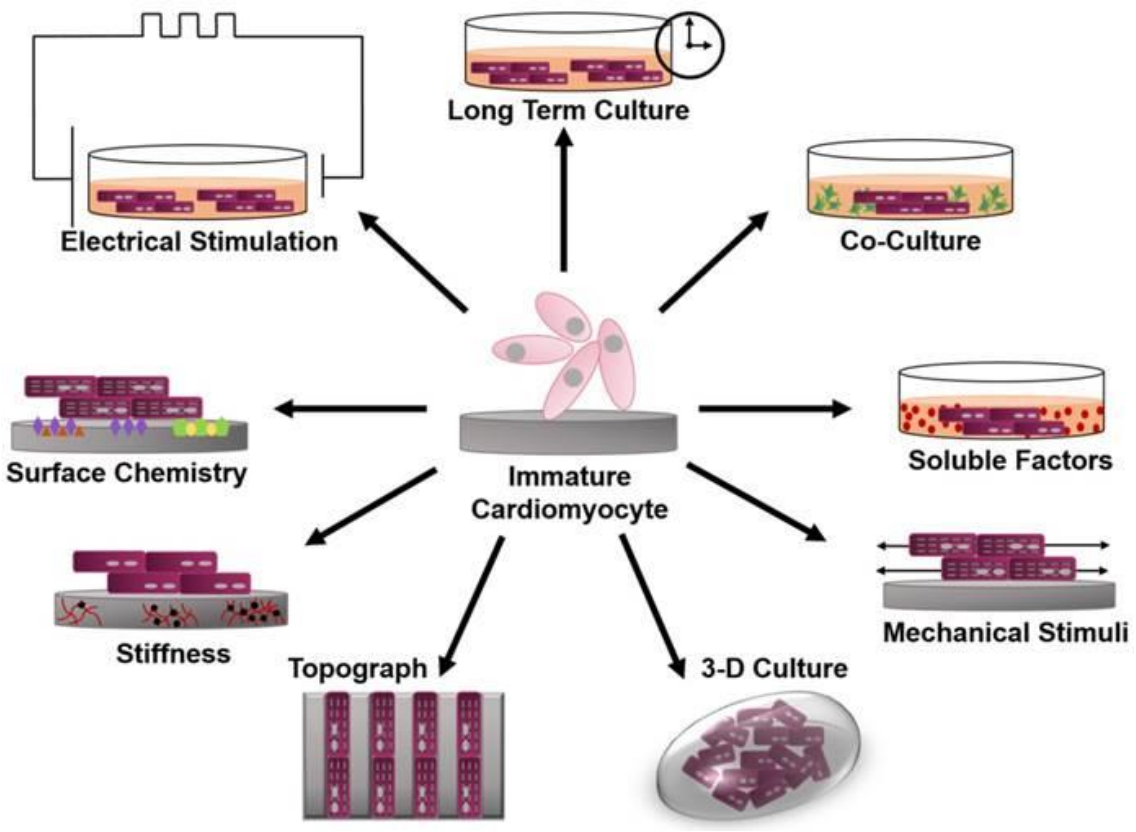

Figure 1-6 Schematic of engineered microenvironments used to mature human pluripotent stem cell-derived cardiomyocytes. Reprinted with permission from [103]. Copyright © Ivyspring International Publisher.

It is difficult to meet all the criteria set forth above in a single system, and all studies, including this thesis, necessarily focus more on some aspects than others. Table 1-3 gives an overview over the criteria addressed directly or more implicitly in this thesis. The main focus points are in bold.

Table 1-3 Regulatory signals and design criteria implemented in this thesis.

Criterion	Addressed here	Details
Matrix suitability	**Yes, part II**	**Comparison of different matrices, particularly an optimized defined matrix (collagen-fibrin) vs. an optimized complete matrix (dECM-fibrin)**
3D	**Yes, all parts**	**Based on 3D matrix (part II), efforts to obtain 3D alignment (part III) and 3D mechanical stimulation (part IV)**
Alignment	**Yes**	**Geometrical (part III) and mechanical influences (part IV)**
Mechanical	**Yes, with limitations**	**Stiffness-matching (part II); mechanical stimulation (part IV), although load not synchronized to electrical activity**
Electrical	Partly	We rely on spontaneous activity due to embedded rhythmic cells in cardiomyocyte extract, which we quantify, but do not perform stimulation
Co-Culture	**Yes, with limitations**	**Co-cultures were performed explicitly with cell-lines, but cell composition was not adjusted for native cardiomyocyte isolations**
Chemically defined	Attempted	Collagen-fibrin as an attempt to substitute for undefined dECM, but not as successful.
Applications	Partly	The materials are in principal compatible with implantation and well-plate-based screening, although further optimization would be required depending on specific needs.

While matrix aspects have been discussed in the prior sections, in the following sections, the state of the art and research efforts in the remaining focus areas (bold in Table 1-3) are discussed below.

1.4.2.1 Alignment: Chemical and topographical patterning

Biological and mechanical properties of the heart is defined by its microarchitecture. 70% of volume of the myocardium is composed of parallel cardiac muscle cells, or myocytes with elongated shape to produce an anisotropic structure with aligned sarcomeres. To mimic native cardiac tissue, recreating the complex 3D cellular organization while preserving the cell viability and function is crucial [105]. Some research groups found interesting approaches to control cellular organization in 3D, however, it is still a huge challenge to control the alignment in 3D tissue models with bigger dimensions. Some of

the most common approaches in tissue engineering which can provide alignment in the structures including mechanical stimulation, substrate patterning, chemical treatment of the surface, and the combinations of these methods. Using these approaches, the cells will change their intracellular organization (e.g. cytoskeleton reformation, nuclei orientation and shape, and the cell signaling), and modify their spreading and orientation in response to them [106].

Several researchers worked on producing aligned cardiomyocytes *in vitro* with chemical or topographical patterning of the cell substrates. For instance, one study used microcontact printing of laminin in the order of 5-50 µm wide strips to help the elongation of neonatal cardiac cells in 2D. The results suggest the improvement in N-cadherin and connexin-43 expression and localization which indicates the maturation of neonatal cardiac cells in chemically micropatterned substrates [107]. Another example is the patterning of polyethylene glycol (PEG) to form 150-800nm grooves to recapitulate the nanostructure of aligned fibrils in the myocardium ECM. These nanogrooves increased the protein expression, oriented the cardiac cells and showed an anisotropic action potential propagation [108]. Alternative research promoted the alignment of cardiac cells and the calcium transient amplitude by patterning hydrophobic-hydrophilic lines with the dimensions of 10 µm on Parylene C structures [109]. Using Faraday waves, another research group could encourage the iPSCs to form predefined patterns. The results showed the alignment of the cells with increased cellular functionality, intracellular connectivity, and beating rate compared to the random distribution of the cells [110].

Kim *et al*. developed a nanotopographically controlled *in vitro* model based on polyethylene glycol (PEG) hydrogel arrays for recapitulating the structural and functional properties of native myocardial tissue (Figure 1-7A, [108]). On the other hand, Figure 1-7B shows a fabrication method based on the uniaxial shrinkage of polyethylene (PE) to create multiscale grooves ranging from nano to micrometers [111]. Cardiomyocytes were also microcontact-printed (Figure 1-7C) either into aligned stripes (Figure 1-7D) or into circular colonies (Figure 1-7E). Mcdevitt *et al*. micro-printed lanes of laminin onto a non-adhesive surface [112]. In this study, they tried to spatially align neonatal rat cardiomyocytes to recapitulate an *in vivo*-like organization. The cells showed highly aligned myofibrils with normal diameters and bipolar cell junctions with intercalated disc connections. Serena *et al*. cultured circularly organized human cardiomyocytes onto a poly-acrylamide hydrogel with tunable tissue-like mechanical properties [113]. This method allowed a higher throughput compared to aligned stripes. Finally, PEG-patterned substrates were used to geometrically confine hPSC colonies (Figure 1-7F,[114]). This work notably explores further the characteristics of these cells by analyzing differentiation features that appeared after exposing cells to different biochemical and biophysical cues.

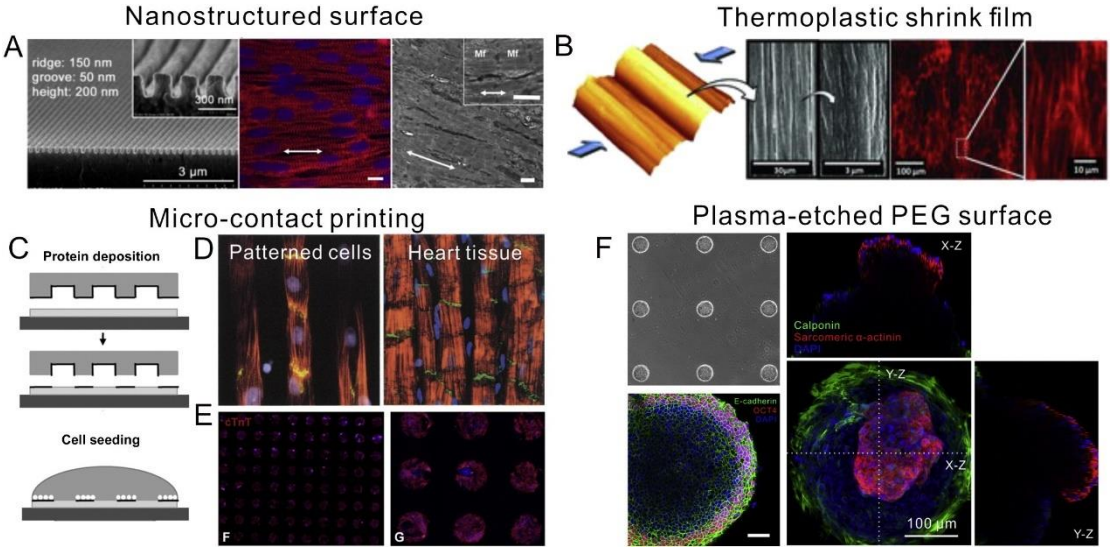

Figure 1-7 different methods of surface patterning. (A) Microfabricated nanostructured surface, [108] ; (B) Prestressed thermoplastic shrink film with tunable multi-scaled wrinkles [111]; and (C) Microcontact-printed patterns of pattern CMs into (D) Aligned stripes to mimic adult cardiac tissue structure [112] and (E) Circular colonies for high-throughput screening [113]. (F) Using oxygen plasma to etch PEG surfaces under a PDMS stencil protection allows micropatterning hiPSCs and determining stem cell fate during cardiac differentiation [114]. Reprint with permission from [17]. Copyright © 2015 Elsevier B.V.

The conclusion of these studies suggests that aligning the cardiomyocytes improve their maturity, functionality, provide a more tissue-like structure which is responding to pharmacological compounds and drugs, and enhance excitation-contraction coupling. However, aligning the cells should be combined with other approaches to encourage producing an adult cardiomyocyte phenotype.

1.4.2.2 3D models of trabeculae carneae

Microfabrication as employed in the studies listed in the previous section and many others focuses on local 3D features on essentially planar substrates. The cardiac trabeculae carnosum units are however 3D. It is therefore an emerging area of cardiac modelling to produce more controlled 3D aligned environments. For example, Xiao produced a cardiac bundle model which is used to create perfusable cardiac biowires based on polytetrafluoroethylene (PTFE) tubing for the drug screening application [115]. However, the use of PTFE as a biomaterial represents a limitation in terms of permeability to the tested drugs as only small molecules can diffuse properly through the tubing wall. Sasano *et al*. used layer-by-layer cell coating technique with fibronectin and gelatin for hiPSC-CMs (human induced pluripotent stem cell-derived cardiomyocytes) and showed synchronous beating [116]. One of the most recent works in providing cardiac models is conducted by Velduizen *et al.* In this work, they developed a microfabricated platform to incorporate surface topography for long term culture and maturation of cardiac cells in a collagen hydrogel. They showed upregulation of maturation genes and synchronized

beating after two weeks. The dimensions of the developed structures were in the range of 100-200 μm and the length of 200-800 μm (figure 1-8) [117]. A major goal in this thesis is to combine this principle with optimized dECM hydrogels to produce aligned cardiomyocyte structures by propagation of cell orientation from micropatterned substrates into the hydrogel. This should afford potentially free-standing hydrogel model units of aligned cardiomyocyte strands.

A

Design #	Micropost shape	Vertical post spacing (μm)
1	Elliptical	200
2	Elliptical	150
3	Hexagonal	200
4	Hexagonal	150

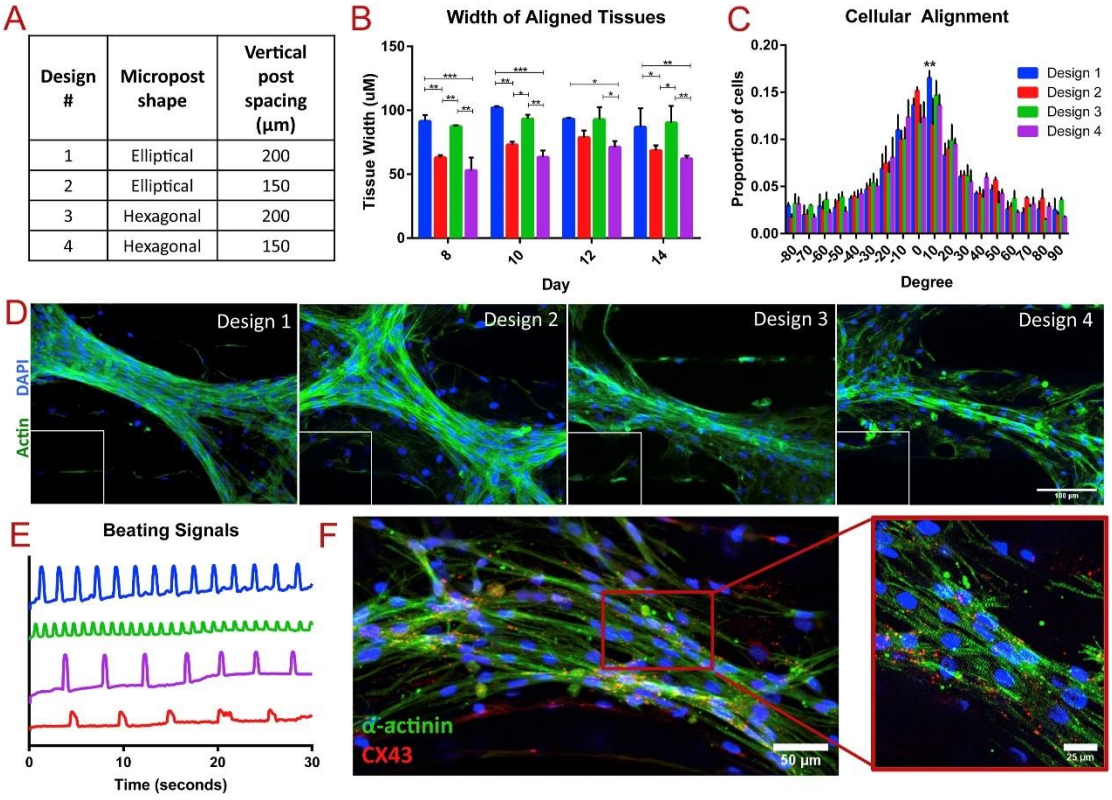

Figure 1-8 Optimization of microfluidic chip design parameters with neonatal rat cardiac cells: (A) Table of microfluidic chip designs with differing post dimensions. (B–F) Characterization of neonatal rat cardiac tissue within each design. (B) Tissue width, (C) cellular alignment, (D) immunostaining of actin and DAPI with inset as FFT, and (E) representative beating signals from tissues formed within each device. (F) Cardiac-specific marker staining of tissues in Design 1, demonstrating aligned sarcomeres (green) and abundant, localized connexin 43 (red), with 40X magnification to right. Statistics performed on two-way ANOVA of (B) n = 2 experiments and (C) n = 3 experiments. Reprinted with permission from [117]. Copyright © 2020 Elsevier Ltd.

1.4.2.3 Mechanical stimulation

The contractile activity of the heart is launched very early in the development; therefore, mechanical forces play an important role during heart morphogenesis. Indeed, Auman and collaborators found evidence of cardiomyocytes contractions and blood flow existing within the earliest ages of the heart, generating forces and stresses essential for correct heart development [118]. Impairment in the contractile function can rapidly lead to fatal outcomes and, therefore, when developing a cardiac model,

the assessment of the contractile activity of such model, as well as its ability to be properly integrated in the endogenous environment, is critical.

During the heart development, the myocardium secretes collagen, which leads to increasing the mechanical stiffness of the ECM from embryonic to the adult tissue [119]. Also, the mechanical stress in the heart, shear force, and the cell-cell and cell-ECM contacts are some of the stresses that cardiomyocytes undergo continuously. In normal healthy tissue, the cells adapt to the environment by changing their genotype and phenotype such as their direction, function, protein and gene expression (figure 1-9) [120], [121], [122], [123], [124], [125]. Cardiomyocytes continuously undergo mechanical forces and alter themselves. If adult cardiomyocytes are cultured in 2D *in vitro* model without applying mechanical stimulation, they dedifferentiate and alter their phenotype. Therefore, as the cells can sense the mechanical alteration in their environment, manipulating these forces will directly have impact on the cell behavior and have a critical role in cardiac tissue development.

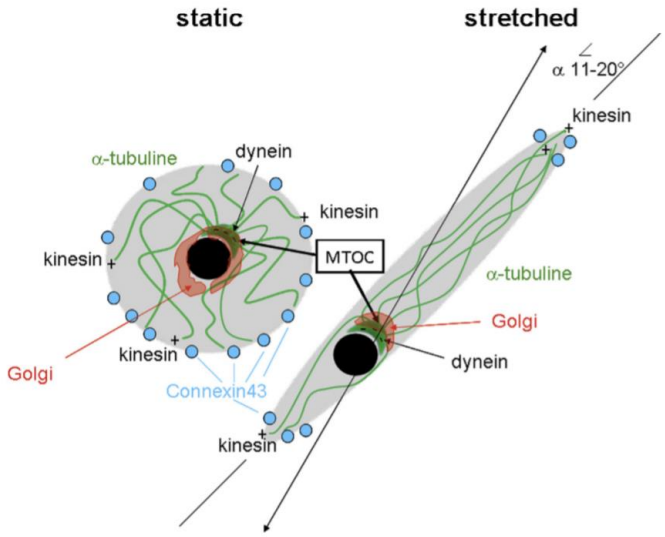

Figure 1-9 The impact of mechanical stress on the cell orientation (reprinted with permission from [121]).

In tissue engineering systems, the mechanical stimulation can be applied to the cells in different ways. One of the approaches is to statically stretch the cells which means that the mechanical force applies to the substrate after the cell are seeded and allowed to settle for a time period. A second approach is to gradually change the applied mechanical stress to the cells, which means that the substrate mechanical stress increases step by step for a long period of time. More physiological are cyclic approaches: in spontaneously beating cultures, an external spring load can mimic the effect of aortic counter pressure. Some cardiac model cell lines do not beat spontaneously, and in this case the external cyclic stretching can be used. Cyclic stretching is thought to better mimic the beating behavior of the cardiac cells in native tissue [126], even though it must be admitted that due to the effect of filling pressure, the stress in the cardiac muscle does not drop to zero even during diastole (Table 1-2). In addition to these

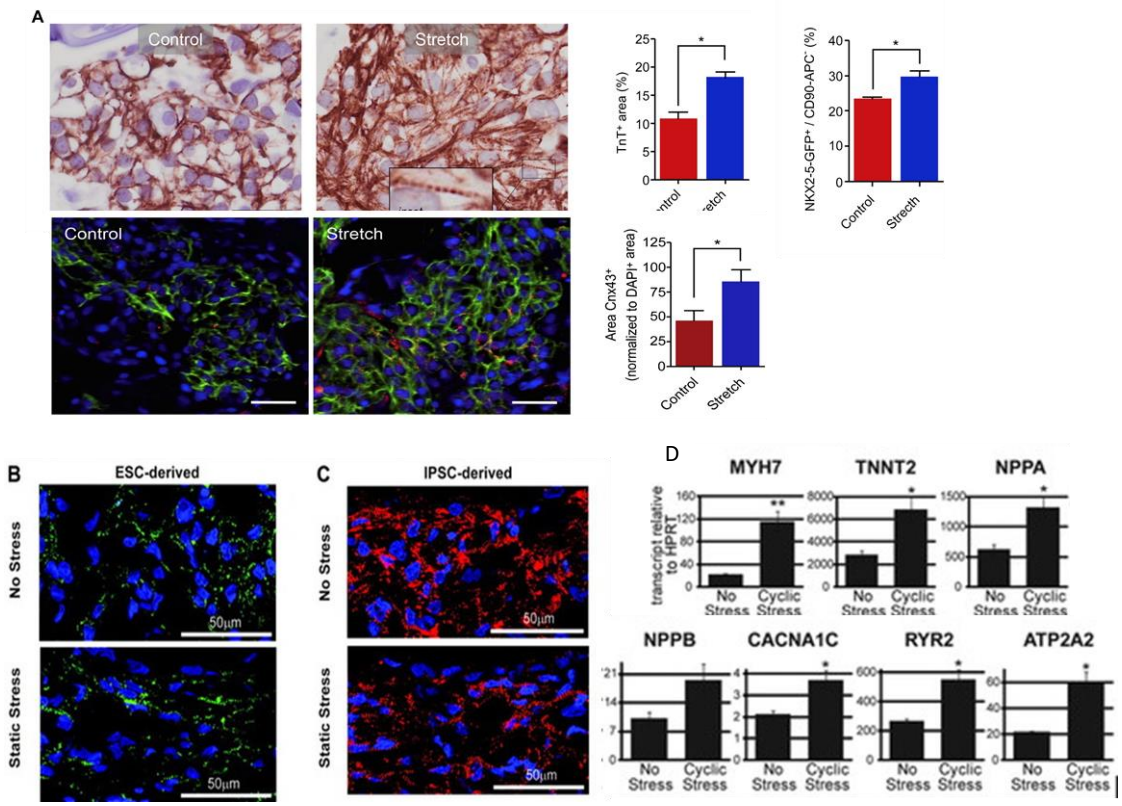

Figure 1-10 1-11 Stretched constructs contained a larger proportion of cardiomyocytes. A. top, Immunostaining for TnT demonstrated greater expression in stretched constructs and well-defined striations with Z-banding running longitudinally along the stretched hESC-CMs (inset) (scale bar 25 μm; *n* = 4/group). Bottom. Immunostaining and quantification of Cnx43 (red) normalized to DAPI (blue) expression showed stretched constructs expressed higher levels of Cnx43 than control constructs (n = 4/group, scale bar 40 μm; TnT immunostained in green). Reprinted with permission from [126]. Copyright © 2014 Elsevier Ltd. B. Constructs generated from ESC-derived cardiomyocytes subjected to static stress conditioning (bottom) or no stress conditioning (top) stained strongly for the sarcomeric protein α-actinin (green). C. Constructs generated from iPSC-derived cardiomyocytes also stained strongly for α-actinin (red). In both cases, myofibrils appear more aligned in the static stress-conditioned constructs. D. Quantitative RT-PCR was performed on iPSC-derived cardiac constructs conditioned with no stress or cyclic stress for 4 days. Reprinted with permission from [125] Copyright © 2011, Wolters Kluwer Health.

methods, based on the application and design of experiment, fluid shear stress or compression instead of stretching can be conducted.

These mechanical loading approaches can be also applied in 3D constructs using either uniaxial, biaxial or multiaxial loading. Several investigations have been conducted on the mechanical stimulation of cardiac cells in 2D and 3D *in vitro*, which all agreed on the influence of mechanical stimulation on intracellular organization of the cardiomyocytes, alteration in gene and protein expression, enhancement of the activity of ion channels, increase of the gap junction proteins which improves the coupling of the cells and transmission of the electrical signals.

For example, one study demonstrated the cardiomyocytes elongation, sarcomeres alignment, gap junction protein expression, and faster calcium cycling in the ESC-CMs or iPSC-CMs cultures in collagen samples with uniaxial mechanical stretching at 1Hz for four days [127]. Another study applied mechanical stretching at 1.25 Hz for 72 hours and reported higher elongation of the cells, increased gap junction protein and ion-channel related genes expressions, and higher beating frequency [128]. Using the incremental stretching method with a 400 µm increase of stretching regime every three to four days, one research group showed higher cell organization and sarcomeres alignment in Collagen I-Matrigel samples [129]. Figure 1-10 summarized two important studies in this field.

Whereas 2D stretching studies in general has been more focused on the nature of the response elicited by the cells upon different stretching regimes, 3D cultures are more interested in the engineering of reliable cardiac models, i.e. models that adequately respond to a specific, *in vivo*-like regime of mechanical stimulation [126]. Indeed, Guan *et al*. notably recapitulated tissue constructs which were mimicking structural and mechanical properties of the myocardium to investigate if such 3D environment has an impact on mesenchymal stem cells (MSC) differentiation into a cardiac lineage [130]. The results showed that, by culturing in a 3D environment that mimic the anisotropic structure and mechanical properties of the myocardium, embedded MSC were properly differentiated. Another work attempted to differentiate human embryonic stem cells by seeding them in Gelfoam sponges on which continuous cyclic stretching of 1.25Hz and 12% elongation was applied for 48 hours [128]. They demonstrated enhanced viability, adhesion, and maturation within the scaffold. Finally, Tulloch *et al*. led a very informative comparative study between uniaxial and cyclic stretches for 3D cultures [127]. They compared three different conditions including unconditioned constructs, uniaxial mechanical stress and cyclic stress on human embryonic and induced pluripotent stem cells-derived cardiomyocytes were seeded in a collagen matrix. The similar results in different conditions demonstrated that the additional factors such as cell culture medium, growth factors, and topography would be imperative in cell responses [104].

All of the studies using mechanical stretching verify the positive impact of using stretching on cardiac cells maturation and functionality including uniform cell distribution enhancement, higher cardiac cell,

myofibrils and sarcomeres alignment and organization, excitation-contraction coupling, morphological improvement of the cardiac cells, and amplified expression of maturity-related genes and proteins compared to the static cardiac models [131], [132].

Besides cell-autonomous benefits, mechanical stimulation could conceivably be important for alignment of the cardiomyocytes. The question of alignment of cardiomyocytes by mechanical stretching has been indeed been investigated by various authors, with conflicting results. For example, Dhein et al. found alignment of neonatal rat cardiomyocytes nearly, but not exactly along the main direction of applied deformation when performing stretch using collagen-modified silicone membranes [121]. However, Salameh et al. [133], in a nearly identical experiment (gelatin- instead of collagen-I coating and some details in media composition), instead found an orientation perpendicular to the main direction of strain. Thus, there are poorly understood subtleties in the experimental conditions that are visibly able to cause radically different cellular responses. One reason might be differential response to cyclic and static deformation: Experiments with fibroblasts have shown perpendicular orientation to cyclic strain [134], but parallel orientation to static strain [135]. Self-alignment of cardiomyocytes in circular collagen-Matrigel structures contracting against a central post [136] also suggest robust parallel alignment of cardiomyocytes along the induced static strain. Whether the unanticipated perpendicular alignment in cyclic stretch is an artefact of experimental conditions and particularly 2D culture is an open question of practical relevance for bioreactor design, but also of fundamental physiological importance: An interplay of perpendicular and parallel responses could indeed be important in the development and maintenance of the helicoidal fibrous structures characteristically found in the heart [137]. Here, my aim was therefore to investigate the influence of mechanical stretching, and particularly cyclic stretching, in a 3D configuration.

Besides mechanical loading, the stiffness of the cell microenvironment can also regulate the behavior and maturation of the cells. A number of studies investigate the impact of substrate stiffness on cardiac cells. For instance, one study investigated the impact of collagen-coated substrate stiffness from 1 kPa to 50 kPa and reported that the optimal stiffness for neonatal cardiac cells in terms of the sarcomere alignment, mechanical force production and calcium transient amplitude was 10 kPa, which is in the range of myocardium stiffness [67]. These results are in agreement with another study introducing the optimal elasticity in the range of 11 kPa to 17 kPa for contractility, signal transmission, and sarcomere alignment [138]. They also displayed that the cell culture made on substrates of higher and lower stiffness do not reach the same results. Stiffer matrices lead to the lack of myofibrils and loss of contractility as the resulting tissue resembles the postinfarct fibrotic tissue scar, however, a lower stiffness alters the functionality of the cells [59], [138].

1.4.2.4 Co-culture with non-cardiomyocytes

As previously mentioned in section 1.3.2, the cardiac tissue is composed of several cell types including cardiomyocytes, fibroblasts, and endothelial cells, that are in close contact with each other and each of them has a critical role in tissue formation, maturation and functionality. By number, healthy cardiac tissue includes around 60-70% fibroblasts, 30% of cardiomyocytes and the remaining for non-cardiomyocyte e.g. endothelial cells. However, in volume, the cardiomyocytes are the dominant cell type and they are surrounded with fibroblasts. Therefore, the fibroblast cells are essential in culture for providing an accurate model. Several studies indicate the cross-talk and communication between cardiomyocytes and fibroblasts, which is leading to higher cell maturity and alignment in the *in vitro* model. Cardiac fibroblasts support the structure and functionality of the cardiac tissue by secreting growth factors and ECM proteins such as collagen. Regarding the generation of an *in vitro* functional cardiac model, the importance of the fibroblast's presence should be considered [139].

Numerous studies evaluate the impact of non-cardiomyocytes on cardiac tissue maturation and functionality. For instance, Sherri *et al*. co-cultured human induced pluripotent stem cell-derived cardiomyocytes with non-cardiomyocytes which were produced in differentiation procedure and showed enhanced electrophysiological maturation in co-culture samples [140]. In another study, Hiroko *et al*. showed that the quantity of the non-cardiomyocytes are essential for preparing a functional engineered cardiac tissue and co-culturing with non-cardiomyocytes increases the cardiotherapeutic potential [141]. Yanzhen *et al*. investigated the importance of fibroblast aging on cardiomyocytes by using fetal and adult cardiac fibroblasts in co-culture with cardiomyocytes and represented higher action potential, stronger contraction, and increased calcium transient amplitude in co-culture with fetal cardiac fibroblasts [142]. Kongpol *et al.* demonstrated the cross-talk between vascular endothelial cells and cardiomyocytes. Their results indicated the cardioprotection role of endothelial cells by secreting the leukocyte protease inhibitor as a protective factor [143]. Kostecki *et al*. showed the electrical connection of fibroblasts to cardiomyocytes which can effectively alter the electrophysiological properties of the cardiac model [144].

In summary, the results of such studies reveal the interesting and critical role of non-cardiomyocytes in co-culture with cardiomyocytes for enhanced maturation and functionality of the cardiac tissue models. In this thesis, we use co-culture with fibroblasts particularly to enhance cardiogenic differentiation.

1.4.2.5 3D cell cultures

3D models represent a significant improvement compared to 2D culture as the environment does not only allow for cell attachment and alignment but constitute a more responsive material enabling load transmission and stiffness modulation to recapitulate values within the physiological range [116], [145], [146]. Creating a tissue model *in vitro* implies to mimic the native structure of the tissue. Therefore,

most of the studies on cardiac tissue models use 3D cell cultures to have a similar organization of the tissue as it is *in vivo* [147]–[150]. The cells *in vivo* are located in the ECM which provides all critical biochemical, biophysical, electrical, and mechanical cues necessary for cell proliferation, survival, differentiation, maturation, and functionality. Several studies indicate the different behavior of the cells in 2D cultures compared to the native tissue and 3D cultures *in vitro* [151]–[154]. The results of numerous studies also suggest better similarity between the behavior of the cells in 3D *in vitro* models and native tissue [155], [156]. 3D cell culture provides spatial cell-cell and cell-ECM interactions which promotes the cell maturation and function. Hence, research groups are progressively focusing on 3D culturing and thus providing more reliable models that more precisely mimic the niche of the cells in native tissue.

Hydrogels in combination with cells or without cells are broadly used in developing the 3D cultures [14]. Moreover, a variety of stimulations and conditions can be applied to the hydrogels which make them an ideal candidate for cardiac tissue model development [157]. The other approaches for providing the 3D constructs include porous scaffolds, bioprinting, cell sheet engineering, tissue decellularization, organoids, etc. [158].

For instance, in one of the studies, neonatal cardiac cells were mixed with collagen I and Matrigel, and produced a 3D tissue-like circular ring to apply mechanical stretching. The cells displayed elongation, organized sarcomeres, and longitudinal organization [136]. Lei *et al*. used electrohydrodynamic printing technique to print polycaprolactone (PCL) microfibers in a layer-by-layer manner scaffold with defined orientation in each layer. The seeded cells in this structure showed improved adhesion, proliferation, gene expression, and conductivity [159].

A number of studies combine 3D cell culture with other methods, such as mechanical, biochemical and electrical stimulation to provide more adult-like tissue structures, and reported higher maturation in 3D cultures. For example, one study combined electrical stimulation with 3D cultures and compared it with the same condition in 2D culture of iPSCs. The results showed lower expression of fetal gene MYH6, higher expression of KCNJ2, and higher action potential, which are suggesting more adult-like and mature structures in the 3D cell culture combined with electrical stimulation.

As the conclusion, it has been shown in several studies that the primary cardiomyocytes grown *in vitro* on 2D substrates dedifferentiate and alter their phenotype. However, 3D cultures with defined characteristics, resemble physiological environment of the cardiac cell in native tissue and is preferable for *in vitro* studies. 3D culturing can be combined with other engineering technique to improve the maturation and functionality of the cardiac cells in *in vitro* conditions. Nevertheless, additional work has to be conducted to understand and optimize the principles behind 3D culture and its importance in cardiac models, drug screening and toxicity [17].

1.5 Applications of bioengineered cardiac models

Bioengineered cardiac models have a variety of applications in the field of regenerative medicine and tissue engineering. These applications include *in vitro* cardiac disease models, drug screening/discovery, patch transplantation and hydrogel injection (similar to cell therapy). In this section, we focus on these applications (figure 1-11).

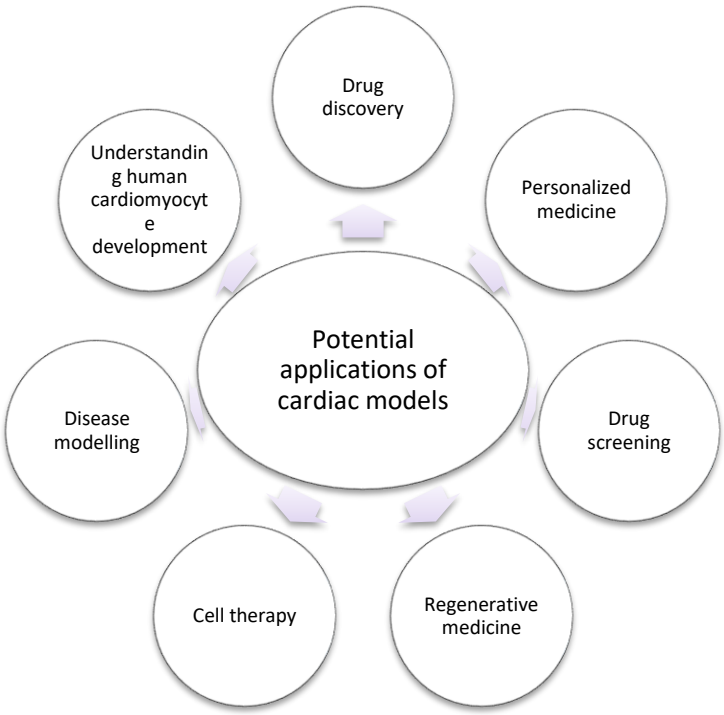

Figure 1-12 Potential applications of cardiac tissue models.

1.5.1 *In vitro* cardiac disease modelling

One of the main reasons of developing cardiac models *in vitro* is their application in understanding the mechanisms and development of different diseases. Many of the cardiac disease are initiated from a mutation in cell genes, the impact of external stimuli, and the side effects of using different drugs [18]. Understanding the mechanisms of the disease, its progress, and the way to prevent or treat it, is an imperative challenge in this field. Therefore, providing a specific cardiac platform *in vitro* to mimic the native heart physiology, pathology, and diseases can be useful to better comprehend such problems [160]–[163]. Several studies used animal models for replicating the diseases, however, the drawback of using animal is the differences between animal and human tissue, in terms of dimensions, beating rate, response to the treatment, and ion channels contributions [164]. These differences affect the

accuracy of these models and lead to questionable results when compared with human tissue [164]. Some researchers isolated the human diseased cells, as the source of their cells for disease modelling. Another source of cells is iPSCs which can be used in disease model investigations. Despite the fact that these cell sources have great potential for disease modeling, without having an accurate platform for culturing these cells, the results obtained with such cells cannot be precise, due to the difference of the cells response in 2D and 3D culture. That would necessitate having an *in vitro* model that can replicate the critical parameters of the native tissue e.g. the alignment of the cell, 3D structure, and different stimuli.

1.5.2 *In vitro* drug screening

Cardiovascular toxicity is one of the major drawbacks of drugs used either for treating the cardiovascular diseases or treating other diseases such as diabetes and cancers, that can prevent them from entering the market [165]. In addition, a noticeable percentage of the new drugs which are approved by FDA are excluded from the market due to their cardiovascular toxicity [166]. Hence, it leads to the significant waste of time and budget for each of the rejected drug [167], [168].

In general, most of the scientists and pharmaceutical companies work on the hypotheses and results on 2D *in vitro* cell culture platforms to investigate and develop new drugs. However, they fail to mimic the main aspects of the living human tissues due to not controlling the biological environment tightly enough [169]. The conventional preclinical studies for drug screening and toxicity tests are composed of either 2D monolayer cell culture models or animal models.

2D monolayer models are informative for understanding the molecular biology and the physiological responses of the cells, however, they suffer from the absence of the important cardiac tissue features such as the cell-cell and cell-ECM interactions, related protein and gene expressions, genetic instability and dedifferentiation, limited survival time *in vitro*, 3D sense of the construct, and lack of mechanical, electrical, and biochemical stimulations. In addition, drug diffusion and response kinetics in 2D models differ from the native *in vivo* responses, which make it problematic to extrapolate reliable and predictable results to preclinical, clinical and animal trials [161]. These limitations result in drug failure before entering the market because of the low efficiency of the models.

Even though testing new drugs on animal models, provides informative results, it also leads to a high failure percentage for drugs in clinical trials due to models that are not totally biologically relevant to the human body [170]–[172]. The *in vivo* animal models offer a platform with multi-organ integration which makes a great benefit compared to 2D models. However, in addition to the ethical concerns, the particular physiological response of a specific tissue cannot be isolated and recognized from the whole model, which adds more complexity [171].

To overcome the limitations and deficiencies of both monolayer platforms and animal models, one should develop *in vitro* models which are faithfully representing the requirements of an adult physiological and pathological human heart tissue such as 3D culturing, cell-cell and cell-ECM interactions, dynamic environment, electrical and mechanical activity, the tissue configuration and geometry. These reliable models are of huge interest for *in vitro* drug screening and disease modeling [146], [173], [174].

Developing new drugs, investigating their side effects and interactions with other drugs or the cells, has always been motivating for researchers, pharmaceutical companies and the medical community. The collaboration between the bioengineering and microengineering fields allows to define promising approaches to provide a cost- and time-efficient pre-clinical drug screening. The functional models made of the collaboration of these two fields are reproducibly high throughput, more complex and can recapitulate the *in vivo* environment precisely and the findings would be profoundly relevant to the human tissue responses [77], [169], [175]–[178].

These models represent an informative platform to understand, study, and develop new drugs. Additionally, they decrease the cost of drug development and can make more personalized platform for testing the drugs on human cells before exposing the patient to the drug. Therefore, it will diminish the cardiovascular toxicity of the drugs and provide relevant information about human physiology.

1.5.3 Cell therapy

One of the interesting approaches to treat the infarcted heart without invasive surgery is injecting the isolated cells from different sources such as embryonic stem cells, induced pluripotent stem cells, skeletal myoblasts, and native cardiac progenitor cells in the heart via pericardium, endocardium or coronary arteries to increase the number of cardiomyocytes in the target zone and enhance the functionality of the infarcted heart [179]. Cell therapies try to prevent the weakening of the heart tissue by providing an abundant number of healthy cardiomyocytes and non-cardiomyocytes in injected zone, resulting in a slight enhancement of the cardiac physiology in animal models with heart diseases. However, these improvements reduce with time and are not long-term solutions for cardiac diseases and heart failure [180], [181]. As in other cell therapy areas, investigations increasingly suggest the improvements seen are more due to paracrine signaling and myogenesis, rather than actual cell replacement, although many doubts prevail [180], [182]. Further studies are required to verify the cause of these enhancements by cell injection and investigate the mechanism behind it [183].

Nevertheless, the correct localization and maintenance of therapeutic cells in the native heart is clearly one of the main problems in cell therapy. Tissue engineering that are generally using biomaterials to protect the cells from shear forces during injection and to ensure proper localization and survival of the cells are therefore emerging[42],[94],[184], [185], [186]. Other challenges that biomaterials may help

address are reduction of immune rejection, as well as suppression of other unwanted cell types by reinforcing correct differentiation [179].

1.6 Limitations of current tissue engineering approaches

The approaches for creating a cardiac model *in vitro* have to produce an adult tissue-like structure in terms of the maturity of the cells and the mechanical and biological properties of the whole structure. Hence, the bioengineered tissue constructs should mimic all the critical factors of the native cardiac tissue, e.g. the alignment of the cell in 3D, the mechanical characteristics, the maturation of the cells, and the presence of non-cardiomyocytes and biochemical cues.

As outlined above, the different aspects of cardiac tissue engineering have brought to light many captivating works that have tried to recapitulate a piece of this fascinating organ. *In vitro* cardiac tissue models are numerous and each of them presents a great opportunity for concrete application in the fields of regenerative medicine, drug screening and disease modeling. However, the recapitulation of such models is associated with several challenges, including finding the right cell source, making the right choice in terms of biomaterial and implement a smart design that fits the application of the model. Whereas stem cells represent a very promising technology to tackle the challenges of cardiac tissue engineering in a near future, their use for the moment is limited to fundamental research due to the difficulty of applying all the necessary cues to differentiate them into the required cell type, as well as to insert stem cells-based grafts in the native environment. Concerning the scaffolding technologies reviewed, 3D biomaterials seem to display several advantages compared to their 2D homolog when the application of the cardiac model tends towards graft use. However, 2D cultures constitute a simple way of determining some key features of cardiac cells, such as elongation or orientation, as well as allowing for the observation of the effects of tuned mechanical stimulations. Also, we have highlighted the importance of recapitulating mechanical cues when implementing a cardiac model. Providing all the parameters in a model makes it ideal for different application such as drug screening, implantation, etc. However, combining them is extremely challenging. For instance, the alignment of the cells in a 3D structure is still not easily achievable. Finally, even with such improvements in the microenvironment of the cells, the real mechanisms of action remain unclear and need more investigation. As an example, the exact difference of the cell responses in 2D and 3D constructs is not yet fully understood.

1.7 Thesis goals and structure

In summary, having an accurate model that is a true representation of the in vivo human myocardium is essential for cell therapy, myocardial disease modelling and drug toxicity screening applications.

Hence, in **chapter 2** of this thesis, our aim is to provide a simple, yet highly efficient *in vitro* model for cardiomyocyte differentiation and maintenance. Three main dimensions enter the model design [41][187]: extracellular matrix composition [81], mechanical stiffness [188] and interaction with stromal fibroblasts [38].

The work was then continued by patterning the hydrogel in a way that we could have highly aligned 3D structures of cardiomyocytes in **chapter 3**. These structures resemble the trabeculae carneae which can be thought to constitute the smallest collection of aligned cardiomyocytes in native heart. In chapter 3, we discussed these structure in more details. Providing the trabeculae carneae-like structure is a promising step toward the 3D cardiac models *in vitro*. This model has potential applications in drug screening, simplifies generation of cardiomyocytes and may provide building blocks for cell transplantation.

This work was extended by adding mechanical stimulation to the provided 3D structure in **chapter 4**. Mechanical stimulation improves the protein expression, maturity of the cells and provides more physiologically relevant model *in vitro* for studying the biophysical, biochemical and biomechanical parameters on cardiac cells, cell maturation, drug screening, and related studies in tissue engineering.

Chapter 5 summarizes all the achieved results and discusses the future of such heart models. In this chapter we will introduce some application of the cardiac model and the criteria that can be added to the present model to improve its functionality.

These results together recommend that three-dimensional tissue engineered models with defined cell niche hold great promise for drug screening and cardiotoxicity testing[17].

Chapter 2 Thrombin-coagulated fibrin enriched with decellularized porcine heart extracellular matrix hydrogel preparation and characterization

This chapter presents the hydrogel composed of porcine heart decellularized extracellular matrix and fibrin for the formation of an *in vitro* 3D cardiac cell culture model. This hydrogel is the scaffold of the 3D structure that provides mechanical and biological support for culturing cells. This hydrogel has been used for the 3D experiments in the subsequent chapters. The content of this chapter has been submitted as an original paper to biomaterials science journal and is at present available as preprint [80]. It is reproduced here with minor changes: additional conceptual and illustrative figures, some additional data, and additional discussion with respect to the thesis introduction and overall concept. Also, contents of the supplementary to the original publication (submitted, not available with the preprint) have been incorporated into the text here.

2.1 Introduction

Our aim here is to provide a simple, yet highly efficient *in vitro* model for cardiomyocyte differentiation and maintenance. We designed this model to simultaneously recapitulate three main dimensions of the native cardiomyocyte environment [41][187]: extracellular matrix cues [81], mechanical stiffness

[188] and interaction with stromal fibroblasts [38]. This model has potential applications in drug screening, simplifies generation of cardiomyocytes and may provide building blocks for cell transplantation in regenerative medicine.

Our first cardiomyocyte environment element is the choice of a specific cardiac extracellular matrix. We opt here for the use of porcine decellularized extracellular matrix (dECM) of cardiac origin to provide organ-specific cues [189], with reinforcement by thrombin-coagulated fibrin [190] for improvement of mechanical properties [191]. Myocardial dECM has indeed been shown to powerfully support cardiomyocyte differentiation and maturation in many cell lineages, including human embryonic stem cells and rat neonatal ventricular cardiomyocytes [81]. Moreover, porcine cardiac dECM hydrogels are ultrastucturally similar to their human analogs [192] and known to provide functional benefits after myocardial infarction in animal models [193]. Preservation of part of the organ-specific cues [194][77], [195], including a fraction of the growth factors contained in the dECM [81][78], is thought to be responsible for correct organ-specific cellular differentiation (Figure 2-1).

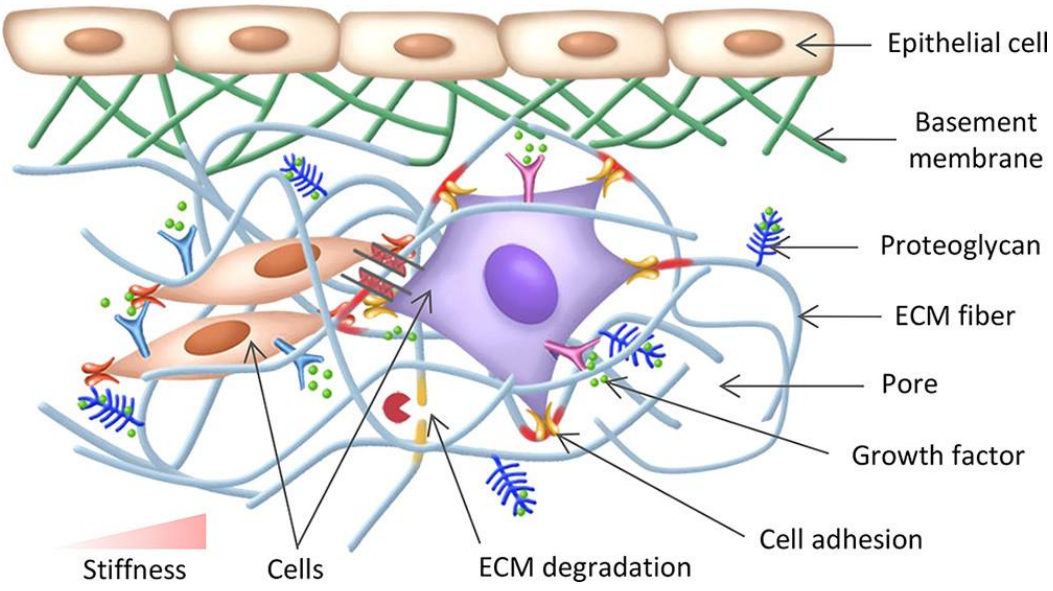

Figure 2-1 Schematic representation of cell-ECM interactions. ECM provides different biochemical and mechanical cues such as proteoglycans, growth factors, mechanical stiffness and structural features which helps the cell survival, proliferation, differentiation, and functional behaviors regulation [59]. Reprinted with permission from [59]. Copyright (2017) American Chemical Society.

Besides dECM, a variety of synthetic and natural matrices have been used for cardiomyocyte culture [196][197][198][199][200]. Collagen I, and mixtures of collagen I with Matrigel have in particular been

reported to be supportive of spontaneous synchronized *in vitro* contractions, albeit requiring mixed cardiac cultures with both contractile and non-contractile cells, either primary or derived from induced pluripotent stem cells [197][201][200]. *In vivo*, collagen foams and Matrigel were further shown to enhance engraftment efficiency of the cardiac model cell line H9c2 [202]. With regard to the extracellular matrix element, an important aim of this study is therefore to quantify possible advantages of the proposed dECM-fibrin composite over readily available commercial controls such as collagen I or Matrigel.

The second element of our *in vitro* cardiomyocyte niche model is the achievement of appropriate mechanical stiffness. Pure cardiac dECM hydrogels have long gelation times [78] and mechanical properties far below native cardiac tissue [203][81]. This is a practical problem, since sedimentation during the extended gelling time will make cell seeding difficult [204]. More importantly, however, it is known that the differentiated phenotype of heart cells is the most prominent on substrates with stiffness comparable to that of the native heart [188].

Various approaches to reinforce cardiac dECM are available, and include for instance covalent crosslinking [205] or combination with additional hydrogels [206]. Williams, *et al*. combined the two approaches by blending fibrin with dECM from neonatal and adult rat hearts, followed by crosslinking with transglutaminase [79]. However, the lack of specificity of transglutaminases rises concerns about cellular toxicity *in vitro* [79] and possible side effects such as autoimmune reaction due to altered self-epitopes *in vivo* [207]. To avoid such side reactions, we here use fibrin obtained by coagulation of fibrinogen with human thrombin [190] to raise the level of stiffness in dECM-fibrin blends in a more specific and safer way. The use of fibrin as opposed to synthetic polymers [206] is motivated by the reported increased efficiency of cardiac reprogramming in the presence of this biopolymer [88].

Finally, the third element of the cardiomyocyte niche to be addressed in this study is the stromal support by fibroblasts. Although the cardiomyocytes in native heart tissue form around 75% of the cardiac tissue volume, they are 30-40% of the total cell number [38], the remainder being mainly endothelial cells and fibroblasts [208]. Fibroblasts are surrounding the cardiomyocytes and connect different layers of the myocardial tissue, which provides mechanical anisotropy due to the cell alignment in this complex structure [209]. The fibroblast cells in native heart tissue have a major and complex roles in cardiac development, myocardial structure, cell signaling, and electromechanical function [38][210]. *In vitro*, co-culture with fibroblasts has been shown to enhance skeletal muscle regeneration from myogenic progenitor cells as well as electrophysiological maturation of iPSC-derived cardiomyocytes [211]. Moreover, this anisotropic structure leads to higher electrical conduction in the direction of fiber orientation. Therefore, developing a model to mimic the spatial organization of the cardiomyocytes is imperative for functional cardiac tissue engineering. We hypothesize here that co-culture with fibroblasts in the context of a mechanically and biologically relevant matrix could be used to enhance differentiation of cardiomyocytes from myoblast progenitor cells.

We use the H9c2 cell line as a model system for cell differentiation [212]. Originally derived from rat embryonic ventricular heart tissue, this immortalized line spontaneously differentiates towards skeletal muscle upon reaching confluence [212]. Yet, upon exposure to retinoic acid, cardiac differentiation can be recovered [213]. The cardiac differentiation efficiency of H9c2 cells can be further enhanced by the presence of fibroblast-derived matrix in addition to the retinoic acid [214]. Our aim is to optimize cardiogenic differentiation of H9c2 by combining fibroblast support with appropriate mechanical and matrix cues in composites of coagulated fibrin and porcine cardiac dECM hydrogels. We aim at replacing the exogenous retinoic acid by endogenous cues to simplify the differentiation protocol. This allows to avoid the presence of the strong, widespread effects of retinoids on gene expression in screening and gene expression profiling experiments [215].

Regarding the development of a cardiac *in vitro* niche with relevant cellular, mechanical and matrix components, a major aim is also to better support physiological electromechanical activity and synchronization of primary neonatal cardiomyocytes. Hence, we also investigate synchrony, beating rate and recovery time of neonatal cardiomyocytes in various hydrogel compositions including fibrin, collagen I and Matrigel, but also the composites fibrin-collagen I and dECM-fibrin. This allows us to further refine our comprehension of niche effects, with relevance to culture of primary neonatal cardiomyocytes and the optimal definition of tissue engineering and transplantation matrices. Figure 2-2 shows a schematic of the work in this chapter, including extracellular matrix decellularization, hydrogel preparation based on dECM and characterization, and cardiac cell functionality in this novel hydrogel.

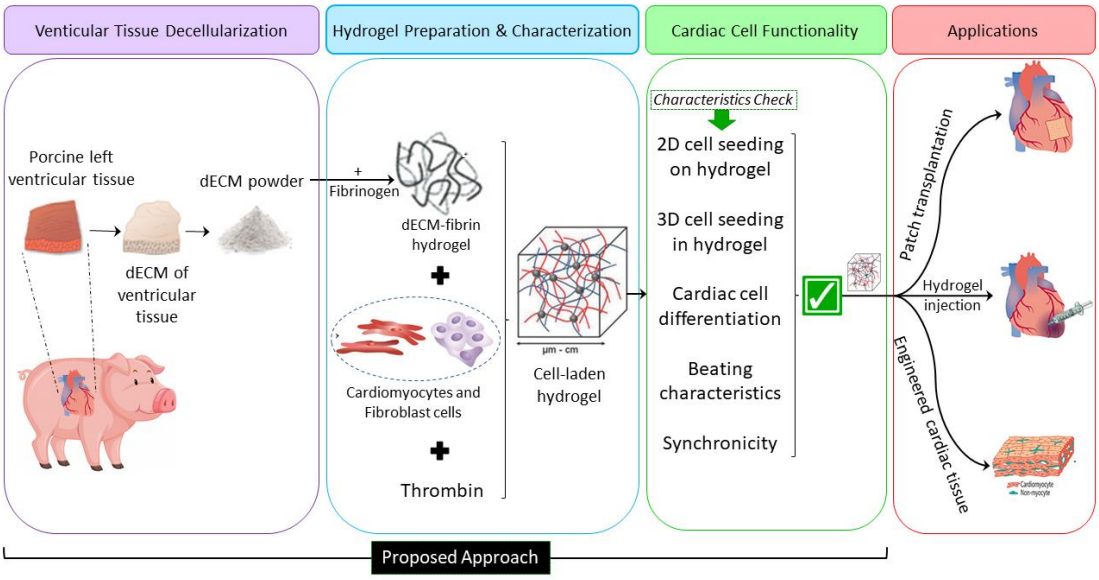

Figure 2-2 Schematic of the proposed approach in this chapter. Phase 1: dECM-fibrin hydrogel preparation, Phase 2: characterization of the hydrogel. Phase 3: investigating the functionality of cardiac cells in the hydrogel. Phase 4: the application of this model.

2.2 Methods

2.2.1 Extracellular matrix decellularization

Decellularized porcine cardiac extracellular matrix forms the basis of the dECM-fibrin hydrogel studied in this chapter. The procedure for decellularization of the cardiac tissue was based on published literature[189]. Briefly, porcine heart tissue was obtained from a local slaughterhouse and the ventricles cut into pieces of about 1 mm in thickness. The pieces were rinsed with deionized water and then stirred in 1% Sodium Dodecyl Sulfate (SDS) in a phosphate buffered saline (PBS) solution for 48-72 h at 4°C, followed by 1% Triton X-100 for an additional 30min. Finally, the preparation was stirred in deionized water overnight and freeze-dried. The dECM powder thus obtained was suspended in 0.1M HCl, followed by pepsin (Sigma P6887) digestion for 72 hours (100mg of dECM and 10mg of pepsin per 1mL of HCl) [189]. The pH was then adjusted to 7.4 by gradual addition of NaOH, yielding a solution of 100 mg/mL dECM. dECM stock solution was finally obtained by adding Dulbecco's Modified Eagle Medium DMEM (Thermofisher, cat# 41965) to reach a final dECM concentration of 50mg/mL. The steps of this procedure are shown in figure 2-3.

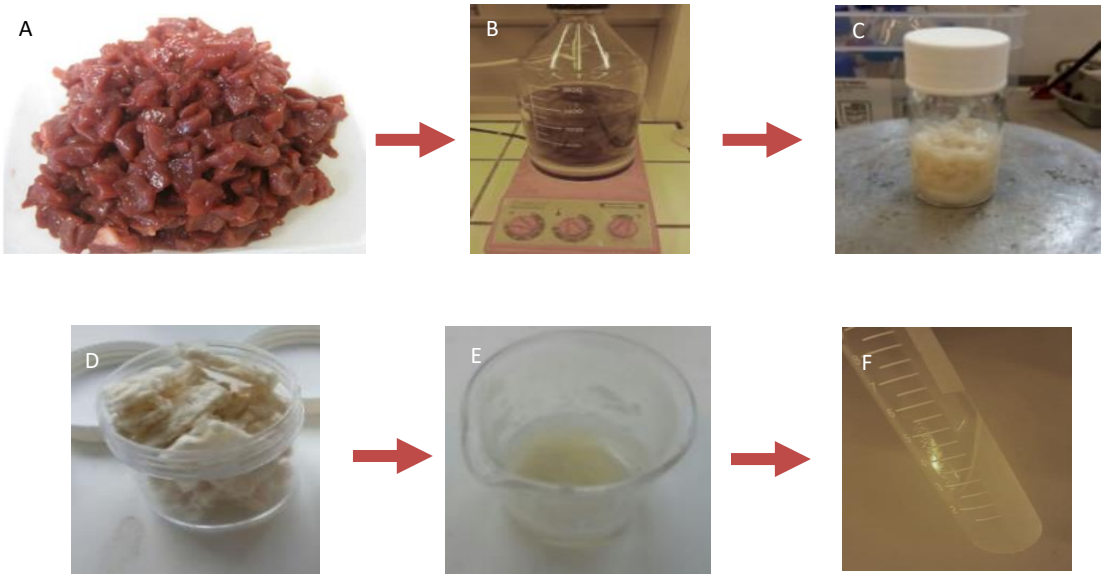

Figure 2-3 ECM decellularization protocol: A. Cutting the ventricles to small pieces, B. Rinsing with deionized water followed by stirring in 1% Sodium Dodecyl Sulfate (SDS) in a phosphate buffered saline (PBS) solution for 48-72 h at 4°C. C. Stirring with 1% Triton X-100 for 30min. D. Freeze drying the decellularized pieces to provide the dECM powder. E. Suspending dECM powder in 0.1M HCl, followed by pepsin digestion for 72 hours. F. pH adjustment to 7.4 by gradual addition of NaOH.

2.2.2 Extracellular matrix characterization

To verify the extent of decellularization, the residual DNA content in both native and decellularized tissue was measured. For this, dECM (respectively intact cardiac tissue) was dissolved in lysis buffer (0.5 M EDTA pH 8.0, 0.5% sodium dodecyl sulfate) and 100µg/mL proteinase K (Sigma, P4850) overnight at 55℃ [216]. The resulting suspension was vortexed, and proteins precipitated with phenol-chloroform, followed by centrifugation at 13700rpm for 40min. DNA was then isolated by recovery of the top (aqueous) phase, followed by addition of 0.5 mL ethanol, resuspension in deionized water, and quantification by Carry 50 spectrophotometer using a quartz cuvette at 260nm. For further quantification of dECM composition, collagen and Glycosaminoglycan (GAG) content in the dECM were measured using the Sircol™ Soluble Collagen Assay kit and Blyscan Sulfated Glycosaminoglycan Assay kit. The protein concentration of the dECM was also measured using Pierce™ BCA Protein Assay Kit to have better understanding of the collagen content of the dECM. For that, we considered collagen as the control sample. Finally, histological sections of dECM were obtained by standard paraffin embedding. The sections were stained with hematoxylin-eosin (H&E), Sirius red, and Miller staining and scanned using an Olympus VS120-L100 microscope slide scanner to verify the presence of collagen and elastin.

2.2.3 Hydrogel preparation

To produce the compound dECM-fibrin hydrogel, we first prepare a pre-gel solution. For this, we mix 100 µl of 50mg/mL dECM stock solution (as described above), 528 µl of 50mg/mL fibrinogen (Sigma, F3879) solution, 100 µl of HEPES 1M pH 7.4 and 269 µl of DMEM. To induce gelling of the pre-gel solution, we then add 1.7 µl of Thrombin (Sigma, T1063, 250U/mL) and 1.3 µl of calcium chloride 1M, and start incubation at 37 ℃. This yields a final composite gel with 5mg/mL dECM and 26.4 mg/mL fibrinogen.

Matrigel (Sigma, E1270, solution supplied at 9mg/mL) was diluted to 3mg/mL before gelation by using DMEM. Collagen I (Sigma, C4243, solution supplied at 3mg/mL) was diluted to 1mg/mL with DMEM prior to gelation. This also neutralized the pH. Finally, the fibrin-collagen I composite was prepared by mixing 157 µl of 3mg/mL collagen stock solution, 314 µl of DMEM, followed by 528 µl of 50mg/mL fibrinogen. Gelling was then induced by adding 1.3 µl of calcium chloride and 1.7 microliters of thrombin (250U/mL).

To include cells, the necessary amount of cells to achieve a final total cell concentration of 10^6 cells/ mL was pelleted, followed by complete removal of the supernatant. The pellet was resuspended in pre-gel, followed by induction of gelation by addition of calcium chloride and thrombin solutions (fibrin-based hydrogels), and placement at 37℃ in 5% CO_2 atmosphere.

2.2.4 Mechanical properties

To measure the mechanical properties, fibrin and dECM-fibrin hydrogels were prepared and pipetted into cryovials where they remained for 30 min at 37°C to gel. The samples were then removed from the cryovials and subjected to compression testing using a dynamic mechanical analyzer (TA Instruments DMA Q800). The storage and loss moduli are defined as follows [217]:

Storage: $E' = \frac{\sigma_0}{\varepsilon_0} \cos\delta$, Loss: $E'' = \frac{\sigma_0}{\varepsilon_0} \sin\delta$

Where σ_0 is stress, ε_0 is strain, and δ is the phase angle or phase lag between the stress and strain.

The Young's modulus is: $E = \sqrt{E'^2 + E''^2}$

2.2.5 Microstructure characterization

The microstructure was analyzed by scanning electron microscopy (SEM). For this, the hydrogel sample was frozen and lyophilized. The lyophilized sample was coated with a few nanometers (5-10nm) of gold prior to performing SEM imaging.

2.2.6 dECM stability study with fluorescently labeled dECM

To investigate the stability of the dECM in our composite hydrogel, we fluorescently labeled the dECM using rhodamine isothiocyanate [218]. For this, we suspended 300mg dECM powder in 10mL of 0.1M HCl. The pH was adjusted to 10.3 with 0.9mL NaOH 1M and 0.3mL of Na_2CO_3 1M. 6mg of rhodamine isothiocyanate was dissolved in 10mL of isopropanol, and this solution was added to the reaction mix, followed by 10mL of distilled water. After overnight incubation, the dECM was precipated and repeatedly washed with excess isopropanol, until a clear washing solution above strongly stained precipitate was obtained. The precipitate was air-dried overnight. dECM-fibrin hydrogels were prepared with fluorescently labeled dECM, using identical procedures as for unlabeled dECM. Fluorescent imaging was conducted after 1, 7, and 14 days of incubation in PBS at 37°C.

2.2.7 H9c2 cell culture

H9c2 cells were obtained from the European Collection of Authenticated Cell Cultures (ECACC) (Lot# 17A028). The cells were cultured in DMEM medium supplemented with 10% fetal bovine serum and 1% penicillin and streptomycin in 75 cm^2 tissue culture flasks at 37°C and 5% CO_2 in an incubator. In

accordance with supplier instructions, the H9c2 cells were passaged before reaching 70-80% confluency to avoid loss of differentiation potential [213].

2.2.8 Nor-10 cell culture

NOR-10 (ECACC 90112701) cells from skeletal muscle were obtained from the European Collection of Authenticated Cell Cultures. The cells were cultured in DMEM medium supplemented with 10% fetal bovine serum and 1% penicillin and streptomycin in 75 cm^2 tissue culture flasks at 37°C and 5% CO_2 in an incubator. They were split before reaching 70-80% confluency according to supplier's notice [219].

2.2.9 H9c2 differentiation

As a starting point in our investigation into use of various hydrogels to enhance cardiogenic differentiation of H9c2 cells, we used a known differentiation procedure of H9c2 cells to cardiomyocytes [220]. This procedure implies simultaneous decrease of the serum percentage to 1% and application of retinoic acid for 5 days, before one to two last days of culture in expansion medium (DMEM with 10% FBS without addition of retinoic acid) [220]. Using this protocol, we studied co-culture with Nor-10 fibroblasts (100/0, 70/30, 50/50, 30/70, 0/100 H9c2: Nor-10 ratios with the total cell density of 10^6cells/mL) in different concentrations of retinoic acid (0-2000nM) for enhancement of the cardiogenic differentiation efficiency. With a fixed 30% H9c2, 70% Nor-10 ratio and in the absence of retinoic acid, we then screened various hydrogels such as collagen I, Matrigel, and the thrombin-coagulated dECM-fibrin hydrogel for their capacity to substitute for retinoic acid in H9c2 cardiogenic differentiation.

2.2.10 Cell seeding onto hydrogel surfaces (2D)

To study the biochemical influence of different hydrogels on cardiomyocyte differentiation in a 2D geometry, we prepared ca. 0.5mm high hydrogel blocks in 48-well plate. For this, we gelled 50µl of dECM-fibrin, collagen or Matrigel in wells of interest. We then applied H9c2 cells mixed with Nor-10 fibroblasts at a ratio of 30% to 70% with density of 2.5×10^5 cells per cm^2 on top of the hydrogels. The differentiation protocol was conducted without addition of retinoic acid: 5 days with 1% FBS in DMEM, followed by 1 day of 10% FBS in DMEM [220].

2.2.11 Cell seeding in 3D hydrogel

To assess whether differentiation could be improved in 3D vs. 2D, we mixed dECM-fibrin pre-gel with Nor-10 and H9c2 cells (70/30 ratio, 10^6 cells/mL). Then thrombin and calcium chloride were added to the solution, and 200µl of the solution was rapidly poured in a 48-well plate where the hydrogel solidified in the incubator. Collagen and Matrigel were used as controls. The differentiation protocol was otherwise identical to the differentiation experiments on the 2D hydrogels, with serum reduction only in the absence of exogenous retinoic acid.

2.2.12 Immunostaining and 3D imaging

For immunostaining, cell culture samples were fixed in 4% of paraformaldehyde (PFA) for 20min at room temperature (RT). Then, 0.1% Triton X-100 was added to permeabilize the cells for 30min at RT. By incubating cells with phalloidin-Atto 488 (Sigma 49409) (1:50) for 45min at 4ºC, actin filaments were made visible in all types of cells [221].

We assessed the differentiation by measuring the fraction of H9c2 cells positive for troponin T by immunofluorescence using the T6277 antibody from Sigma. As this antibody detects both cardiac and skeletal muscle troponin T, we also confirmed cardiac differentiation on dECM-fibrin samples using an antibody specific to cardiac troponin T (Abcam, ab8295).

For immunofluorescence, the cells were first blocked with 1% BSA for 1 hour at 37ºC. Troponin T primary antibody (Sigma, T6277, 1:50) was then added, followed by incubation overnight at 4ºC. Alexa-568 secondary antibody (Sigma, A10037, 1:1000) was added after washing with DPBS (Gibco 2062235) and incubated for 45min at 37ºC, prior to washing with DPBS and staining with 4',6-diamidino-2-phenylindole (DAPI, 1:2000 from 5mg/ml stock solution) for 5min. DAPI was replaced with DPBS before imaging the cells under a fluorescence microscope. We quantify the differentiation percentage as the surface area covered by cells expressing troponin T, relative to the total area of the fluorescent images, and normalize to the percentage of H9c2 cells seeded in co-culture.

2.2.13 Neonatal cardiomyocytes isolation

To study the effect of the thrombin-coagulated dECM-fibrin hydrogel on primary cardiomyocytes, we isolated primary rat neonatal cardiomyocytes. Cardiac cells have been isolated from the neonatal Wistar rat hearts. Hearts are removed and ventricles are finely minced into cubes with 1mm ×1mm dimensions. The minced tissue was washed in an ethylene glycol tetra acetic acid-based heart mincing solution containing 100 mM NaCl, 2 mM EGTA, 5 mM $MgCl_2$, 1 mM dithiothreitol, and 7 mM phosphate

buffer (pH 7) and resuspended in a dissociation solution containing 30 mg collagenase in 50 ml PBS plus 12.5 µl 100 mM CaCl2. This solution was placed in a glass vial with a magnetic stirrer and stirred at 70 rpm at 35°C for 10 min. the supernatant was discarded and fresh dissociation solution was added to dissociate the tissue. This dissociation cycle was repeated for 3 to 5 times. After the tissue is completely disaggregated, the solution is centrifuged for 5 min at 1000 rpm, the supernatant discarded and the cells are resuspended in culture medium. The cells were filtered using 70 µm cell strainer, pre-plated for 2h, recollected and filtered again to obtain a pure population of neonatal cardiomyocytes.

2.2.14 Calcium imaging

For calcium imaging, we seeded the primary rat cardiomyocytes (2.5×10^5cells/cm^2) onto hydrogel slabs prepared in 48-well plates (50 µl of hydrogel per well, as before). Tissue culture controls were prepared by leaving out the hydrogel polymerization step. After 3 days of culture in DMEM with 10% FBS, the cultures were loaded with 2 µM Fluo-4 AM (F14217) for 30 min at 37°C. Calcium transients were then recorded using fluorescent microscopy at room temperature. Temporal peak detection was based on a custom ImageJ plugin, implementing the publicly available findpeaks function of Octave [222] in Java. The plugin is available for download at https://github.com/tbgitoo/calciumImaging, along with source code and a user manual. We used this plugin to evaluate local beating frequency and temporal phase shift from the calcium imaging videos.

2.2.15 Beating characteristics

To assess the contractile properties of primary cardiomyocytes in 3D cultures, we suspended the primary rat cardiomyocytes at a cell density of 10^6 cells/mL in pre-gel mixtures of dECM-fibrin, fibrin, and fibrin-collagen I composite. After gelling of 200 µL of cell-hydrogel mixture per well in a 48-well plate, the cultures were followed both visually and videographically. Synchrony and onset of beating was judged visually on a per-well basis. To quantify the mechanical beating rate of the cells, movies were acquired by connecting a video camera to the microscope, while maintaining the samples at 37℃ in a temperature-controlled chamber. For quantification of the beating frequency, we used the Pulse software (Cellogy Inc.) [223].

2.2.16 Statistical analysis

Data were compared using unpaired t-test (two-tailed, equal variances) in the GraphPad software. Error bars represent the mean ± standard deviation (SD) of the measurements ($*$ $p < 0.05$, $**$ $p < 0.01$, and $***$ $p < 0.001$).

2.3 Results

2.3.1 Decellularization characteristics

We successfully decellularized porcine cardiac extracellular matrix. As shown in Figure 2-4A, the total amount of remaining DNA is less than 50ng/mg of tissue, indicating essentially complete removal of cells [224]. The concentration of the extracellular matrix components collagen and glycosaminoglycans (GAG) was measured in the native tissue and after decellularization, and shows no loss of these components in the resulting dECM (Fig. 2-4B, 2-4C). H&E, Sirius red for collagen and Miller for elastin staining confirmed the absence of cells and cell debris and the presence of collagen and elastin in the matrix after decellularization (Fig. 2-4D). The result of BCA test for dECM and collagen suggests that the protein content of the 3mg/ml dECM is almost the same as protein content of 1.5mg/ml collagen. Hence, it shows that around 50% of the dECM components are protein (mainly collagen).

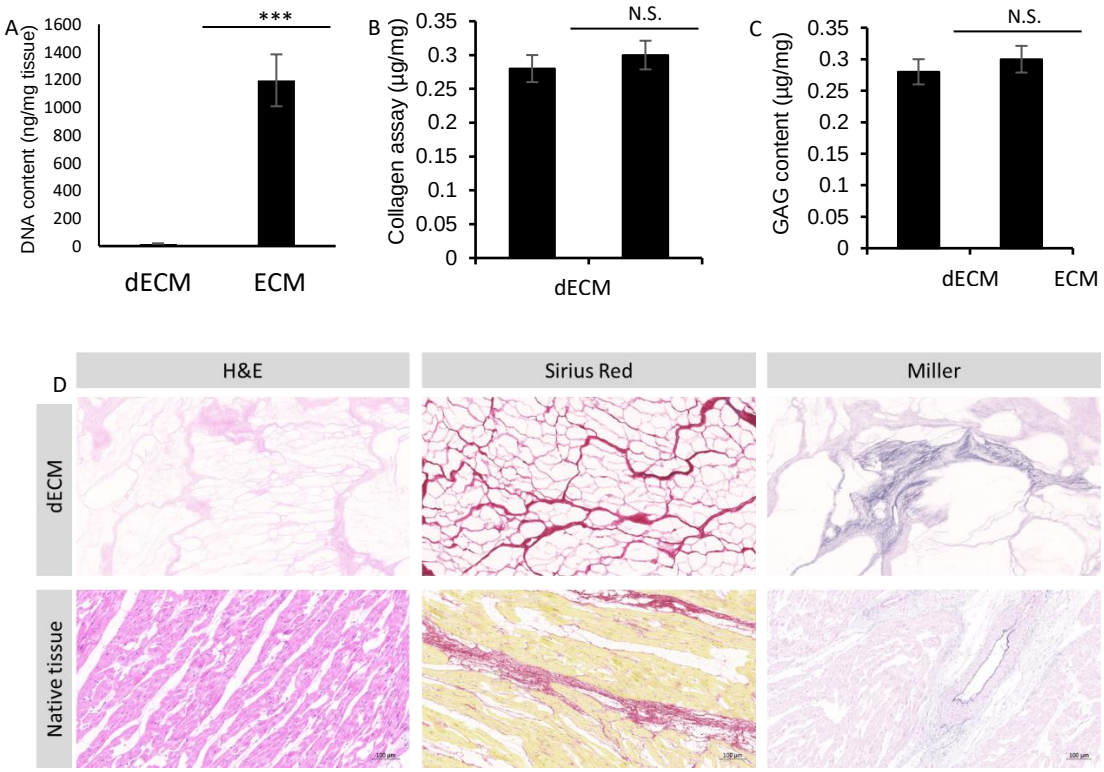

Figure 2-4 dECM and ECM characterization. A, B, C. DNA, Collagen, and GAG content of the dECM after lyophilization and dissolving in lysis buffer D. H&E, Sirius red and Miller staining used for staining the nuclei, Collagen and Elastin respectively, which proves the presence of collagen and elastin and removal of the DNA. *** = significant difference for $p < 0.001$ (N = 3-4 per condition). Scale bar: 100µm.

2.3.2 Mechanical properties

Figure 2-5A shows the relation of between the elastic modulus and fibrinogen concentration in pure fibrin gels. In agreement with literature [191], higher fibrinogen concentrations are associated with higher Young moduli, although at the highest concentrations, a saturation effect can be seen. The evaluation of the storage and loss moduli in dECM-fibrin gels in a linear temperature scan is presented in Figure 2-5B.

At 37°C, the Young's modulus of the dECM-fibrin hydrogel stabilizes at about 21 kPa, falling into the reported range of native adult myocardium from 11.9 to 46.2 kPa [188]. This confirms that mechanical properties adequate for heart cell culture can be achieved with the thrombin coagulation method chosen, eliminating the need for less specific crosslinking agents [188], [225].

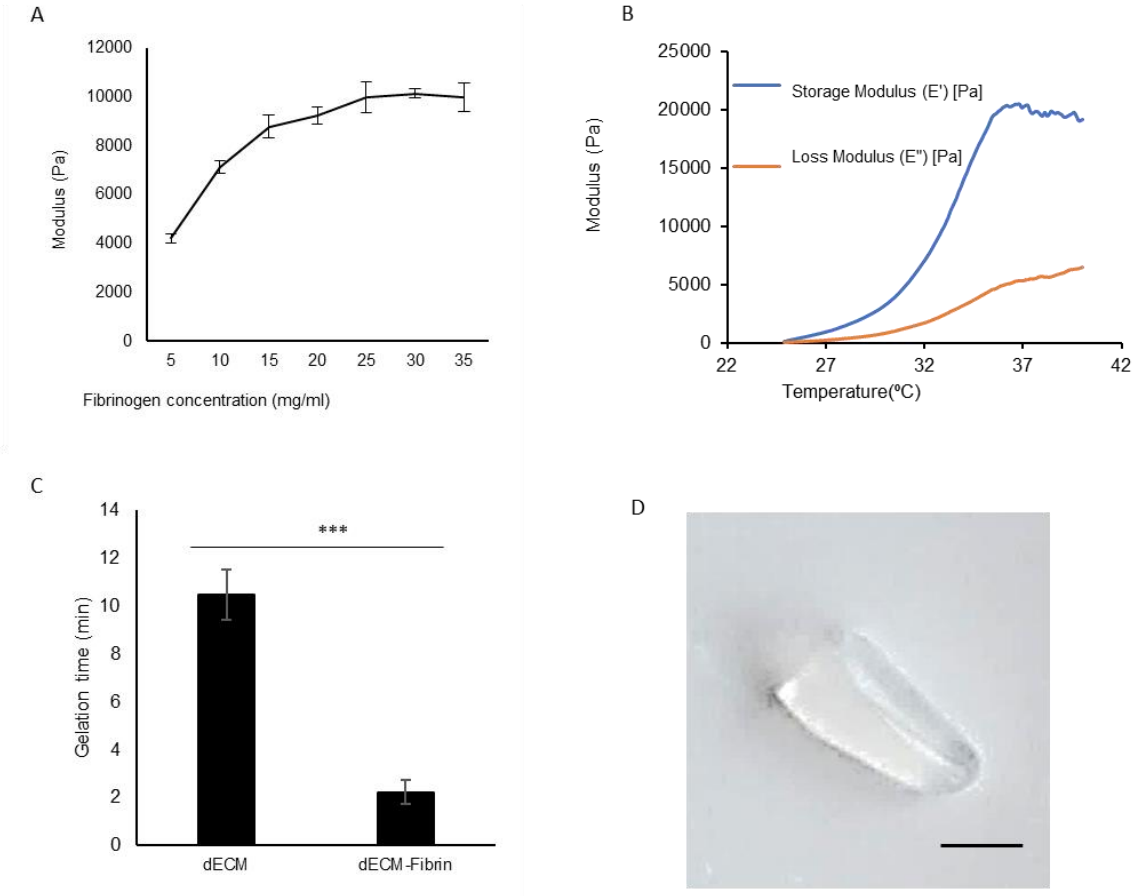

Figure 2-5 Mechanical characterization. A. Stiffness of fibrin gels at different concentrations at room temperature. This allows to determine the optimum concentration of fibrinogen in the hydrogel. B. Storage and loss moduli of the dECM-fibrin hydrogel in a temperature scan (from 25 to 40). The Young's modulus of the hydrogel can be calculated from these measurements. It is comparable to the one of the native heart. C. Gelation time of the dECM and dECM-Fibrin hydrogels at 37°C. In the case of the dECM-Fibrin hydrogel, 2 minutes are sufficient for handling

the gel *** = significant difference, $p < 0.001$ (N = 3-4 per condition). D. Macroscopic appearance of the gelated hydrogels (Scale bar: 5mm).

2.3.3 Gelation time

Fig. 2-5C shows that the gelation time of dECM alone, in the absence of cells, is about 10 minutes. By adding fibrinogen and thrombin to the hydrogel, the gelation time is reduced to about 1-2 minutes, which is sufficient for handling the cells in 3D while avoiding cell sedimentation. Figure 2-5D shows the macroscopic structure of the dECM-fibrin hydrogel after gelation.

2.3.4 Structural characterization and dECM stability

Fig. 2-6A shows a scanning electron micrography image of the dECM-Fibrin hydrogel, whereas Fig. 2-6B shows specifically the spatial distribution of rhodamine-labelled dECM within the dECM-fibrin composite. The heterogeneous structure of the hydrogel can be observed in both imaging modes. This implies that coherent pieces of dECM subsist and are embedded into fibrin, rather than forming a spatially homogeneous mixture, with heterogeneity probably defining local niche structures. Fig. 2-6C and 2-6D indicate stable maintenance of dECM within the dECM-fibrin composite at 7 and 14 days, with no loss of dECM detected. The confocal stack of control dECM-fibrin hydrogel without rhodamine labeling shown in Fig. 2-6E validates the specific detection of rhodamine-labelled dECM as it shows virtual absence of autofluorescence at the exposure settings used for Fig. 2-6B-2-6D.

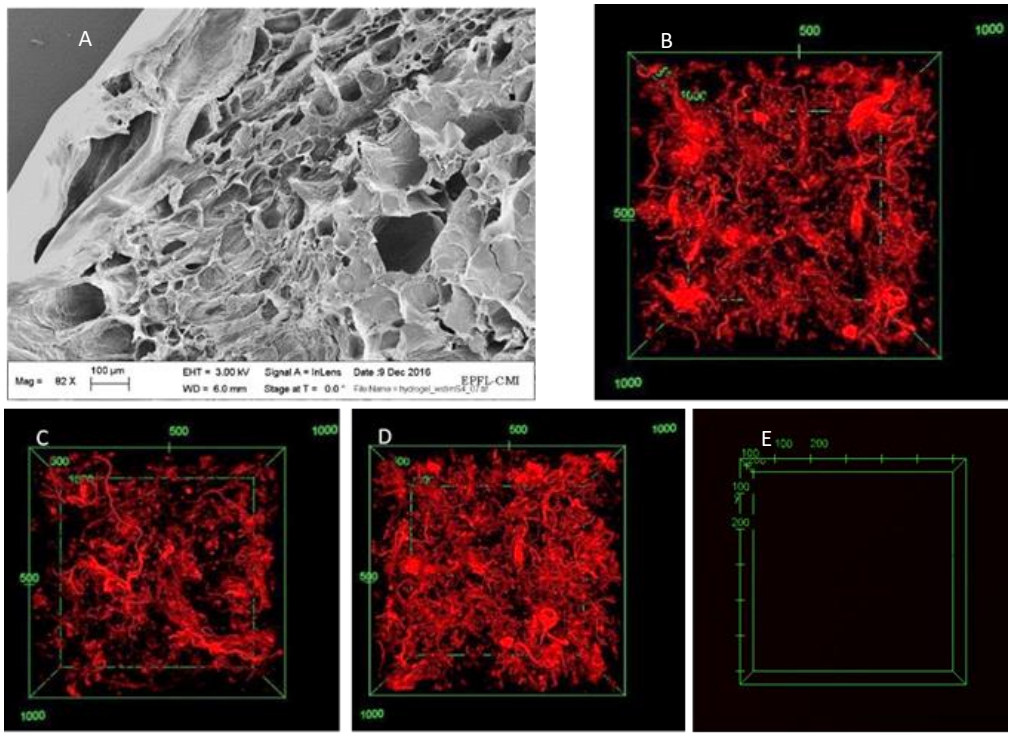

Figure 2-6 Microstructural analysis of dECM-fibrin gels. A. Scanning electron microscopy image of the dECM-fibrin hydrogel. B-D. dECM was labeled with rhodamine isothiocyanate and gelled together with fibrin. Confocal images were taken after B) 1 day, C) 7 days, and D) 14 days, E) the dECM-fibrin hydrogel without rhodamine-labelling. The distribution of dECM is locally heterogeneous. No significant loss of dECM occurs during this time. Scale bar: 100µm

2.3.5 H9c2 in co-culture with fibroblast cells

To investigate the role of extracellular matrix components, and particularly dECM-fibrin as compared to control matrices such as collagen and Matrigel, we used cardiogenic differentiation of the H9c2 myoblast line as a model system[226]. The differentiation of H9c2 cells to cardiomyocytes is traditionally initiated by reducing the serum in the culture medium to 1% in the presence of all-trans-retinoic acid[220].

In preliminary trials to adapt this procedure for use with our hydrogel systems, we found that retinoic acid induces fibrinolysis. This led to dissolution of fibrin-based gels. Retinoic acid is a known transcriptional activator for the expression of fibrinolytic enzymes[227][228]. In addition, we find the dissolution effect to partly persist even in cell-free systems, indicating a chemical effect as well. Hence, our first step is to optimize cardiac differentiation in H9c2 cells in the absence of retinoids.

Fibroblast-derived matrix has been shown to enhance retinoid-based differentiation of H9c2 cells[214]. Here, we assess whether a similar favorable effect on the H9c2 cardiogenic differentiation can be obtained by direct co-culture with Nor-10 fibroblasts[229].

We first optimize the co-culture ratio of H9c2 cells to Nor-10 fibroblasts. The aim is to increase cardiogenic differentiation of H9c2 cells in the presence of a minimal amount of retinoic acid. For the sake of simplicity, we investigate this in 2D co-culture, without hydrogel, but systematically vary both the H9c2: Nor-10 seeding ratio and retinoic acid concentrations. Confirmation of specific cardiac markers is further given in figure 2-7. These preliminary experiments were carried out on regular tissue culture plates to better quantify the effect of co-culture on H9c2 differentiation, and also to evaluate whether Three important conclusions can be drawn: First, in pure Nor-10 fibroblast cultures ("0-100" in Figure 2-7), no troponin T could be detected, regardless of the retinoic acid concentration. This indicates that cardiogenic differentiation is specific to the H9c2 cells. Second, in the absence of retinoic acid, cardiogenic differentiation remains always low on tissue culture plates, regardless of the co-culture conditions. Finally, co-culture with Nor-10 fibroblasts lowers the concentration of retinoic acid necessary to achieve efficient differentiation.

Overall, we see that on tissue culture plates, Nor-10 fibroblasts can partially substitute for addition of retinoic acid to induce cardiogenic differentiation in H9c2 cells. A minimal amount of retinoic acid (below 15nM) remains however necessary. This contrasts with the co-cultures on and in 3D hydrogels, where efficient cardiogenic differentiation was obtained in the complete absence of exogeneous retinoic acid. This indicates that the combination of co-culture with Nor-10 fibroblasts and culture in the presence of various hydrogels completely substitutes for addition of retinoid acid.

Table 2-1 shows the percentage of cardiogenically differentiated H9c2 cells, evaluated as the relative surface area covered by cells expressing troponin T corrected for the proportion of H9c2 seeded. The heatmap (Table 2-1A), outlines the differentiation percentage of the H9c2 cells thus calculated for different values of the ratio of fibroblast cells to H9c2 cells and different concentrations of retinoic acid after 7 days in culture. The results demonstrate that the lower the fraction of H9c2 seeded, the higher the relative differentiation efficiency, indicating that neighboring Nor10 cells help drive the cardiac differentiation of H9c2 cells. As a compromise between high relative differentiation efficiency and achievable absolute numbers of differentiated cells, we choose the seeding ratio of 30% H9c2 cells to 70% fibroblast cells as the preferred condition for subsequent experiments. Of note, even this optimized co-culture could not completely substitute for the addition of retinoic acid, as below 62.5nM the differentiation efficiency started dropping, to reach only about 7% in the absence of the retinoid (Table 2-1B). Overall, we retain that performing co-culture with fibroblasts improves the differentiation efficiency and dramatically reduces the required concentration of retinoic acid for differentiation.

A

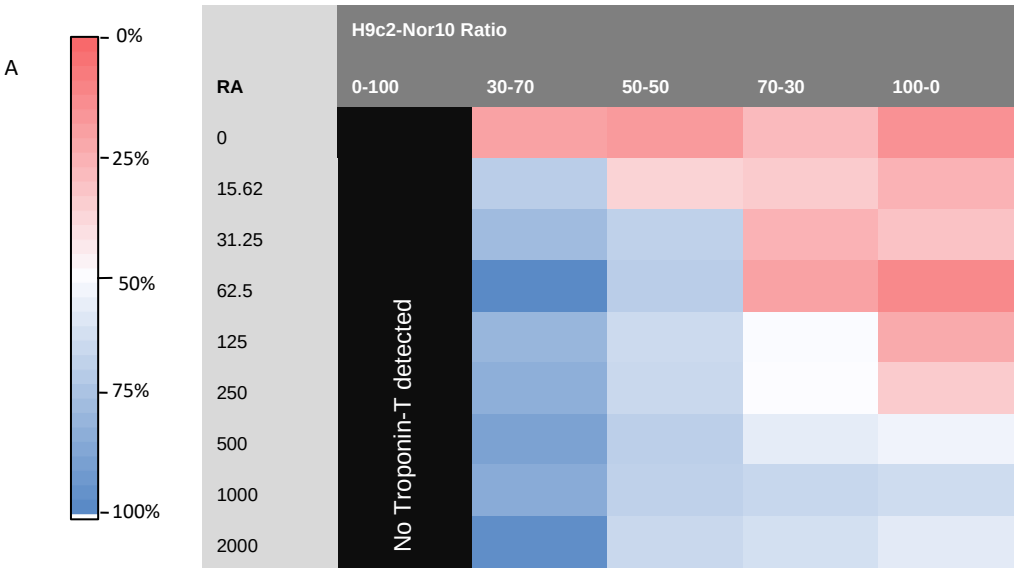

B

Retinoic acid Concentration(nM)	*H9c2/ Fibroblast cells*	
	30/70	**100/0**
0	7±0.87	5±0.69
62.5	81±11.89	4±1.03
2000	79±10.43	28±5.71

Table 2-1 Differentiation of H9c2 cells in mono- and co-culture on tissue culture plates. A) The heat map of normalized differentiation percentage of H9c2 cells for different concentrations of retinoic acid and for different ratios of H9c2 to fibroblast cells. Cultures in 2D, without hydrogel, for 7 days (differentiation duration). B) Selected numerical values for the differentiation percentages for the 30/70 ratio and 100/0 ratio.

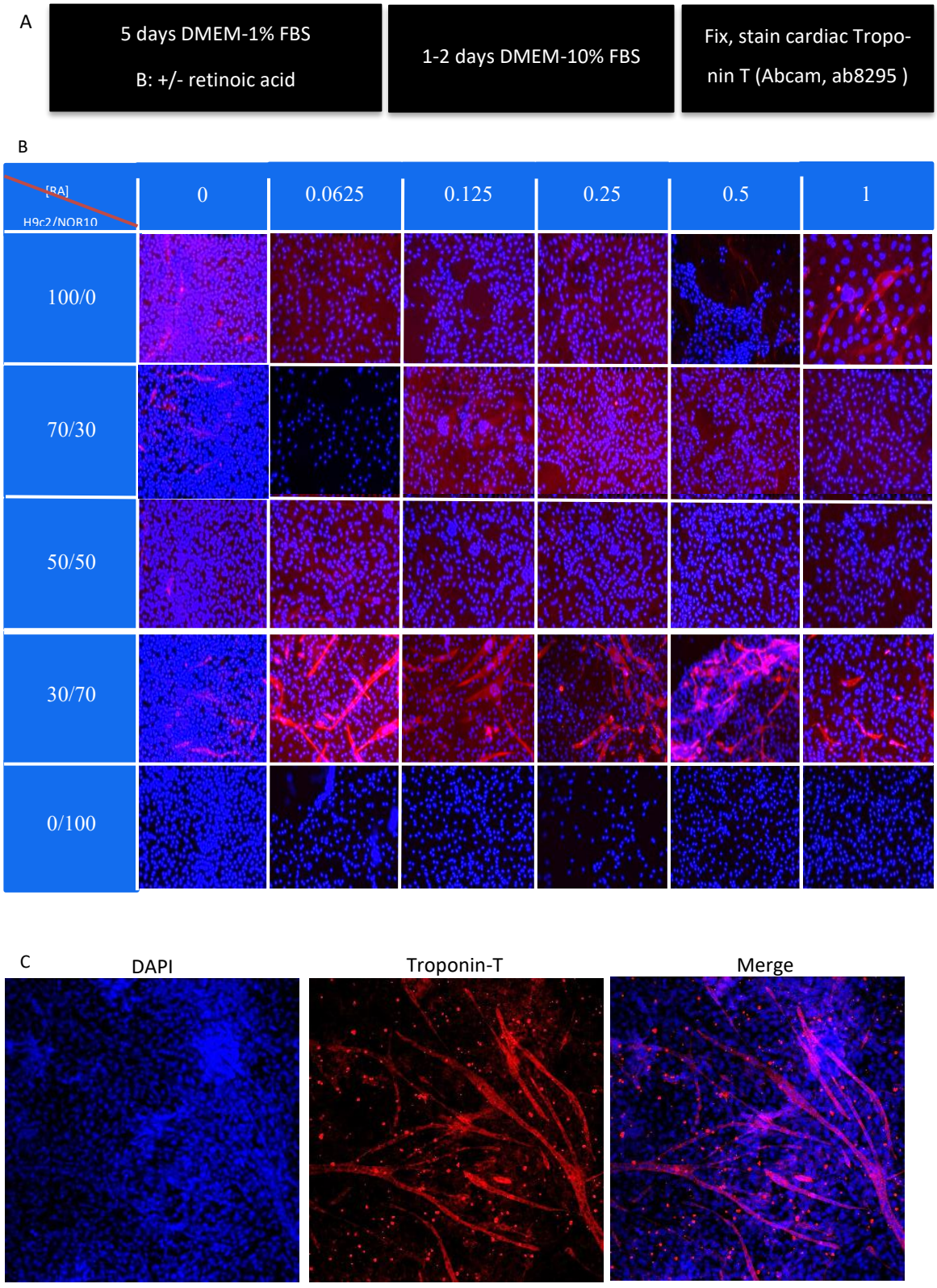

Figure 2-7 Specific cardiac troponin T staining. A) Differentiation protocol B) Co-culturing and differentiation of H9c2 and fibroblast cells (30%/70% seeding ratio) with different concentrations of retinoic acid RA (0-1 micromolar), on tissue culture plates C) Co-culturing and differentiation of H9c2 and fibroblast cells (30%/70% seeding ratio) on dECM-fibrin, no retinoic acid added.

2.3.6 Cell seeding and differentiation on hydrogel-coated surface

We next assessed the capacity of various hydrogels to enhance cardiogenic differentiation in H9c2 cells. We also aimed at replacing the retinoic acid in the H9c2 differentiation protocol by similar favorable effects mediated by the microenvironment.

Having confirmed that Nor-10 fibroblasts favor cardiogenic differentiation of H9c2 cells, we seeded H9c2 cells and Nor-10 fibroblasts at a ratio of 30%:70% onto hydrogel slabs in 48 well plates. Figure 2-8A to 2-8D show the extent of troponin T expression on dECM-fibrin, Matrigel, collagen and tissue culture plate control after 1 week of differentiation. Figure 2-8H quantifies the percentage of differentiation of H9c2 in co-culture with fibroblasts on the different materials. The proportion of differentiated H9c2 cells is larger on the dECM-fibrin hydrogel than on cell culture plates (P=0.0001) and Matrigel (P=0.0024), but similar to the one on collagen (P=0.645). These results suggest that the influence of dECM on the differentiation of H9c2 cells is likely mediated by its collagen content.

The effect of suitable extracellular matrix is striking: The combination of co-culturing the H9c2 cells with Nor-10 fibroblasts and the presence of either dECM-fibrin or collagen outperforms even the highest concentrations of retinoic acid in H9c2 monoculture in 2D (comparison to Table 2-1B, 100/0 ratio, 2000nM retinoic acid, P=0.0059 between dECM-fibrin and 2D, and P= 0.0106 between collagen and 2D).

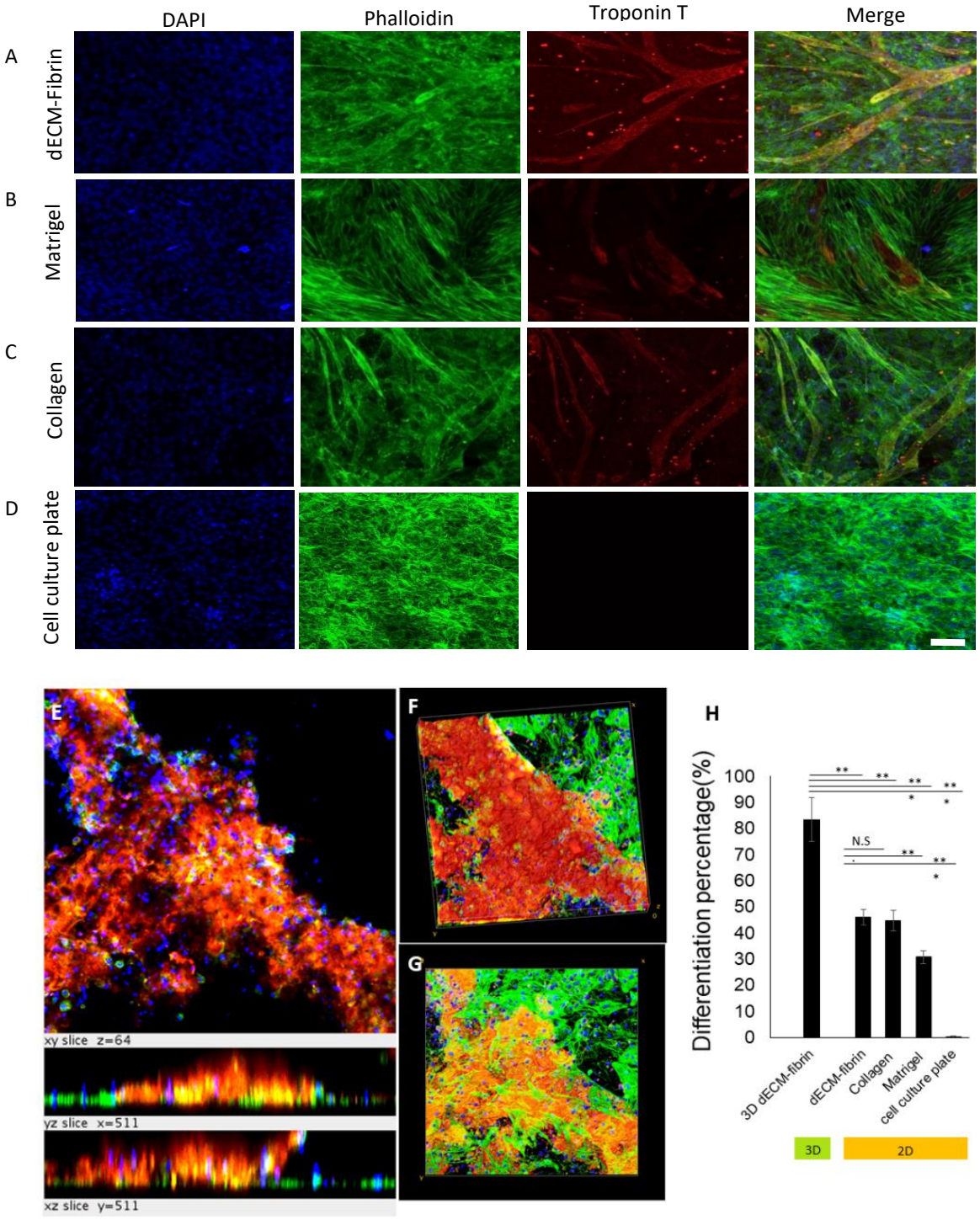

Figure 2-8 Differentiation of H9c2 cells in co-culture with fibroblasts on different hydrogels (2D) and in the dECM-fibrin hydrogel (3D) in the absence of retinoic acid. Differentiation A) on dECM-fibrin, B) on Matrigel, C) on collagen I, and D) on cell culture plates after 7 days of differentiation E) Confocal images of the differentiation of H9c2 cells in the 3D co-culture of 30% of H9c2 cells and 70% fibroblasts in dECM-fibrin hydrogel after 7 days (differentiation duration). F) top view, and G) bottom view of the cells in dECM-fibrin hydrogel. H) Percentage of differentiation of H9c2 cells on different hydrogels in 2D and 3D. Troponin T staining shows the differentiated cells in red. Phalloidin stains the actin filaments of all the cells in green and DAPI in blue stains the nuclei. Scale bar: 100µm (P=0.0024 for dECM-fibrin vs. Matrigel, P=0.0001 for dECM-fibrin vs. cell culture plate, and P=0.645 for dECM-fibrin vs. collagen).

2.3.7 Cell seeding and differentiation in 3D hydrogels

Having evaluated and optimized differentiation efficiency on the surface of various hydrogels, our next step was to proceed to a truly 3D co-culture configuration. For this, we included the suspended cells H9c2 and Nor-10 cells to be co-cultured in the dECM-fibrin hydrogel prior to gel formation. Cells cultured in the 3D structure of the dECM-fibrin hydrogel attached, spread, and formed a network throughout the wells. We also attempted 3D culture in collagen I and Matrigel[230], [231], but could not carry out the entire differentiation protocol in 3D, since after about 2 days, the gels had become very soft with a large part of the cells attached to the floor of the wells.

Figure 2-8E shows the H9c2 cell differentiation in the 3D hydrogel using Troponin T staining. The top and bottom view of the 3D hydrogel has been shown in figure 2-8F, and 2-8G. The cells attached, spread, and formed a network throughout the wells. The differentiation percentage of H9c2 cells in co-culture with fibroblasts in 3D dECM-fibrin hydrogel was 83±8% (Figure 2-8H). This is significantly better than the 2D co-cultures of H9c2 and fibroblast cells on top of dECM-fibrin coated surfaces ($P = 0.0007$), indicating a specific advantage of the 3D configuration. To achieve a similar differentiation efficiency in 2D, the combination of retinoic acid and co-culture is required ($P=0.77$).

Due to the fragile nature of the pure collagen I gels, we could not assess whether there is a difference between dECM-fibrin and collagen I regarding H9c2 differentiation in 3D. However, from the 2D results given in Figure 2-8H, it seems that the primary advantage of the dECM-fibrin gel over collagen I in the H9c2 system is mechanical ruggedness, both gels showing high differentiation capacity.

Overall, we conclude that the very high differentiation efficiency in our 3D co-culture system affords the freedom to avoid retinoids altogether. Co-culture with Nor-10 fibroblasts, the 3D environment, and a collagen-based matrix all have a positive effect on cardiac differentiation of H9c2 cells.

2.3.8 Neonatal cardiac cells on 2D and in 3D hydrogels

To study the effect of different hydrogels with a more physiologically relevant cell system, we next cultured primary neonatal cardiomyocytes on surfaces (2D culture) of dECM-fibrin hydrogel, in comparison with various controls: tissue culture plates, the commercial matrices collagen I and Matrigel, as well as a fibrin-collagen I composite. This latter is the closest analog to dECM-fibrin with chemically defined composition. To assess electrophysiological activity, we videographically recorded intracellular calcium ionic concentration variations by using the Ca^{2+} indicator Fluo-4 AM at 3 days of culture. Sample videos are provided as supplementary Videos S4 (dECM-fibrin), S5 (fibrin-collagen I), S6 (collagen I), S7 (Matrigel), S8 (tissue culture plate). From the calcium oscillation videos, we evaluated local frequency

(Figure 2-9A to 2-9E) and local phase (Figure 2-9F to 2-9J). The results indicate essentially perfect synchrony on the dECM-fibrin hydrogel, regarding both frequency (2-9E) and phase (2-9J). This is followed by fibrin-collagen I where the phase analysis (2-9I) shows some individual desynchronized cells and regions with increased lag. The other conditions show even higher degrees of variability in phase and frequency, common timing being nearly lost on Matrigel (2-9G). This indicates that dECM-fibrin performs best regarding synchronization of calcium influx. The result correlates with morphological observation: cell spread and morphological connectivity improve in parallel with synchrony along the series Matrigel, collagen I and tissue culture plates, fibrin-collagen I, culminating in dECM-fibrin hydrogels.

Having established optimal properties of the dECM-fibrin matrix regarding synchronization of calcium influx, we next investigated mechanical contraction activity. In light of the results obtained by calcium imaging, we compared 3D cultures of rat neonatal cardiomyocytes in dECM-fibrin hydrogels to similar cultures in fibrin alone and fibrin-collagen I.

The normal beating rate of the neonatal rat heart is around 276-423 beats per minute (bpm)[232], whereas for isolated primary cells *in vitro* on standard cell culture conditions it is about 100-115 bpm, (manufacturer's notice[233], confirmed in preliminary trials). Figure 2-9K shows a profound effect of the extracellular matrix environment on the beating rate. At 77 bpm at 5 days of culture, pure fibrin gels sustain a relatively low beating rate, whereas fibrin-collagen I (166bpm, P=0.0001 vs. fibrin) and even more so dECM-fibrin cultures (206bpm, P=0.0001 vs. fibrin-collagen I) approach the expected rate of the neonatal heart. The recovery of the mechanical beating function was gradual as indicated by the progressive rise of beating frequency for all conditions in Figure 2-9K, and started earlier in the dECM-fibrin hydrogel as compared to the other conditions.

Finally, in Figure 2-9L, we visually quantified the synchrony of the neonatal cardiac cell cultures. The neonatal cardiomyocyte extracts seeded in dECM-fibrin gel displayed synchronous contractions from the first day on, and for at least 10 days. In contrast, cardiomyocytes seeded in fibrin did not show synchronous beating until day 5 and typically stopped beating after 7 days. The cardiomyocytes cultured in fibrin-collagen I showed intermediate behavior by reaching synchronicity at day 3, but similar to fibrin, they did not beat after 7 days. These results confirm the superior results obtained with the dECM-fibrin hydrogel in calcium imaging (Figure 2-9A to 2-9J), and make dECM-fibrin the optimal hydrogel for primary neonatal cardiomyocyte culture among the various options compared here.

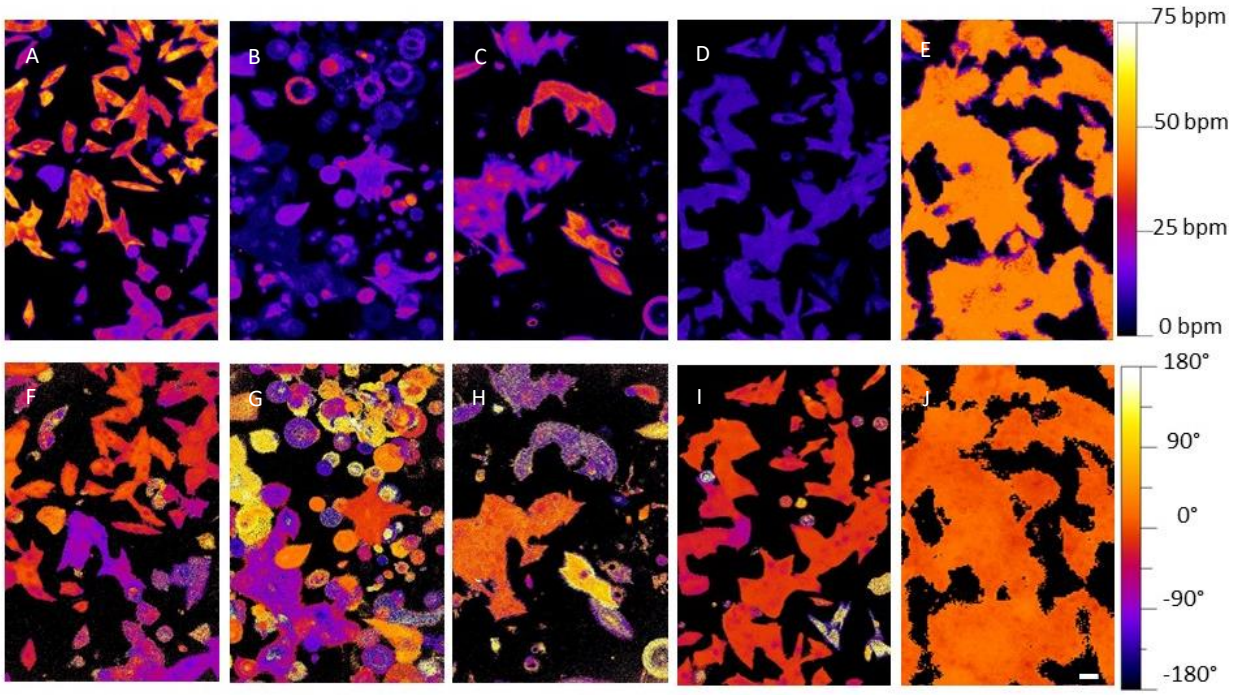

K

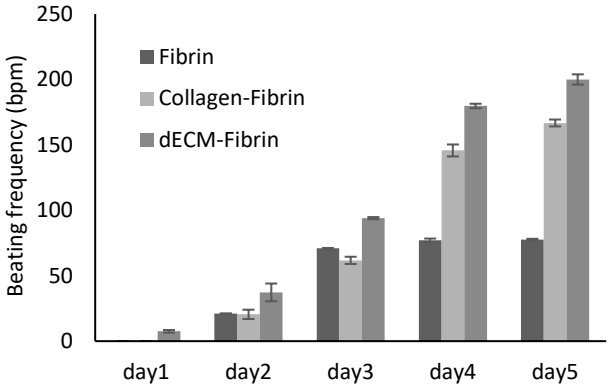

L

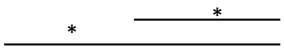

Synchronicity

Days	Fibrin	Fibrin-collagen I	dECM-fibrin
1	-	-	+ (100%)
2	- (25%)	- (50%)	+ (100%)
3	- (50%)	+ (75%)	+ (100%)
4	- (50%)	+ (100%)	+ (100%)
5	+ (100%)	+ (100%)	+ (100%)

Figure 2-9 Calcium transients and beating characteristics of cardiomyocytes interacting with different hydrogels. A-J) Calcium imaging for neonatal cardiomyocytes seeding onto different hydrogels, and tissue culture plate (control). A-E) Frequency, F-J) Phase (positive values indicate earlier beating, negative value retardation). Hydrogels used in calcium imaging: tissue culture control (A and F), Matrigel (B and G), collagen I (C and H), fibrin-collagen I (D and I) and dECM-fibrin (E and J). K) Beating rate for the first 5 days for neonatal cardiomyocytes seeded 3D in fibrin, fibrin-collagen I and dECM-fibrin hydrogels. L) Synchronization as the percentage of synchronously beating wells (four wells per condition) during 5 days in the 3D hydrogels. Scale bar: 100µm.

2.4 Discussion

In this study, we develop a hydrogel blend of fibrin and decellularized porcine cardiac matrix to improve the cellular niche for cardiomyocyte cell culture. For this, we successfully decellularized porcine ventricular tissue, with maintenance of collagen, glycosaminoglycans and elastin components. The addition of fibrinogen to the dECM thus obtained, followed by coagulation with thrombin, provided a Young modulus of about 20kPa, in the range of adult cardiac tissue[188]. We used this system in conjunction with fibroblast co-culture to robustly differentiate the H9c2 myoblast line into a cardiomyocyte phenotype while avoiding retinoic acid. Finally, we demonstrated excellent maintenance of electromechanical activity in neonatal cardiomyocytes by quantification of beating activity as well as calcium imaging.

An important aim in the design of the hydrogel system was to match the physical stiffness of native myocardium (10-50kPa range, [67], [188]). To mechanically reinforce the intrinsically soft cardiac dECM, we chose the specific coagulation of fibrinogen by thrombin, as opposed to more generic agents such as transglutaminase[79][234] or genipin[214][235] We find the thrombin-coagulated fibrin gels to be softer than similar gels crosslinked by transglutaminase[79], but we could compensate for this by increasing the fibrinogen concentration correspondingly. The specificity of thrombin[236] is advantageous for both *in vitro* and anticipated *in vivo* applications, and probably allowed us to avoid cellular toxicity observed in transglutaminase crosslinking[79].

We used the H9c2 cell line to investigate cardiogenic differentiation. By combining 3D embedding into dECM fibrin hydrogels with co-culture with Nor-10 fibroblasts, we obtained over 80% differentiation efficiency. While the utility of adding fibroblasts or fibroblast-derived matrix in H9c2 differentiation has repeatedly been demonstrated[237][29][60], the differentiation efficiency in our system is rather high compared to previous reports[237][214]. *Nota bene*, we obtain our results in the absence of retinoids. We achieved this by stepwise optimization of three key elements of the cardiac cell environment: choice of the extracellular matrix, its physical properties, and the co-culture composition. The result should simplify pharmacological screening, as retinoids are known to broadly affect cellular processes beyond specific cardiac differentiation[239]. Further, avoiding the strong transcriptional effects of retinoids[239] could also simplify investigation of communication between cardiac fibroblasts and cardiomyocyte, which today remains only partially understood[240].

The ultimate aim of an *in vitro* cardiac model should be to replicate the electromechanical beating function. Comparative culture of freshly isolated rat cardiomyocytes on dECM-fibrin, fibrin-collagen I and fibrin control hydrogels indicate specific advantages of the dECM-fibrin composite as it performs best regarding recovery of physiological beating frequency and reacquisition of synchrony. In line with these results, dECM-fibrin also outperformed collagen I, Matrigel, tissue culture plates, and also fibrin-collagen I regarding synchronization in calcium imaging. The result correlates well with morphological analysis: cell spreading and enhanced geometric contacts are overall associated with higher frequency and

better synchrony, with reinforcement by mechano-electrical feedback on substrates with physiological stiffness[241]. Given that we seed a native cardiomyocyte population including various pacemaker cells, these results replicate native cardiac physiology[242]: better connectivity directly provides better synchrony, but also better spread of the highest pacemaker frequency. This subtly graded response of the native cardiomyocyte population contrasts with the differentiation of the H9c2 cell line, where the presence of collagen was as efficient as the dECM-fibrin composite in inducing cardiogenic differentiation, in essence independently on mechanical properties.

Interaction of cardiomyocytes with extracellular matrix proteins is known to be of prime importance for cardiac differentiation and electrophysiological maintenance. For example, a multitude of integrins with affinity for collagen I, but also laminin and fibronectin are expressed on cardiomyocytes[243][244][241][245]. It is fully conceivable that the presence of a more complete mixture of extracellular matrix components in the cardiac dECM is important not only for fine electrophysiological regulation, but also for cell spreading and thus geometrical connectivity of neonatal cardiomyocytes. In contrast, collagen I may suffice in H9c2 to induce a pro-cardiogenic, but ultimately non-functional cell state.

Mechanical aspects probably play a more important role in mechanically beating cells as well. Ideal energy transmission to the substrate is expected to occur at near physiological stiffness (neither too soft, preventing force development, nor too stiff, preventing substrate deformation)[138], [246], [247]. Mechanical feedback [241], could therefore help explain why the most physiological frequency and best synchrony for the neonatal cardiomyocytes are indeed found for the composite hydrogels, and not for the softer collagen, Matrigel or pure fibrin or on the other hand the hard tissue culture plates.

This chapter answered a number of questions regarding the impact of 3D culture, hydrogel characteristics and the functionality of the cardiac cells. There are some technical and conceptual issues being addressed in the review process of the original publication. There is above all and foremost the need to constitute a fibrin-collagen control that precisely matches the collagen concentration in the dECM-fibrin hydrogels. This is required to define exactly the utility of performing the time-consuming dECM isolation vs. simple usage of purified commercial collagen I. This implies more precise efforts to quantify the collagen concentration in the final dECM. Therefore, while the comparison in figure 2-4b and c holds and allows to state that indeed, relatively little change of composition in terms of GAG and collagen is observed during decellularization, it is necessary to further investigate the absolute amounts in order to explain or resolve the discrepancies with literature. Hence, we conducted BCA test to measure the exact concentration of the collagen in dECM and the results showed that around half of the dECM concentration is collagen which is matched with the literature.

As knowledge of the absolute composition of the dECM extract is necessary to constitute a matching fibrin-collagen I control, these investigations are ongoing. Beyond this work, one can then consider

conducting more biological experiments such as cell differentiation to cardiac lineage, gene expression, and long-term functionality assays. Using the introduced hydrogel in this chapter, we will proceed to provide more tissue-like structures in chapter 3, by aligning the cardiac cells in this hydrogel in 3D structure.

Chapter 3 Trabeculae carneae *in vitro* model as the smallest cardiac tissue unit

This chapter presents an *in vitro* trabeculae carneae model as the smallest cardiac tissue unit which will be made by using the hydrogel presented in chapter 2. It has been indicated in the previous chapter that dECM-fibrin hydrogel can be considered as an effective environment for cardiac cell survival, differentiation and functionality. Motivated by the fact that the cell alignment in native cardiac tissue is one of the critical parameters of functionality of the tissue, and also the trabeculae carneae can be extrapolated to represent the tiniest building blocks of the cardiac tissue which resembles the myocardium characteristics and functionality, the main focus of the following chapter is on developing trabeculae carneae model *in vitro* by aligning the cardiac cells in 3D with dimensions comparable with trabeculae carneae structures using the hydrogel and investigate the impact of 3D surface topography and spatial geometry on the alignment and function of the cardiac cells in the hydrogel.

3.1 Introduction

To improve our understanding of cardiovascular physiology, diseases, and related therapies, there is a need to perform studies on cardiac models *in vitro* [17]. This implies to recapitulate the complex microenvironment of the heart. Studies made using such *in vitro* cardiac models can be a step towards

reaching more accurate pharmacological responses when developing new drugs targeting cardiovascular diseases (CVDs), compared with the existing drug screening [248] methods.

In native myocardial tissue the arrangement of the cardiomyocytes and fibroblasts within the ECM plays an important role in tissue function, in particular in the generation of contractile force as well as in biological, electrical and mechanical functions [249]. The three-dimensional nature of this tissue structure and the appropriate distribution of cell patterns within it, is directly related to the operative and active forces it produces [209]. Additionally, the electrical conduction in the heart is anisotropic and depends on cardiomyocyte fibers orientation as electric current spreads faster in the long axis of cardiac fibers [210]. Therefore, a precise and realistic knowledge of the myocardial fiber architecture and its physiology is essential to accurately understand and interpret cardiac contraction and propagation of the electrical stimulus and mechanical functions [250]–[252]. Consequently, to have a reliable *in vitro* model of the heart tissues, recapitulating the anisotropic spatial arrangement of the cardiomyocytes seems to be a significant criterion and still an open question that should be considered in designing the 3D functional cardiac models *in vitro* [249], [106].

In the recent years, 2D and 3D micro-physiological models of the heart have been the subject of studies, as they can be used as platforms for drug screening, for testing drug delivery and for developing tissue engineering methods [253]. Several studies performed the alignment of cells in 2D cell culture using different methods and demonstrated that the cardiomyocyte cell alignment provided a higher expression of related genes and a better differentiation of the aligned cells [254],[255]: Grosberg *et al*. cultured heart muscle cells on polydimethylsiloxane (PDMS) thin films patterned with fibronectin using microfabrication techniques, such that the myocytes self-organized into an anisotropic tissue. The obtained contractile structures were later electrically stimulated and exposed to drugs to evaluate their cardiotoxicity [256]. Bursac *et al.* modified coverslips by creating linear grooves made by micro abrasion or by depositing micropatterned fibronectin lines. They studied the effect of such patterned substrates on cardiomyocyte organization and on the anisotropy of the propagation of action potentials [257]. Au *et al.* seeded neonatal rat cardiomyocytes on micro-grooved polystyrene substrates fabricated by embossing and showed that the myocytes aligned with the grooves [258]. Agarwal *et al.*[259] patterned fibronectin lines on microcantilevers and showed sarcomeric alignment in the seeded cardiac tissues. Their system was used to evaluate the *in vitro* response of the engineered cardiac tissues to isoproterenol, a pharmacological agent. Annabi *et al.* covered the surface of PDMS micro-channels with methacrylated gelatin (GelMA) and methacrylated tropoelastin (MeTro) to promote the adhesion of cardiomyocytes. The presence of MeTro in the micro-channels enabled the formation of well-defined elongated sarcomere structures, and induced a better adhesion and contractility of the myocytes compared with the GelMA-covered channels [260]. Zhao *et al.* showed that in 2D, the myotubes formed on the microstructures were highly aligned along the longitudinal axis of the structures and propagated their alignment to the 200µm gap area with a slanting angle around 70°, while the myotubes formed

on smooth surface or the gaps in order of mm, had no special direction[261]. They also showed that by adding another layer of cells on top of the aligned myotubes, the alignment spread and although the top layer was not in close contact with the grooves, they followed a similar highly aligned structure. However, the thickness of their observed structure was limited to 40µm.

Although many studies have provided methods to engineering cardiomyocyte alignment *in vitro* in a 2D environment, there are still several challenges that need to be addressed as cells naturally reside in a 3D micro-environment *in vivo* and a variety of studies suggest that cells may behave differently in 2D and 3D constructs [262],[106]. There are a few studies evaluating cell alignment in 3D cellular constructs *in vitro* using simple methods without the need for external stimulation to the cells [105] (e.g. no mechanical stretching, electrical stimulation or flow induced shear-stress). Very successfully, large ring-shaped self-condensing structures made from a collagen-Matrigel mix seeded with neonatal rat cardiomyocytes causes alignment of the cells along the along the tangential direction [136][82]. Elevated oxygen pressure and high insulin levels were however necessary to ensure the possibility to the high metabolic needs and unfavorable diffusion characteristics of the large constructs [82]. More fundamentally, the reason for cardiomyocyte self-alignment remains unclear. In order to better dissect and reproduce the elementary mechanisms for cardiomyocyte alignment, a number of researchers resorted to microfabrication techniques. For instance, Mosiewicz *et al.* demonstrated the spatiotemporal *in situ* modulation of the mesenchymal stem cells invasion of a PEG hydrogel, using light activated patterning of the hydrogel with desired ECM proteins and growth factors [263]. Norman *et al.* prepared PDMS parallel channels with dimensions of 40×70×25µm. Fibroblast-seeded collagen was molded and confined in these channels to induce the cell alignment in 3D [264]. Aubin *et al.* encapsulated different cell types such as cardiomyocytes, fibroblast, and endothelial cells in a photosensitive GelMA-based prepolymer and pipetted this photosensitive hydrogel between a PEG-coated glass slide and an untreated coverslip. Using UV light, they could pattern the cell-laden hydrogel and quantify the cell elongation and alignment [249]. Mathur *et al.* [165] presented a microfabricated chip in which human stem cell derived cardiomyocytes were cultured in 3D in a central chamber and where lateral channels surrounding the main chamber acted as vasculature, allowing nutrient delivery via diffusion, while protecting the tissue in culture from shear forces. The system was used to confirm the drug response of the cardiac cells to two pharmacological agents, verapamil and isoproterenol. Sidorov *et al.*[265] assembled cardiac cells loaded in fibrin gel into a 3D tube-like structure and used these constructs to assess their passive and active mechanical and electrical characteristics. Engelmayr Jr *et al.* developed an accordion-like honeycomb scaffold in poly (glycerol sebacate), using microfabrication techniques. This design provided a porous, elastomeric 3D anisotropic scaffold in which neonatal rat heart cells were cultured. The obtained cell constructs demonstrated mechanical properties similar to the one of the native ventricular myocardium, controllable stiffness, directionally-dependent electrical excitation, and better heart cell

alignment than isotropic control scaffolds[266]. Although several research groups are mimicking the cardiac tissue with various approaches to align the cells in a 3D structure, there are still challenges for 3D alignment in larger constructs and investigating the impact of 3D cell alignment on cell behavior and functionality[106].

Many studies indicate the influence of micro and nano grooves on cell alignment in 2D and 3D structures, however, these models might not sufficiently resemble the native cell microenvironment. For this reason, understanding the smallest physiologically relevant, functional myocardium tissue unit in the native heart is imperative. The answer to this question is the trabeculae carneae (Figure 3-1), which are irregular muscular structures that pattern the inner surface of both ventricles of the heart [29]. These structures are the smallest collections of aligned cardiomyocytes in the heart, with dimensions of 0.5 to 3 mm in length and from 50 to 500 µm in diameter [28]. Because of the dimensions of the trabeculae carneae, oxygen and nutrient can diffuse easily in these structures [267]. The vascularization in the trabeculated myocardium is less than that of the compact myocardium, which is why it is often favored by researchers for the study of ionic, mechanical and metabolic activity of the cardiac muscle [28],[268]. Therefore, a cardiac model which mimics the trabeculae carneae, can provide interesting knowledge in this field.

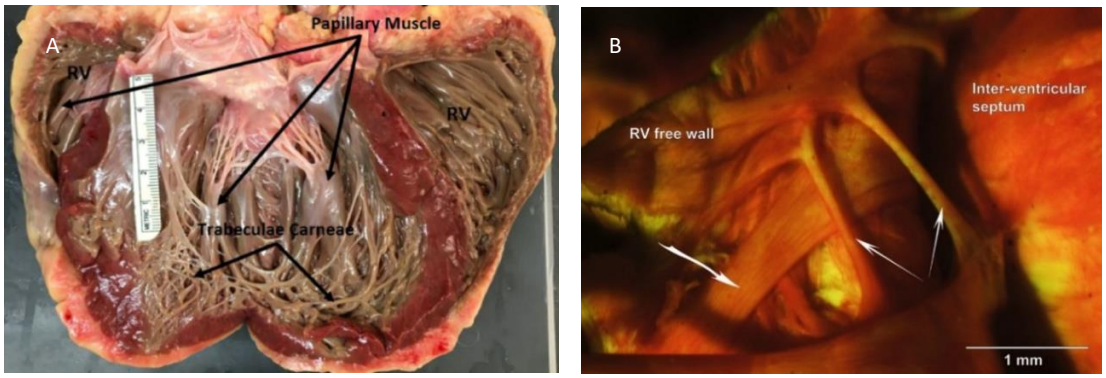

Figure 3-1 A. Photograph of a human heart opened by a frontal incision illustrating the trabeculae carneae and papillary muscles[29]. B. Rat right ventricular trabeculae in situ. Photomicrograph of a Bouin's-fixed, PSR-stained rat RV in which the free wall has been reflected to reveal the presence of trabeculae. The two narrow arrows point to thin, free-running preparations of the sort sought by experimentalists. The heavier arrow points to a wider, apparently strap-like, specimen[28]. Copyright © 2020 Rockefeller University Press.

The main difficulty for creating such a model is obtaining the orientation of the cells in large 3D culture which develops our goal for this chapter. The hydrogel composition and also the physical restriction which is forced by the patterning play a critical role in cell alignment. The physical environment affects the function of the cells through the mechano-transduction process. Cells have the ability to sense and

respond to a large variety of signals, namely biochemical or biophysical cues. This means, the physical cues around the cells are integrated by being converted to biochemical intracellular signaling responses that results in changes in cell function [269]. When an outside-in force is applied to cell-ECM, almost every aspect of the ECM is deformed and rearranged. On the other hand, an inside-out force transmission path also exists [269]. Polymerization and de-polymerization of microtubules generates pushing and pulling forces which controls the position of mitotic spindles, chromosomes and nuclei [270]. When the head of actin filaments are pulled, traction forces are generated which deforms the ECM [271]. Forces can affect the protein domains existing in the ECM which can lead to revealing cryptic sites for engagement and signaling of cellular receptors [269]. All of these signals can lead to the change of orientation of the cells in a predefined microenvironment.

Our hypothesis in this chapter is that if we can make oriented 3D constructs of the size of trabeculae carneae. For that, we present a simple method to control cell alignment in 3D cell-laden hydrogels, which are patterned using microfabricated PDMS grooves with large dimensions (from 100 μm to 350 μm) similar to the dimensions of the trabeculae carneae. The alignment of the cells in the grooves with dimensions less than 100 μm has been proved in several studies [17], [272]. Here, we expect to provide more relevant model of trabeculae carneae with larger dimensions. The dimensions more than 350 μm are also less relevant due to the lack of vascularization and cell apoptosis in the middle of the 3D structure. Figure 3-2 demonstrates a schematic of the work in this chapter. Hence, the questions that we answer in this chapter is that whether the cells in proximity to the corners of the grooves will follow the alignment and if so, how far this alignment can be propagated. Finally, we evaluate the model in terms of its dimensions compared to trabeculae carneae, detachability, alignment stability, and contractility maintenance.

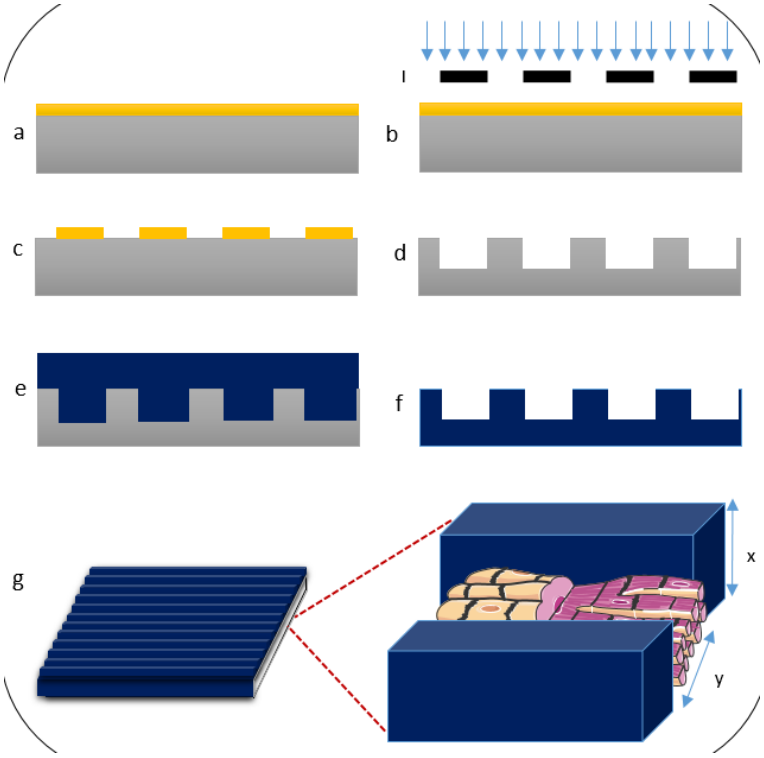

Figure 3-2 Grooves microfabrication and their use for cell culture: a. photoresist deposition b. direct laser writing photolithography c. development d. Bosch process e. PDMS molding f. obtained PDMS component g. cell culture and differentiation leading to 3D aligned cell constructs. In this work we used dimensions of 100 µm to 350 µm.

3.2 Methods

3.2.1 Hydrogel preparation

As we discussed in chapter 2, one of the most promising approaches for creating the 3D cardiac tissue models is using hydrogels, because of their biocompatibility, physical, mechanical and chemical properties. In this part of the work, we used the dECM-fibrin hydrogel which is described in the previous chapter, and proved to provide appropriate mechanical and biological environment for the cells. It has been shown that the mechanical properties of this hydrogel are in the range of native cardiac tissue (~ 20 kPa) and it can provide a microenvironment for the cells to improve their biological properties, such as differentiation, beating rate and synchronicity *in vitro*. In this chapter, the same hydrogel is used as the basis of the 3D structure preparation.

3.2.2 Microfabricated grooves for cell alignment

To prepare the mold for patterning the hydrogel, microfabricated grooves were designed and manufactured with different dimensions on a silicon wafer. Figure 3-3 determines the main steps of silicon wafer etching. The samples were fabricated using direct laser writing photolithography and deep silicon etching using the standard Bosch process.

A silanization step is conducted after the fabrication of the wafer by exposing the wafer to the evaporation of Trimethylsilyl chloride (TMCS) under the chemical hood. Silanization is a covalent effective surface modification which reacts with hydroxyl groups of the material surface and act as a non-sticky surface layer. Hence, it finally enables to detach easily the PDMS from the silicon surface. Six different channel size were produced (channel size × spacing: 100 × 100 µm, 150 × 150 µm, 200 × 200 µm, 250 × 250 µm, 300 × 300 µm, and 350 × 350 µm) on a single sided 100mm Si wafer. These master molds have been used to pattern polydimethylsiloxane (PDMS). PDMS is inexpensive, easy to pattern, flexible, biocompatible, optically transparent and permeable to gases which makes it ideal for cell experiments.

The PDMS used in this work is a well-mixed 1:10 combination of the curing agent and PDMS polymer. This mixture has been degassed before use, for removing the air bubbles, and then poured on the silicon wafer. It was kept at 80°C for two hours for PDMS curing. After removing the patterned PDMS from the silicon wafer, it was exposed to an oxygen plasma to make it hydrophilic on the PDMS surface which is crucial for hydrogel patterning and cell culture.

Step	Process description	Cross-section after process
Mask 1_ Silicon mold for PDMS		
01	*HMDS + Positive Photoresists Coating* *Machine: ACS* *PR : AZ 1512HS – 1.5um*	
02	*Direct Writing* Machine: MLA150	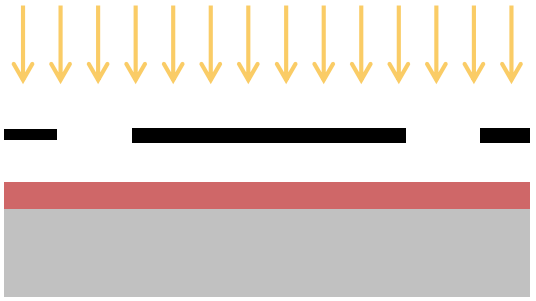
03	*Development* Machine: ACS	
04	*Deep silicon etching*	
05	*Stripping*	

Figure 3-3 The steps of groove microfabrication including photoresist coating, direct laser writing, developing, deep silicon etching using the standard Bosch process, and stripping.

3.2.3 Cell culture

In this chapter, we used the same cell model as described in previous chapter which is based on coculturing the H9c2 cells with fibroblast cells in the presence of hydrogel. As it is mentioned in the previous chapter, in general, the H9c2 cells need retinoid acid for differentiation. However, in co-culture with fibroblast cells in dECM-fibrin 3D hydrogel, they can differentiate properly. We, also, used neonatal cardiac cells to investigate the behavior of the CMs in terms of their beating and synchronicity. The details of culturing have been explained in the previous chapter.

3.2.4 Cell seeding on PDMS (2D) and in 3D hydrogel

To demonstrate the impact of 3D culture on cell alignment and functionality and compare it with 2D cell culture, H9c2 cells in co-culture with fibroblasts as well as neonatal cardiac cells have been cultured on the PDMS molds presenting grooves, with and without hydrogel. For the 2D culture, the cells were just attached on the plasma treated PDMS substrate and for the 3D culture with hydrogel, the cells were mixed with pre-gel. Thrombin and calcium chloride were added to the pre-gel solution for its gelation. 200µl of the cell-suspended solution was rapidly poured in the PDMS mold to fill, solidify and pattern the hydrogel. The medium was changed every two days. Therefore, in the case of 2D mono-layer, the cardiac cells directly attached and spread on plasma treated PDMS, however, in the case of 3D hydrogel, the cells attached to the polymer chains of the hydrogels and formed a 3D network of the cells in the gel.

3.2.5 Immunostaining and 3D imaging

To investigate the expression of specific proteins of the cardiac cells, the samples were stained for different antibodies. Prior to staining, the cell samples were fixed with 4% paraformaldehyde (PFA) for 20min at room temperature. Then, 0.1% TritonX-100 is added to permeabilize the cells for 30min at room temperature. Actin filaments are stained by incubating the cells with phalloidin-Atto 488 (1:50) for 45min at 4ºC. Finally, cells were stained with DAPI (1:2000) for 5min, for labelling DNA. DAPI is then removed and replaced with DPBS before imaging the cells under the ZEISS LSM 700 inverted confocal microscope.

3.2.6 Cell orientation

To examine the orientation of cells in 2D, the H9c2 cells were cultured on patterned, plasma-treated PDMS chips, without the use of hydrogel. For 3D investigations, the cells were first mixed with Fibrin-dECM hydrogel and then cultured on the patterned, plasma-treated PDMS chips. The resulting PDMS microgrooves containing cell-laden hydrogel were soaked in culture media at 37°C. Cells cultured in unpatterned gel were prepared and used as control. To quantify the orientation of cells, the orientation index was measured in 100µm x 100µm images area, repeated 3 times, using OrientationJ, a plugin for ImageJ software. The analyzed results are the normalized ratio of oriented cells to the total number of cells counted.

3.2.7 Beating characteristics

To investigate the beating characteristics of the cardiomyocytes in 3D cultures with and without patterning, the cardiac cells were cultured at the cell density of 10^6 cells/mL in pre-gel mixtures of dECM-fibrin on patterned or unpatterned substrates. Synchrony and onset of beating was judged visually on a per-well basis.

3.2.8 Statistical analysis

Data were compared using unpaired t-test (two-tailed, equal variances) in the GraphPad software. Error bars represent the mean ± standard deviation (SD) of the measurements ($* p < 0.05$, $** p < 0.01$, and $*** p < 0.001$).

3.3 Results

3.3.1 Microfabricated grooves for cell alignment

The microfabricated grooves with different dimensions have been fabricated using silicon wafers as a mold for PDMS chips. This standard photolithography and dry silicon etching process has been done at the center of micronanotechnology (CMi) at EPFL. Figure 3-4C shows the scanning electron microscopy images of the fabricated grooves. Si etching with pulsed process (Bosch process) using AMS200 etcher machine which is an optimized Deep Reactive Ion Etching (DRIE) system for Silicon wafers, is well-defined and accurate process. Therefore, as it is shown in the figure 3-4, the grooves are nicely fabricated in the predefined dimensions.

The surface treatment of the silicon wafers is critical to prevent PDMS sticking. Thus, a silanization step after wafer fabrication allows passivation of the surfaces and removing the PDMS from the silicon wafer. For that, a few droplets of TMCS were placed in the small cup located in desiccator. The fabricated wafer has to be totally clean and without any dust or particles. So, before placing the wafer in the desiccator, the wafer has to be cleaned with nitrogen gun. By placing the desiccator under vacuum, the TMCS evaporates and provides a passive layer on silicon wafer (figure 3-5).

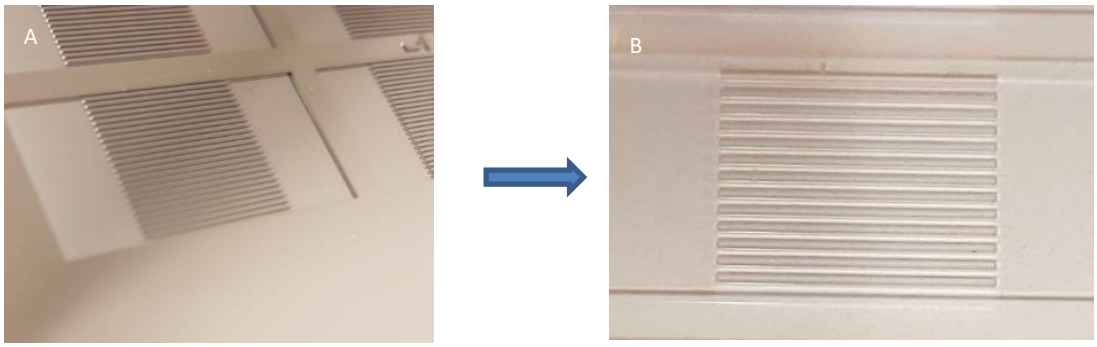

C

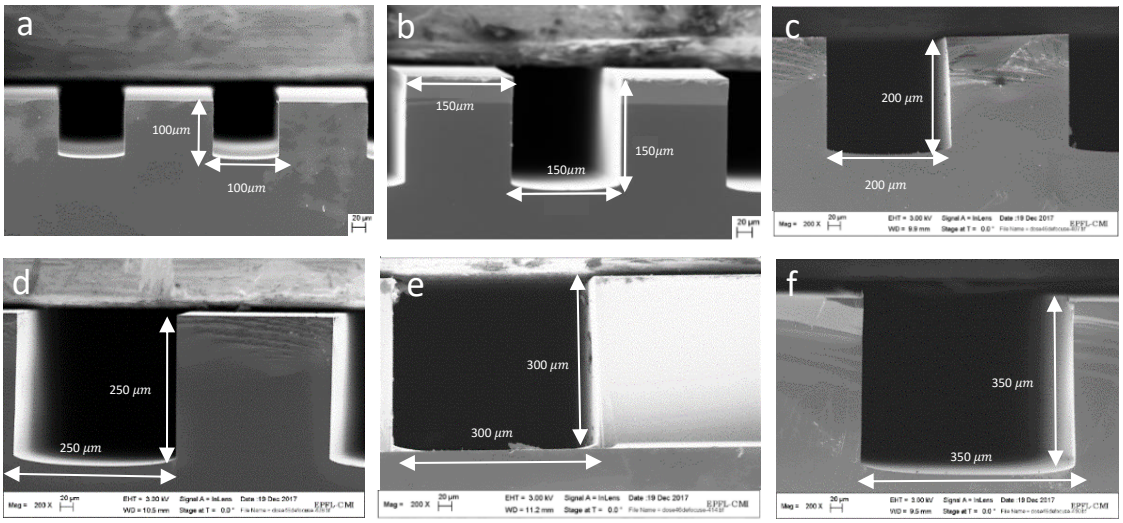

Figure 3-4 A. Etched silicon wafer for microgroove's fabricating. B. patterned PDMS which is molded from the silicon wafer. C. SEM pictures of Microfabricated grooves patterned in silicon wafer using direct laser writing photolithography and deep silicon etching using the standard the fabrication process described in Figure 1, and based on the Bosch process. Grooves of different dimensions were made: (a)100×100 µm, (b)150×150 µm, (c)200×200 µm, (d)250×250 µm, (e)300×300 µm, (f)350×350µm.

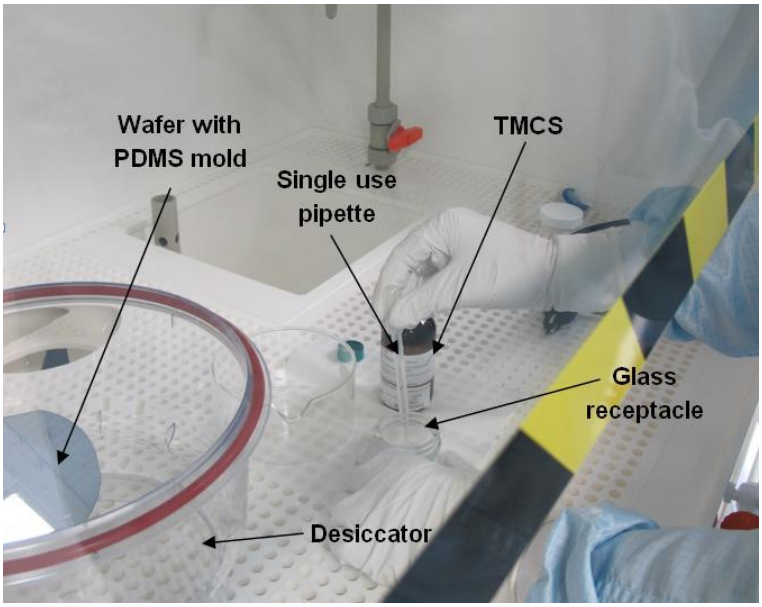

Figure 3-5 the passivation step of silicon wafer using TMCS [273].

To provide the patterned PDMS substrate, first, Sylgard 184 silicone base, and Sylgard curing agent were prepared with the ratio of 10:1, mixed for 1 min at 2000 rpm and degassed for 2 min at 2200 rpm. Then the mixture was placed in a vacuum desiccator for final degassing. The PDMS mixture was poured over the passivated silicon wafer and degassed again to both remove the bubbles and enhance the filling of the microfabricated structures. The final step for preparing the PDMS mold is curing the PDMS by placing the sample in an oven at 80°C for 2 hours. After cooling, the PDMS can be easily peeled off from the silicon wafer while preserving the microstructures.

PDMS is hydrophobic with no reactive surface. To use it as a substrate for culturing the cells, a surface activation step has to be done. By treating the PDMS samples with oxygen plasma before use, one can make the surface hydrophilic. Hence, we exposed the PDMS samples to oxygen plasma with 100 W power for 60s. This step should be done right before the use of PDMS substrate due to the fact that the PDMS surface try to reconstruct the hydrophobic surface within hours.

3.3.2 H9c2 cell culture in 2D and 3D

Controlling the patterns and mechanical anisotropy of *in vitro* cell cultures in order to develop functional tissue is highly important [274]. Hence, the size of the 3D structure containing the aligned cells is critical. To achieve this goal, confocal images of the 3D cell cultured inside the hydrogel were acquired and the orientation of the cells in different stacks has been observed. Figure 3-6 describes a schematic of the whole procedure for aligning the cells, and the confocal images of the cell alignment in 2D and 3D cell cultures on patterned PDMS chips. Briefly, the cells were cultured on the patterned PDMS substrate in two manners: first, culturing a monolayer of H9c2 in co-culture with fibroblasts on patterned PDMS substrate to provide a 2D configuration of the cell alignment, and second, 3D culturing of the same cell combination in the dECM-fibrin hydrogel to provide a 3D structure which is confined with the walls of microfabricated patterns on PDMS. Hence, they provide a tubular structure of the cell-laden hydrogel with defined dimensions. In all cases, for 2D and 3D cell cultures and regardless of the groove dimensions, the cells show an elongated shape and a preferential alignment with the groove's direction. The images show that the cells are aligned in the designed pattern in the hydrogel. It can be justified with the fact that the contact guidance of the wall corner, orientation of the cells in proximity and the formation of gap junctions forced the cells to orient. Even though the cells are not in direct contact with the mold, the contact guidance from the corner of the microstructure forces the cells to align in the direction of the grooves. This orientation propagates to the cells that are far from the walls in 2D, or in the bulk of the hydrogel in 3D culturing.

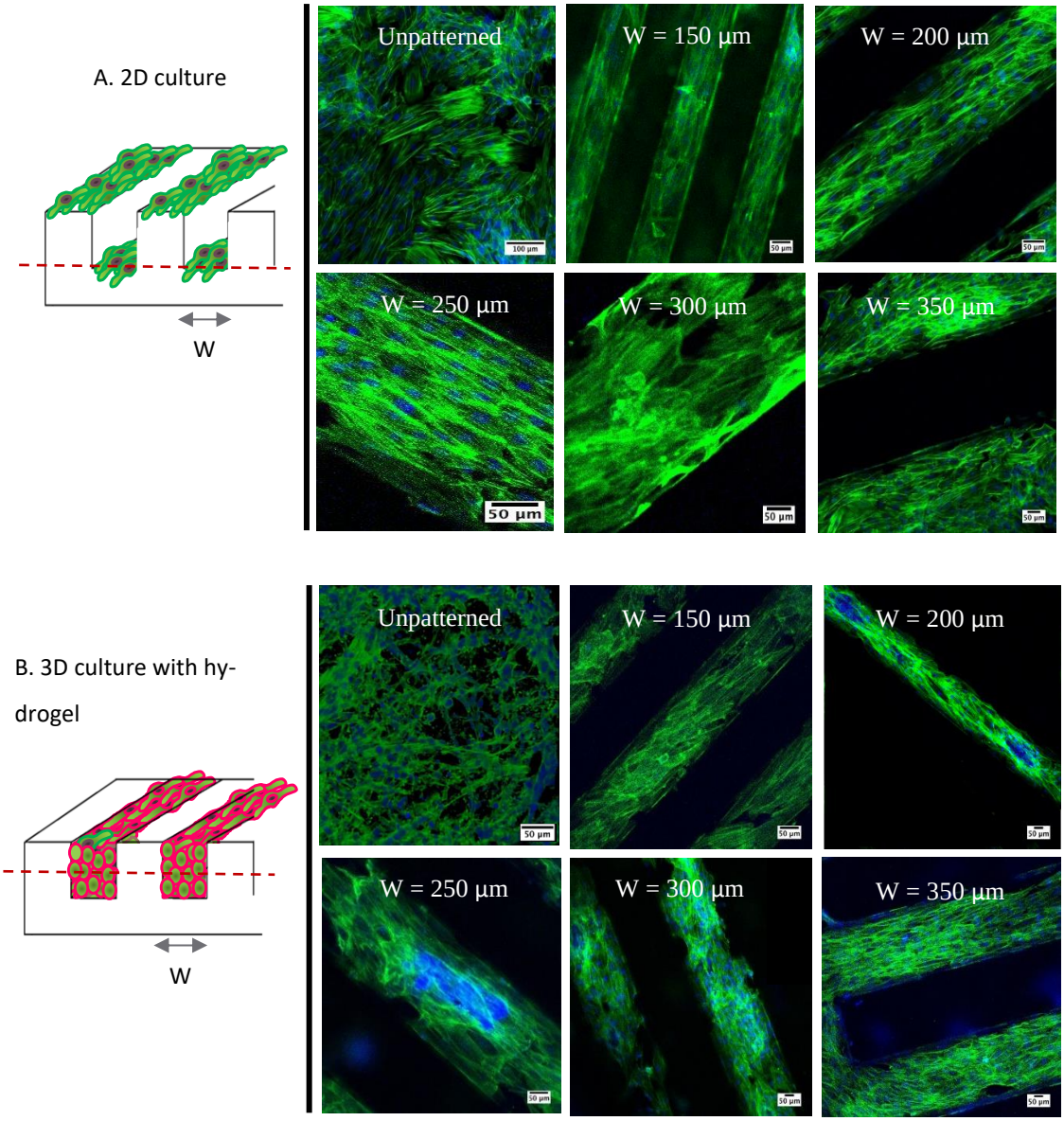

Figure 3-6 Confocal imaging of cell alignment using microfabricated grooves. A. Cells cultured on patterned PDMS molds without hydrogel, creating the 2D stripes, B. Cells encapsulated in the dECM-fibrin hydrogel and cultured in patterned PDMS mold in 3D. Cell alignment is observed in all cases, regardless of the structure dimensions, in both 2D and 3D. the red dash line indicates the confocal image stack. For 2D culture the observation took place at the bottom of the grooves and for 3D culture, the middle stack, means 175 µm distance from the bottom of the groove was observed.

3.3.3 Cell orientation measurement

The alignment of the cells in 3D hydrogel was observed by examining the orientation in different stacks of confocal images. Figure 3-7 shows the middle stack for the 3D structure and the orientation of the cells. The orientation in the same direction of the grooves has been investigated in all the stacks. Figure 3-7 illustrates two important results: Firstly, the cells aligned in the patterned hydrogel, however, by increasing the dimensions, this alignment cannot propagate anymore. Moreover, the alignment of the

cells has impact on the shape of the nuclei as it displays the pulled and elongated nuclei in the direction of the microgrooves, which verifies the effect of alignment on intracellular structure and organization.

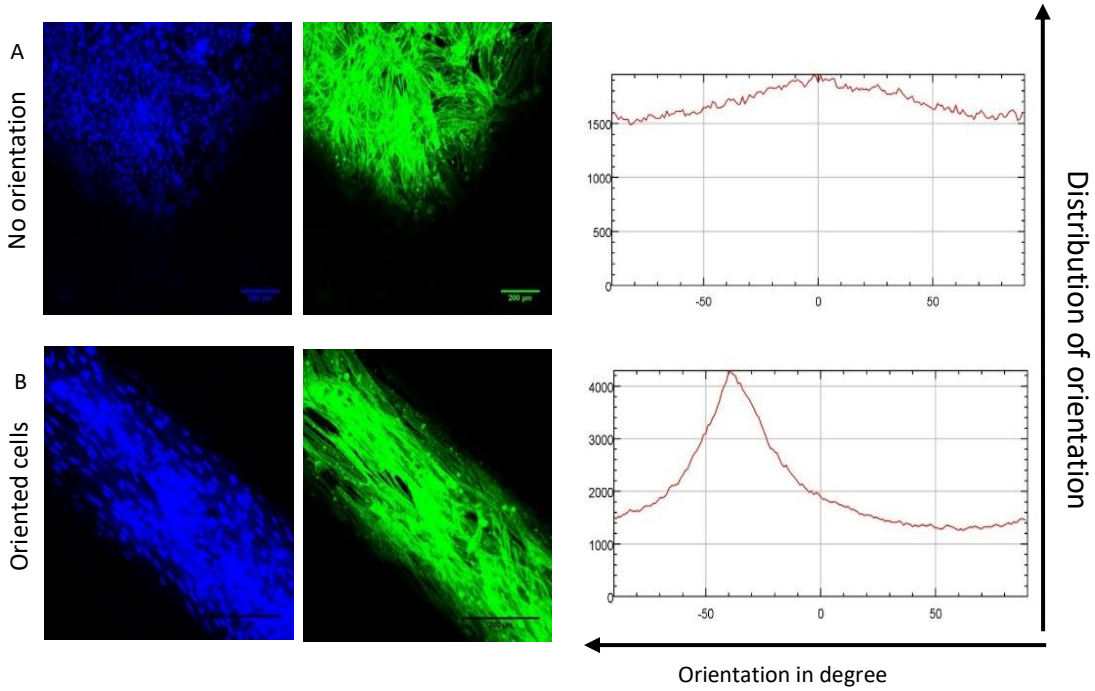

Figure 3-7 The confocal images of the alignment measurement of H9c2 in co-culture with fibroblasts in A.3D culture in hydrogel, on flat substrate (no grooves), and B. 3D culture in hydrogel, inside a 300 μm wide groove (at h = 175 μm). Phalloidin staining in green shows the alignment and organization of the actin filaments in the cells. Nuclei staining with DAPI in blue displays the elongation and orientation of nuclei in patterned substrate. The middle stack of the confocal images (h= 175 μm) has been selected for this alignment observation. Scale bar: 200 μm.

To quantify the alignment of the cells, calculate the maximum distance of cell alignment in 3D hydrogel and also verify the impact of inner corner contact guidance on cell alignment, different stacks of the confocal images with the height of 0, 150, 250, and 350 μm from the bottom of the groove were selected. Using OrientationJ plugin in ImageJ software, three regions of interest in each stack with the area of 100 μm × 100 μm close to each wall and in the middle of the stack were identified (figure 3-8). Each sample was experimentally repeated three times. The analyzed results are an index of orientation which is the normalized ratio of oriented cells to the total number of cells counted. The maximum of the orientation index is 1.

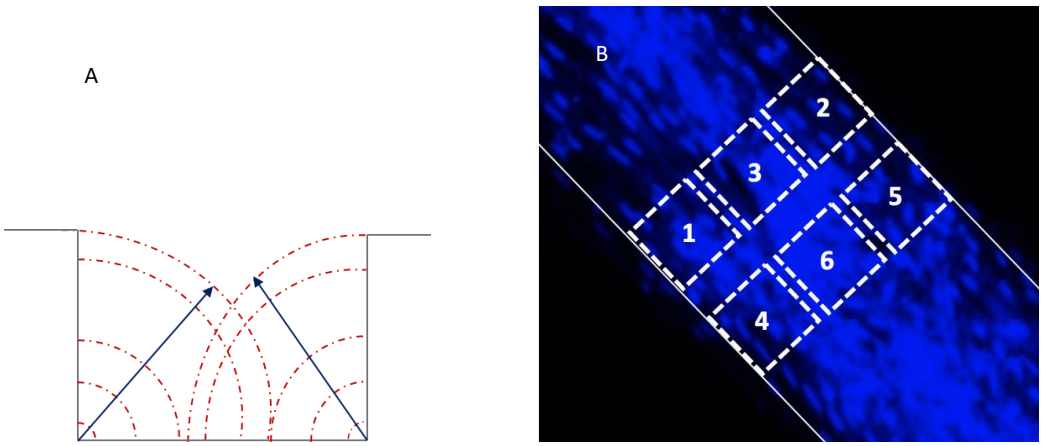

Figure 3-8 A. the contact guidance of the corners to improve the cell alignment in a groove. B. the regions of interest (ROI) in a stack of confocal image for measuring the alignment of the cells. Measurements are repeated for several heights. ROI area 100x100 µm. Positions: 1 and 2 = near the wall, 3 = center of the groove. 4, 5 and 6: repeat of analysis in proximal position in the groove.

Therefore, the orientation of the cells in different distances can be quantified. Figure 3-9A indicates the orientation of the cells in different stacks from 0 to 350 µm. by increasing the height from the bottom of the groove, the orientation index decreases, however, this reduction is not significant (the 50 and 300 µm distance from the inner corner are identical. It is showed differently to be able to recognize two sides).

Figure 3-9B shows the distance from the inner corner versus the orientation index. In this measurement, we considered a groove with 350 µm by 350 µm dimensions. Hence, the maximum distance from the corner is 391 µm (350 µm from the bottom and 175 µm from the corner). The middle ROI of the 350 µm stack has the maximum distance from the corner (391 µm) and lowest orientation index. However, as the index is 0.6, it is still considered as the oriented sample. Therefore, we can conclude from these measurements that we could align the cell in 3D structures up to 350 µm by 350 µm.

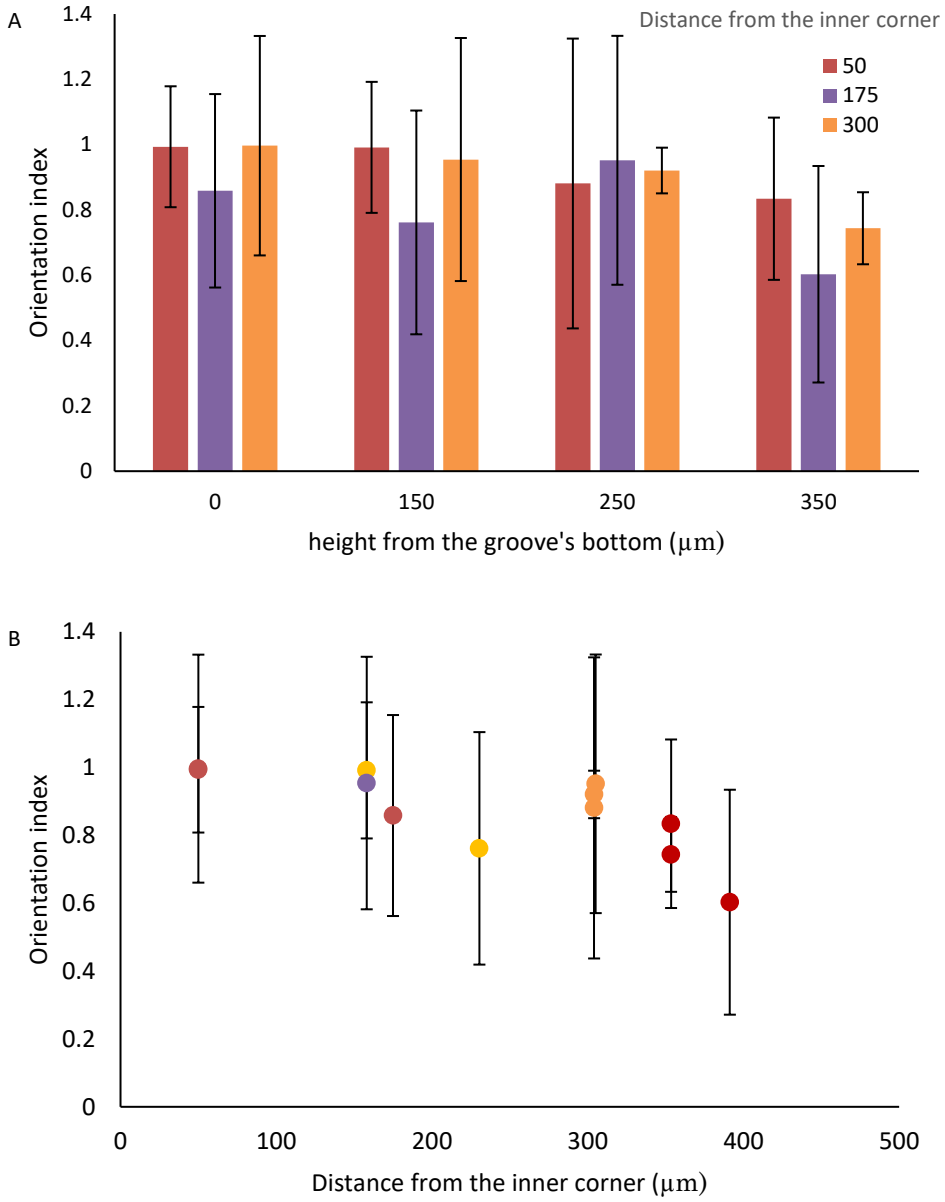

Figure 3-9 The measurement of cell alignment and its relation with distance from the groove's corner in a groove with 350 µm by 350 µm dimensions. A. the cell alignment in different height from the bottom of the groove. B. the orientation index in different distance from the inner corner of the groove. Maximum distance from the corner in this case is 391 µm.

How far from the corner can the cell align? To investigate the maximum distance of the alignment propagation in the 3D hydrogel and whether the alignment is due to the corner edges of the grooves or not, we fabricated a groove with large width (2mm) to be considered as a single edge (figure 3-10). Hence, the cells in 3D hydrogels in this structure are just restricted in one side. The measurements on confocal images were conducted using OrientationJ as described above.

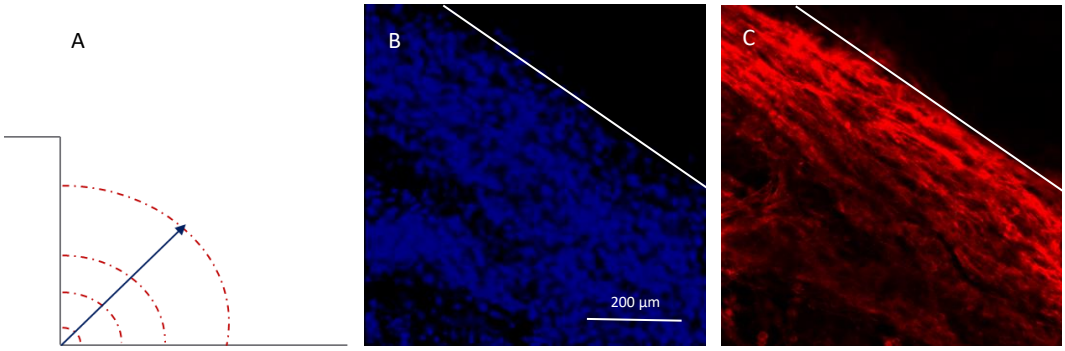

Figure 3-10 A. the contact guidance of the corner in a groove with infinite width. The middle confocal stack of H9c2 cells in co-culture with fibroblasts in 3D dECM-fibrin hydrogel B. DAPI staining, and C. Phalloidin staining. The cells are restricted in one side. The height of the groove is 350 µm and the width is 2mm which can be considered as infinite. Scale bar: 200 µm.

Figure 3-11 shows the distance from inner corner in each confocal stack. The results display that by increasing the distance from the side wall and the bottom of the groove the orientation gradually loses. In the layer of 400 µm above the substrate plane, no orientation can be detected. To have better understanding of the impact of distance from the inner corner on cell alignment, we calculated the distance by knowing the vertical and horizontal distance of each ROI and plot it versus the orientation index. Figure 3-11B demonstrates that the orientation of the cells can be retained up to ~250-300 µm distance from the inner corner of the wall. The alignment of the cells with distances more than that is gradually disappeared.

In the case of the groove with 350 µm by 350 µm dimensions, as the cells constraint with two walls, they will sense the contact guidance from both side, which leads to the extension of the orientation up around 500 µm distance.

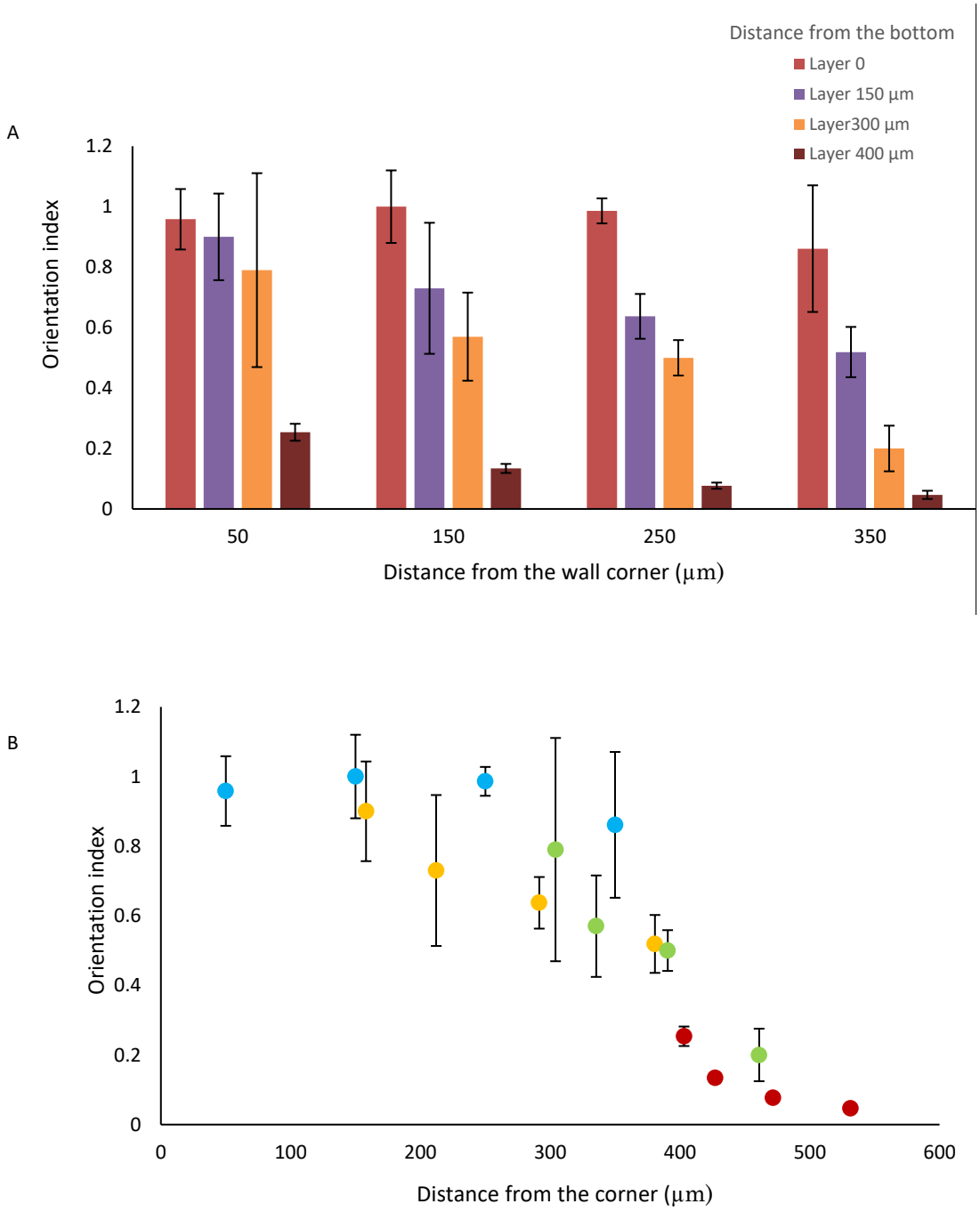

Figure 3-11 The measurement of cell alignment and its relation with distance from the groove's corner in a single edge configuration. A. the cell alignment in different height from the bottom of the groove. B. the orientation index in different distance from the inner corner of the groove. Maximum distance with the orientation of the cells is around 250-300 µm from the inner corner.

We continue the experiments with 350 µm groove dimension, due to the fact that in this size, we have the highly aligned 3D structure with the dimensions comparable to trabeculae carneae, and also, we are not concerned about the vascularization and oxygen and nutrient deficiency.

3.3.4 Detachability and stability of the hydrogel from PDMS substrate

One of the most important criteria for a 3D model is its ability to maintain the structure without external supports. It makes the structure more similar to the native tissue and provides a platform to study different parameters on the cells without limitations regarding the supportive material. Especially, in this case, although the PDMS is a great material in terms of its flexibility and transparency, its porous structure leads to absorption of media and compounds, which makes it not reliable for drug discovery studies. Therefore, having a 3D free-standing structure of the cells is a huge improvement. Using the introduced platform, we can easily peel off the cell-laden hydrogel and have the free-standing structure as it is shown in figure 3-12. The dimensions of this structure can be modified based on the application.

Figure 3-12A shows the cardiac cells in 3D patterned hydrogel in culture. The peeled off hydrogel in figure3-12B indicates the ease of handling and the stability of the patterned structure. Figure 3-12C is the macroscopic view of the cultured cells in 3D hydrogel without the support of PDMS mold for one week after detaching from the patterned surface. Finally, in figure 3-12D, the alignment of the cells in free-standing hydrogel is observed by staining the actin filaments of the cells with phalloidin.

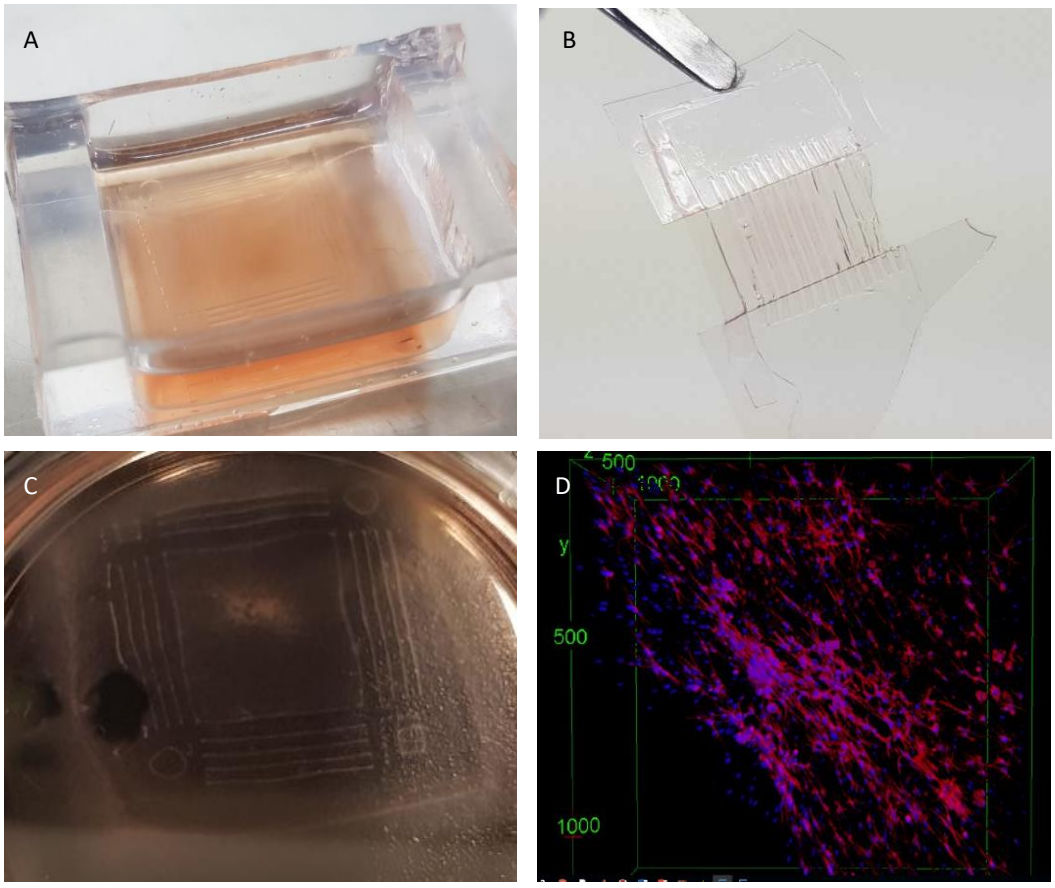

Figure 3-12 Patterned hydrogel A. the patterned hydrogel in culture. B. peeled off from the PDMS mold. It is easy to handle such a free-standing structure. C. the H9c2 cells alignment has been preserved in the peeled structure. The lines of aligned cells in the hydrogel are visible. D. the cells are stained with phalloidin and DAPI to show the alignment stability in the free-standing structure for 1 week after the detachment from the PDMS mold.

3.3.5 Beating characteristics

The beating rate of the neonatal cardiac cells in the patterned hydrogel was compared with the random distribution sample without any pattern. The results showed that the maximum frequency of the beating has not changed significantly. However, 3D patterned hydrogel maintained the beating for longer time than non-patterned. It is been shown that the contractility in random distributed sample last for approximately 10 days with the gradual loss of the beating rate from day 5. In the patterned sample, the beating loss happened after 14 days and it maintained the physiological beating till day 10. Figure 3-13 displays the alignment of the neonatal cardiac cells in the microgrooves and the comparison of beating rate in patterned and unpatterned hydrogel.

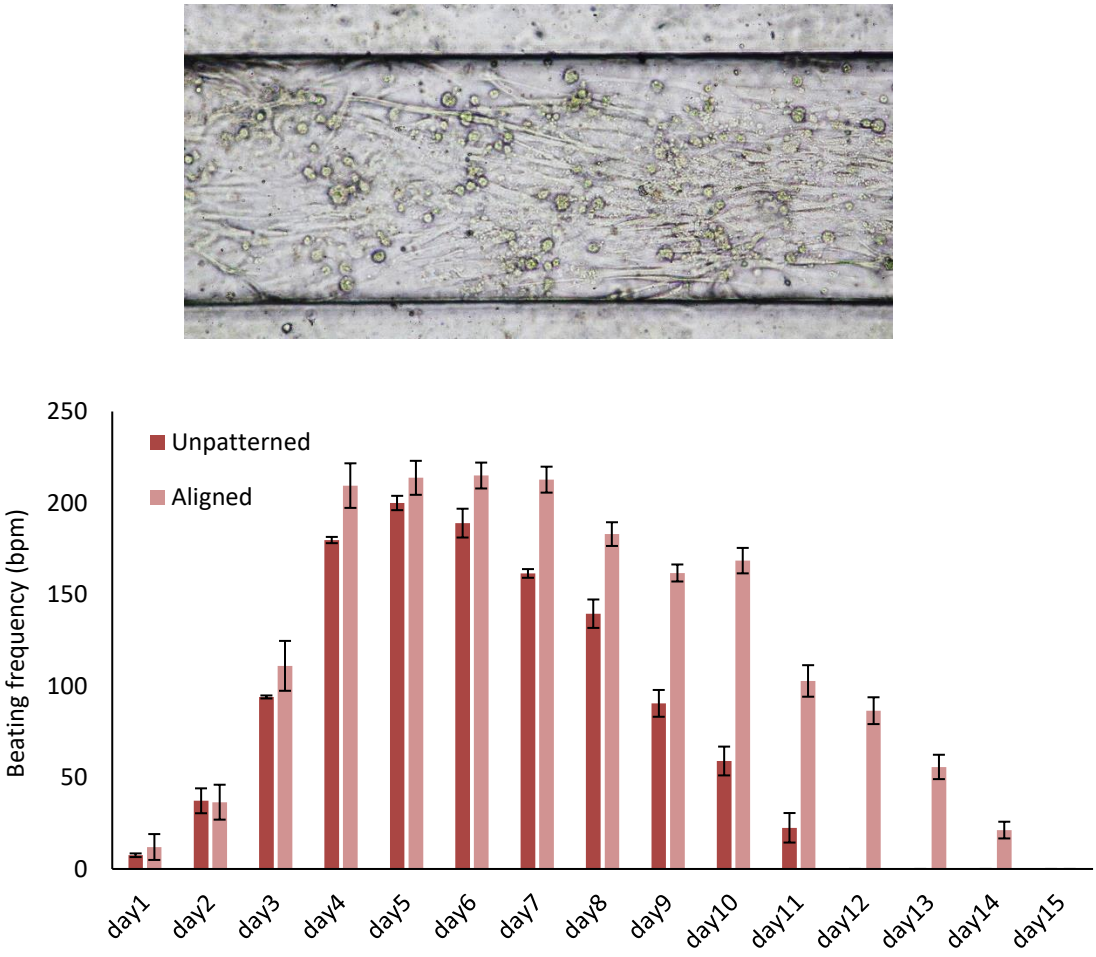

Figure 3-13 the comparison between the beating frequency in the 3D dECM-fibrin hydrogel, with and without pattern.

3.4 Discussion

The aim of this chapter was to develop a platform for aligning the cells in 3D environment in a size comparable with trabeculae carneae which is the smallest physiologically relevant part of the myocardium. Hence, we described a simple method to align the cells in free-standing condition and showed that the cardiac cells encapsulated in micropatterned dECM-fibrin hydrogel can self-organize into a 3D aligned structure without an external force. This alignment is due to the contact guidance of the inner corner of the grooves. Seeding cardiomyocytes in grooves of dimensions between 100 and 350μm in a 3D cell culture without any other interactions during cell culture is sufficient to obtain highly aligned 3D cardiac cells. We investigated the maximum dimensions of cell alignment propagation in an infinite groove to realize how far the cell orientation can be propagated from a corner, which is up to ~250-300 μm based on the measurements. This 3D constructs can detach from the PDMS surface that makes it an ideal model for drug screening studies. In addition, the neonatal cardiac cells cultured in this model displayed longer time maintenance of the contractility. Overall, this model can be considered as a recapitulation of the trabeculae carneae in *in vitro* condition which is the basis of many pharmaceutical, biological, and bioengineering studies.

One of the critical factors in cell orientation propagation is the stiffness of the microenvironment. It can define the distance that the cells can sense each other and their signals. The stiffer niche provides shorter distance. As it has been discussed in the previous chapter, the dECM-fibrin hydrogel that we have used in this work has interesting features for the differentiation, and functionality of the cardiac cells. The modulus of the native myocardium is in the range of 11.9 to 46.2 kPa. The mechanical properties of trabeculae carneae is also in the same range (around 20kPa)[275]. In the case of this study, the mechanical stiffness of dECM-fibrin hydrogel is around 20 kPa (as it is measured in chapter 2) and comparable with the native cardiac tissue, which suggest providing a microenvironment similar to the native heart myocardium *in vivo*. This means that the cells have almost the same physical environment and effect on their neighboring cells as they face in native tissue. On the other hand, the main component of the hydrogel is ECM which provides different biochemical and mechanical cues such as proteoglycans, growth factors, mechanical stiffness and structural features which helps the cell survival, proliferation, differentiation, and functional behaviors regulation.

In this study the cytoskeleton morphology of the cells was examined by staining the actin filaments of the cardiac cells, to confirm that the cell alignment is not just an artifact due to topographical restrictions, and it is originated from the cellular response to the guidance. Several studies indicated that cellular orientation leads to long actomyosin bundles formation [276]. F-actin filaments staining of the cardiac cells in patterned structure both in 2D and 3D shows that the actomyosin fibers are aligned in the direction of the microfabricated grooves. This actomyosin fiber alignment has also been reported

in the patterned substrates with subcellular dimension, in which the spatial constraints is not the problem [277]–[279].

Along with actin filaments alignment, nuclei elongation was also observed in 2D and 3D patterned structures. However, the nuclei were mainly spherical in the case of unpatterned surfaces. The observed elongation is comparable with the studies showing the cell orientation in a wide range of width and depth from nano to micro dimensions [5], [280]–[287], which confirm the response of the cells to the contact guidance and propagation of the alignment in bigger dimensions, in our case 350 μm width and depth.

We indicated that the cells which are sensing the groove's corner constraint are forced to reorient. This is in agreement with the study reporting that the cell orientation is initiated with sensing the edges of the microgrooves by filopodia [288]. As discussed in the introduction of this chapter, when the cells are culturing on microfabricated substrates, the contact guidance of the micropatterned structure encourages the cell to remodel and adapt to the environment. It is been verified that between surface topography and microenvironment properties, the topographical features have greater influence on cell alignment [289]. Based on this remodeling and reorganization, the cells which are close to the edge of the patterned substrate will get the directional growth in the direction of the pattern, and this topographical changes considerably influence the cytoskeletal organization, alignment, and cell morphology [5], [289]–[291]. One study investigated the 2D cell alignment in different microchannel dimensions and suggest that for the channels wider that 500 μm the orientation cannot be observed [292]. This is in agreement with our results in this study for 3D cell patterning, which observed clear alignment in the approximately wide microgrooves up to 350 μm by 350 μm width and depth and the loss of orientation for wider grooves. When the cells are limited in one side by the wall of the groove, the results showed that the alignment can propagate to around 250-300 μm from the corner in 3D environment.

The cells in native tissue perform mechano-electric feedback. It means that the neighboring cells can sense each other and remotely control their microenvironment and transfer the deformations through the ECM. Therefore, this alignment can be propagated to the neighboring cells and in the bulk of the 3D structure, as it is shown in the results.

One study used 3D printing of gelatin hydrogel for patterning the substrate and determined that the cells cultured on the patterned hydrogel in 2D which are in contact with the wall of microchannels align to the direction of channel and these aligned cells guide the neighboring cells to induce more alignment. Therefore, the cells within the channel respect the same direction. They reported that on wider channels (~800 μm), the guidance of the cells in contact with the edge is less effective, and no special orientation can be observed [292], [293]. Similarly, our study totally confirms the orientation in these dimensions and also use the same assumption to justify the alignment in 3D patterned hydrogel. Therefore,

the cell orientation in 3D hydrogel can be explained by edge sensing of the cells, contact guidance of the nearby cells and the propagation of the alignment in the whole structure.

The neonatal cardiac cells were aligned to the direction of the microgrooves. Their beating frequency has not altered, and was similar to the beating rate of the 3D random cell culture (~200 bpm) which is discussed in previous chapter. The dECM-fibrin hydrogel induced cardiac cell beating in the range of rat neonatal rate (around 276-423 bpm). However, the beating last for at least 2 weeks in aligned structures, which was a benefit compared to the non-patterned samples. These results are in agreement with several papers where they show the longer beating time and retaining the activity of the cardiac cells in the patterned samples. Whereas, a gradual loss of the contractility was observed on unpatterned substrates [5], [294]–[296]. The beating behavior of the cardiac cells *in vitro* is dependent on the density of the pacemaker channels [297]. It can be concluded that the alignment of the cells in addition to the mechanical and physical properties of the hydrogel can improve the recovery of the synchronicity and contractility of the cardiac cells *in vitro*. Hence, conducting q-PCR for quantifying the density of different ion channels in the cells in different states will provide evidences to explain the beating behavior.

The cellular alignment in the cardiac tissue dictates most of the physical, mechanical, and electrical properties of the cells and plays a vital role in tissue functionality. Using microfabricated grooves with dimensions up to 350µm × 350µm, we could align the cardiac cells encapsulated in the dECM-fibrin hydrogel, while preserving their viability and function, to create an *in vitro* trabeculae carneae.

In principle, the groove's size more than 350 µm are less relevant because of the deprivation of nutrients and oxygen for larger structures and lack of microvasculature. In addition, larger dimensions are not needed in this step, because of the fact that trabeculae carneae is limited to these dimensions. Controlling the alignment of the cardiac cells in 3D *in vitro* tissue models was a challenge, however, using this model, we can provide the smallest aligned myocardium tissue unit of the heart in the lab for more research in different fields.

One group of possible end-users of *in vitro* trabeculae carneae model is toxicologists and the pharmaceutical industry. They require realistic cardiac models in order to perform relevant pharmacokinetics and pharmacodynamics studies [172]. It is proved that the kinetics of drug diffusion obtained in 3D cardiac cell models have a behavior closer to native tissues compared to 2D tissue cultures. In 3D cardiac models that mimic the native tissue architectures, the cell–cell and cell–matrix interactions improve the cell function [298].

This chapter was dedicated to the alignment of the cardiac cells in 3D structure with defined dimensions to provide an *in vitro* trabeculae carneae model as the smallest cardiac tissue unit. Next chapter will focus on the mechanical stimulation application in 3D hydrogel. The reason of continuing the study with

applying mechanical stimulation is that, since the impact of external stimuli on the maturation of the tissues has been proved, we would like to improve cell functionality and maturity by providing more native tissue-like structure.

Chapter 4 Mechanical stimulation in the 3D cardiac cells cultured in hydrogel

Previous chapters have introduced the hydrogel for 3D cardiac cell culturing and a simple and efficient method to align cells in 3D constructs. This chapter presents the impact of mechanical stimulation on the functionality and alignment of 3D cardiac model and its relevance to the native tissue behavior.

4.1 Introduction

4.1.1 The native mechanical environment of cardiac cells

Mechanotransduction is the transformation of mechanical signals to the intracellular biochemical activities which regulates and alters the cell response to the external and internal forces [299], [126], [300]. In general, the cells can sense their microenvironment such as substrate elasticity, mechanical signals and biochemical cues, and respond accordingly, for example by reorganization or changing the protein expressions [300].

The cardiac cells in native cardiac tissues are located in a dynamic environment with a numerous mechanical (contractility of the heart), physical (blood shear flow), biochemical (gradient of different components), and electrical (signal transmission between cells) stimulations. This dynamic structure plays a great role in tissue metabolism, functionality, and the fate of cells. Cardiovascular diseases lead to

dramatic alteration, remodeling and reorganization in cardiac tissue, which finally leads to the heart failure and death [301]. Cardiomyocytes within the myocardium are locally orientated parallel to each other, and the resulting locally dominant myocyte orientation is referred to as 'fiber-orientation' [301], [296]. Native ventricular myocardium is composed of several sheets of oriented cardiac cells and myofibers. This orientation differs from endocardium to epicardium and forms a helical rotation which makes the complex cardiac tissue structure (figure 4-1) [301], [302], [303], [304], [305].

The mechanical cycle undergone by the cardiac muscle is known and has been outlined in the introduction of this thesis. The strain (elongation followed by contraction) amplitude in each cycle is about 20%, although the stress does not completely return to zero due to incomplete emptying of the ventricles (Table 1-2). As also illustrated in Table 1-2, the cardiomyocytes are both passively elongated (during cellular relaxation in diastole) and work actively against high load will contracting (systole). A static stress component remains at all points of time due to incomplete emptying of the ventricles (Table 1-2).

Locally, mathematical models of cardiac mechanics as well as the experimental measurements in animal cardiac tissue indicate that this overall complex mechanical setting leads to uniformity in the direction of cardiac fibers [306]. This in turn provides strong conduction and optimal distribution of the contractile forces of the heart as a result of mechanical anisotropy in this tissue [302]. How the different components of the local stress- and strain-cycles interact to produce or maintain such optimal local geometry is not fully understood at present.

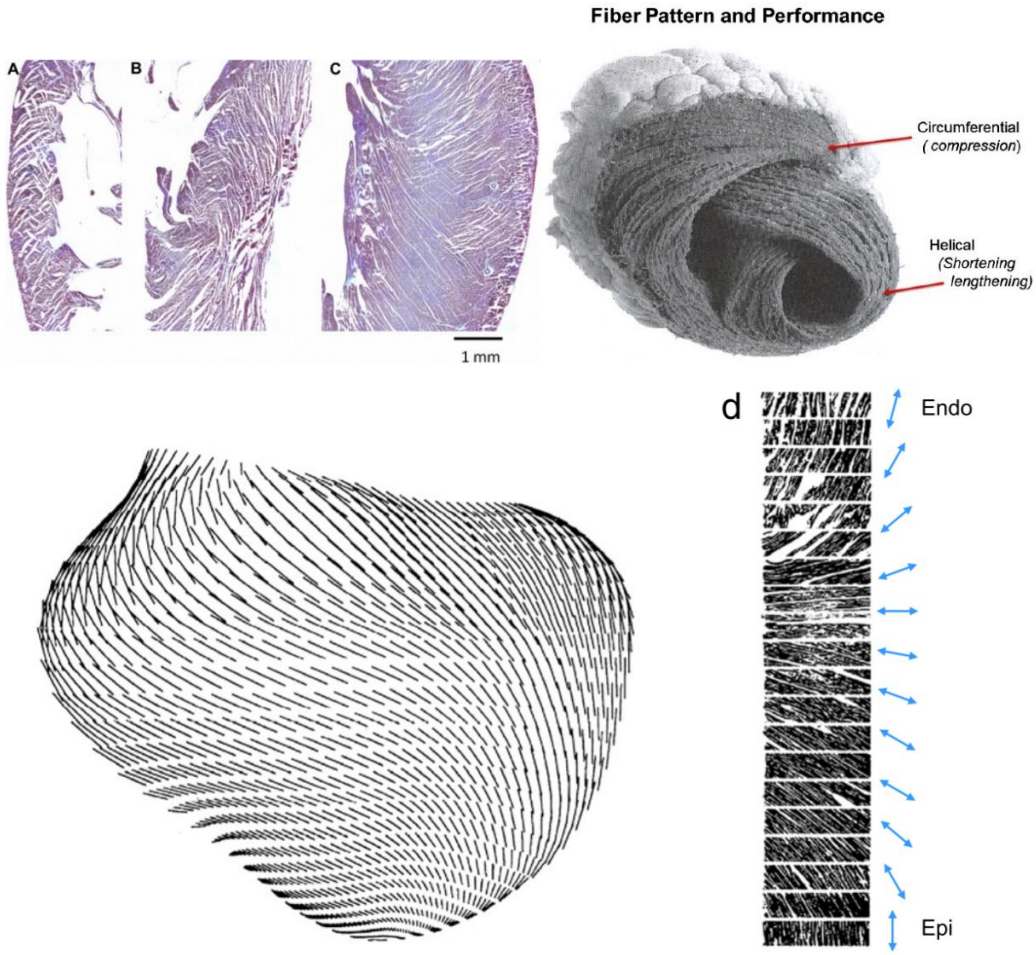

Figure 4-1 the configuration of the cells and fibers in native cardiac tissue. This organization differs from endocardium to epicardium which provides a helical rotation in the alignment of the cells [301], [307].

Beyond the local alignment of fibers along the main stress and strain direction, there is also a complex helicoidal organization evident at the macroscopic scale (figure 4-1). Indeed it is known that the heart muscle twists along its long-axis during ejection, which is supported by helical rotation in the fiber alignment of the tissue [50]. Indeed, ventricular contraction is accompanied not only by circumferential shortening, but importantly by clockwise basal rotation and counterclockwise apical rotation. Altogether, this produces a wringing motion. Mechanistically, this rotational motion arises not uniformly, but because superficially (subepicardially) generated rotation overpowers opposing forces generated more deeply (subendocardially) located fibers with opposing rotational orientation (figure 4-1). Indeed, due to the difference in the radius of the cross section in both base and apex of the heart, subepicardium creates higher torque than the subendocardium. The wringing motion during contraction also helps ejection because it progressively aligns both the superficial (subepicardial) and deep fibers (subendocardial) along the vertical (base to apex) axis of the heart, further enhancing shortening (figure 4-2). Similarly to the efficiency of wringing motions in drying tissue fabrics, this twist motion is critical for

heart function: without this torsion, the 20% circumferential contraction would at best lead to an ejection fraction of the human of about 15-20%, while physiologically, it reaches 60-70% [51]. Quantitatively, the rotation is major: the subendocardial fibers find a 60° angle to the long axis and the fibers in subepicardial run at an angle of 60° in opposite direction [51]. Any cardiac problem which leads to the alteration in the heart shape, can change the rotation of the heart and the angles of the myocardial fibers (figure 4-2) [51].

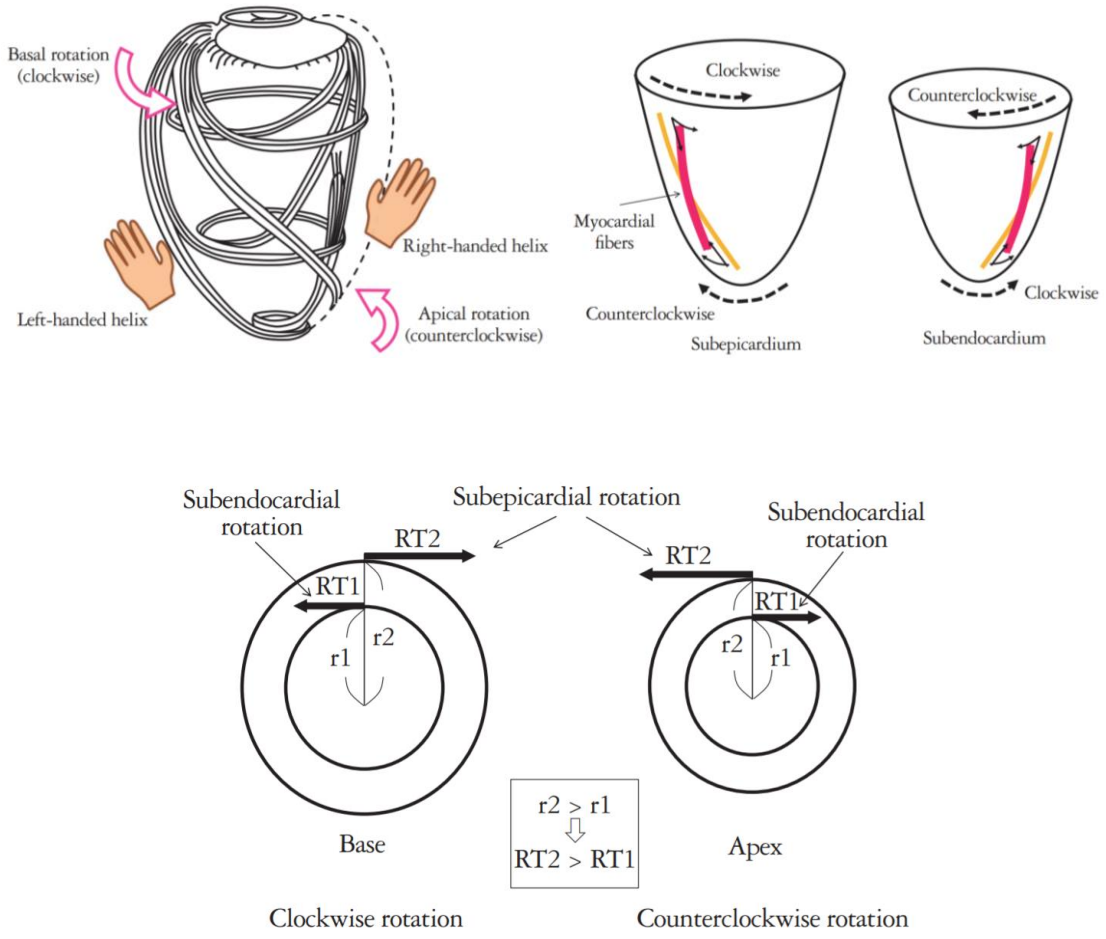

Figure 4-2 A. Myocardial fiber orientation and direction of rotation. Myocardial fibers in the subepicardium helically run in a left-handed direction, fibers in the mid layer run circumferentially, and fibers in the subendocardium helically run in a right-handed direction. B. Myocardial contraction and rotation. When myocardial fibers on the subepicardial side contract, clockwise rotational torque is produced at the base and counterclockwise rotational torque at the apex. When myocardial fibers on the subendocardial side contract, counterclockwise rotational torque is produced at the base and clockwise rotational torque at the apex. C. Opposite rotation at the base and apex. Subepicardial radius is larger than subendocardial radius (r2 > r1). Therefore, subepicardial rotational torque is larger than subendocardial rotational torque (R2 > R1). Reprinted with permission from [51]. Copyright © 2011 Korean Society of Echocardiography.

4.1.2 Mechanical environment and cellular phenotype

Based on this fundamental knowledge, one should consider that the repair of damaged cardiac tissue or providing a reliable cardiac model *in vitro* requires a special consideration of the mechanical behavior and function of the cardiac cells in dynamic microenvironment [308]. The ECM is composed of organized collagen fibers which contribute in mechanical stiffness and 3D structure of the native heart [309]. Therefore, the hydrogel that we introduced in this work, will be advantageous in promoting the cells to reorganize themselves in the direction of the collagen fibers. However, in static, stress-free conditions the mechanical microenvironment of the cells in native tissue is not appropriately recapitulated. Several studies have indeed shown that long-term culture of the cardiac cells in static conditions leads to a loss of their phenotype, functionality, and dedifferentiation [310]. For that, applying a mechanical stimulation to the system is a step forward to have a 3D cardiac model with the most similarity to the physical and mechanical properties of the native tissue [311].

Overall, it has been proven that the mechanical stimulation, for instance by uniaxial stretching, enhances the organization, functionality, cell morphology, proliferation, lineage commitment, differentiation and strength of engineered tissues [126], [145], [312], [313] [314]. Cellular responses to stretch stimulation may depend on the properties of extracellular matrix (ECM) and vary in different cell types and different mechanical stimulation regimes [126]. Figure 4-3 displays some of the most important effects of mechanical stimulation on cells, including the cell-cell, and cell-ECM communication, gene and protein expression, cell survival, and ion channel function.

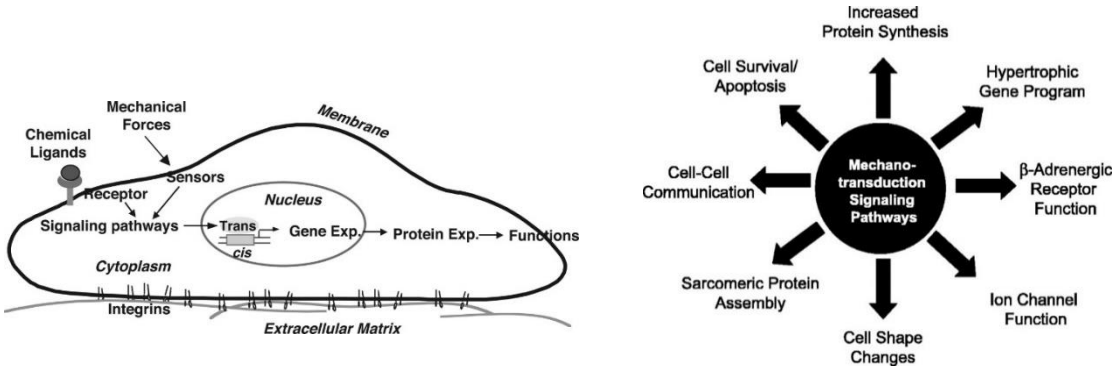

Figure 4-3 the impact of mechanical stimulation on cells. Mechanical forces to the cells alter the intracellular organization and response of the cell, which finally leads to promotion in cell-cell communication, survival, protein and gene expression, ion channel functionality alteration, etc. Reprinted with permission from[315], [316]. Copyright © 2005 by the American Physiological Society and Copyright © 2007, The American Physiological Society

Several research groups worked on applying mechanical stimulation in 2D and 3D constructs. This stimulation in 2D culture is mostly based on either the stiffness of the substrate material (as discussed in chapter 2), or the mechanical stretching of the substrate (e.g. uniaxial, biaxial, multiaxial) with different approaches (e.g. cyclic stretch, step-wise increasing the stretch, or holding a stretching regime for an extended period of time). The impact of mechanical stiffness on the substrate has been discussed in detail in chapter 2. Here, we focus more on the stretching of the cells in 2D and 3D. Overall, the interesting outcomes of all of these studies include cellular and sarcomere organization, gene and protein expression change, and improvement in functional properties.

Several investigations suggest that mechanical cyclic stretching in 2D leads to the proper excitation-contraction maintenance, activity of the stretch-sensitive ion channels, enhancement of gene expressions [126], [317]. Other studies investigate the impact of mechanical stretching on cardiomyocytes maturation by comparing the alignment, expression of myosin heavy chain and gap junction content, and increase of the binucleated cardiomyocytes [66], [128]. Dynamic stretching in 2D has impact on intracellular and extracellular organization [318]. Some studies showed the effect of stretching on augmentation of growth factors such as VEGF secretion [319]. Although these results are promising for developing a cardiac model *in vitro*, they do not meet the main criteria of the human tissues which is 3D tissue constructs.

The elasticity and stiffness of the biomaterial matrix due to the complexity of cell distribution and focal adhesions is more difficult to define in a 3D structure rather than 2D [145], with maybe the exception of simple cylindrical or ribbon-like geometries [82]. The presence of a variety of parameters such as cytoskeleton reorganization, cell-cell and cell-ECM interactions, limited nutrient and oxygen diffusion, as well as complex force distribution make the 3D models more difficult to design and understand. It is been shown in different studies [105], [116], [151], as well as this thesis, that the cardiac cells in 3D environment, even without mechanical stimulation promotes tissue function and maturity. Adding mechanical stimulation improves it even more, with improvements in cellular organization and integrity, increasing in cell length and width, increasing the mitochondrial density, upregulating the metabolic activity, and maintenance of cardiomyocytes phenotype[320]. The 4D (3D+time, figure 4-4) aspect is however a challenge in experimental design, as not only the hydrogel parameters, but also the stimulation parameters such as frequency, stress axes, amplitude and duration make it harder to compare

the studies (Figure 4-3, [315]). In any case, to potentially guide and manipulate matrix anisotropy, more insight in 3D is required [145].

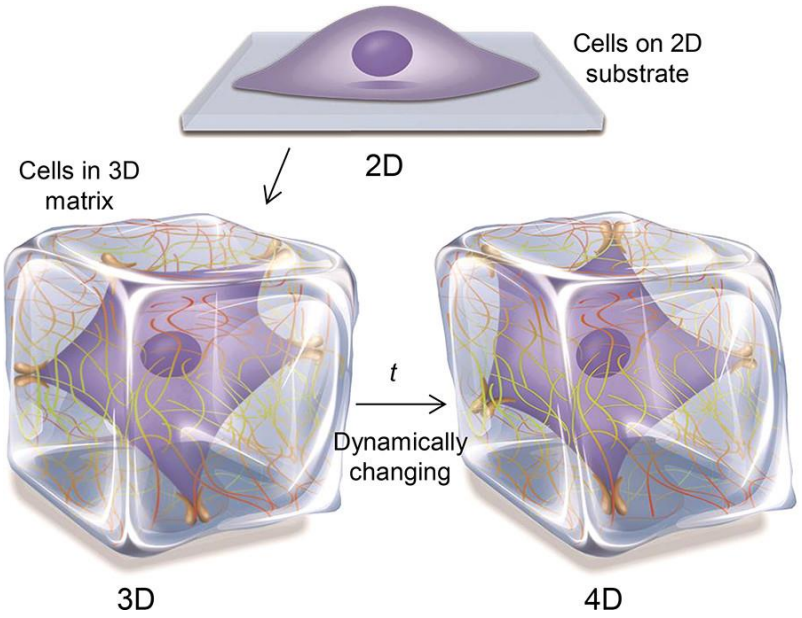

Figure 4-4 Schematic of engineering the cell microenvironment from 2D to 3D and 4D[59]. Reprinted with permission from [59]. Copyright (2017) American Chemical Society.

There are known synergistic effects between mechanical stimulation and use of other cues. For example, Gu et al. focused on the effect of mechanical stretching combined with substrate topography in 2D cultures of human mesenchymal stem cells. They observed significantly higher expression levels of desired markers, confirming a synergistic effect of a biomimetic environment (such as substrate pattern) and mechanical stimulation in their system [320].

4.1.3 Mechanical stimulation and cellular alignment

Understanding and predicting cell orientation in 3D structures to obtain functional tissue engineered constructs is crucial, since the cell orientation strongly influences tissue mechanics [308]. The strong geometric and also the unusual helicoidal organization of the native heart raises the question of the mechanisms of cell alignment. Beyond a favorable biochemical influence, one would expect the cardiomyocytes to use mechanical cues of their particular static and dynamic environment for the purpose of optimizing cell orientation.

To investigate this, stretching experiments in various configurations have been performed in the literature. Stretching of cells in general and cardiomyocytes in particular can fundamentally be carried out in a static mode (extension or force maintained) or a dynamic mode (cyclic), in 2D or 3D [104], [126]. Due to the spontaneous beating in activity cardiomyocytes, dynamic stretching can be further synchronous with electrical excitation (for example, by working against an external spring load [82]) or be imposed irrespective of spontaneous electrical and contractile activity. Given the many parameters involved, the research field at present is at the stage of assembling the elements.

Based on the Zimmermann *et al work, n*early perfect parallel cardiomyocyte arrangement including in 3D millimetric structures was obtained by self-condensation in defined extensional geometries (presumably mostly static stress [82]). This alignment was maintained during auxotonic contraction (with both deformation and force varying over time, synchronized with beating activity by the use of an external spring as a load [82]). However, no trace of helicoidal cell orientation was found in such geometries.

In 2D cultures, conflicting results regarding cell alignment were found when applying external cyclic stretch. Indeed, both Dhein *et al*. [121] and Salameh *et al*. [133, p. 43] performed uniaxial cyclic stretching of neonatal cardiomyocytes on ECM-functionalized PDMS membranes. Dhein *et al*. [121] observed nearly parallel, Salameh *et al*. [133, p. 43] essentially perfectly perpendicular orientation with regard to the stretch axis. These results are not only conflicting, but challenging to interpret. Dhein's observation of parallel alignment seems in intuitive agreement with the self-condensation experiments [82] and the native structure of the heart and its alignment of cardiomyocyte along the collagen-fibers and direction of local contraction [51]. Yet, in cyclic stretch experiments, perpendicular alignment is observed for a wide range of cells [308], rather in agreement with the observations by Salameh *et al*. [133, p. 43].

The conflicting results and apparent inconsistencies point towards a lack of understanding of the full set of experimentally important conditions. A first aim of this chapter is to evaluate what type of alignment cyclic stretch in a 3D environment would produce, as the observed conflicting results might result from non-physiological 2D effects.

An important observation in this regard is that a substrate of sufficient stiffness is required for efficient cellular orientation. Ghibaudo et al. [300] indeed investigated the morphological changes and migration responses in 3T3 fibroblasts cultured on PDMS pillar arrays. By varying the shape and length of the pillars, they could produce virtual surfaces of defined overall rigidity and anisotropy. In this setting, they found that the fibroblasts aligned along the direction of strongest rigidity, by development of stress fibers and focal adhesions in the direction where the substrate deformation was least. On overall softer substrates, this mechanism was less efficient, as focal adhesions remained less defined [300]. Therefore, for experiments implicating cellular orientation sufficiently stiff substrates are required. This basic requirement for the study of cellular orientation by mechanical cues is met by dECM-fibrin composites,

as the minimal requirement is that cells should be able to successfully spread [300]. As shown in chapter 2, this is indeed the case for the H9c2 cells, fibroblasts, and neonatal cardiomyocytes.

Beyond the question of 3D vs. 2D conditions, it seems probable that the cells integrate a variety of local mechanical microenvironment cues, some leading to perpendicular, and others to parallel orientation, to determine their final alignment angle. An insufficiently understood component in cyclic stretch experiments could explain the inconsistencies. To address this possibility, it is necessary to develop a deeper fundamental understanding of how cells integrate mechanical cues to determine alignment.

The alignment of fibroblasts has been comparatively well studied, and so we shall use experimental and theoretical results from their study to develop a more fundamental view here. For fibroblasts, it is well established that cyclic strain leads to alignment perpendicular to the direction of deformation, a phenomenon referred to as strain avoidance [134], [308]. At first glance paradoxically, it is also well accepted that fibroblasts align parallel to the main axis of stress in self-organization experiments [135].

Detailed mechanical modelling resolves this apparent contradiction and simultaneously provides a possible cellular integration mechanism [308]. The fibroblasts cells constantly probe their environment by excreting traction [308]. If the substrate gives way to this traction, stress fibers in that direction are depolymerized, and their actin monomers redistributed to the remaining stress fibers, that are correspondingly reinforced [308]. The cells ultimately align to the axis with most stress fibers. In this view cyclic strains leads to periodic compression of the stress fibers oriented along the main cyclic strain direction. This leads to their depolymerization [308], with a resulting re-orientation perpendicular to oscillatory principal strain and stress axis [308].

In self-condensation experiments (fibroblasts:[135], similarly with cardiomyocytes: [46]), the substrate can be condensed in all directions, except the externally maintained long axis imposed by the experimental geometry. The substrate giving way in all but this preferred direction, the stress fiber model [308] predicts that the stress fibers will be maintained preferentially along this preferred direction. Given the pulling action of the cells, this is also the main direction of stress, and this result in parallel alignment to the main axis of the experiment, as opposed to perpendicular one in cyclic stretch.

Hence, according to the stress fiber dynamic model [308], although the fundamental mechanism of depolymerization of stress fibers upon loss of tension, or worse compression, is the same in both cyclic stretch and self-condensation experiments, the macroscopic observations are different. Alignment occurs perpendicular to both main stress and strain direction in cyclic stretch, but along the main stress and minimal strain direction in self-condensation experiments. Self-evidently, this analysis should serve as guard against overly inaccurate generalizations of cell alignment along or perpendicular to main stress or strain directions in a given experiment. In fact, in the cyclic strain experiments, the linear static

strain component is typically neither controlled nor specified, and the analysis above suggests that this unspecified component may account for major experimental discrepancy.

Besides clarifying possible differences between 2D and 3D geometries, it is also an aim of this chapter to evaluate the possibility to produce oblique alignments between 0° and 90°, to lay a basis of future developments of helicoidal structures as found in the native heart.

There are indeed signs in the literature that by more subtle force interplay, intermediate angles are possible. In the cyclic strain experiment by Dhein et al. [121], cardiomyocytes show only nearly, but not fully parallel orientation with the main strain axis. A deviation of 11-20° was indeed observed [121]. The precise reason for this observation could not be elucidated in the study by Dhein et al [121]. A temptative hypothesis would be that the cell integration mechanism for determining the preferred long axis is not digital, but analogous, with different influences being integrated by the actin polymerization and depolymerization dynamics [308]. Such an integration mechanism between different alignment cues has indeed been observed before, namely in a 2D setting by the interaction of chemical pattern in 2D with cyclic stretch stimulation , using the myoblast cell line C2C12[321].

With the insights provided here, and the results of chapter 3, intermediate angles to a preferred direction should be possible to achieve experimentally: Cyclic stretch should produce a perpendicular orientation, geometric alignment in grooves a parallel one. If the cells can integrate both cues through their cytoskeleton dynamics [308], applying both should lead to intermediate orientations. Orientation at oblique angles also suggests a connection to the helicoidal structure of the heart, with incremental small rotations through the layers from endocardium to epicardium (figure 4-2). However, while suggestive, we cannot possibly prove such a hypothesis here. The experiments performed here are indeed purely *in vitro*, and the complex process of the embryonic development of the heart by itself contributes to laying down appropriately oriented tissue. These processes result from the coordination of migration, growth, contraction and physical forces [322] that are far beyond the scope of this thesis.

Therefore, the first goal of this chapter is to understand how cardiomyocytes orient in response to mechanical stimuli in 3D constructs. The second aim is to evaluate whether the cells are capable of integrating the geometric alignment cues (chapter 3) with mechanical stimulation cues to achieve intermediate orientation angles. This understanding of the impact of mechanical forces on the alignment of the ECM is important in developing cardiac models, where providing appropriate mechanical anisotropy is essential [323]. In future work, it may be the basis of a more complex helicoidal alignment unit.

Here, we develop a platform to culture and align the cardiac cells as realistically as possible to native tissue. We design and fabricate a user-friendly stretching device for studying the impact of mechanical stretching on 3D structures. An interface is developed to control different parameters like the frequencies and elongation. Also, a mold is designed for fabricating a flexible chamber of 4 cm^2 with grooves at

the bottom as a platform for 3D cell culturing. Cell stretching within 3D constructs is one of the most effective and physiologically relevant stimulations for tissues. We provide here a reliable and realistic platform for 3D mechanical stretching with appropriate function to use in *in vitro* cardiovascular tissue engineering[312], and use it to provide proof of principle of off-axis alignment.

4.2 Materials and methods

4.2.1 Stretching device and working principle

The fabricated device is designed to culture cells especially cardiac cells in a standard CO_2 incubator and impose controllable uniaxial stretching motion on the cell-seeded transparent PDMS chamber during the culture procedure. The designed stretching device can precisely manage the elongation and frequency of the stretching motion using a software interface written in MATLAB. This stretching device can be easily installed in and removed from a CO_2 incubator.

The apparatus consists of three parts, as shown in Figure 4-5. The first part (figure 4-5A) is a computerized control system used outside of the incubator composed of an electrical board (Step motor controller, TMCM-1110 STEPROCKER, Trinamic) which is connected to the mechanical stimulator device using wires and can be controlled easily by a user-friendly interface to adjust the desired elongation and frequency. The second part is (figure 4-5B) the mechanical device which is composed of a stepper motor (5 mm, 1.8°, 0.06 Nm, QSH2818-32-07-006, Trinamic) which is used to apply the mechanical cyclic stretching motion to the PDMS chamber using a stainless-steel screw connected to the movable part of the stretching jaw. The third part (figure 4-5C) is a transparent PDMS chamber for culturing the cells in 3D constructs. This PDMS chamber can be fabricated either with or without the microgrooves on its surface. This part can be easily fixed to four pins provided on the device. The PDMS chamber is fixed in one side and movable in the other side to apply the stimulation to the cells in culture.

The PDMS chamber is autoclavable and is covered with a PDMS lid to prevent the contamination of the cell culture. The working place of the device can also be sterilized with 70% ethanol. Hence, the risk of contamination is low.

4.2.2 Design of control system

To control the frequency and elongation of the chamber, we wrote a MATLAB code. This code provides a user-friendly interface which is shown in figure 4-6 to control different related parameters such as the elongation and frequency.

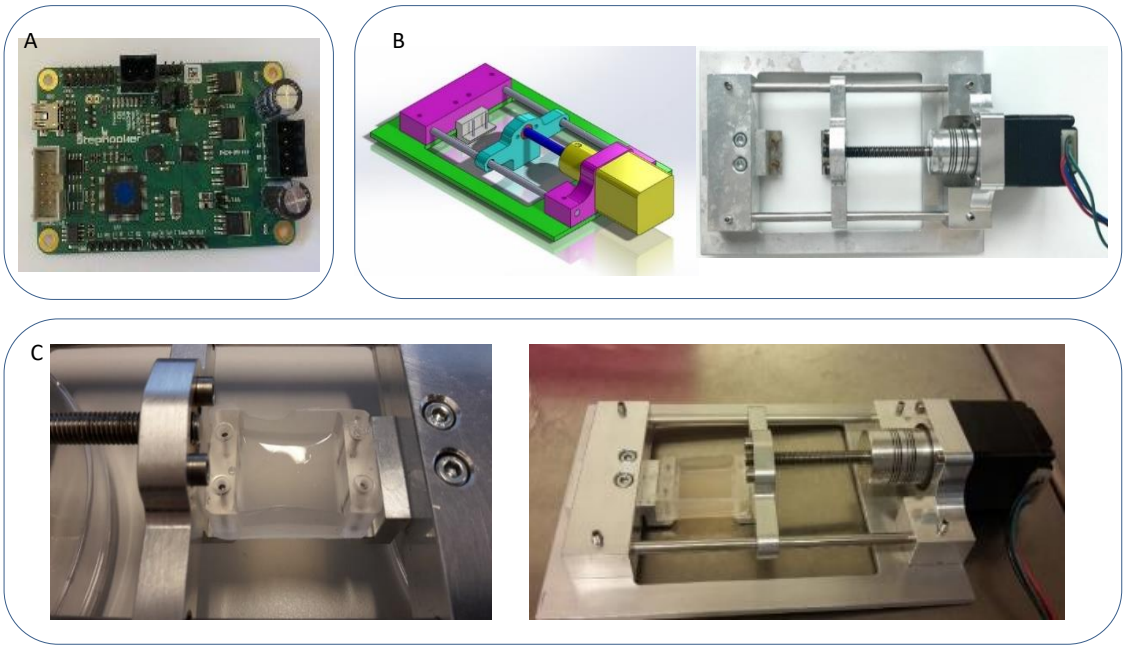

Figure 4-5 Schematic of the mechanical stretching device. A. electronic board for controlling the device, B. Schematic of the mechanical system, and the real fabricated mechanical device. C. flexible, PDMS chamber placed in the device.

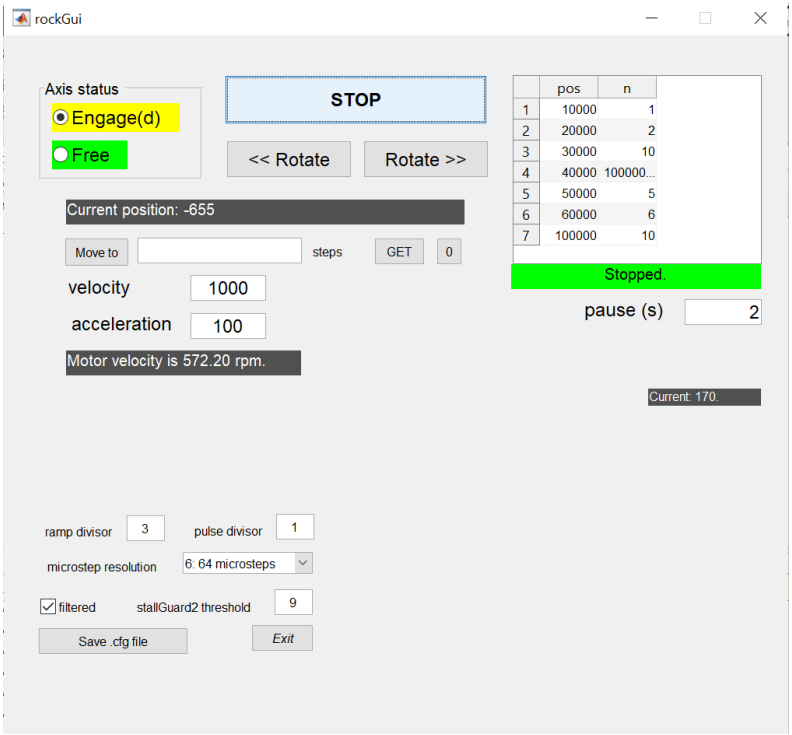

Figure 4-6 The interface of the mechanical stimulator. Different parameters can be adjusted.

4.2.3 Design of transparent chamber for cell culture

PDMS has several features such as mechanical stability and elasticity, chemical inertness, optical transparency, gas permeability, ease of fabrication, and biocompatibility which makes it well suited for cell experiment applications [324]. The schematic design of the mold for PDMS chamber preparation is shown in figure 4-7A. We use Polytetrafluoroethylene (PTFE) to fabricate the mold which enables us to inject PDMS in it (figure 4-7B). After the PDMS injection, it is placed in an 80°C oven for 2 hours to cure. For the PDMS chamber with the grooves, microgrooves were fabricated using direct laser writing photolithography and deep silicon etching using the standard Bosch process with channel size × spacing of 350 × 350 µm (As it is described in detail in chapter 3). This master molds have been used to pattern polydimethylsiloxane (PDMS) and the patterned PDMS was replaced manually at the bottom of the chamber (figure 4-7C).

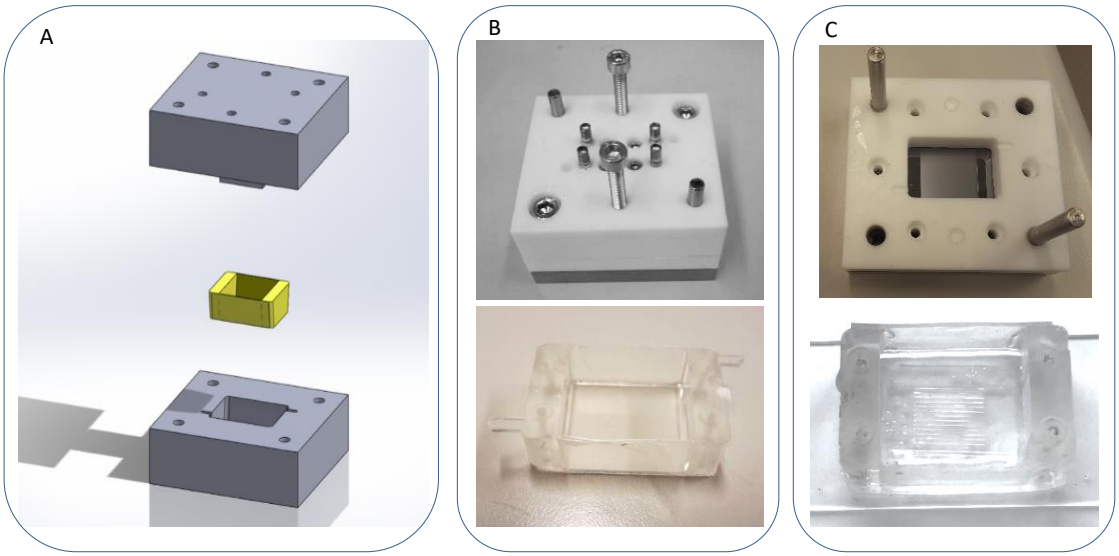

Figure 4-7 PDMS chamber fabrication, A. the schematic of the mold design, B. the PDMS chamber fabrication without grooves, C. PDMS chamber fabrication with grooves.

4.2.4 Cell culture

We conducted experiments with two groups of cells: H9c2 in co-culture with fibroblasts, and neonatal cardiac cells from rats. The H9c2 cell line, obtained from the European Collection of Authenticated Cell Cultures (ECACC) (Lot# 17A028), was cultured in DMEM medium supplemented with 10% fetal bovine serum and 1% penicillin and streptomycin in 75 cm^2 tissue culture flasks at 37°C and 5% CO_2 in an incubator. The neonatal cardiac cells were isolated from newborn rat's heart and used freshly after isolation. The neonatal cells also were cultured in DMEM supplemented with 10% fetal bovine serum and 1% penicillin and streptomycin.

4.2.5 dECM-fibrin hydrogel preparation and cell seeding

To demonstrate the impact of mechanical stimulation on 3D cardiac cell culturing, we used the same dECM-fibrin hydrogel, that has introduced and characterized in chapter 2. Briefly, it was obtained by mixing dECM and fibrinogen at a final concentration of 5 mg/mL and 26.4 mg/mL, respectively. Once all components have been mixed, the H9c2 cells in co-culture with fibroblast cells were added to the pre-gel at a concentration of 1×10^6 cells/mL. Lastly, thrombin and calcium chloride were added to the pre-gel solution to trigger the gelation of the hydrogel. 500 µl of the cell-suspended solution was rapidly poured in the PDMS chamber with and without the grooves to solidify and pattern the hydrogel. The medium was changed every two days. The same cells have been cultured on the substrates without the hydrogels, as the control group for comparison between 2D and 3D mechanical stimulation effects.

4.2.6 Hydrogel adhesion to the PDMS chamber

Although PDMS has properties of interest for cell culture, its extremely hydrophobic nature often limits its applicability[325]. Therefore, various methods have been proposed to modify the PDMS surface to convey hydrophilicity ranging from oxygen plasma treatment to chemical modifications[324]. In this work we used plasma treatment (as described in chapter 3) to modify the chemical surface groups of PDMS and right after the plasma treatment, the hydrogel was placed in the chamber. The connection between the hydrophilic surface and the hydrogel provides sufficient bonding to prohibit the detachment of the hydrogel from the PDMS chamber. We suggest that coating the PDMS chamber with hydrophilic hydrogel would be effective enough and enhance the attachment of the hydrogel to the PDMS chamber as no detachment has be observed during mechanical stimulation time period. The resulting PDMS-patterned hydrogel environment was used as an *in vitro* cell culture platform to study 3D cellular behavior in response to cyclic mechanical strain.

4.2.7 Mechanical stimulation

The cells in 3D dECM-fibrin hydrogels were incubated 48 hours before mechanical stimulation to have enough time for cell attachment and spreading either in the hydrogel or to the plasma-treated PDMS surface. In this work, we chose 15% elongation and 1Hz frequency which is the physiological range of mechanical stimulation in native heart. This regime was applied to the samples 4hours/day for one week. The reason of choosing an intermittent stretching regime is that it is confirmed that intermittent mechanical stimulation compared to continuous stimulation, leads to higher tissue regeneration and improve the expression of cardiac related genes and proteins [326].

4.2.8 Immunostaining and 3D imaging

To investigate the expression of proteins, the samples were stained. For that, the samples were washed with PBS and fixed with 3% paraformaldehyde (PFA) for 15 min at room temperature. Then, they were washed again with PBS and permeabilized with Triton 0.3% in PBS for 15 min. In the case of phalloidin staining for actin filaments, the cells were incubated with phalloidin-Atto 488 (1:50) for 45 min at 4°C. For α-actinin, and connexin-43, the staining procedure continued by another washing step with PBS, and blocking with PBS-BSA 1% for 10 min at room temperature. The primary antibody in PBS -Tween 0.1% - BSA 1% was added to the samples for either 1 hour at 37°C or overnight at 4°C. They were washed another time with PBS-Tween 0.1%, and the secondary antibody in PBS -Tween 0.1% - BSA 1% was added to the sample for 1 hour at 37°C. Finally, the cells were washed and stained with DAPI for 5min, for labelling DNA. DAPI is then removed and replaced with DPBS before imaging the cells under the ZEISS LSM 700 inverted confocal microscope.

4.2.9 Beating characteristics

To assess the contractile properties of primary cardiomyocytes in 3D cultures, we suspended the primary rat cardiomyocytes at a cell density of 10^6 cells/mL in pre-gel mixtures of dECM-fibrin and poured it in the PDMS chamber to apply mechanical stretching. The cultures with and without mechanical stimulation were followed both visually and videographically. To quantify the mechanical beating rate of the cells, movies were acquired by connecting a video camera to the microscope. Temporal peak detection was based on a custom ImageJ plugin in Java, which was introduced in chapter 2 [222]. We used this plugin to evaluate local beating frequency and temporal phase shift from the heatmap videos of the samples with and without mechanical stimulation.

4.3 Results

4.3.1 Mechanical stimulator

The fabricated mechanical stimulator device integrated well into the cell culture condition without any special problem. The PDMS chamber fabrication was also replicable and easy to handle. Using the MATLAB code, one can control the elongation and the frequency of the stimulation. Also, the hydrogel was completely attached and connected along all the corners to the PDMS chamber. We assume similar tissue strains in different 3D structure layers.

4.3.2 Cell orientation in 2D and 3D culture, with and without patterning

Based on the findings of the previous chapter, in the static condition, the cardiac cells cultured in the 3D hydrogel without any pattern, distribute homogenously in the dECM-fibrin hydrogel, according to the polymer chains of the hydrogel and no specific orientation can be observed. However, using micro-grooves for patterning the hydrogel encourage the cells to align in the direction of grooves. This alignment can propagate to the whole structure with the dimensions of 350 µm × 350 µm. Figure 3-6 in chapter 3 shows these results.

In this chapter we studied the impact of dynamic stretching by applying mechanical stimulation to the cells which are cultured in 2D or 3D, with and without pattern. This allows to address the influence of mechanical stimulation in 3D, and also the interplay with geometric alignment. In 2D, the cells align along the grooves in the absence of mechanical stimulation (chapter 3). They orient perpendicularly to the stretch direction on flat PDMS substrates, in agreement with the results by Salameh *et al*. [133], but not Dhein *et al*. [121]. When applying stretch to cells cultured on patterned substrates, the effect of stretch dominates and orientation nearly perpendicularly to the axis of stretch is observed (figure 4-8A to C).

The cell responses in 3D structures was different. By applying the mechanical stimulation to the samples in the hydrogel without patterning, slight orientation perpendicular to the stretch axis is found (figure 4-8D, P= 0.013 against 45° for random orientation between 0° and 90°). However, possibly due to difficulties in coupling of the mechanical stretch from the flat PDMS to the hydrogel, the effect remains comparatively weak. When the mechanical stimulation is applied cells cultured in 3D, on grooved substrates, the result depends on the configuration between stretch and groove direction. When the cyclic stretch is applied in the same direction of the microgrooves, the cells orient themselves to a direction with an angle around 40 to 60° to the direction of the mechanical stretching. Figure 4-8F shows the orientation of the cardiac cell in 3D culture with the mechanical stimulation parallel to the direction of microgrooves. On the contrary, as it is shown in figure 4-8E, if the cyclic stretch is applied perpendicularly to the grooves, the orientation of the cells along the grooves (and perpendicular to the stretch) is reinforced (t-test between grooves only and grooves + perpendicular stretch, P= 0.21). Figure 4-8G shows explicitly the combination of two stimuli due to mechanical stimulation and topographical alignment which leads to the formation of a competition and orienting the cells at an angle around 45°. Figure 4-8H quantifies the orientation degree based on different conditions.

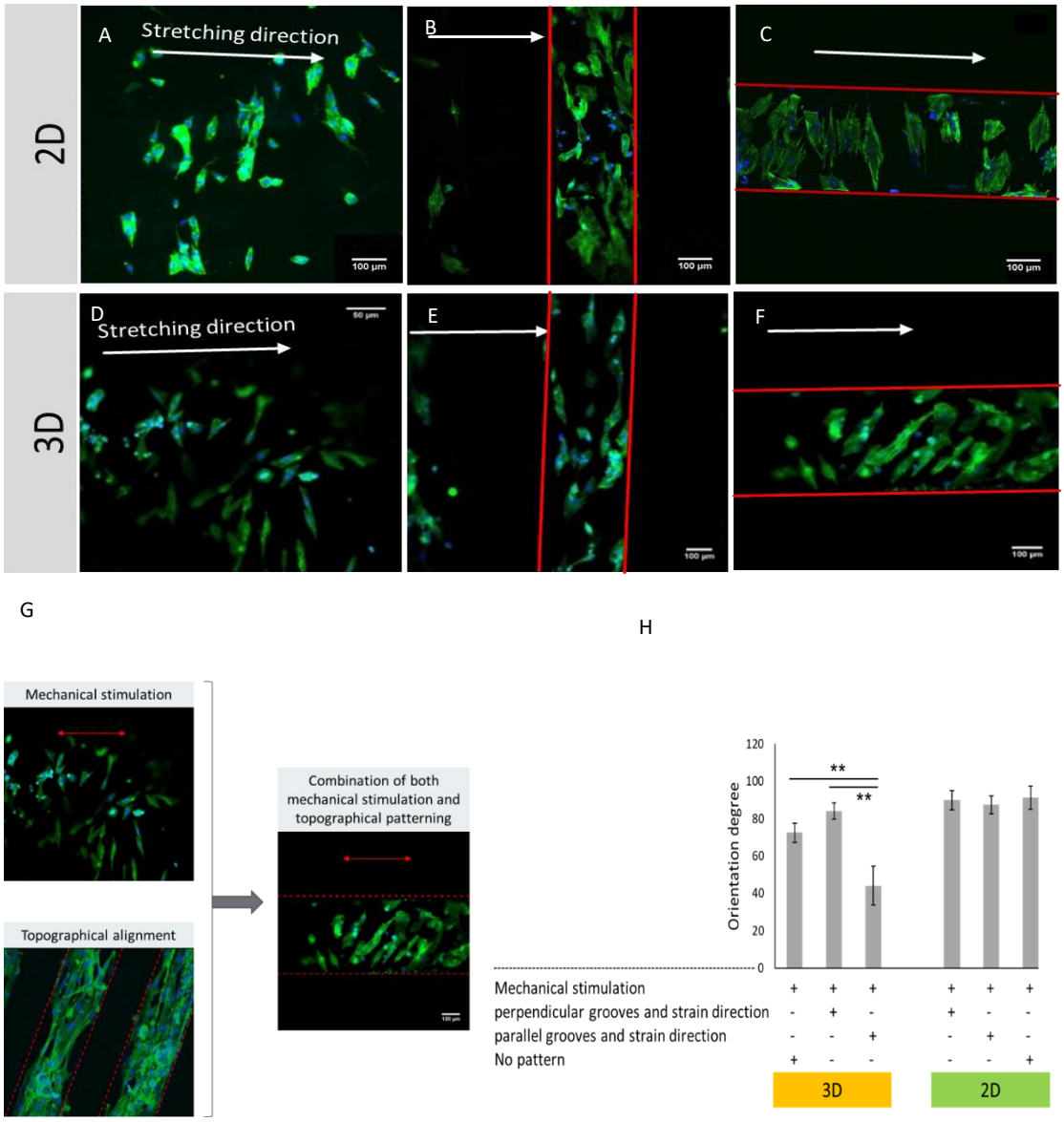

Figure 4-8 H9c2 co-cultured cells in 350µm width and height grooves stimulated under A, B, C. 2D culture, and D. 3D condition without pattern, E. 3D condition with pattern perpendicular to the direction of stimulation, and F. 3D condition with the pattern parallel to the stretching (15%, 1Hz). Stained with Phalloidin and DAPI. Cell concentration (1 million cells/mL). G. the competition between mechanical and topological patterning. H. the degree of orientation in different culture conditions.

Overall, our results confirm strain-avoidance in cyclic stretch [133], [308] in 2D and 3D, and show that cell alignment by topography and cyclic stretch interact and can produce intermediate angles.

4.3.3 Expression of cardiomyocytes related markers

We performed immunofluorescence staining for α-actinin and connexin-43 in both groups of cells, with and without mechanical stretching after one week, and quantitatively analyzed their expression to

compare these two groups. According to the images of the staining, the expression of connexin-43 and α-actinin increased strongly in the sample with applied mechanical stimulation (figure 4-9).

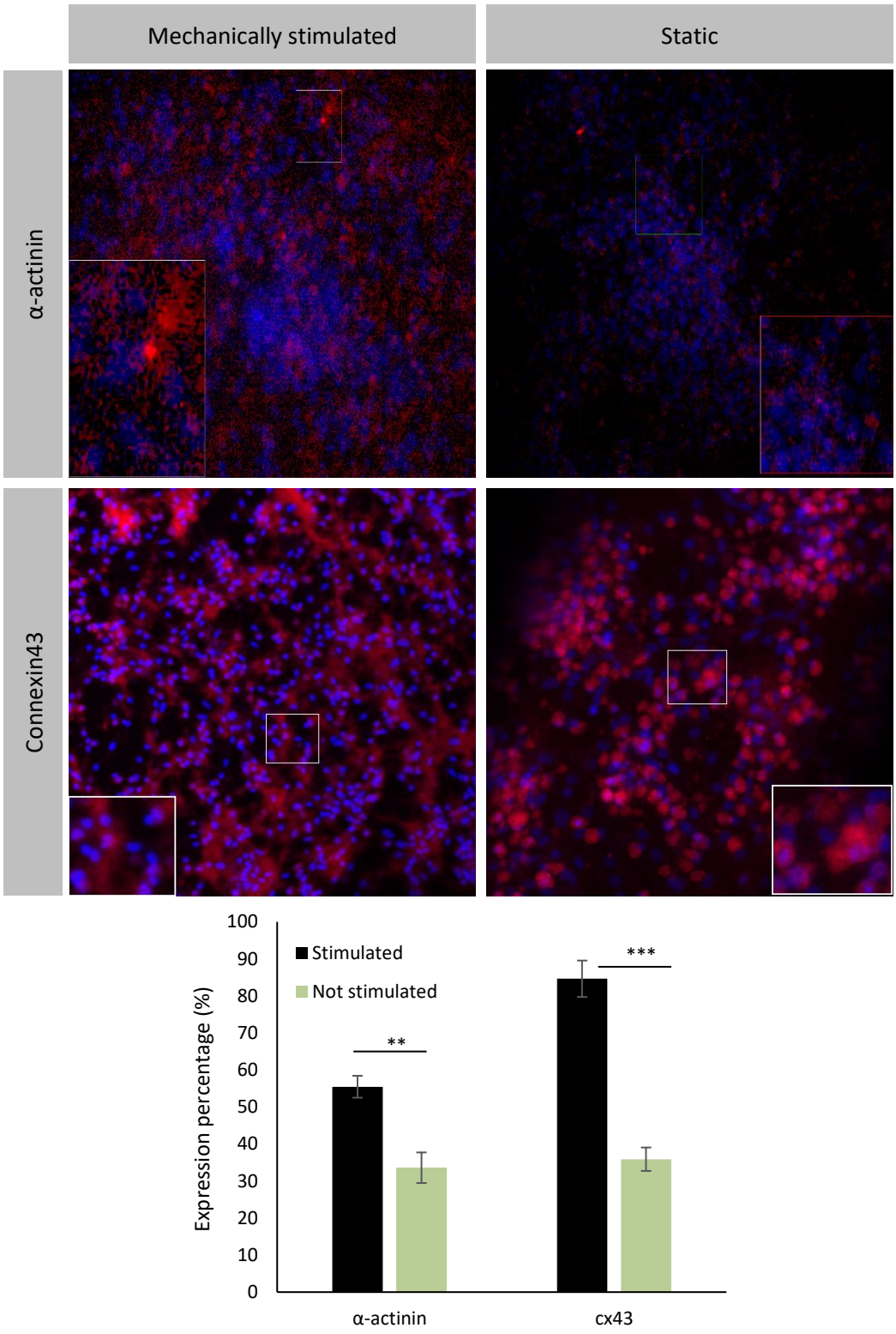

Figure 4-9 The expression of α-actinin and connexin-43 in neonatal cardiac cells cultured in 3D dECM-fibrin hydrogel under mechanical stimulation and static condition (without mechanical stimulation). A. the immunofluorescence stainingof the neonatal cardiac cells, B. the expression percentage of the proteins.

We quantified the protein expression percentage as the surface area covered by cells expressing the marker, relative to the total area of the fluorescent images. This approach assumes that there is little cell growth in our conditions, and near 100% confluency. The expression of α-actinin and connexin-43 which are more mature genes increases (P= 0.0017 for α-actinin, and 0.00013 for connexin-43). Hence, the combination of both 3D culture and mechanical stimulation improves cardiomyocytes maturation, confirming prior results also in our particular setting [320].

4.3.4 Beating characteristics of neonatal cardiac cells

From the videos of neonatal cardiac cells cultured under mechanical stimulation or without stimulation, we evaluated local frequency (Figure 4-10) and local phase (Figure 4-11). The results indicate essentially perfect synchrony in the 3D dECM-fibrin hydrogel, in both conditions. The noises are mostly because of the 3D culture condition. The local frequency results show higher frequency in the sample with applied mechanical stimulation. The results of visual quantifying the beating rate, 10 days after the culture and applied mechanical stimulation, shows around two times higher beating rate in the stimulated sample (120bpm vs. 60bpm).

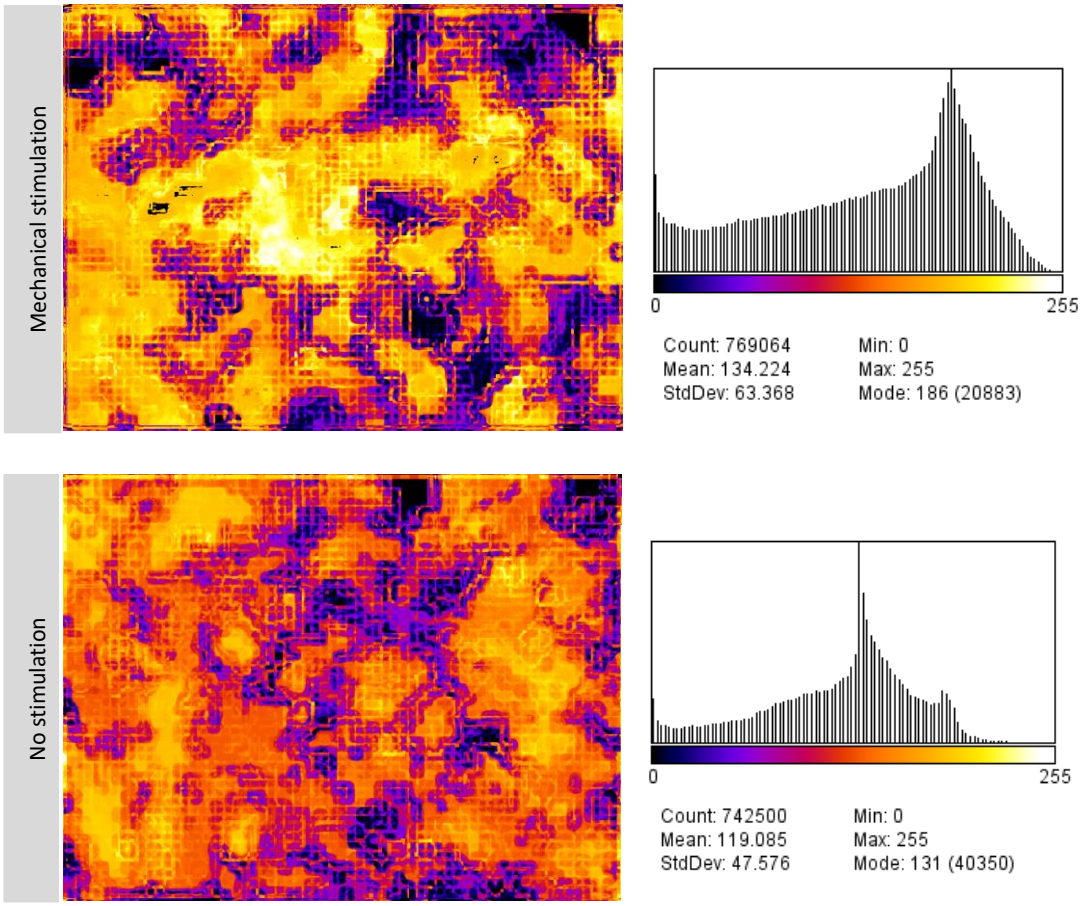

Figure 4-10 Local frequency of neonatal cardiac cells cultured in 3D hydrogel, top. With and bottom. Without mechanical stimulation.

The local phase shows the synchrony in both conditions. The slight difference between two groups could be because of 3D culturing of the cells, which adds complexity to the observation and analysis of the movies.

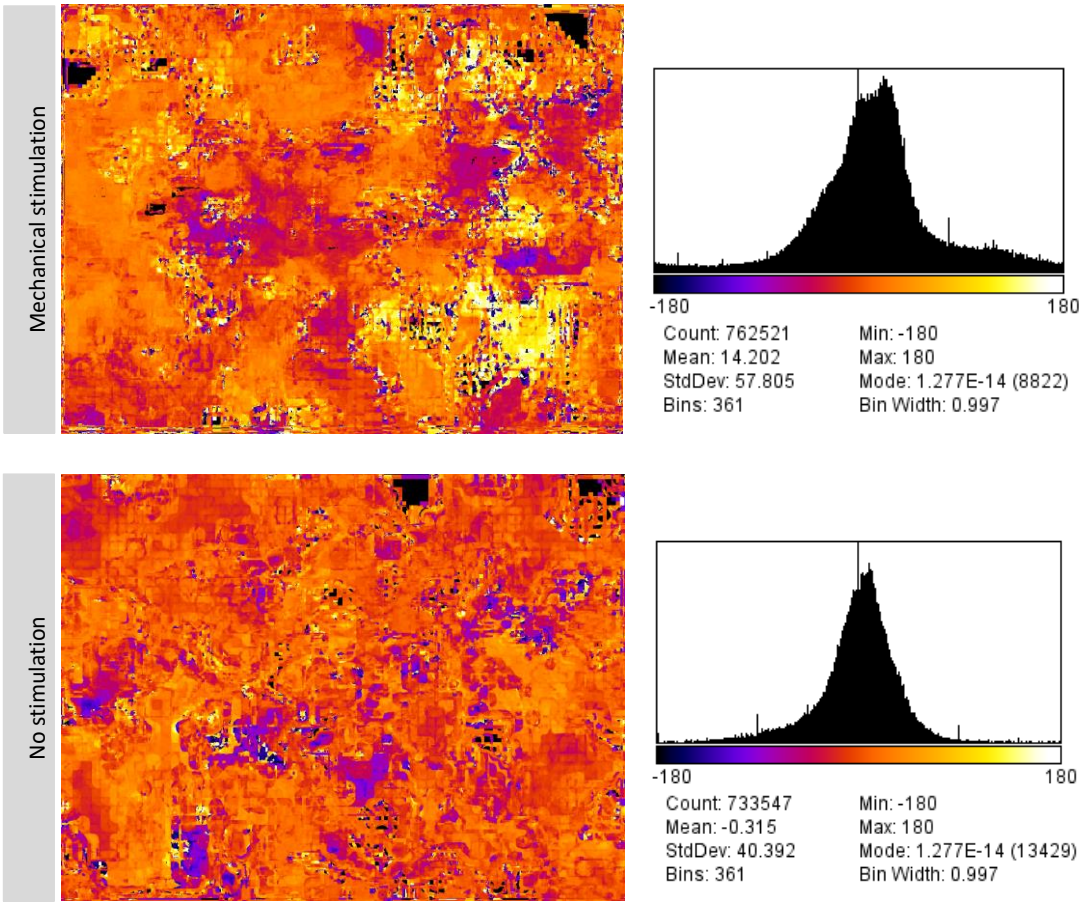

Figure 4-11 Local phase of neonatal cardiac cells cultured in 3D hydrogel, top. With and bottom. Without mechanical stimulation.

4.4 Discussion

The main focus of this chapter was on the impact of mechanical stimulation on the cardiac cells in 3D and simultaneous engagement of mechanical stretching and hydrogel patterning on cardiac cell functionality, orientation and protein expression. In principle, mechanical stimulation of the constructs can be coupled with the mechanisms that modify gene and protein expression, orientation, and functionality of the cells [104]. Hence, understanding the impact of dynamic environment on cell fate is crucial for the development of cardiac tissue models. In this work, we combined the mechanical stimulation and 3D culture in dECM-fibrin hydrogel to provide more desirable and tissue-like environment for the cardiac cells *in vitro* and compared it with 2D culture, and the static condition.

As demonstrated with the results of this work and other studies, in 2D culture, mechanical stimulation leads to cellular reorganization in a direction nearly perpendicular to the stretching direction to minimize the substrate deformation and the internal strain on each cell in response to extracellular stresses, which is called strain avoidance response [145], [308], [327], [328], [106]. It is been investigated in several studies that the stretch avoidance response is cell type dependent and it mainly alter by strain amplitude, stretch magnitude, and the duration of stimulation [329]. The result of Dhein *et al*. [121], with nearly parallel alignment of cardiomyocytes to the cyclic stretch axis seems to be an outlier in light of this well-established theoretical framework, our results, and also the results of Salameh *et al*. [133].

The combination of mechanical stimulation and surface topography in 3D improves the recapitulation of the *in vivo* conditions, as judged by the enhanced expression of the maturity markers α-actinin and connexin 43. However, the primary question is what the impact of simultaneous application of mechanical stimulation by cyclic stretch and anisotropic geometrical cues would be. By applying cyclic stretch to 3D cultures undergoing topographical alignment by grooved substrates, we find the two effects interact approximately additively. When cyclic stretch and grooves are aligned the applied mechanical strain reorients the cells nearly perpendicular to the direction of stretching, while the microgrooves promote the cell alignment in the direction of their axis. An oblique orientation of the cells (around 45°) in 3D patterned hydrogel with applied mechanical stimulation in the direction of the microgrooves results, and indicates interaction between the alignment mechanisms. When the mechanical stimulation is perpendicular to the groove's orientation, both forces encourage the same orientation (the grooves promotes the alignment in the direction of their axis, which is already perpendicular to the direction of the stretching motion). In the case, the alignment along the grooves is reinforced by the cyclic stretch. These results are in agreement with known results obtained in 2D, using a myoblast cell line [321]. In this study, an intermediate angle at 47.9° reflecting competition of chemical patterning and cyclic stretch was found. Our results transpose these results to a 3D setting with cardiomyocytes and alignment by 3D geometry rather than 2D chemical patterns.

There remains the question of physiological relevance of the results obtained in our 3D hydrogel system with cyclic stretch. The mechanical stimulation on neonatal cardiac cells in 3D enhanced the expression of connexin-43 and α-actinin. This means that the stimulation improves the integrity and maturation of the 3D constructs. Moreover, the beating analysis of the 3D structures with and without mechanical stimulation confirm the higher beating rate and more integrity of the cardiac cells in dynamic condition. Hence, overall, providing a dynamic environment for the cardiac cell in *in vitro* condition promotes their maturity and functionality, and, in terms of orientation, it provides more physiologically relevant cardiac model in 3D. This is in line with reported results.

The oblique cellular orientation upon physiological orientation of aligned stretch and geometry at first glance seems at odds with the parallel alignment in myocardial bundles and the *trabeculae carneae*. To interpret these results, one has to come back to the origins of cell orientation. The cells are known to

avoid compressive strain on their cytoskeleton, favoring tension instead [308]. Contrary to our *in vitro* setting, in the physiological setting, cardiomyocytes are to a first approximation protected from such compressive strain.

First, the myocardium does not relax completely during diastole, the ejection fraction is below 100% and ventricular filling starts immediately and rapidly [64]. So, there is a continuous tensile stretch superimposed on the cyclic strain (Table 1-2). This static part of the native mechanical microenvironment is not replicated here, primarily due to experimental difficulties with permanent hydrogel deformation under constant stretch. However, as self-condensation experiments [46] show, such continuous tensile stress favors parallel alignment. Hence, an essential part of the mechanical physiological environment that favors parallel alignment of cardiomyocytes is not replicated here. It could be included, but to avoid problems with differences in permanent deformation between the substrates and the hydrogels, the freestanding structures would have to be used instead (Chapter 3). In addition, it would be necessary to integrate force-monitoring during stretch experiments, as the length of the freestanding structures might change permanently. Based on the self-condensation experiments, adding and controlling the static part of the stress would be beneficial; this lack of control and knowledge of static stress may indeed explain the partly contradictory results reported in the literature [121], [133]. In any case, it would favor a more parallel alignment and thus narrow the gap between the *in vivo* alignment and *in vitro* observations.

A second important consideration is that cells avoid loss of tensile stress in their cytoskeleton, but this is limited during the active part of the contraction cycle in native cardiomyocyte. Indeed, the molecular acto-myosin interaction during electrically activated contraction produces additional tension, rather than decreasing it [330]. This tension is maintained because the cells work against a high external load (aortic pressure, as transduced to high active wall stress, Table 1-2. In this sense, the passive compressive part of the strain cycle as applied here is unphysiological. To avoid this problem, further sophistication of the stretch system would be required. Not only would one have to monitor and impose high forces during contraction, but actually ensure synchrony between electrical activity and applied forces. This requires integration with electrophysiological monitoring, beyond the scope of this thesis. This is partly addressed by using an external spring load in self-condensation experiments[82], although the constant spring load in this case is unsuitable to emulate the much higher loads during active contraction.

Following these considerations, one may wonder whether at all the compressive part of the cyclic stretch experiments, which presumably cause the off-axis alignment [308], have some physiological relevance. To try to answer this question, one has to consider in full detail the cardiac contraction cycle. By subtle regionally variable ion channel functionality and expression, the contraction time span is known to be shorter in superficial (subepicardial) as compared to the deep (subendocardial) regions, and also shorter at the basal part of the ventricular walls than at the apex [51]. Thus, subepicardial and

basal regions contract slightly after, and relax slightly before the apical and subendocardial parts [50], [51]. This means that there is indeed a short time-window at the beginning and end of active contraction, where the neighboring already respectively still active tissues have the potential to cause significant loss of tension along the main local stress axis. These time-windows being short compared to the overall cardiac cycle, one would expect only minor local deviations from perfect parallel alignment. The helical orientation of the fibers throughout the wall thickness (figure 4-1) is however precisely characterized by slowly progressive rather than abrupt angle change. It is therefore conceivable that there is an *a priori* unexpected link between the subtly timed excitation and relaxation in the native myocardium and the helical arrangement of the cardiac fibers. Clearly more elements are involved, since the considerations here do not give rise the chirality (handedness) observed in the hearts of most people [51], and also since the argument relies on pre-established regionality. But a slight off-axis orientation imparted by minor compressive elements could indeed help stabilize and optimize helicality once the major regions and characteristics are in place after embryonic development.

Overall, our results of 3D cell alignment in the condition of applying both mechanical stimulation and groove constraint provides a possible mechanism for generation and optimization of helicoidal structures in the myocardium. Cyclic stretch is fully compatible with cells survival and development in our 3D fibrin-dECM model system. In agreement with literature [320], maturation markers are indeed enhanced in neonatal cardiomyocytes under mechanical stretch condition, and the beating culture period is extended. As it has been mentioned in the introduction, the native heart muscle twists along its long axis because of the opposite rotation of the subepicardium and subendocardium. Structurally, this is reflected by a helical arrangement of cell and fiber alignment throughout the ventricle walls. The change of orientation is gradual, and our large off-axis orientations are probably to some extent unphysiological due to experimental shortcomings. This concerns mainly the lack of static stress and lack of synchronization with electrical activity. Nevertheless, fundamentally, a mechanism capable of creating off-axis alignment is crucial for the generation of helical structures. Therefore, our developed model can be considered not only as physiological model regarding cardiomyocyte maturation, alignment and 3D activity, but also as a first-of-its kind *in vitro* model to recapitulate and investigate an unexpected relation between the dynamic mechanical niche of cardiomyocytes and the helicoidal structures of the heart.

It is worthwhile at this point to take a step back and relate the results obtained to the original hypothesis regarding mechanical stimulation at the outset of this thesis. Outlined in the introduction, our hypothesis was that mechanical stimulation would improve cell alignment and functionality. In line with literature [104], [126], our results leave little doubt about the usefulness of cyclic stretch regarding cell maturation. Cellular alignment however turns out to be governed by a multitude of effects. With cyclic stretch (as compared to static stress [46]), we seem to have chosen a mechanical stimulation regime that causes off-axis, rather than the intended parallel cardiomyocyte alignment. Therefore, this chapter

is an example of scientific work where the primary original hypothesis needs to be rejected. However, the unexpected negative answer is technically sound, theoretically founded and points toward a novel mechanism that could at least partially explain biological helicality in the heart. Although intellectually more challenging, this outcome is many ways more interesting than a simple confirmation of an anticipated result.

Technical future directions include the addition of static stress and synchronization with electrical activity to improve matching with the physiological niche. This is expected to better reflect alignment of the cells with the main stress axis. It comes however at the cost of increased sophistication of the device. On a more fundamental level, it would be interesting to better understand the exact mechanisms behind the behavior of cells in 3D constrained and dynamic environment and its combination with pre-patterning has to be investigated in both cellular and tissue levels. Also, different physiological and pathological range of mechanical stimulation should be conducted and evaluated to understand the impact of specific regimes on cell behavior and functionality. Numerous investigations can be applied to validate the maturity of the cells in this dynamic environment, such as more specific gene and protein expression, patch clamping, and drug testing. Understanding the details of this field eventually lead to the design and fabrication of more relevant *in vitro* models for study the diseases which are coming from mechanotransduction defects. On the translational level, the fundamental advance in understanding of the cell alignment could one day be used to use smart mechanical design to align cells seeded randomly by external forces only – with the potential to create not only a local trabeculae carneae unit, but a full helicoidal trans-ventricular unit or even transplantable, physiologically pre-oriented patches.

Chapter 5 Conclusion

In this chapter, the summary of the main results of the project and their impact on future developments of cardiac *in vitro* models will be presented.

5.1 Summary of the achieved results and conclusion

Currently, the development of *in vitro* models of human tissues is one of the most challenging subjects for experimentalists in biology and can have an impact on cell biology, developmental biology, drug screening, cell therapy, and disease modeling. Recent advances in bioengineering and microtechnology have led to the numerous interdisciplinary ideas to overcome the difficulties related to the development of *in vitro* models of organs. Motivated by the fact that heart diseases cause one out of four deaths in developed countries, this thesis aims are developing a cardiac model which can find applications in decreasing the side effects of cardiac drugs, understanding the cell-cell and cell-ECM interactions, and investigating the maturation and functionality of cardiac tissues in *in vitro* conditions. Cardiac models are promising platforms to conduct cost-efficient and time-efficient biological analysis before starting animal and clinical trials. The main objective of this thesis is to design and fabricate a novel model that can be used for 3D cardiac cell culture, differentiation, maturation and stimulation. This cardiac model will allow us to have a 3D-oriented cell structure on a stretchable substrate, which is useful for cell differentiation, studying the impact of different stimulation methods (mechanical, biochemical, and electrical) on cell fate, and also investigate the response of cells to different drugs or stimuli.

In general, making a stable 3D cellular construct requires the use of a biomaterial with sufficient mechanical stiffness. In this work, we studied a new combination of two natural hydrogels for myocardium regeneration: decellularized extracellular matrix from porcine ventricular heart tissue, admixed with fibrinogen and coagulated under cell-compatible conditions with thrombin. Its mechanical properties are adjusted to match the ones of the native heart tissue (around 20 KPa), while the choice of thrombin as a specific crosslinking agent eliminates concerns of toxicity with more generic agents such as transglutaminase. We successfully tested this new hydrogel in the context of highly efficient, retinoid-free cardiac differentiation of the myoblast line H9c2. In neonatal cardiomyocytes, we show enhanced recovery, synchrony and beating frequency, as compared to various controls, demonstrating the specific advantage of using the dECM-fibrin hydrogel over collagen analogs, fibrin alone, Matrigel and tissue culture plates.

A simple and efficient microengineering technique, enabled us to develop a 3D platform with oriented cardiac cells which resembles the trabeculae carneae structures in native cardiac tissue, which can be considered as the building blocks of heart tissue. There are two important features in the trabeculae which makes it interesting for experimentalists to study the mechanical, biological and functional properties of the heart muscle; the cardiac cells are parallel to the direction of the trabeculae, and also they can easily exchange nutrients and oxygen by diffusion [331]. The proposed method for aligning the cardiac cells in microgrooves with similar dimensions to trabeculae carneae units, provides the structures with rational dimensions and aligned cardiomyocytes comparable to these units. Hence, it can be considered as a valuable model for further investigations. Concerning the access to oxygen and nutrients, there is no need for adding further complexity in the structure due to their small size. Regardless of the efforts for presenting this model and confirming the cell orientation in this 3D constructs, it still requires several validations in terms of developmental biology, differentiation, and functionality of the whole structure.

As the cardiac cells in their native niche are living in a dynamic environment with several stimulations, applying a mechanical stimulation to cardiomyocytes in culture mimics the native tissue behavior and improves the functionality of the platform for having a more reliable *in vitro* model. A cost-effective and user-friendly mechanical stimulator was designed and fabricated, which is compatible with cell culture conditions, i.e. the cell culture incubator and the stage of the microscope. One can control the mechanical stimulation regime for the cells in culture. The PDMS, flexible, transparent chamber for culturing the cells, provides a broad range of possibilities of experimental conditions, which makes it a great device for understanding the impact of this stimulation on cell fate and functionality. The obtained results suggest that mechanical stimulation enhances the integrity of the cells in the tissue by increasing the expression of gap-junction and cardiac-specific

proteins, and it alters the orientation of cells in 3D. This orientation can partially explain biological helicality in the heart. The preliminary results we obtained suggest promising opportunities towards a more cardiac tissue-like structure.

We anticipate the system we developed will be used both as robust a cardiac 3D cell model for drug screening, and as a building block for 3D printing, tissue engineering and transplantation in regenerative medicine.

5.2 Outlook

This work opened up several challenges and future prospective to investigate more in the field of cardiac tissue engineering and *in vitro* models. In this section, I summarize some of the future works and the potential applications of this model that can be evaluated in more details in future explorations for understanding the cause of different biological responses of the cells in *in vitro* conditions. The outlook will be discussed in four main aspects: cell source, material, technologies, and applications.

5.2.1 Cell sources

Regarding the cell sources, as it is mentioned, cardiomyocytes are not the only cells in cardiac tissue. In this thesis, we already investigated the role of fibroblasts and its importance in cardiac tissue differentiation and maturation. Nevertheless, to make more reliable and precise cardiac models, one should consider the contribution of non-cardiomyocytes such as endothelial and smooth muscle cells in physiological and pathological behavior of cardiac cells. Hence, another important point to be considered in this case is the addition of these different cell types to the co-culture system and to understand the significance of cell-cell communication in myocardial cell fate.

In this research to proof the concept of providing a 3D aligned cardiac model, we limited the experiments to just two cell types, i.e. H9c2 cells in co-culture with fibroblasts and neonatal cardiac cells. However, since another approach for future work will be the use of this model for studying molecular and developmental biology, other cell sources such as iPSCs or ESCs can be used for more advanced investigations for clarifying the mechanisms behind the different behaviors of the cells in 2D and 3D, cell fate, and optimizing the ESCs/iPSCs differentiation into cardiac lineage. This consideration will enable the researchers to improve the personalized medicine studies and would

revolutionize current complex differentiation procedures for having mature cardiac cells in *in vitro* condition.

5.2.2 Material selection

In terms of the material for 3D culture, dECM alone, it not well-understood yet. It is composed of a number of components that might have an impact on the cell culture. The combination of collagen I content and appropriate mechanical stiffness explain most of the favorable properties, although further investigation is needed to assess whether non-collagen I components of the dECM could be responsible for more subtle differences in early synchronization and long-term maintenance of primary cardiomyocytes.

In addition, currently, most of the microfabrication and microfluidic chips are based on PDMS because of its excellent properties. Although PDMS is a great material in terms of biocompatibility, transparency, porosity, and flexibility, it absorbs chemical compounds which makes it not totally applicable in drug screening/discovery. Hence, one technical points that is necessary to be considered is the use of PDMS in different applications. One needs to consider another appropriate material as a substitute for PDMS, for instance tetrafluoroethylene-propylene (FEPM) elastomer[332], Polyurethane elastomer[333], styrene-ethylene/butylene-styrene (SEBS) triblock copolymer[334], or modifying the normal PDMS to decrease the abruption of small molecules, for example by using PDMS-PEG-modified PDMS [335].

5.2.3 Technology

Concerning the technology point of view, merging microtechnology with bioengineering provide promising ideas to tackle the challenges in the regenerative medicine field. Taking advantage of microfluidic systems can ease the assessment of different biochemical stimuli such as growth factors, drugs, differentiation media, and toxic or non-toxic compounds by precise dynamic control of the concentration, flow rate, and the time of exposure over the culture. This technology also, can be applied to provide nutrients and oxygen and remove the byproducts from the culture. In addition, microfluidic techniques are replicable and precise in their fabrication which can be perfect for high throughput applications.

One of the key challenges in tissue engineering is vascularization, due to the fact that by increasing the size of the bioengineered tissue, the middle part of the structure will face the oxygen deficiency

and the lack of sufficient nutrition and growth factors which leads to the cell apoptosis. In our model, we did not experience this problem because of the size of our model which is in the range of trabeculae carneae dimensions. However, vascularization must be considered as an important factor especially for larger dimensions. Using microfluidic systems and designing channels for fluid flow, we can integrate the vasculature network in our model to overcome this limitation. In addition, the other idea regarding this limitation could be integrating oxygen-generator microparticles such as (PEG-H_2O_2) in our hydrogel which release oxygen in their microenvironment and is confirmed to decrease the fibrotic tissue formation and increase the vascular density in the infarct area after in vivo injection.

Cardiac cells in native tissue are living in a dynamic environment with a variety of internal and external stimuli. Adding mechanical stimulation to our model reveals extremely interesting results in terms of the maturation and the alignment of the cells, because of the fact that it mimics more tissue-like environment for the cells. However, the mechanisms of this phenomena are not understood and require further investigation in both cellular and tissue levels in 3D structure with different conditions.

Electrical stimulation and recording would be another factor that can be applied to the 3D cardiac models. It can improve the maturity of the model to provide more consistent response of the cells *in vitro*. In addition, as the heart tissue is totally interconnected and the electromechanical signals between the cells have a key effect on tissue maturation and functionality, the electrophysiological properties of the 3D constructs has to be carefully understood and considered. In the future, merging different stimulations such as mechanical, biochemical and electrical stimuluses in the same model using microengineering techniques would be a great step towards a more tissue-like structure in *in vitro* conditions.

5.2.4 Applications

Although in this work we could introduce a cardiac model which meets some of the important features of cardiac tissue, the applications of this platform need to be investigated and validated more in depth. Motivated by the fact that the induced hydrogel can be injected and solidified in situ, other applications can be considered. One of these applications is bioprinting and 3D printing applications to fabricate platforms or scaffolds with desired spatial design[336]. In this application, synthesizing a biomaterial as the “biopaper” for printing and forming the expected 3D construct is needed. Besides the biocompatibility and mechanical properties of this material, its printability is the main criteria to choose the right one. It should be liquid during the printing process and

solidified by an external stimulus such as temperature, light, and ions. Therefore, the introduced hydrogel which has a short gelation time would be an ideal material in this application.

One of the main drawbacks of cell therapy is losing a great number of injected healthy cells during and after injection due to the lack of critical support. This hydrogel can enhance the efficiency of cell therapy by providing a pre-supportive environment which can reinforce cell survival and proliferation and encourage the cells to maintain their integrity, maturation and functionality. Hence, the hydrogel, either without cells and just as a supportive material, or in combination with different cells to improve their functionality, can be injected in diseased soft tissues to control the therapy which leads to positive clinical outcomes.

Another approach would be transplantation of this model in *in vivo* conditions, for instance as a cardiac patch to facilitate the delivery of healthy cardiac cells in the target zone and improve the efficiency of the cardiac regeneration. In addition, it can be considered as the long-oriented cell fibers for injection. Since this model provides pre-oriented, well-integrated and functional cardiac cell platform, it can augment the rate of success in animal infarct models and clinical trials.

In this thesis, we worked with cardiac cell lines and neonatal cardiac cells. However, as the aligned cardiac tissue in 3D was successfully prepared with this method, one can apply the same method for the other human tissues in which the orientation of the cells is crucial, such as nervous system, musculoskeletal and vascular tissues. The 3D alignment in different tissues will provide promising results and a powerful model to evaluate cell behavior and tissue function *in vitro*.

Reliable and robust results in *in vitro* conditions will arise from years of follow-up rather than weeks or months. Hence, to provide an applicable and consistent model, one needs long-term culturing and follow-up. Also, reproducibility, handling procedure, and standardization of the whole process should be carefully considered in the way towards further pre-clinical the clinical applications.

One of the main concideration in fabricating an engineered tissue is its correspondence with Advanced Therapy Medicinal Products (ATMPs) regulatory. In this case, the relevance of the animal cells and tissues, the working conditions and all the details of the experiments has to be checked with the standards. In this thesis the main concept of the work has been proved, however, the use of cell lines from different origins such as mouse and rat would not be accepted in standards. The use of pig heart would not make any special problem, as it is totally decellularized and the immune response would be negligible.

This works provided all the components for providing a reliable heart-on-a-chip system. However, the next step would be considering the high-throughput production of the chips for the experiments by adding microfluidic channels or applying mechanical stimulation on several chambers at athe same time. Also, in this work, we investigated the trabeculae carneae, however, one could study bigger tissue by assembling these building blocks and providing microfluidic channels and shear stress to the engineered tissue for advanced investigations. These considerations will provide more interesting and reliable results.

This work introduced a new biomaterial for cardiac tissue engineering and regeneration medicine and highlighted different parameters that have to be considered in this field to make more reliable and accurate model. The model validated with a variety of physical, mechanical and biological experiments. However, definitely further works and validations are required to reach the ideal platform representing the mature and functional cardiac tissue in different applications.

References

[1] D. S. Celermajer, C. K. Chow, E. Marijon, N. M. Anstey, and K. S. Woo, "Cardiovascular Disease in the Developing World: Prevalences, Patterns, and the Potential of Early Disease Detection," *J. Am. Coll. Cardiol.*, vol. 60, no. 14, pp. 1207–1216, Oct. 2012, doi: 10.1016/j.jacc.2012.03.074.

[2] F. An, Y. Qu, X. Liu, R. Zhong, and Y. Luo, "Organ-on-a-Chip : New Platform for Biological Analysis," pp. 39–45, 2015, doi: 10.4137/ACI.S28905.TYPE.

[3] T. Kalogeris, C. P. Baines, M. Krenz, and R. J. Korthuis, "Ischemia/Reperfusion," *Compr. Physiol.*, vol. 7, no. 1, pp. 113–170, Dec. 2016, doi: 10.1002/cphy.c160006.

[4] W. Richardson, S. Clarke, T. Quinn, and J. Holmes, "Physiological Implications of Myocardial Scar Structure," *Compr. Physiol.*, vol. 5, no. 4, pp. 1877–1909, Sep. 2015, doi: 10.1002/cphy.c140067.

[5] A. Tijore, S. A. Irvine, U. Sarig, P. Mhaisalkar, V. Baisane, and S. Venkatraman, "Contact guidance for cardiac tissue engineering using 3D bioprinted gelatin patterned hydrogel," *Biofabrication*, vol. 10, no. 2, p. 025003, Jan. 2018, doi: 10.1088/1758-5090/aaa15d.

[6] D. Kuraitis, K. Hosoyama, N. J. R. Blackburn, C. Deng, Z. Zhong, and E. J. Suuronen, "Functionalization of soft materials for cardiac repair and regeneration," *Crit. Rev. Biotechnol.*, vol. 39, no. 4, pp. 451–468, May 2019, doi: 10.1080/07388551.2019.1572587.

[7] J. W. Holmes, Z. Laksman, and L. Gepstein, "Making better scar: Emerging approaches for modifying mechanical and electrical properties following infarction and ablation," *Prog. Biophys. Mol. Biol.*, vol. 120, no. 1, pp. 134–148, Jan. 2016, doi: 10.1016/j.pbiomolbio.2015.11.002.

[8] P. S. Azevedo *et al.*, "Cardiac Remodeling: Concepts, Clinical Impact, Pathophysiological Mechanisms and Pharmacologic Treatment," *Arq. Bras. Cardiol.*, vol. 106, no. 1, pp. 62–69, Jan. 2016, doi: 10.5935/abc.20160005.

[9] Murry Charles E., Field Loren J., and Menasché Philippe, "Cell-Based Cardiac Repair," *Circulation*, vol. 112, no. 20, pp. 3174–3183, Nov. 2005, doi: 10.1161/CIRCULATIONAHA.105.546218.

[10] K. Cheng *et al.*, "Human Cardiosphere-Derived Cells From Advanced Heart Failure Patients Exhibit Augmented Functional Potency in Myocardial Repair," *JACC Heart Fail.*, vol. 2, no. 1, pp. 49–61, Feb. 2014, doi: 10.1016/j.jchf.2013.08.008.

[11] P. Jakob and U. Landmesser, "Current Status of Cell-Based Therapy for Heart Failure," *Curr. Heart Fail. Rep.*, vol. 10, no. 2, pp. 165–176, Jun. 2013, doi: 10.1007/s11897-013-0134-z.

[12] P. Überfuhr *et al.*, "Heart transplantation: an approach to treating primary cardiac sarcoma?," *J. Heart Lung Transplant.*, vol. 21, no. 10, pp. 1135–1139, Oct. 2002, doi: 10.1016/S1053-2498(02)00409-6.

[13] A. R. Horak, "Physiology and Pharmacology of the Transplanted Heart," in *The Transplantation and Replacement of Thoracic Organs: The Present Status of Biological and Mechanical Replacement of the Heart and Lungs*, D. K. C. Cooper and D. Novitzky, Eds. Dordrecht: Springer Netherlands, 1990, pp. 101–108.

[14] G. Camci-Unal, N. Annabi, M. R. Dokmeci, R. Liao, and A. Khademhosseini, "Hydrogels for cardiac tissue engineering," *NPG Asia Mater.*, vol. 6, no. 5, p. e99, May 2014, doi: 10.1038/am.2014.19.

[15] G. Vunjak-Novakovic *et al.*, "Challenges in Cardiac Tissue Engineering," *Tissue Eng. Part B Rev.*, vol. 16, no. 2, pp. 169–187, Aug. 2009, doi: 10.1089/ten.teb.2009.0352.

[16] X. Ma *et al.*, "3D bioprinting of functional tissue models for personalized drug screening and in vitro disease modeling," *Adv. Drug Deliv. Rev.*, vol. 132, pp. 235–251, Jul. 2018, doi: 10.1016/j.addr.2018.06.011.

[17] A. Mathur, Z. Ma, P. Loskill, S. Jeeawoody, and K. E. Healy, "In vitro cardiac tissue models: Current status and future prospects," *Adv. Drug Deliv. Rev.*, vol. 96, pp. 203–213, Jan. 2016, doi: 10.1016/j.addr.2015.09.011.

[18] M. F. Hoes, N. Bomer, and P. van der Meer, "Concise Review: The Current State of Human In Vitro Cardiac Disease Modeling: A Focus on Gene Editing and Tissue Engineering," *STEM CELLS Transl. Med.*, vol. 8, no. 1, pp. 66–74, 2019, doi: 10.1002/sctm.18-0052.

[19] L. M. Biga *et al.*, "19.3 Cardiac Cycle," in *Anatomy & Physiology*, OpenStax/Oregon State University, 2019.

[20] M. Suhaeri *et al.*, "Cardiomyoblast (H9c2) Differentiation on Tunable Extracellular Matrix Microenvironment | Tissue Engineering Part A," 2015. .

[21] Q. Jallerat and A. W. Feinberg, "Extracellular Matrix Structure and Composition in the Early Four-Chambered Embryonic Heart," *Cells*, vol. 9, no. 2, Art. no. 2, Feb. 2020, doi: 10.3390/cells9020285.

[22] A. Padhi and A. S. Nain, "ECM in Differentiation: A Review of Matrix Structure, Composition and Mechanical Properties," *Ann. Biomed. Eng.*, vol. 48, no. 3, pp. 1071–1089, Mar. 2020, doi: 10.1007/s10439-019-02337-7.

[23] J. Halper and M. Kjaer, “Basic Components of Connective Tissues and Extracellular Matrix: Elastin, Fibrillin, Fibulins, Fibrinogen, Fibronectin, Laminin, Tenascins and Thrombospondins,” in *Progress in Heritable Soft Connective Tissue Diseases*, J. Halper, Ed. Dordrecht: Springer Netherlands, 2014, pp. 31–47.

[24] J. M. Mattson, R. Turcotte, and Y. Zhang, “Glycosaminoglycans Contribute to Extracellular Matrix Fiber Recruitment and Arterial Wall Mechanics,” *Biomech. Model. Mechanobiol.*, vol. 16, no. 1, pp. 213–225, Feb. 2017, doi: 10.1007/s10237-016-0811-4.

[25] S. Hinds, W. Bian, R. G. Dennis, and N. Bursac, “The role of extracellular matrix composition in structure and function of bioengineered skeletal muscle,” *Biomaterials*, vol. 32, no. 14, pp. 3575–3583, May 2011, doi: 10.1016/j.biomaterials.2011.01.062.

[26] F. Wang and J. Guan, “Cellular cardiomyoplasty and cardiac tissue engineering for myocardial therapy,” *Adv. Drug Deliv. Rev.*, vol. 62, no. 7, pp. 784–797, Jun. 2010, doi: 10.1016/j.addr.2010.03.001.

[27] M. L. Munro, X. Shen, M. Ward, P. N. Ruygrok, D. J. Crossman, and C. Soeller, “Highly variable contractile performance correlates with myocyte content in trabeculae from failing human hearts,” *Sci. Rep.*, vol. 8, no. 1, Art. no. 1, Feb. 2018, doi: 10.1038/s41598-018-21199-y.

[28] S. Goo *et al.*, “Trabeculae carneae as models of the ventricular walls: implications for the delivery of oxygen,” *J. Gen. Physiol.*, vol. 134, no. 4, pp. 339–350, Oct. 2009, doi: 10.1085/jgp.200910276.

[29] F. Fatemifar, M. D. Feldman, M. Oglesby, and H.-C. Han, “Comparison of Biomechanical Properties and Microstructure of Trabeculae Carneae, Papillary Muscles, and Myocardium in the Human Heart,” *J. Biomech. Eng.*, vol. 141, no. 2, Feb. 2019, doi: 10.1115/1.4041966.

[30] M. Belleza and R.N., “Cardiovascular System Anatomy and Physiology: Study Guide for Nurses,” *Nurseslabs*, Apr. 24, 2017. https://nurseslabs.com/cardiovascular-system-anatomy-physiology/ (accessed Nov. 28, 2020).

[31] I. Banerjee, J. W. Fuseler, R. L. Price, T. K. Borg, and T. A. Baudino, “Determination of cell types and numbers during cardiac development in the neonatal and adult rat and mouse,” *Am. J. Physiol.-Heart Circ. Physiol.*, vol. 293, no. 3, pp. H1883–H1891, Sep. 2007, doi: 10.1152/ajpheart.00514.2007.

[32] I. C. Parrag, P. W. Zandstra, and K. A. Woodhouse, “Fiber alignment and coculture with fibroblasts improves the differentiated phenotype of murine embryonic stem cell-derived cardiomyocytes for cardiac tissue engineering,” *Biotechnol. Bioeng.*, vol. 109, no. 3, pp. 813–822, 2012, doi: 10.1002/bit.23353.

[33] O. Y. Antúnez Montes, “Anatomical Correlation of the Helical Structure of the Ventricular Myocardium Through Echocardiography,” *Rev. Esp. Cardiol. Engl. Ed.*, vol. 73, no. 2, pp. 153–160, Feb. 2020, doi: 10.1016/j.rec.2018.10.016.

[34] A. F. Huxley and R. Niedergerke, “Structural Changes in Muscle During Contraction: Interference Microscopy of Living Muscle Fibres,” *Nature*, vol. 173, no. 4412, pp. 971–973, May 1954, doi: 10.1038/173971a0.

[35] A. Vreeker, L. van Stuijvenberg, T. J. Hund, P. J. Mohler, P. G. J. Nikkels, and T. A. B. van Veen, “Assembly of the Cardiac Intercalated Disk during Pre- and Postnatal Development of the Human Heart,” *PLOS ONE*, vol. 9, no. 4, p. e94722, Apr. 2014, doi: 10.1371/journal.pone.0094722.

[36] D. M. Bers, “Cardiac excitation–contraction coupling,” *Nature*, vol. 415, no. 6868, Art. no. 6868, Jan. 2002, doi: 10.1038/415198a.

[37] P. Camelliti, T. K. Borg, and P. Kohl, “Structural and functional characterisation of cardiac fibroblasts,” *Cardiovasc. Res.*, vol. 65, no. 1, pp. 40–51, Jan. 2005, doi: 10.1016/j.cardiores.2004.08.020.

[38] T. A. Baudino, W. Carver, W. Giles, and T. K. Borg, “Cardiac fibroblasts: friend or foe?,” *Am. J. Physiol.-Heart Circ. Physiol.*, vol. 291, no. 3, pp. H1015–H1026, Sep. 2006, doi: 10.1152/ajpheart.00023.2006.

[39] P. Kohl and R. G. Gourdie, “Fibroblast–myocyte electrotonic coupling: Does it occur in native cardiac tissue?,” *J. Mol. Cell. Cardiol.*, vol. 70, pp. 37–46, May 2014, doi: 10.1016/j.yjmcc.2013.12.024.

[40] N. C. for B. Information, U. S. N. L. of M. 8600 R. Pike, B. MD, and 20894 Usa, “Signal transduction from the extracellular matrix,” *J. Cell Biol.*, vol. 120, no. 3, p. 577, Feb. 1993, doi: 10.1083/jcb.120.3.577.

[41] L. Hortells, A. K. Z. Johansen, and K. E. Yutzey, “Cardiac Fibroblasts and the Extracellular Matrix in Regenerative and Nonregenerative Hearts,” *J. Cardiovasc. Dev. Dis.*, vol. 6, no. 3, Aug. 2019, doi: 10.3390/jcdd6030029.

[42] R. Chaudhuri, M. Ramachandran, P. Moharil, M. Harumalani, and A. K. Jaiswal, “Biomaterials and cells for cardiac tissue engineering: Current choices,” *Mater. Sci. Eng. C*, vol. 79, pp. 950–957, Oct. 2017, doi: 10.1016/j.msec.2017.05.121.

[43] P. C. H. Hsieh, M. E. Davis, L. K. Lisowski, and R. T. Lee, “Endothelial-Cardiomyocyte Interactions in Cardiac Development and Repair,” *Annu. Rev. Physiol.*, vol. 68, no. 1, pp. 51–66, 2006, doi: 10.1146/annurev.physiol.68.040104.124629.

[44] G. Yang, B. Mahadik, J. Y. Choi, and J. P. Fisher, "Vascularization in tissue engineering: fundamentals and state-of-art," *Prog. Biomed. Eng.*, vol. 2, no. 1, p. 012002, Jan. 2020, doi: 10.1088/2516-1091/ab5637.

[45] "Muscle Tissue - Cardiac Muscle," *purkinje fibers*. http://purkinjefibers.weebly.com/muscle-tissue---cardiac-muscle.html (accessed Aug. 13, 2020).

[46] W. Pearce, "The Cardiovascular Autonomic Nervous System and Anaesthesia," *South. Afr. J. Anaesth. Analg.*, vol. 8, no. 3, pp. 8–24, Jul. 2002, doi: 10.1080/22201173.2002.10872967.

[47] Y. Kurachi, A. Terzic, and M. V. Cohen, *Heart Physiology and Pathophysiology*. Elsevier, 2000.

[48] Sarnoff S. J., Brockman S. K., Gilmore J. P., Linden R. J., and Mitchell J. H., "Regulation of Ventricular Contraction," *Circ. Res.*, vol. 8, no. 5, pp. 1108–1122, Sep. 1960, doi: 10.1161/01.RES.8.5.1108.

[49] A. M. Katz, *Physiology of the Heart*. Lippincott Williams & Wilkins, 2010.

[50] I. K. Rüssel, M. J. W. Götte, J. G. Bronzwaer, P. Knaapen, W. J. Paulus, and A. C. van Rossum, "Left Ventricular Torsion: An Expanding Role in the Analysis of Myocardial Dysfunction," *JACC Cardiovasc. Imaging*, vol. 2, no. 5, pp. 648–655, May 2009, doi: 10.1016/j.jcmg.2009.03.001.

[51] S. Nakatani, "Left ventricular rotation and twist: why should we learn?," *J. Cardiovasc. Ultrasound*, vol. 19, no. 1, pp. 1–6, 2011, doi: 10.4250/jcu.2011.19.1.1.

[52] K. C. Vinnakota and J. B. Bassingthwaighte, "Myocardial density and composition: a basis for calculating intracellular metabolite concentrations," *Am. J. Physiol.-Heart Circ. Physiol.*, vol. 286, no. 5, pp. H1742–H1749, May 2004, doi: 10.1152/ajpheart.00478.2003.

[53] D. E. Oken and R. J. Boucek, "Quantitation of Collagen in Human Myocardium," *Circ. Res.*, vol. 5, no. 4, pp. 357–361, Jul. 1957, doi: 10.1161/01.RES.5.4.357.

[54] A. Atala, "Tissue Engineering and Regenerative Medicine: Concepts for Clinical Application," *Rejuvenation Res.*, vol. 7, no. 1, pp. 15–31, May 2004, doi: 10.1089/154916804323105053.

[55] K. S. M. Smalley, M. Lioni, and M. Herlyn, "Life ins't flat: Taking cancer biology to the next dimension," *Vitro Cell. Dev. Biol. - Anim.*, vol. 42, no. 8, pp. 242–247, Sep. 2006, doi: 10.1290/0604027.1.

[56] N. Milani-Nejad and P. M. L. Janssen, "Small and large animal models in cardiac contraction research: Advantages and disadvantages," *Pharmacol. Ther.*, vol. 141, no. 3, pp. 235–249, Mar. 2014, doi: 10.1016/j.pharmthera.2013.10.007.

[57] J. E. Pomeroy, A. Helfer, and N. Bursac, "Biomaterializing the promise of cardiac tissue engineering," *Biotechnol. Adv.*, vol. 42, p. 107353, Sep. 2020, doi: 10.1016/j.biotechadv.2019.02.009.

[58] A. D. Theocharis, S. S. Skandalis, C. Gialeli, and N. K. Karamanos, "Extracellular matrix structure," *Adv. Drug Deliv. Rev.*, vol. 97, pp. 4–27, Feb. 2016, doi: 10.1016/j.addr.2015.11.001.

[59] G. Huang *et al.*, "Functional and Biomimetic Materials for Engineering of the Three-Dimensional Cell Microenvironment," *Chem. Rev.*, vol. 117, no. 20, pp. 12764–12850, Oct. 2017, doi: 10.1021/acs.chemrev.7b00094.

[60] A. S. Theus *et al.*, "Biomaterial approaches for cardiovascular tissue engineering," *Emergent Mater.*, vol. 2, no. 2, pp. 193–207, Jun. 2019, doi: 10.1007/s42247-019-00039-3.

[61] G. Khang, S. J. Lee, M. S. Kim, and H. B. Lee, "Biomaterials: Tissue Engineering and Scaffolds," in *Encyclopedia of Medical Devices and Instrumentation*, American Cancer Society, 2006.

[62] L. A. Reis, L. L. Y. Chiu, N. Feric, L. Fu, and M. Radisic, "Biomaterials in myocardial tissue engineering," *J. Tissue Eng. Regen. Med.*, vol. 10, no. 1, pp. 11–28, 2016, doi: 10.1002/term.1944.

[63] A. Scatteia, A. Baritussio, and C. Bucciarelli-Ducci, "Strain imaging using cardiac magnetic resonance," *Heart Fail. Rev.*, vol. 22, no. 4, pp. 465–476, 2017, doi: 10.1007/s10741-017-9621-8.

[64] H. L. Falsetti, R. E. Mates, C. Grant, D. G. Greene, and I. L. Bunnell, "Left Ventricular Wall Stress Calculated from One-Plane Cineangiography: AN APPROACH TO FORCE-VELOCITY ANALYSIS IN MAN," *Circ. Res.*, vol. 26, no. 1, pp. 71–83, Jan. 1970, doi: 10.1161/01.RES.26.1.71.

[65] H. A. Shiels and E. White, "The Frank–Starling mechanism in vertebrate cardiac myocytes," *J. Exp. Biol.*, vol. 211, no. 13, pp. 2005–2013, Jul. 2008, doi: 10.1242/jeb.003145.

[66] M. Tallawi, R. Rai, Aldo. R. Boccaccini, and K. E. Aifantis, "Effect of Substrate Mechanics on Cardiomyocyte Maturation and Growth," *Tissue Eng. Part B Rev.*, vol. 21, no. 1, pp. 157–165, Aug. 2014, doi: 10.1089/ten.teb.2014.0383.

[67] J. G. Jacot, A. D. McCulloch, and J. H. Omens, "Substrate Stiffness Affects the Functional Maturation of Neonatal Rat Ventricular Myocytes," *Biophys. J.*, vol. 95, no. 7, pp. 3479–3487, Oct. 2008, doi: 10.1529/biophysj.107.124545.

[68] V. Schwach and R. Passier, "Native cardiac environment and its impact on engineering cardiac tissue," *Biomater. Sci.*, vol. 7, no. 9, pp. 3566–3580, 2019, doi: 10.1039/C8BM01348A.

[69] M. L. Rodriguez *et al.*, "Substrate Stiffness, Cell Anisotropy, and Cell–Cell Contact Contribute to Enhanced Structural and Calcium Handling Properties of Human Embryonic Stem Cell-Derived Cardiomyocytes," *ACS Biomater. Sci. Eng.*, vol. 5, no. 8, pp. 3876–3888, Aug. 2019, doi: 10.1021/acsbiomaterials.8b01256.

[70] E. A. Corbin *et al.*, "Tunable and Reversible Substrate Stiffness Reveals a Dynamic Mechanosensitivity of Cardiomyocytes," *ACS Appl. Mater. Interfaces*, vol. 11, no. 23, pp. 20603–20614, Jun. 2019, doi: 10.1021/acsami.9b02446.

[71] M. C. Watson, E. M. Cherry-Kemmerling, and L. D. Black, "Cell-Matrix Interactions in Cardiac Development and Disease," in *Multi-scale Extracellular Matrix Mechanics and Mechanobiology*, Y. Zhang, Ed. Cham: Springer International Publishing, 2020, pp. 311–342.

[72] M. Urbanczyk, S. L. Layland, and K. Schenke-Layland, "The role of extracellular matrix in biomechanics and its impact on bioengineering of cells and 3D tissues," *Matrix Biol.*, vol. 85–86, pp. 1–14, Jan. 2020, doi: 10.1016/j.matbio.2019.11.005.

[73] C. F. Guimarães, L. Gasperini, A. P. Marques, and R. L. Reis, "The stiffness of living tissues and its implications for tissue engineering," *Nat. Rev. Mater.*, vol. 5, no. 5, Art. no. 5, May 2020, doi: 10.1038/s41578-019-0169-1.

[74] A. H. Nguyen *et al.*, "Cardiac tissue engineering: state-of-the-art methods and outlook," *J. Biol. Eng.*, vol. 13, no. 1, p. 57, Jun. 2019, doi: 10.1186/s13036-019-0185-0.

[75] R. Gauvin, R. Parenteau-Bareil, M. R. Dokmeci, W. D. Merryman, and A. Khademhosseini, "Hydrogels and microtechnologies for engineering the cellular microenvironment," *WIREs Nanomedicine Nanobiotechnology*, vol. 4, no. 3, pp. 235–246, 2012, doi: 10.1002/wnan.171.

[76] E. Jabbari, "Challenges for Natural Hydrogels in Tissue Engineering," *Gels*, vol. 5, no. 2, Art. no. 2, Jun. 2019, doi: 10.3390/gels5020030.

[77] M. Verhulsel, M. Vignes, S. Descroix, L. Malaquin, D. M. Vignjevic, and J. Viovy, "Biomaterials A review of microfabrication and hydrogel engineering for micro-organs on chips," *Biomaterials*, vol. 35, no. 6, pp. 1816–1832, 2014, doi: 10.1016/j.biomaterials.2013.11.021.

[78] L. T. Saldin, M. C. Cramer, S. S. Velankar, L. J. White, and S. F. Badylak, "Extracellular Matrix Hydrogels from Decellularized Tissues: Structure and Function," *Acta Biomater.*, vol. 49, pp. 1–15, Feb. 2017, doi: 10.1016/j.actbio.2016.11.068.

[79] C. Williams *et al.*, "Cardiac Extracellular Matrix-Fibrin Hybrid Scaffolds with Tunable Properties for Cardiovascular Tissue Engineering," *Acta Biomater.*, vol. 14, pp. 84–95, Mar. 2015, doi: 10.1016/j.actbio.2014.11.035.

[80] F. Navaee, P. Renaud, and T. Braschler, "Highly efficient cardiac differentiation and maintenance by thrombin-coagulated fibrin hydrogels enriched with decellularized porcine heart extracellular matrix," *bioRxiv*, p. 2020.01.30.927319, Jan. 2020, doi: 10.1101/2020.01.30.927319.

[81] G. Agmon and K. L. Christman, "Controlling stem cell behavior with decellularized extracellular matrix scaffolds," *Curr. Opin. Solid State Mater. Sci.*, vol. 20, no. 4, pp. 193–201, 2016, doi: 10.1016/j.cossms.2016.02.001.

[82] W.-H. Zimmermann *et al.*, "Engineered heart tissue grafts improve systolic and diastolic function in infarcted rat hearts," *Nat. Med.*, vol. 12, no. 4, Art. no. 4, Apr. 2006, doi: 10.1038/nm1394.

[83] K. Bakunts, N. Gillum, Z. Karabekian, and N. Sarvazyan, "Formation of cardiac fibers in Matrigel matrix," *BioTechniques*, vol. 44, no. 3, pp. 341–348, Mar. 2008, doi: 10.2144/000112682.

[84] E. E. Antoine, P. P. Vlachos, and M. N. Rylander, "Review of Collagen I Hydrogels for Bioengineered Tissue Microenvironments: Characterization of Mechanics, Structure, and Transport," *Tissue Eng. Part B Rev.*, vol. 20, no. 6, pp. 683–696, Dec. 2014, doi: 10.1089/ten.teb.2014.0086.

[85] A. E. T. Al, "Fibrin : A Versatile Scaffold for Tissue Engineering Applications," vol. 14, no. 2, 2008, doi: 10.1089/ten.teb.2007.0435.

[86] B. Peña *et al.*, "Injectable Hydrogels for Cardiac Tissue Engineering," *Macromol. Biosci.*, vol. 18, no. 6, p. 1800079, 2018, doi: 10.1002/mabi.201800079.

[87] K. Y. Ye, K. E. Sullivan, and L. D. Black, "Encapsulation of Cardiomyocytes in a Fibrin Hydrogel for Cardiac Tissue Engineering," no. September, pp. 1–7, 2011, doi: 10.3791/3251.

[88] Y. P. Kong, B. Carrion, R. K. Singh, and A. J. Putnam, "Matrix identity and tractional forces influence indirect cardiac reprogramming," *Sci. Rep.*, vol. 3, no. 1, Dec. 2013, doi: 10.1038/srep03474.

[89] Y. Zhang *et al.*, "Tissue-specific extracellular matrix coatings for the promotion of cell proliferation and maintenance of cell phenotype," *Biomaterials*, vol. 30, no. 23, pp. 4021–4028, Aug. 2009, doi: 10.1016/j.biomaterials.2009.04.005.

[90] B. S. Kim, H. Kim, G. Gao, J. Jang, and D.-W. Cho, “Decellularized extracellular matrix: a step towards the next generation source for bioink manufacturing,” *Biofabrication*, vol. 9, no. 3, p. 034104, Aug. 2017, doi: 10.1088/1758-5090/aa7e98.

[91] S. Chlopcikova, J. Psotova, and P. Miketova, “NEONATAL RAT CARDIOMYOCYTES - A MODEL FOR THE STUDY OF MORPHOLOGICAL, BIOCHEMICAL AND ELECTROPHYSIOLOGICAL CHARACTERISTICS OF THE HEART,” *Biomed. Pap.*, vol. 145, no. 2, pp. 49–55, Dec. 2001, doi: 10.5507/bp.2001.011.

[92] J. T. Hinson *et al.*, “Titin mutations in iPS cells define sarcomere insufficiency as a cause of dilated cardiomyopathy,” *Science*, vol. 349, no. 6251, pp. 982–986, Aug. 2015, doi: 10.1126/science.aaa5458.

[93] Z. Li and J. Guan, “Hydrogels for Cardiac Tissue Engineering,” *Polymers*, vol. 3, no. 2, Art. no. 2, Jun. 2011, doi: 10.3390/polym3020740.

[94] Q.-Z. Chen, S. E. Harding, N. N. Ali, A. R. Lyon, and A. R. Boccaccini, “Biomaterials in cardiac tissue engineering: Ten years of research survey,” *Mater. Sci. Eng. R Rep.*, vol. 59, no. 1, pp. 1–37, Feb. 2008, doi: 10.1016/j.mser.2007.08.001.

[95] M. P. Lutolf and J. A. Hubbell, “Synthetic biomaterials as instructive extracellular microenvironments for morphogenesis in tissue engineering,” *Nat. Biotechnol.*, vol. 23, no. 1, Art. no. 1, Jan. 2005, doi: 10.1038/nbt1055.

[96] Y. Orlova, N. Magome, L. Liu, Y. Chen, and K. Agladze, “Electrospun nanofibers as a tool for architecture control in engineered cardiac tissue,” *Biomaterials*, vol. 32, no. 24, pp. 5615–5624, Aug. 2011, doi: 10.1016/j.biomaterials.2011.04.042.

[97] M. R. Badrossamay *et al.*, “Engineering hybrid polymer-protein super-aligned nanofibers via rotary jet spinning,” *Biomaterials*, vol. 35, no. 10, pp. 3188–3197, Mar. 2014, doi: 10.1016/j.biomaterials.2013.12.072.

[98] L. Ghasemi-Mobarakeh, M. P. Prabhakaran, M. Morshed, M.-H. Nasr-Esfahani, and S. Ramakrishna, “Electrospun poly(ε-caprolactone)/gelatin nanofibrous scaffolds for nerve tissue engineering,” *Biomaterials*, vol. 29, no. 34, pp. 4532–4539, Dec. 2008, doi: 10.1016/j.biomaterials.2008.08.007.

[99] Z. Ma *et al.*, “Three-dimensional filamentous human diseased cardiac tissue model,” *Biomaterials*, vol. 35, no. 5, pp. 1367–1377, Feb. 2014, doi: 10.1016/j.biomaterials.2013.10.052.

[100] X. Ma *et al.*, “3D printed micro-scale force gauge arrays to improve human cardiac tissue maturation and enable high throughput drug testing,” *Acta Biomater.*, vol. 95, pp. 319–327, Sep. 2019, doi: 10.1016/j.actbio.2018.12.026.

[101] T. Hu *et al.*, “Micropatterned, electroactive, and biodegradable poly(glycerol sebacate)-aniline trimer elastomer for cardiac tissue engineering,” *Chem. Eng. J.*, vol. 366, pp. 208–222, Jun. 2019, doi: 10.1016/j.cej.2019.02.072.

[102] G. V. Novakovic, T. Eschenhagen, and C. Mummery, “Myocardial Tissue Engineering: In Vitro Models,” *Cold Spring Harb. Perspect. Med.*, vol. 4, no. 3, p. a014076, Mar. 2014, doi: 10.1101/cshperspect.a014076.

[103] R. R. Besser, M. Ishahak, V. Mayo, D. Carbonero, I. Claure, and A. Agarwal, “Engineered Microenvironments for Maturation of Stem Cell Derived Cardiac Myocytes,” *Theranostics*, vol. 8, no. 1, pp. 124–140, 2018, doi: 10.7150/thno.19441.

[104] W. L. Stoppel, D. L. Kaplan, and L. D. Black, “Electrical and mechanical stimulation of cardiac cells and tissue constructs,” *Adv. Drug Deliv. Rev.*, vol. 96, pp. 135–155, Jan. 2016, doi: 10.1016/j.addr.2015.07.009.

[105] H. Aubin *et al.*, “Directed 3D cell alignment and elongation in microengineered hydrogels,” *Biomaterials*, vol. 31, no. 27, pp. 6941–6951, Sep. 2010, doi: 10.1016/j.biomaterials.2010.05.056.

[106] Y. Li *et al.*, “Engineering cell alignment in vitro,” *Biotechnol. Adv.*, vol. 32, no. 2, pp. 347–365, 2014, doi: 10.1016/j.biotechadv.2013.11.007.

[107] P. Camelliti, J. O. Gallagher, P. Kohl, and A. D. McCulloch, “Micropatterned cell cultures on elastic membranes as an in vitro model of myocardium,” *Nat. Protoc.*, vol. 1, no. 3, Art. no. 3, Aug. 2006, doi: 10.1038/nprot.2006.203.

[108] D.-H. Kim *et al.*, “Nanoscale cues regulate the structure and function of macroscopic cardiac tissue constructs,” *Proc. Natl. Acad. Sci.*, vol. 107, no. 2, pp. 565–570, Jan. 2010, doi: 10.1073/pnas.0906504107.

[109] T. Trantidou, C. M. Terracciano, D. Kontziampasis, E. J. Humphrey, and T. Prodromakis, “Biorealistic cardiac cell culture platforms with integrated monitoring of extracellular action potentials,” *Sci. Rep.*, vol. 5, no. 1, Art. no. 1, Jun. 2015, doi: 10.1038/srep11067.

[110] V. Serpooshan *et al.*, “Bioacoustic-enabled patterning of human iPSC-derived cardiomyocytes into 3D cardiac tissue,” *Biomaterials*, vol. 131, pp. 47–57, Jul. 2017, doi: 10.1016/j.biomaterials.2017.03.037.

[111] A. Chen *et al.*, “Shrink-Film Configurable Multiscale Wrinkles for Functional Alignment of Human Embryonic Stem Cells and their Cardiac Derivatives,” *Adv. Mater.*, vol. 23, no. 48, pp. 5785–5791, 2011, doi: 10.1002/adma.201103463.

[112] T. C. McDevitt *et al.*, “In vitro generation of differentiated cardiac myofibers on micropatterned laminin surfaces,” *J. Biomed. Mater. Res.*, vol. 60, no. 3, pp. 472–479, 2002, doi: 10.1002/jbm.1292.

[113] E. Serena *et al.*, “Micro-Arrayed Human Embryonic Stem Cells-Derived Cardiomyocytes for In Vitro Functional Assay,” *PLOS ONE*, vol. 7, no. 11, p. e48483, Nov. 2012, doi: 10.1371/journal.pone.0048483.

[114] Z. Ma *et al.*, “Self-organizing human cardiac microchambers mediated by geometric confinement,” *Nat. Commun.*, vol. 6, no. 1, Art. no. 1, Jul. 2015, doi: 10.1038/ncomms8413.

[115] Y. Xiao *et al.*, “Microfabricated perfusable cardiac biowire: a platform that mimics native cardiac bundle,” *Lab. Chip*, vol. 14, no. 5, pp. 869–882, 2014, doi: 10.1039/C3LC51123E.

[116] Y. Sasano, K. Fukumoto, Y. Tsukamoto, T. Akagi, and M. Akashi, “Construction of 3D cardiac tissue with synchronous powerful beating using human cardiomyocytes from human iPS cells prepared by a convenient differentiation method,” *J. Biosci. Bioeng.*, vol. 129, no. 6, pp. 749–755, Jun. 2020, doi: 10.1016/j.jbiosc.2020.01.001.

[117] J. Veldhuizen, J. Cutts, D. A. Brafman, R. Q. Migrino, and M. Nikkhah, “Engineering anisotropic human stem cell-derived three-dimensional cardiac tissue on-a-chip,” *Biomaterials*, vol. 256, p. 120195, Oct. 2020, doi: 10.1016/j.biomaterials.2020.120195.

[118] H. J. Auman, H. Coleman, H. E. Riley, F. Olale, H.-J. Tsai, and D. Yelon, “Functional Modulation of Cardiac Form through Regionally Confined Cell Shape Changes,” *PLOS Biol.*, vol. 5, no. 3, p. e53, Feb. 2007, doi: 10.1371/journal.pbio.0050053.

[119] A. M. Handorf, Y. Zhou, M. A. Halanski, and W.-J. Li, “Tissue Stiffness Dictates Development, Homeostasis, and Disease Progression,” *Organogenesis*, vol. 11, no. 1, pp. 1–15, Jan. 2015, doi: 10.1080/15476278.2015.1019687.

[120] Yang Xiulan, Pabon Lil, and Murry Charles E., “Engineering Adolescence,” *Circ. Res.*, vol. 114, no. 3, pp. 511–523, Jan. 2014, doi: 10.1161/CIRCRESAHA.114.300558.

[121] S. Dhein *et al.*, “Mechanical control of cell biology. Effects of cyclic mechanical stretch on cardiomyocyte cellular organization,” *Prog. Biophys. Mol. Biol.*, vol. 115, no. 2, pp. 93–102, Aug. 2014, doi: 10.1016/j.pbiomolbio.2014.06.006.

[122] J. G. Jacot, J. C. Martin, and D. L. Hunt, “Mechanobiology of cardiomyocyte development,” *J. Biomech.*, vol. 43, no. 1, pp. 93–98, Jan. 2010, doi: 10.1016/j.jbiomech.2009.09.014.

[123] Y. S. Prakash, M. J. Cody, P. R. Housmans, J. D. Hannon, and G. C. Sieck, “Comparison of cross-bridge cycling kinetics in neonatal vs. adult rat ventricular muscle,” *J. Muscle Res. Cell Motil.*, vol. 20, no. 7, pp. 717–723, Oct. 1999, doi: 10.1023/A:1005585807179.

[124] C. C. Veerman, G. Kosmidis, C. L. Mummery, S. Casini, A. O. Verkerk, and M. Bellin, “Immaturity of Human Stem-Cell-Derived Cardiomyocytes in Culture: Fatal Flaw or Soluble Problem?,” *Stem Cells Dev.*, vol. 24, no. 9, pp. 1035–1052, Jan. 2015, doi: 10.1089/scd.2014.0533.

[125] C. C. Veerman, G. Kosmidis, C. L. Mummery, S. Casini, A. O. Verkerk, and M. Bellin, “Immaturity of stem-cell derived cardiomyocytes: fatal flaw or soluble problem?,” p. 36.

[126] B. D. Riehl, J.-H. Park, I. K. Kwon, and J. Y. Lim, “Mechanical Stretching for Tissue Engineering: Two-Dimensional and Three-Dimensional Constructs,” *Tissue Eng. Part B Rev.*, vol. 18, no. 4, pp. 288–300, Feb. 2012, doi: 10.1089/ten.teb.2011.0465.

[127] N. L. Tulloch *et al.*, “Growth of Engineered Human Myocardium With Mechanical Loading and Vascular Coculture,” *Circ. Res.*, vol. 109, no. 1, pp. 47–59, Jun. 2011, doi: 10.1161/CIRCRESAHA.110.237206.

[128] A. Mihic *et al.*, “The effect of cyclic stretch on maturation and 3D tissue formation of human embryonic stem cell-derived cardiomyocytes,” *Biomaterials*, vol. 35, no. 9, pp. 2798–2808, Mar. 2014, doi: 10.1016/j.biomaterials.2013.12.052.

[129] G. Kensah *et al.*, “Murine and human pluripotent stem cell-derived cardiac bodies form contractile myocardial tissue in vitro,” *Eur. Heart J.*, vol. 34, no. 15, pp. 1134–1146, Apr. 2013, doi: 10.1093/eurheartj/ehs349.

[130] J. Guan *et al.*, “The stimulation of the cardiac differentiation of mesenchymal stem cells in tissue constructs that mimic myocardium structure and biomechanics,” *Biomaterials*, vol. 32, no. 24, pp. 5568–5580, Aug. 2011, doi: 10.1016/j.biomaterials.2011.04.038.

[131] A. Leychenko, E. Konorev, M. Jijiwa, and M. L. Matter, “Stretch-Induced Hypertrophy Activates NFkB-Mediated VEGF Secretion in Adult Cardiomyocytes,” *PLOS ONE*, vol. 6, no. 12, p. e29055, Dec. 2011, doi: 10.1371/journal.pone.0029055.

[132] C. R. Haggart, E. G. Ames, J. K. Lee, and J. W. Holmes, “Effects of stretch and shortening on gene expression in intact myocardium,” *Physiol. Genomics*, vol. 46, no. 2, pp. 57–65, Dec. 2013, doi: 10.1152/physiolgenomics.00103.2013.

[133] A. Salameh *et al.*, “Cyclic Mechanical Stretch Induces Cardiomyocyte Orientation and Polarization of the Gap Junction Protein Connexin43,” *Circ. Res.*, vol. 106, no. 10, pp. 1592–1602, May 2010, doi: 10.1161/CIRCRESAHA.109.214429.

[134] J. L. Balestrini, J. K. Skorinko, A. Hera, G. R. Gaudette, and K. L. Billiar, “Applying controlled non-uniform deformation for in vitro studies of cell mechanobiology,” *Biomech. Model. Mechanobiol.*, vol. 9, no. 3, pp. 329–344, Jun. 2010, doi: 10.1007/s10237-009-0179-9.

[135] D. Huang, “Mechanisms and dynamics of mechanical strengthening in ligament-equivalent fibroblast-populated collagen matrices,” *Ann. Biomed. Eng.*, vol. 21, pp. 289–305, 1993.

[136] Zimmermann W.-H. *et al.*, “Tissue Engineering of a Differentiated Cardiac Muscle Construct,” *Circ. Res.*, vol. 90, no. 2, pp. 223–230, Feb. 2002, doi: 10.1161/hh0202.103644.

[137] A. K. Capulli, L. A. MacQueen, S. P. Sheehy, and K. K. Parker, “Fibrous scaffolds for building hearts and heart parts,” *Adv. Drug Deliv. Rev.*, vol. 96, pp. 83–102, Jan. 2016, doi: 10.1016/j.addr.2015.11.020.

[138] A. J. Engler *et al.*, “Embryonic cardiomyocytes beat best on a matrix with heart-like elasticity: scar-like rigidity inhibits beating,” *J. Cell Sci.*, vol. 121, no. 22, pp. 3794–3802, Nov. 2008, doi: 10.1242/jcs.029678.

[139] C. M. Kofron and U. Mende, “In vitro models of the cardiac microenvironment to study myocyte and nonmyocyte crosstalk: bioinspired approaches beyond the polystyrene dish,” *J. Physiol.*, vol. 595, no. 12, pp. 3891–3905, 2017, doi: 10.1113/JP273100.

[140] S. M. Biendarra-Tiegs, D. J. Clemens, F. J. Secreto, and T. J. Nelson, “Human Induced Pluripotent Stem Cell-Derived Non-Cardiomyocytes Modulate Cardiac Electrophysiological Maturation Through Connexin 43-Mediated Cell-Cell Interactions,” *Stem Cells Dev.*, vol. 29, no. 2, pp. 75–89, Nov. 2019, doi: 10.1089/scd.2019.0098.

[141] H. Iseoka *et al.*, “Pivotal Role of Non-cardiomyocytes in Electromechanical and Therapeutic Potential of Induced Pluripotent Stem Cell-Derived Engineered Cardiac Tissue,” *Tissue Eng. Part A*, vol. 24, no. 3–4, pp. 287–300, May 2017, doi: 10.1089/ten.tea.2016.0535.

[142] Y. Li, H. Asfour, and N. Bursac, “Age-dependent functional crosstalk between cardiac fibroblasts and cardiomyocytes in a 3D engineered cardiac tissue,” *Acta Biomater.*, vol. 55, pp. 120–130, Jun. 2017, doi: 10.1016/j.actbio.2017.04.027.

[143] K. Kongpol, N. Nernpermpisooth, E. Prompunt, and S. Kumphune, “Endothelial-Cell-Derived Human Secretory Leukocyte Protease Inhibitor (SLPI) Protects Cardiomyocytes against Ischemia/Reperfusion Injury,” *Biomolecules*, vol. 9, no. 11, Art. no. 11, Nov. 2019, doi: 10.3390/biom9110678.

[144] G. Kostecki, Y. Shi, C. Chen, D. H. Reich, E. Entcheva, and L. Tung, “Optogenetic currents in myofibroblasts acutely alter electrophysiology and conduction of co-cultured cardiomyocytes,” *bioRxiv*, p. 2020.06.02.124529, Jun. 2020, doi: 10.1101/2020.06.02.124529.

[145] J. Foolen, V. S. Deshpande, F. M. W. Kanters, and F. P. T. Baaijens, “The influence of matrix integrity on stress-fiber remodeling in 3D,” *Biomaterials*, vol. 33, no. 30, pp. 7508–7518, Oct. 2012, doi: 10.1016/j.biomaterials.2012.06.103.

[146] D. Huh, G. A. Hamilton, and D. E. Ingber, “From 3D cell culture to organs-on-chips,” *Trends Cell Biol.*, vol. 21, no. 12, pp. 745–754, 2011, doi: 10.1016/j.tcb.2011.09.005.

[147] O. Caspi *et al.*, “Transplantation of human embryonic stem cell-derived cardiomyocytes improves myocardial performance in infarcted rat hearts,” *J. Am. Coll. Cardiol.*, vol. 50, no. 19, pp. 1884–1893, Nov. 2007, doi: 10.1016/j.jacc.2007.07.054.

[148] J. L. Young and A. J. Engler, “Hydrogels with time-dependent material properties enhance cardiomyocyte differentiation in vitro,” *Biomaterials*, vol. 32, no. 4, pp. 1002–1009, Feb. 2011, doi: 10.1016/j.biomaterials.2010.10.020.

[149] P. Beauchamp *et al.*, “3D Co-culture of hiPSC-Derived Cardiomyocytes With Cardiac Fibroblasts Improves Tissue-Like Features of Cardiac Spheroids,” *Front. Mol. Biosci.*, vol. 7, 2020, doi: 10.3389/fmolb.2020.00014.

[150] C. Sacchetto, L. Vitiello, L. J. de Windt, A. Rampazzo, and M. Calore, “Modeling Cardiovascular Diseases with hiPSC-Derived Cardiomyocytes in 2D and 3D Cultures,” *Int. J. Mol. Sci.*, vol. 21, no. 9, Art. no. 9, Jan. 2020, doi: 10.3390/ijms21093404.

[151] M. Kapałczyńska *et al.*, “2D and 3D cell cultures – a comparison of different types of cancer cell cultures,” *Arch. Med. Sci. AMS*, vol. 14, no. 4, pp. 910–919, Jun. 2018, doi: 10.5114/aoms.2016.63743.

[152] M. Ravi, V. Paramesh, S. R. Kaviya, E. Anuradha, and F. D. P. Solomon, "3D Cell Culture Systems: Advantages and Applications," *J. Cell. Physiol.*, vol. 230, no. 1, pp. 16–26, 2015, doi: 10.1002/jcp.24683.

[153] K. Duval *et al.*, "Modeling Physiological Events in 2D vs. 3D Cell Culture," *Physiology*, vol. 32, no. 4, pp. 266–277, Jun. 2017, doi: 10.1152/physiol.00036.2016.

[154] J. Hoarau-Véchot, A. Rafii, C. Touboul, and J. Pasquier, "Halfway between 2D and Animal Models: Are 3D Cultures the Ideal Tool to Study Cancer-Microenvironment Interactions?," *Int. J. Mol. Sci.*, vol. 19, no. 1, Art. no. 1, Jan. 2018, doi: 10.3390/ijms19010181.

[155] K. Wolf *et al.*, "Collagen-based cell migration models in vitro and in vivo," *Semin. Cell Dev. Biol.*, vol. 20, no. 8, pp. 931–941, Oct. 2009, doi: 10.1016/j.semcdb.2009.08.005.

[156] W. Peng, D. Unutmaz, and I. T. Ozbolat, "Bioprinting towards Physiologically Relevant Tissue Models for Pharmaceutics," *Trends Biotechnol.*, vol. 34, no. 9, pp. 722–732, Sep. 2016, doi: 10.1016/j.tibtech.2016.05.013.

[157] A. Korolj, E. Y. Wang, R. A. Civitarese, and M. Radisic, "Biophysical stimulation for in vitro engineering of functional cardiac tissues," *Clin. Sci.*, vol. 131, no. 13, pp. 1393–1404, Jul. 2017, doi: 10.1042/CS20170055.

[158] L. Saludas, S. Pascual-Gil, F. Prósper, E. Garbayo, and M. Blanco-Prieto, "Hydrogel based approaches for cardiac tissue engineering," *Int. J. Pharm.*, vol. 523, no. 2, pp. 454–475, May 2017, doi: 10.1016/j.ijpharm.2016.10.061.

[159] Q. Lei, J. He, and D. Li, "Electrohydrodynamic 3D printing of layer-specifically oriented, multiscale conductive scaffolds for cardiac tissue engineering," *Nanoscale*, vol. 11, no. 32, pp. 15195–15205, 2019, doi: 10.1039/C9NR04989D.

[160] B. Nugraha, M. F. Buono, L. von Boehmer, S. P. Hoerstrup, and M. Y. Emmert, "Human Cardiac Organoids for Disease Modeling," *Clin. Pharmacol. Ther.*, vol. 105, no. 1, pp. 79–85, 2019, doi: 10.1002/cpt.1286.

[161] A. Skardal, T. Shupe, and A. Atala, "Organoid-on-a-chip and body-on-a-chip systems for drug screening and disease modeling," *Drug Discov. Today*, vol. 21, no. 9, pp. 1399–1411, Sep. 2016, doi: 10.1016/j.drudis.2016.07.003.

[162] A. D. Ebert, P. Liang, and J. C. Wu, "Induced Pluripotent Stem Cells as a Disease Modeling and Drug Screening Platform," *J. Cardiovasc. Pharmacol.*, vol. 60, no. 4, pp. 408–416, Oct. 2012, doi: 10.1097/FJC.0b013e318247f642.

[163] H. Savoji *et al.*, "Cardiovascular disease models: A game changing paradigm in drug discovery and screening," *Biomaterials*, vol. 198, pp. 3–26, Apr. 2019, doi: 10.1016/j.biomaterials.2018.09.036.

[164] B. Fine and G. Vunjak-Novakovic, "Shortcomings of Animal Models and the Rise of Engineered Human Cardiac Tissue," *ACS Biomater. Sci. Eng.*, vol. 3, no. 9, pp. 1884–1897, Sep. 2017, doi: 10.1021/acsbiomaterials.6b00662.

[165] A. Mathur *et al.*, "Human iPSC-based Cardiac Microphysiological System For Drug Screening Applications," *Sci. Rep.*, vol. 5, p. 8883, Mar. 2015, doi: 10.1038/srep08883.

[166] I. J. Onakpoya, C. J. Heneghan, and J. K. Aronson, "Post-marketing withdrawal of 462 medicinal products because of adverse drug reactions: a systematic review of the world literature," *BMC Med.*, vol. 14, no. 1, p. 10, Feb. 2016, doi: 10.1186/s12916-016-0553-2.

[167] S. R. Braam, R. Passier, and C. L. Mummery, "Cardiomyocytes from human pluripotent stem cells in regenerative medicine and drug discovery," *Trends Pharmacol. Sci.*, vol. 30, no. 10, pp. 536–545, Oct. 2009, doi: 10.1016/j.tips.2009.07.001.

[168] H. Inoue and S. Yamanaka, "The Use of Induced Pluripotent Stem Cells in Drug Development," *Clin. Pharmacol. Ther.*, vol. 89, no. 5, pp. 655–661, 2011, doi: 10.1038/clpt.2011.38.

[169] N. Gaio *et al.*, "Cytostretch, an Organ-on-Chip Platform," *Micromachines*, vol. 7, no. 7, Art. no. 7, Jul. 2016, doi: 10.3390/mi7070120.

[170] S. J. Engle and D. Puppala, "Integrating Human Pluripotent Stem Cells," *Stem Cell*, vol. 12, no. 6, pp. 669–677, 2013, doi: 10.1016/j.stem.2013.05.011.

[171] M. Wu, S. Huang, and G. Lee, "Microfluidic cell culture systems for drug research," no. October 2009, pp. 939–956, 2010, doi: 10.1039/b921695b.

[172] A. D. van der Meer and A. van den Berg, "Organs-on-chips: breaking the in vitro impasse," *Integr. Biol.*, vol. 4, no. 5, pp. 461–470, May 2012, doi: 10.1039/C2IB00176D.

[173] K. Ejner *et al.*, "Alternative (non-animal) methods for cosmetics testing : current status and future prospects — 2010," pp. 367–485, 2011, doi: 10.1007/s00204-011-0693-2.

[174] Y. Zhao *et al.*, "Towards chamber specific heart-on-a-chip for drug testing applications," *Adv. Drug Deliv. Rev.*, p. S0169409X20300016, Jan. 2020, doi: 10.1016/j.addr.2019.12.002.

[175] A. M. Ghaemmaghami, M. J. Hancock, H. Harrington, H. Kaji, and A. Khademhosseini, “Biomimetic tissues on a chip for drug discovery,” *Drug Discov. Today*, vol. 17, no. 3–4, pp. 173–181, 2012, doi: 10.1016/j.drudis.2011.10.029.

[176] C. Luni, E. Serena, and N. Elvassore, “ScienceDirect Human-on-chip for therapy development and fundamental science,” *Curr. Opin. Biotechnol.*, vol. 25, pp. 45–50, doi: 10.1016/j.copbio.2013.08.015.

[177] B. Gradient and H. For, “NIH Public Access,” vol. 88, no. 6, pp. 899–911, 2011, doi: 10.1002/cjce.20411.BIOMIMETIC.

[178] Y. Zhao *et al.*, “Engineering microenvironment for human cardiac tissue assembly in heart-on-a-chip platform,” *Matrix Biol.*, vol. 85–86, pp. 189–204, Jan. 2020, doi: 10.1016/j.matbio.2019.04.001.

[179] L. Wang, M. Neumann, T. Fu, W. Li, X. Cheng, and B.-L. Su, “Porous and responsive hydrogels for cell therapy,” *Curr. Opin. Colloid Interface Sci.*, vol. 38, pp. 135–157, Nov. 2018, doi: 10.1016/j.cocis.2018.10.010.

[180] M. A. Alaiti, M. Ishikawa, and M. A. Costa, “Bone marrow and circulating stem/progenitor cells for regenerative cardiovascular therapy,” *Transl. Res.*, vol. 156, no. 3, pp. 112–129, Sep. 2010, doi: 10.1016/j.trsl.2010.06.008.

[181] L. W. van Laake *et al.*, “Human embryonic stem cell-derived cardiomyocytes survive and mature in the mouse heart and transiently improve function after myocardial infarction,” *Stem Cell Res.*, vol. 1, no. 1, pp. 9–24, Oct. 2007, doi: 10.1016/j.scr.2007.06.001.

[182] Gnecchi Massimiliano, Zhang Zhiping, Ni Aiguo, and Dzau Victor J., “Paracrine Mechanisms in Adult Stem Cell Signaling and Therapy,” *Circ. Res.*, vol. 103, no. 11, pp. 1204–1219, Nov. 2008, doi: 10.1161/CIRCRESAHA.108.176826.

[183] M. Mirotsou, T. M. Jayawardena, J. Schmeckpeper, M. Gnecchi, and V. J. Dzau, “Paracrine mechanisms of stem cell reparative and regenerative actions in the heart,” *J. Mol. Cell. Cardiol.*, vol. 50, no. 2, pp. 280–289, Feb. 2011, doi: 10.1016/j.yjmcc.2010.08.005.

[184] Dohmann Hans F.R. *et al.*, “Transendocardial Autologous Bone Marrow Mononuclear Cell Injection in Ischemic Heart Failure,” *Circulation*, vol. 112, no. 4, pp. 521–526, Jul. 2005, doi: 10.1161/CIRCULATIONAHA.104.499178.

[185] L. D. Black, J. D. Meyers, J. S. Weinbaum, Y. A. Shvelidze, and R. T. Tranquillo, “Cell-Induced Alignment Augments Twitch Force in Fibrin Gel–Based Engineered Myocardium via Gap Junction Modification,” *Tissue Eng. Part A*, vol. 15, no. 10, pp. 3099–3108, Oct. 2009, doi: 10.1089/ten.tea.2008.0502.

[186] K. J. Hansen *et al.*, “Functional Effects of Delivering Human Mesenchymal Stem Cell-Seeded Biological Sutures to an Infarcted Heart,” *BioResearch Open Access*, vol. 5, no. 1, pp. 249–260, May 2016, doi: 10.1089/biores.2016.0026.

[187] P. Bajaj, X. Tang, T. A. Saif, and R. Bashir, “Stiffness of the substrate influences the phenotype of embryonic chicken cardiac myocytes,” *J. Biomed. Mater. Res. A*, vol. 95A, no. 4, pp. 1261–1269, 2010, doi: 10.1002/jbm.a.32951.

[188] B. Bhana *et al.*, “Influence of substrate stiffness on the phenotype of heart cells,” *Biotechnol. Bioeng.*, vol. 105, no. 6, pp. 1148–1160, doi: 10.1002/bit.22647.

[189] J. M. Singelyn, J. A. DeQuach, S. B. Seif-Naraghi, R. B. Littlefield, P. J. Schup-Magoffin, and K. L. Christman, “Naturally derived myocardial matrix as an injectable scaffold for cardiac tissue engineering,” *Biomaterials*, vol. 30, no. 29, pp. 5409–5416, Oct. 2009, doi: 10.1016/j.biomaterials.2009.06.045.

[190] S. Canonico, “The use of human fibrin glue in the surgical operations,” *Acta Bio-Medica Atenei Parm.*, vol. 74 Suppl 2, pp. 21–25, 2003.

[191] J. Brouwers, “Influence of fibrinogen concentration on the Young’s modulus in fibrin gels,” Master Thesis, Eindhoven, 2002.

[192] T. D. Johnson *et al.*, “Human versus porcine tissue sourcing for an injectable myocardial matrix hydrogel,” *Biomater Sci*, vol. 2, no. 5, pp. 735–744, 2014, doi: 10.1039/C3BM60283D.

[193] S. B. Seif-Naraghi *et al.*, “Safety and Efficacy of an Injectable Extracellular Matrix Hydrogel for Treating Myocardial Infarction,” *Sci. Transl. Med.*, vol. 5, no. 173, pp. 173ra25-173ra25, Feb. 2013, doi: 10.1126/scitranslmed.3005503.

[194] F. Gattazzo, A. Urciuolo, and P. Bonaldo, “Extracellular matrix: A dynamic microenvironment for stem cell niche,” *Biochim. Biophys. Acta*, vol. 1840, no. 8, pp. 2506–2519, Aug. 2014, doi: 10.1016/j.bbagen.2014.01.010.

[195] “2015 4th TERMIS World CongressBoston, MassachusettsSeptember 8–11, 2015,” *Tissue Eng. Part A*, vol. 21, no. S1, p. S-1, Aug. 2015, doi: 10.1089/ten.tea.2015.5000.abstracts.

[196] N. Annabi *et al.*, “Highly Elastic Micropatterned Hydrogel for Engineering Functional Cardiac Tissue,” *Adv. Funct. Mater.*, vol. 23, no. 39, Oct. 2013, doi: 10.1002/adfm.201300570.

[197] M. J. A. van Luyn *et al.*, “Cardiac tissue engineering: characteristics of in unison contracting two- and three-dimensional neonatal rat ventricle cell (co)-cultures,” *Biomaterials*, vol. 23, no. 24, pp. 4793–4801, Dec. 2002, doi: 10.1016/S0142-9612(02)00230-2.

[198] H. Park, B. L. Larson, M. E. Kolewe, G. Vunjak-Novakovic, and L. E. Freed, “Biomimetic scaffold combined with electrical stimulation and growth factor promotes tissue engineered cardiac development,” *Exp. Cell Res.*, vol. 321, no. 2, pp. 297–306, Feb. 2014, doi: 10.1016/j.yexcr.2013.11.005.

[199] Y. Xing *et al.*, “Construction of engineered myocardial tissues in vitro with cardiomyocyte-like cells and a polylactic-co-glycolic acid polymer,” *Mol. Med. Rep.*, vol. 20, no. 3, pp. 2403–2409, Sep. 2019, doi: 10.3892/mmr.2019.10434.

[200] R. Feiner *et al.*, “Engineered hybrid cardiac patches with multifunctional electronics for online monitoring and regulation of tissue function,” *Nat. Mater.*, vol. 15, no. 6, pp. 679–685, Jun. 2016, doi: 10.1038/nmat4590.

[201] B. W. Streeter and M. E. Davis, “Therapeutic Cardiac Patches for Repairing the Myocardium,” *Adv. Exp. Med. Biol.*, vol. 1144, pp. 1–24, 2019, doi: 10.1007/5584_2018_309.

[202] Kutschka Ingo *et al.*, “Collagen Matrices Enhance Survival of Transplanted Cardiomyoblasts and Contribute to Functional Improvement of Ischemic Rat Hearts,” *Circulation*, vol. 114, no. 1_supplement, p. I–167, Jul. 2006, doi: 10.1161/CIRCULATIONAHA.105.001297.

[203] L. T. Saldin, M. C. Cramer, S. S. Velankar, L. J. White, and S. F. Badylak, “Acta Biomaterialia Extracellular matrix hydrogels from decellularized tissues : Structure and function,” *Acta Biomater.*, vol. 49, pp. 1–15, 2017, doi: 10.1016/j.actbio.2016.11.068.

[204] Z. Wang and J. M. Belovich, “A simple apparatus for measuring cell settling velocity,” *Biotechnol. Prog.*, vol. 26, no. 5, pp. 1361–1366, Sep. 2010, doi: 10.1002/btpr.432.

[205] M. E. Jeffords, J. Wu, M. Shah, Y. Hong, and G. Zhang, “Tailoring Material Properties of Cardiac Matrix Hydrogels To Induce Endothelial Differentiation of Human Mesenchymal Stem Cells,” *ACS Appl. Mater. Interfaces*, vol. 7, no. 20, pp. 11053–11061, May 2015, doi: 10.1021/acsami.5b03195.

[206] L. G. Bracaglia and J. P. Fisher, “ECM-Based Biohybrid Materials for Engineering Compliant, Matrix-Dense Tissues,” *Adv. Healthc. Mater.*, vol. 4, no. 16, pp. 2475–2487, Nov. 2015, doi: 10.1002/adhm.201500236.

[207] L. M. Sollid and B. Jabri, “Celiac disease and transglutaminase 2: a model for posttranslational modification of antigens and HLA association in the pathogenesis of autoimmune disorders,” *Curr. Opin. Immunol.*, vol. 23, no. 6, pp. 732–738, Dec. 2011, doi: 10.1016/j.coi.2011.08.006.

[208] P. Zhou and W. T. Pu, “Recounting cardiac cellular composition,” *Circ. Res.*, vol. 118, no. 3, pp. 368–370, Feb. 2016, doi: 10.1161/CIRCRESAHA.116.308139.

[209] P. Helm, F. Beg, M. I. Miller, and R. L. Winslow, “Measuring and Mapping Cardiac Fiber and Laminar Architecture Using Diffusion Tensor MR Imaging,” vol. 307, pp. 296–307, 2005, doi: 10.1196/annals.1341.026.

[210] P. Camelliti, T. K. Borg, and P. Kohl, “Structural and functional characterisation of cardiac fibroblasts,” *Cardiovasc. Res.*, vol. 65, no. 1, pp. 40–51, 2005, doi: 10.1016/j.cardiores.2004.08.020.

[211] Kane Christopher and Terracciano Cesare M, “Abstract 18700: Cardiac Fibroblast Co-Culture Promotes More Adult-Like Electrophysiological Properties in Human Induced Pluripotent Stem Cell-Derived Cardiomyocytes,” *Circulation*, vol. 134, no. suppl_1, pp. A18700–A18700, Nov. 2016, doi: 10.1161/circ.134.suppl_1.18700.

[212] B. W. Kimes and B. L. Brandt, “Properties of a clonal muscle cell line from rat heart,” *Exp. Cell Res.*, vol. 98, no. 2, pp. 367–381, Mar. 1976, doi: 10.1016/0014-4827(76)90447-X.

[213] A. F. Branco, S. P. Pereira, S. Gonzalez, O. Gusev, A. A. Rizvanov, and P. J. Oliveira, “Gene Expression Profiling of H9c2 Myoblast Differentiation towards a Cardiac-Like Phenotype,” *PLOS ONE*, vol. 10, no. 6, p. e0129303, Jun. 2015, doi: 10.1371/journal.pone.0129303.

[214] M. Suhaeri *et al.*, “Cardiomyoblast (H9c2) Differentiation on Tunable Extracellular Matrix Microenvironment,” *Tissue Eng. Part A*, vol. 21, no. 11–12, pp. 1940–1951, Jun. 2015, doi: 10.1089/ten.tea.2014.0591.

[215] J. E. Balmer and R. Blomhoff, “Gene expression regulation by retinoic acid,” *J. Lipid Res.*, vol. 43, no. 11, pp. 1773–1808, Nov. 2002, doi: 10.1194/jlr.R100015-JLR200.

[216] D. Y. Yang, B. Eng, J. S. Waye, J. C. Dudar, and S. R. Saunders, “Improved DNA extraction from ancient bones using silica-based spin columns,” *Am. J. Phys. Anthropol.*, vol. 105, no. 4, pp. 539–543, 1998, doi: 10.1002/(SICI)1096-8644(199804)105:4<539::AID-AJPA10>3.0.CO;2-1.

[217] M. A. Meyers and K. K. Chawla, *Mechanical behavior of materials*, 2nd ed. Cambridge ; New York: Cambridge University Press, 2009.

[218] A. Béduer *et al.*, “Additive manufacturing of hierarchical injectable scaffolds for tissue engineering,” *Acta Biomater.*, vol. 76, pp. 71–79, Aug. 2018, doi: 10.1016/j.actbio.2018.05.056.

[219] “detail.” https://www.phe-culturecollections.org.uk/products/celllines/generalcell/detail.jsp?refId=90112701&collection=ecacc_gc (accessed Oct. 28, 2019).

[220] A. F. Branco, S. P. Pereira, S. Gonzalez, O. Gusev, A. A. Rizvanov, and P. J. Oliveira, “Gene Expression Profiling of H9c2 Myoblast Differentiation towards a Cardiac-Like Phenotype,” *PLOS ONE*, vol. 10, no. 6, p. e0129303, Jun. 2015, doi: 10.1371/journal.pone.0129303.

[221] “Phalloidin-Atto 488 49409,” *Sigma-Aldrich*. https://www.sigmaaldrich.com/catalog/product/sigma/49409 (accessed Oct. 08, 2019).

[222] “findpeaks.m in octave-signal | source code search engine.” https://search-code.com/codesearch/view/64213481/ (accessed Nov. 13, 2019).

[223] M. Maddah *et al.*, “A Non-invasive Platform for Functional Characterization of Stem-Cell-Derived Cardiomyocytes with Applications in Cardiotoxicity Testing,” *Stem Cell Rep.*, vol. 4, no. 4, pp. 621–631, Mar. 2015, doi: 10.1016/j.stemcr.2015.02.007.

[224] F. Pati *et al.*, “Printing three-dimensional tissue analogues with decellularized extracellular matrix bioink,” *Nat. Commun.*, vol. 5, Jun. 2014, doi: 10.1038/ncomms4935.

[225] B. Schoen *et al.*, “Electrospun Extracellular Matrix: Paving the Way to Tailor-Made Natural Scaffolds for Cardiac Tissue Regeneration,” *Adv. Funct. Mater.*, vol. 27, no. 34, p. 1700427, doi: 10.1002/adfm.201700427.

[226] S. J. Watkins, G. M. Borthwick, and H. M. Arthur, “The H9C2 cell line and primary neonatal cardiomyocyte cells show similar hypertrophic responses in vitro,” *Vitro Cell. Dev. Biol. - Anim.*, vol. 47, no. 2, pp. 125–131, Feb. 2011, doi: 10.1007/s11626-010-9368-1.

[227] A. C. Gidlöf, P. Ocaya, O. Krivospitskaya, and A. Sirsjö, “Vitamin A: a drug for prevention of restenosis/reocclusion after percutaneous coronary intervention?,” *Clin. Sci. Lond. Engl. 1979*, vol. 114, no. 1, pp. 19–25, Jan. 2008, doi: 10.1042/CS20070090.

[228] M. S. Tallman *et al.*, “Effects of all-trans retinoic acid or chemotherapy on the molecular regulation of systemic blood coagulation and fibrinolysis in patients with acute promyelocytic leukemia,” *J. Thromb. Haemost. JTH*, vol. 2, no. 8, pp. 1341–1350, Aug. 2004, doi: 10.1111/j.1538-7836.2004.00787.x.

[229] “Cellosaurus cell line NOR-10 (CVCL_3939).” https://web.expasy.org/cellosaurus/CVCL_3939 (accessed Sep. 30, 2019).

[230] M. G. McCoy, J. M. Wei, S. Choi, J. P. Goerger, W. Zipfel, and C. Fischbach, “Collagen Fiber Orientation Regulates 3D Vascular Network Formation and Alignment,” *ACS Biomater. Sci. Eng.*, vol. 4, no. 8, pp. 2967–2976, Aug. 2018, doi: 10.1021/acsbiomaterials.8b00384.

[231] K. Zhang and A. Manninen, “3D Cell Culture Models of Epithelial Tissues,” in *Kidney Organogenesis: Methods and Protocols*, S. Vainio, Ed. New York, NY: Springer New York, 2019, pp. 77–84.

[232] C. M. Zehendner, H. J. Luhmann, and J.-W. Yang, “A Simple and Novel Method to Monitor Breathing and Heart Rate in Awake and Urethane-Anesthetized Newborn Rodents,” *PLOS ONE*, vol. 8, no. 5, p. e62628, May 2013, doi: 10.1371/journal.pone.0062628.

[233] “One-Hour Procedure to Isolate Primary Cardiomyocytes from Neonatal Mouse and Rat Hearts - CH.” https://www.thermofisher.com/uk/en/home/life-science/protein-biology/protein-biology-learning-center/protein-biology-resource-library/protein-biology-application-notes/one-hour-procedure-isolate-primary-cardiomyocytes-neonatal-mouse-rat-hearts.html (accessed Sep. 19, 2019).

[234] M. T. Gundersen, J. W. Keillor, and J. N. Pelletier, “Microbial transglutaminase displays broad acyl-acceptor substrate specificity,” *Appl. Microbiol. Biotechnol.*, vol. 98, no. 1, pp. 219–230, Jan. 2014, doi: 10.1007/s00253-013-4886-x.

[235] M. F. Butler, Y.-F. Ng, and P. D. A. Pudney, “Mechanism and kinetics of the crosslinking reaction between biopolymers containing primary amine groups and genipin,” *J. Polym. Sci. Part Polym. Chem.*, vol. 41, no. 24, pp. 3941–3953, 2003, doi: 10.1002/pola.10960.

[236] M. Gallwitz, M. Enoksson, M. Thorpe, and L. Hellman, “The Extended Cleavage Specificity of Human Thrombin,” *PLOS ONE*, vol. 7, no. 2, p. e31756, Feb. 2012, doi: 10.1371/journal.pone.0031756.

[237] M. Suhaeri *et al.*, “Novel Platform of Cardiomyocyte Culture and Coculture via Fibroblast-Derived Matrix-Coupled Aligned Electrospun Nanofiber,” Dec. 20, 2016. https://pubs.acs.org/doi/full/10.1021/acsami.6b14020 (accessed Oct. 07, 2019).

[238] R. J. Bick, M. B. Snuggs, B. J. Poindexter, L. M. Buja, and W. B. V. Winkle, “Physical, contractile and calcium handling properties of neonatal cardiac myocytes cultured on different matrices,” *Cell Adhes. Commun.*, vol. 6, no. 4, pp. 301–310, Jan. 1998, doi: 10.3109/15419069809010789.

[239] F.-J. Huang *et al.*, "Adverse effects of retinoic acid on embryo development and the selective expression of retinoic acid receptors in mouse blastocysts," *Hum. Reprod.*, vol. 21, no. 1, pp. 202–209, Jan. 2006, doi: 10.1093/humrep/dei286.

[240] J. Pellman, J. Zhang, and F. Sheikh, "Myocyte-Fibroblast Communication in Cardiac Fibrosis and Arrhythmias: Mechanisms and Model Systems," *J. Mol. Cell. Cardiol.*, vol. 94, pp. 22–31, May 2016, doi: 10.1016/j.yjmcc.2016.03.005.

[241] O. Cohen and S. A. Safran, "Theory of frequency response of mechanically driven cardiomyocytes," *Sci. Rep.*, vol. 8, no. 1, pp. 1–8, Feb. 2018, doi: 10.1038/s41598-018-20307-2.

[242] H. C. Pape *et al.*, *Physiologie*. Stuttgart: Georg Thieme Verlag, 2018.

[243] B. Liu *et al.*, "Role of Cyclic Strain Frequency in Regulating the Alignment of Vascular Smooth Muscle Cells In Vitro," *Biophys. J.*, vol. 94, no. 4, pp. 1497–1507, Feb. 2008, doi: 10.1529/biophysj.106.098574.

[244] S. Israeli-Rosenberg, A. M. Manso, H. Okada, and R. S. Ross, "Integrins and Integrin-Associated Proteins in the Cardiac Myocyte," *Circ. Res.*, vol. 114, no. 3, pp. 572–586, Jan. 2014, doi: 10.1161/CIRCRESAHA.114.301275.

[245] Ross Robert S. and Borg Thomas K., "Integrins and the Myocardium," *Circ. Res.*, vol. 88, no. 11, pp. 1112–1119, Jun. 2001, doi: 10.1161/hh1101.091862.

[246] I. Nitsan, S. Drori, Y. E. Lewis, S. Cohen, and S. Tzlil, "Mechanical communication in cardiac cell synchronized beating," *Nat. Phys.*, vol. 12, no. 5, Art. no. 5, May 2016, doi: 10.1038/nphys3619.

[247] S. Majkut, T. Idema, J. Swift, C. Krieger, A. Liu, and D. E. Discher, "Heart-Specific Stiffening in Early Embryos Parallels Matrix and Myosin Expression to Optimize Beating," *Curr. Biol.*, vol. 23, no. 23, pp. 2434–2439, Dec. 2013, doi: 10.1016/j.cub.2013.10.057.

[248] Y. K. Kurokawa and S. C. George, "Tissue engineering the cardiac microenvironment: Multicellular microphysiological systems for drug screening," *Adv. Drug Deliv. Rev.*, vol. 96, pp. 225–233, Jan. 2016, doi: 10.1016/j.addr.2015.07.004.

[249] H. Aubin *et al.*, "Directed 3D cell alignment and elongation in microengineered hydrogels," *Biomaterials*, vol. 31, no. 27, pp. 6941–6951, 2010, doi: 10.1016/j.biomaterials.2010.05.056.

[250] I. N. Vasserman, V. P. Matveenko, I. N. Shardakov, and A. P. Shestakov, "Numerical simulation of the propagation of electrical excitation in the heart wall taking its fibrous laminar structure into account," *Biophysics*, vol. 60, no. 4, pp. 613–621, Jul. 2015, doi: 10.1134/S0006350915040259.

[251] E. W. Hsu and C. S. Henriquez, "Myocardial Fiber Orientation Mapping Using Reduced Encoding Diffusion Tensor Imaging," *J. Cardiovasc. Magn. Reson.*, vol. 3, no. 4, pp. 339–347, Jan. 2001, doi: 10.1081/JCMR-100108588.

[252] M. McLean and J. Prothero, "Determination of relative fiber orientation in heart muscle: Methodological problems," *Anat. Rec.*, vol. 232, no. 4, pp. 459–465, 1992, doi: 10.1002/ar.1092320402.

[253] H. Jo, H.-W. Jun, J. Shin, and S. Lee, Eds., *Biomedical Engineering: Frontier Research and Converging Technologies*. Springer International Publishing, 2016.

[254] M. Nikkhah, F. Edalat, S. Manoucheri, and A. Khademhosseini, "Biomaterials Engineering microscale topographies to control the cell e substrate interface," *Biomaterials*, vol. 33, no. 21, pp. 5230–5246, 2012, doi: 10.1016/j.biomaterials.2012.03.079.

[255] M. M. Stevens and J. H. George, "Exploring and Engineering the Cell Surface Interface," pp. 1135–1139, 2005.

[256] A. Grosberg, P. W. Alford, M. L. McCain, and K. K. Parker, "Ensembles of engineered cardiac tissues for physiological and pharmacological study: Heart on a chip," *Lab. Chip*, vol. 11, no. 24, pp. 4165–4173, Nov. 2011, doi: 10.1039/C1LC20557A.

[257] N. Bursac, K. K. Parker, S. Iravanian, and L. Tung, "Cardiomyocyte cultures with controlled macroscopic anisotropy: a model for functional electrophysiological studies of cardiac muscle," *Circ. Res.*, vol. 91, no. 12, pp. e45-54, Dec. 2002.

[258] H. T. Heidi Au, B. Cui, Z. E. Chu, T. Veres, and M. Radisic, "Cell culture chips for simultaneous application of topographical and electrical cues enhance phenotype of cardiomyocytes," *Lab. Chip*, vol. 9, no. 4, pp. 564–575, Feb. 2009, doi: 10.1039/b810034a.

[259] A. Agarwal, J. A. Goss, A. Cho, M. L. Mccain, and K. K. Parker, "Lab on a Chip," no. ii, pp. 3599–3608, 2013, doi: 10.1039/c3lc50350j.

[260] N. Annabi *et al.*, "Hydrogel-coated microfluidic channels for cardiomyocyte culture," *Lab. Chip*, vol. 13, no. 18, pp. 3569–3577, Aug. 2013, doi: 10.1039/C3LC50252J.

[261] Y. Zhao, H. Zeng, J. Nam, and S. Agarwal, “Fabrication of skeletal muscle constructs by topographic activation of cell alignment.,” *Biotechnol. Bioeng.*, vol. 102, no. 2, pp. 624–631, Feb. 2009, doi: 10.1002/bit.22080.

[262] B. Chen, B. Wang, W. Jie, G. Zhou, Y. Cao, and W. Liu, “Biomaterials In vivo tendon engineering with skeletal muscle derived cells in a mouse model,” *Biomaterials*, vol. 33, no. 26, pp. 6086–6097, 2012, doi: 10.1016/j.biomaterials.2012.05.022.

[263] K. A. Mosiewicz *et al.*, “hydrogel photopatterning,” vol. 12, no. November, 2013, doi: 10.1038/nmat3766.

[264] J. J. Norman and T. A. Desai, “Control of Cellular Organization in Three Dimensions Using a Microfabricated Polydimethylsiloxane–Collagen Composite Tissue Scaffold,” *Tissue Eng.*, vol. 11, no. 3–4, pp. 378–386, Mar. 2005, doi: 10.1089/ten.2005.11.378.

[265] V. Y. Sidorov, P. C. Samson, T. N. Sidorova, J. M. Davidson, C. C. Lim, and J. P. Wikswo, “Acta Biomaterialia I-Wire Heart-on-a-Chip I : Three-dimensional cardiac tissue constructs for physiology and pharmacology,” *Acta Biomater.*, vol. 48, pp. 68–78, 2017, doi: 10.1016/j.actbio.2016.11.009.

[266] G. C. E. Jr, M. Cheng, C. J. Bettinger, J. T. Borenstein, R. Langer, and L. E. Freed, “Accordion-like honeycombs for tissue engineering of cardiac anisotropy,” *Nat. Mater.*, vol. 7, no. 12, pp. 1003–1010, Dec. 2008, doi: 10.1038/nmat2316.

[267] J.-C. Han, A. J. Taberner, P. M. F. Nielsen, and D. S. Loiselle, “Interventricular comparison of the energetics of contraction of trabeculae carneae isolated from the rat heart,” *J. Physiol.*, vol. 591, no. 3, pp. 701–717, 2013, doi: 10.1113/jphysiol.2012.242719.

[268] G. Sands, S. Goo, D. Gerneke, I. LeGrice, and D. Loiselle, “The collagenous microstructure of cardiac ventricular trabeculae carneae,” *J. Struct. Biol.*, vol. 173, no. 1, pp. 110–116, Jan. 2011, doi: 10.1016/j.jsb.2010.06.020.

[269] J. Eyckmans, T. Boudou, X. Yu, and C. S. Chen, “A hitchhiker’s guide to mechanobiology,” *Dev. Cell*, vol. 21, no. 1, pp. 35–47, Jul. 2011, doi: 10.1016/j.devcel.2011.06.015.

[270] M. Dogterom, J. W. J. Kerssemakers, G. Romet-Lemonne, and M. E. Janson, “Force generation by dynamic microtubules,” *Curr. Opin. Cell Biol.*, vol. 17, no. 1, pp. 67–74, Feb. 2005, doi: 10.1016/j.ceb.2004.12.011.

[271] M. Vicente-Manzanares, X. Ma, R. S. Adelstein, and A. R. Horwitz, “Non-muscle myosin II takes centre stage in cell adhesion and migration,” *Nat. Rev. Mol. Cell Biol.*, vol. 10, no. 11, pp. 778–790, Nov. 2009, doi: 10.1038/nrm2786.

[272] S. Yang, J. H. Min, K. Cho, I. H. Seo, W. Ryu, and W.-G. Koh, “Fabrication of microgrooved scaffolds using near-field electrospinning-assisted lithography (NFEAL),” *J. Ind. Eng. Chem.*, vol. 80, pp. 471–478, Dec. 2019, doi: 10.1016/j.jiec.2019.08.025.

[273] “PDMS line.” https://www.epfl.ch/research/facilities/cmi/cmi-home-page/equiment/packaging-miscellaneous/pdms-line/ (accessed Aug. 21, 2020).

[274] M. E. Kolewe, H. Park, C. Gray, X. Ye, R. Langer, and L. E. Freed, “3D Structural Patterns in Scalable, Elastomeric Scaffolds Guide Engineered Tissue Architecture,” *Adv. Mater. Deerfield Beach Fla*, vol. 25, no. 32, pp. 4459–4465, Aug. 2013, doi: 10.1002/adma.201301016.

[275] F. Fatemifar, M. D. Feldman, and H.-C. Han, “CHARACTERIZATION OF BIOMECHANICAL PROPERTIES OF HUMAN TRABECULAE CARNEAE,” p. 3.

[276] M. Prager-Khoutorsky *et al.*, “Fibroblast polarization is a matrix-rigidity-dependent process controlled by focal adhesion mechanosensing,” *Nat. Cell Biol.*, vol. 13, no. 12, Art. no. 12, Dec. 2011, doi: 10.1038/ncb2370.

[277] M. D. Cabezas, B. Meckes, C. A. Mirkin, and M. Mrksich, “Subcellular Control over Focal Adhesion Anisotropy, Independent of Cell Morphology, Dictates Stem Cell Fate,” *ACS Nano*, vol. 13, no. 10, pp. 11144–11152, Oct. 2019, doi: 10.1021/acsnano.9b03937.

[278] N. J. Sniadecki, R. A. Desai, S. A. Ruiz, and C. S. Chen, “Nanotechnology for Cell–Substrate Interactions,” *Ann. Biomed. Eng.*, vol. 34, no. 1, pp. 59–74, Mar. 2006, doi: 10.1007/s10439-005-9006-3.

[279] D. Baptista, L. Teixeira, C. van Blitterswijk, S. Giselbrecht, and R. Truckenmüller, “Overlooked? Underestimated? Effects of Substrate Curvature on Cell Behavior,” *Trends Biotechnol.*, vol. 37, no. 8, pp. 838–854, Aug. 2019, doi: 10.1016/j.tibtech.2019.01.006.

[280] A. S. T. Smith *et al.*, “Micro- and nano-patterned conductive graphene–PEG hybrid scaffolds for cardiac tissue engineering,” *Chem. Commun.*, vol. 53, no. 53, pp. 7412–7415, 2017, doi: 10.1039/C7CC01988B.

[281] J. Y. Lim and H. J. Donahue, “Cell Sensing and Response to Micro- and Nanostructured Surfaces Produced by Chemical and Topographic Patterning,” *Tissue Eng.*, vol. 13, no. 8, pp. 1879–1891, Jun. 2007, doi: 10.1089/ten.2006.0154.

[282] C. Y. Tay, S. A. Irvine, F. Y. C. Boey, L. P. Tan, and S. Venkatraman, “Micro-/Nano-engineered Cellular Responses for Soft Tissue Engineering and Biomedical Applications,” *Small*, vol. 7, no. 10, pp. 1361–1378, 2011, doi: 10.1002/smll.201100046.

[283] S. M. Naseer *et al.*, “Surface acoustic waves induced micropatterning of cells in gelatin methacryloyl (GelMA) hydrogels,” *Biofabrication*, vol. 9, no. 1, p. 015020, Feb. 2017, doi: 10.1088/1758-5090/aa585e.

[284] S. Jana, M. Leung, J. Chang, and M. Zhang, “Effect of nano- and micro-scale topological features on alignment of muscle cells and commitment of myogenic differentiation,” *Biofabrication*, vol. 6, no. 3, p. 035012, May 2014, doi: 10.1088/1758-5082/6/3/035012.

[285] B. Zhang, Y. Xiao, A. Hsieh, N. Thavandiran, and M. Radisic, “Micro- and nanotechnology in cardiovascular tissue engineering,” *Nanotechnology*, vol. 22, no. 49, p. 494003, Nov. 2011, doi: 10.1088/0957-4484/22/49/494003.

[286] T. Trantidou *et al.*, “Selective hydrophilic modification of Parylene C films: a new approach to cell micropatterning for synthetic biology applications,” *Biofabrication*, vol. 6, no. 2, p. 025004, Mar. 2014, doi: 10.1088/1758-5082/6/2/025004.

[287] R. K. Kankala, K. Zhu, X.-N. Sun, C.-G. Liu, S.-B. Wang, and A.-Z. Chen, “Cardiac Tissue Engineering on the Nanoscale,” *ACS Biomater. Sci. Eng.*, vol. 4, no. 3, pp. 800–818, Mar. 2018, doi: 10.1021/acsbiomaterials.7b00913.

[288] R. You, X. Li, Z. Luo, J. Qu, and M. Li, “Directional cell elongation through filopodia-steered lamellipodial extension on patterned silk fibroin films,” *Biointerphases*, vol. 10, no. 1, p. 011005, Mar. 2015, doi: 10.1116/1.4914028.

[289] E. K. F. Yim, E. M. Darling, K. Kulangara, F. Guilak, and K. W. Leong, “Nanotopography-induced changes in focal adhesions, cytoskeletal organization, and mechanical properties of human mesenchymal stem cells,” *Biomaterials*, vol. 31, no. 6, pp. 1299–1306, Feb. 2010, doi: 10.1016/j.biomaterials.2009.10.037.

[290] K. Kolind, K. W. Leong, F. Besenbacher, and M. Foss, “Guidance of stem cell fate on 2D patterned surfaces,” *Biomaterials*, vol. 33, no. 28, pp. 6626–6633, Oct. 2012, doi: 10.1016/j.biomaterials.2012.05.070.

[291] B. H. Lee, “Engineering Stem Cell Niche and Stem Cell–Material Interactions,” p. 34.

[292] C.-L. Chou *et al.*, “Micrometer scale guidance of mesenchymal stem cells to form structurally oriented large-scale tissue engineered cartilage,” *Acta Biomater.*, vol. 60, pp. 210–219, Sep. 2017, doi: 10.1016/j.actbio.2017.07.016.

[293] M. R. Salick *et al.*, “Micropattern width dependent sarcomere development in human ESC-derived cardiomyocytes,” *Biomaterials*, vol. 35, no. 15, pp. 4454–4464, May 2014, doi: 10.1016/j.biomaterials.2014.02.001.

[294] M. Kharaziha *et al.*, “PGS:Gelatin nanofibrous scaffolds with tunable mechanical and structural properties for engineering cardiac tissues,” *Biomaterials*, vol. 34, no. 27, pp. 6355–6366, Sep. 2013, doi: 10.1016/j.biomaterials.2013.04.045.

[295] P.-Y. Wang, J. Yu, J.-H. Lin, and W.-B. Tsai, “Modulation of alignment, elongation and contraction of cardiomyocytes through a combination of nanotopography and rigidity of substrates,” *Acta Biomater.*, vol. 7, no. 9, pp. 3285–3293, Sep. 2011, doi: 10.1016/j.actbio.2011.05.021.

[296] A. C. C. van Spreeuwel *et al.*, “The influence of matrix (an)isotropy on cardiomyocyte contraction in engineered cardiac microtissues,” *Integr. Biol.*, vol. 6, no. 4, pp. 422–429, Apr. 2014, doi: 10.1039/c3ib40219c.

[297] L. Sartiani, E. Bettiol, F. Stillitano, A. Mugelli, E. Cerbai, and M. E. Jaconi, “Developmental Changes in Cardiomyocytes Differentiated from Human Embryonic Stem Cells: A Molecular and Electrophysiological Approach,” *STEM CELLS*, vol. 25, no. 5, pp. 1136–1144, 2007, doi: 10.1634/stemcells.2006-0466.

[298] A. Skardal, T. Shupe, and A. Atala, “chip systems for drug screening and disease modeling,” *Drug Discov. Today*, vol. 21, no. 9, pp. 1399–1411, 2016, doi: 10.1016/j.drudis.2016.07.003.

[299] D. E. Ingber, N. Wang, and D. Stamenović, “Tensegrity, cellular biophysics, and the mechanics of living systems,” *Rep. Prog. Phys.*, vol. 77, no. 4, p. 046603, Apr. 2014, doi: 10.1088/0034-4885/77/4/046603.

[300] M. Ghibaudo *et al.*, “Traction forces and rigidity sensing regulate cell functions,” *Soft Matter*, vol. 4, no. 9, p. 1836, 2008, doi: 10.1039/b804103b.

[301] P. W. Hales, J. E. Schneider, R. A. B. Burton, B. J. Wright, C. Bollensdorff, and P. Kohl, “Histo-anatomical structure of the living isolated rat heart in two contraction states assessed by diffusion tensor MRI,” *Prog. Biophys. Mol. Biol.*, vol. 110, no. 2, pp. 319–330, Oct. 2012, doi: 10.1016/j.pbiomolbio.2012.07.014.

[302] P. Helm, M. F. Beg, M. I. Miller, and R. L. Winslow, “Measuring and Mapping Cardiac Fiber and Laminar Architecture Using Diffusion Tensor MR Imaging,” *Ann. N. Y. Acad. Sci.*, vol. 1047, no. 1, pp. 296–307, 2005, doi: 10.1196/annals.1341.026.

[303] Z. Qu, G. Hu, A. Garfinkel, and J. N. Weiss, “Nonlinear and stochastic dynamics in the heart,” *Phys. Rep.*, vol. 543, no. 2, pp. 61–162, Oct. 2014, doi: 10.1016/j.physrep.2014.05.002.

[304] Y. Jiang, K. Pandya, O. Smithies, and E. W. Hsu, “Three-dimensional diffusion tensor microscopy of fixed mouse hearts,” *Magn. Reson. Med.*, vol. 52, no. 3, pp. 453–460, 2004, doi: 10.1002/mrm.20191.

[305] S. Fleischer, A. Shapira, R. Feiner, and T. Dvir, “Modular assembly of thick multifunctional cardiac patches,” *Proc. Natl. Acad. Sci.*, vol. 114, no. 8, pp. 1898–1903, Feb. 2017, doi: 10.1073/pnas.1615728114.

[306] J. H.-C. Wang, F. Jia, T. W. Gilbert, and S. L.-Y. Woo, “Cell orientation determines the alignment of cell-produced collagenous matrix,” *J. Biomech.*, vol. 36, no. 1, pp. 97–102, Jan. 2003, doi: 10.1016/S0021-9290(02)00233-6.

[307] G. Buckberg, N. Nanda, C. Nguyen, and M. Kocica, “What Is the Heart? Anatomy, Function, Pathophysiology, and Misconceptions,” *J. Cardiovasc. Dev. Dis.*, vol. 5, no. 2, p. 33, Jun. 2018, doi: 10.3390/jcdd5020033.

[308] C. Obbink-Huizer, C. W. J. Oomens, S. Loerakker, J. Foolen, C. V. C. Bouten, and F. P. T. Baaijens, “Computational model predicts cell orientation in response to a range of mechanical stimuli,” *Biomech. Model. Mechanobiol.*, vol. 13, no. 1, pp. 227–236, Jan. 2014, doi: 10.1007/s10237-013-0501-4.

[309] N. de Jonge, F. M. W. Kanters, F. P. T. Baaijens, and C. V. C. Bouten, “Strain-induced Collagen Organization at the Micro-level in Fibrin-based Engineered Tissue Constructs,” *Ann. Biomed. Eng.*, vol. 41, no. 4, pp. 763–774, Apr. 2013, doi: 10.1007/s10439-012-0704-3.

[310] Y. Zhang *et al.*, “Dedifferentiation and Proliferation of Mammalian Cardiomyocytes,” *PLoS ONE*, vol. 5, no. 9, Sep. 2010, doi: 10.1371/journal.pone.0012559.

[311] T. C. McDevitt, K. A. Woodhouse, S. D. Hauschka, C. E. Murry, and P. S. Stayton, “Spatially organized layers of cardiomyocytes on biodegradable polyurethane films for myocardial repair,” *J. Biomed. Mater. Res. A*, vol. 66A, no. 3, pp. 586–595, 2003, doi: 10.1002/jbm.a.10504.

[312] F. Navaee, N. Piacentini, and P. Renaud, “Design And Fabrication Of A Well-set, Cost-effective Device For Mechanical And Biochemical Stimulation In Cardiac Tissue Engineering Applications,” *TISSUE ENGINEERING: Part A*, 2016. https://infoscience.epfl.ch/record/225618 (accessed Jun. 02, 2020).

[313] Q. Pang, J. W. Zu, G. M. Siu, and R.-K. Li, “Design and Development of a Novel Biostretch Apparatus for Tissue Engineering,” *J. Biomech. Eng.*, vol. 132, no. 1, Jan. 2010, doi: 10.1115/1.3005154.

[314] P. C. Dartsch, H. Hämmerle, and E. Betz, “Orientation of Cultured Arterial Smooth Muscle Cells Growing on Cyclically Stretched Substrates,” *Cells Tissues Organs*, vol. 125, no. 2, pp. 108–113, 1986, doi: 10.1159/000146146.

[315] A. M. Samarel, “Costameres, focal adhesions, and cardiomyocyte mechanotransduction,” *Am. J. Physiol.-Heart Circ. Physiol.*, vol. 289, no. 6, pp. H2291–H2301, Dec. 2005, doi: 10.1152/ajpheart.00749.2005.

[316] S. Chien, “Mechanotransduction and endothelial cell homeostasis: the wisdom of the cell,” *Am. J. Physiol.-Heart Circ. Physiol.*, vol. 292, no. 3, pp. H1209–H1224, Mar. 2007, doi: 10.1152/ajpheart.01047.2006.

[317] A. Livne, E. Bouchbinder, and B. Geiger, “Cell reorientation under cyclic stretching,” *Nat. Commun.*, vol. 5, no. 1, Art. no. 1, May 2014, doi: 10.1038/ncomms4938.

[318] J. Y. Kresh and A. Chopra, “Intercellular and extracellular mechanotransduction in cardiac myocytes,” *Pflüg. Arch. - Eur. J. Physiol.*, vol. 462, no. 1, pp. 75–87, Jul. 2011, doi: 10.1007/s00424-011-0954-1.

[319] E. Saygili *et al.*, “Mechanical stretch of sympathetic neurons induces VEGF expression via a NGF and CNTF signaling pathway,” *Biochem. Biophys. Res. Commun.*, vol. 410, no. 1, pp. 62–67, Jun. 2011, doi: 10.1016/j.bbrc.2011.05.105.

[320] S. R. Gu, Y. G. Kang, J. W. Shin, and J.-W. Shin, “Simultaneous engagement of mechanical stretching and surface pattern promotes cardiomyogenic differentiation of human mesenchymal stem cells,” *J. Biosci. Bioeng.*, vol. 123, no. 2, pp. 252–258, Feb. 2017, doi: 10.1016/j.jbiosc.2016.07.020.

[321] W. W. Ahmed *et al.*, “Myoblast morphology and organization on biochemically micro-patterned hydrogel coatings under cyclic mechanical strain,” *Biomaterials*, vol. 31, no. 2, pp. 250–258, Jan. 2010, doi: 10.1016/j.biomaterials.2009.09.047.

[322] C. M. J. Tan and A. J. Lewandowski, “The Transitional Heart: From Early Embryonic and Fetal Development to Neonatal Life,” *Fetal Diagn. Ther.*, vol. 47, no. Suppl. 5, pp. 373–386, 2020, doi: 10.1159/000501906.

[323] N. K. Weidenhamer and R. T. Tranquillo, “Influence of Cyclic Mechanical Stretch and Tissue Constraints on Cellular and Collagen Alignment in Fibroblast-Derived Cell Sheets,” *Tissue Eng. Part C Methods*, vol. 19, no. 5, pp. 386–395, Nov. 2012, doi: 10.1089/ten.tec.2012.0423.

[324] R. Kemkemer *et al.*, “Surface modification of Polydimethylsiloxane by hydrogels for microfluidic applications,” *Curr. Dir. Biomed. Eng.*, vol. 5, no. 1, pp. 93–96, Sep. 2019, doi: 10.1515/cdbme-2019-0024.

[325] C. Cha *et al.*, “Tailoring Hydrogel Adhesion to Polydimethylsiloxane Substrates Using Polysaccharide Glue,” *Angew. Chem. Int. Ed.*, vol. 52, no. 27, pp. 6949–6952, Jul. 2013, doi: 10.1002/anie.201302925.

[326] M. Shachar, N. Benishti, and S. Cohen, “Effects of mechanical stimulation induced by compression and medium perfusion on cardiac tissue engineering,” *Biotechnol. Prog.*, vol. 28, no. 6, pp. 1551–1559, 2012, doi: 10.1002/btpr.1633.

[327] D. Ea, M. S, Y. L, and R. Ch, “[Responses of ligamentous fibroblasts to mechanical stimulation],” *Ann. Chir.*, vol. 49, no. 8, pp. 768–774, Jan. 1995.

[328] R. C. Buck, “Reorientation response of cells to repeated stretch and recoil of the substratum,” *Exp. Cell Res.*, vol. 127, no. 2, pp. 470–474, Jun. 1980, doi: 10.1016/0014-4827(80)90456-5.

[329] C. Tamiello, A. B. C. Buskermolen, F. P. T. Baaijens, J. L. V. Broers, and C. V. C. Bouten, “Heading in the Right Direction: Understanding Cellular Orientation Responses to Complex Biophysical Environments,” *Cell. Mol. Bioeng.*, vol. 9, no. 1, pp. 12–37, Mar. 2016, doi: 10.1007/s12195-015-0422-7.

[330] F. Sbrana *et al.*, “Role for stress fiber contraction in surface tension development and stretch-activated channel regulation in C2C12 myoblasts,” *Am. J. Physiol.-Cell Physiol.*, vol. 295, no. 1, pp. C160–C172, Jul. 2008, doi: 10.1152/ajpcell.00014.2008.

[331] M. Serrani, M. L. Costantino, and R. Fumero, “The Influence of Cardiac Trabeculae on Ventricular Mechanics,” p. 4.

[332] E. Sano *et al.*, “Tetrafluoroethylene-Propylene Elastomer for Fabrication of Microfluidic Organs-on-Chips Resistant to Drug Absorption,” *Micromachines*, vol. 10, no. 11, Nov. 2019, doi: 10.3390/mi10110793.

[333] K. Domansky *et al.*, “Clear Castable Polyurethane Elastomer for Fabrication of Microfluidic Devices,” *Lab. Chip*, vol. 13, no. 19, pp. 3956–3964, Oct. 2013, doi: 10.1039/c3lc50558h.

[334] M. D. Borysiak, K. S. Bielawski, N. J. Sniadecki, C. F. Jenkel, B. D. Vogt, and J. D. Posner, “Simple Replica Micromolding of Biocompatible Styrenic Elastomers,” *Lab. Chip*, vol. 13, no. 14, pp. 2773–2784, Jul. 2013, doi: 10.1039/c3lc50426c.

[335] A. Gökaltun, Y. B. (Abraham) Kang, M. L. Yarmush, O. B. Usta, and A. Asatekin, “Simple Surface Modification of Poly(dimethylsiloxane) via Surface Segregating Smart Polymers for Biomicrofluidics,” *Sci. Rep.*, vol. 9, no. 1, Art. no. 1, May 2019, doi: 10.1038/s41598-019-43625-5.

[336] M. D. Sarker, S. Naghieh, N. K. Sharma, and X. Chen, “3D biofabrication of vascular networks for tissue regeneration: A report on recent advances,” *J. Pharm. Anal.*, vol. 8, no. 5, pp. 277–296, Oct. 2018, doi: 10.1016/j.jpha.2018.08.005.

Curriculum Vitae

FATEMEH NAVAEE

Doctoral Assistant

@ fatemeh.navaee@epfl.ch +41-787668255 https://www.linkedin.com/in/fatemeh-navaee/
Rue de Verdeaux, 7d, 1020, Renens, Switzerland Lausanne, Switzerland

STRENGTHS

- Result-driven professional with 10+ years of comprehensive experience working in cell culture labs, developing and proposing new biomaterials, organ-on-a-chip platforms using microfabrication techniques, as well as working on bioprinting and tissue engineering
- Industry experience in manufacturing companies on safety product toxicology, electrophysiology, and cellular biology
- Superb project leadership abilities and personal management skills with strong expertise in the area of biomaterials in cardiovascular, skin and cartilage tissue engineering, microengineering, heart-on-chip, microfabrication, hydrogels, bioprinting, cell culture, and cell differentiation
- Proven problem solving, analytical thinking, working on parallel tasks, a fast-learning curve, and ability to adapt to evolving industry trends

PROFESSIONAL EXPERIENCE

Research Intern

Philip Morris International

January 2020 – July 2020 Neucahtel, Switzerland

- Product safety toxicity. Early detection of the effect of genotoxic compounds on DNA damage.
- Effect of different compounds on Na and K channels of cardiac cells using Patch-clamp and FLIPR techniques.

Research Assistant

LMIS4, Microengineering Department, EPFL

Sep 2015 – Sep 2016 Lausanne, Switzerland

- Project: Heart-on-a-chip
- Developing a heart-on-a-chip platform using 3D culturing of the cardiac cells in an innovative hydrogel, and microfabricating a platform for stimulating the cells physically and mechanically. The final aim of the project is recreating a relevant 3D cardiac microenvironment in-vitro for drug testing

Tissue Scientist

Department of Stem Cells and Developmental Biology, Royan institute

Sep 2011 – Sep 2015 Tehran, Iran

- Project: Development of bioprinting platform for reconstruction of human beating heart tube; Task: Team leader, responsible for the grant

Biomaterial Engineer

Cell Bank, Pasteur Institute of Iran

Sep 2010 – Sep 2011 Tehran, Iran

- Project: Preparation and evaluation of ovalbumin film cross-linked by HMDI as a cartilage tissue engineering scaffold

Intern

Iran Polymer and Petrochemical Institute (IPPI)

June 2010 – Sep 2010 Tehran, Iran

- Project: Bioprinting of sodium alginate hydrogel into vessel-like geometries using a novel microdispenser system

CORE COMPETENCIES

Organ-on-chip | Biomaterials | Cardiovascular, Skin and cartilage T.E. | Microengineering | Bioprinting | Micro-Biofabrication | Smart Hydrogels | Cell culture and differentiation

HONORS

- Swiss Government Excellence Scholarship holder for Ph.D. studies 2015-2018
- Directly admitted to the M.Sc. program as an excellent student award, Amirkabir University of Technology 2011
- Top 5% student in M.Sc. and B.Sc.
- Ranked 918^{th} in B.Sc. nationwide university entrance exam among 120,000

LANGUAGES

Persian	**Native**
English	**C2**
French	**B2**
German	**A1**

REFEREES

Prof. Philippe Renaud
@ EPFL university
philippe.renaud@epfl.ch

Prof. Thomas Braschler
@ University of Geneva
thomas.braschler@unige.ch

Dr. Omar Alijevic
@ Philip Morris International
Omar.Alijevic@contracted.pmi.com

Prof. Shahin Bonakdar
@ Pasteur Institute of Iran (IPI)
sh_bonakdar@pasteur.ac.ir

PERSONAL DETAILS

Date of Birth
22.12.1988

Marital Status
Single

EDUCATION

Ph.D. candidate in microsystems and microengineering

LMIS4, Microengineering Department, EPFL

Sep 2016 – Nov 2020 Lausanne, Switzerland

- Thesis title: "The impact of 3D dynamic microenvironment on cardiac cell fate and functionality"
- Achievement: Enhancing 3D cardiac models in terms of cell alignment, differentiation efficiency, cardiac cell frequency, synchrony, and maintenance of spontaneous beating

M.Sc. in Biomedical Engineering, Tissue Engineering

Amir Kabir University of Technology (AUT)

Sep 2011 – Oct 2013 Tehran, Iran

- Thesis title: "Vascular tissue engineering using embryonic stem cell aggregates in Alginate and Fibrin hydrogels"
- Patent: 3D bioprinter in cylindrical coordinate, M. Halvaee, **F. Navaee**, N. Abolfathi, *filed to State Organization for Registration of Deeds and Properties*
- GPA: 19.17/20

B.Sc. in Biomedical Engineering, Biomaterials

Amir Kabir University of Technology (AUT)

Sep 2007 – Aug 2011 Tehran, Iran

- Thesis Title: "Evaluation of different cross linkers on egg-white film properties in wound dressing application"
- GPA: 17.22/20

MANAGEMENT EXPERIENCE

- "Electrospining in stem cell nanoengineering", at Royan Institute, 2012
- Bioprinting in tissue engineering symposium, 2013
- 9^{th} training course of polymers in medicine entitled: "investigation and improvement of cell behavior on the surface of tissue engineering scaffolds, at Iran Polymer and Petrochemical Institute, 2009
- "Functional nanoporous biomaterials: modeling, design, and application", at Tissue Engineering and Biomaterials Division, National Institute of Genetic Engineering and Biotechnology, 2010
- 12^{th} Royan International Twin Congress, 2011
- 2^{nd} Royan International Summer School: "stem cells and developmental biology", 2011

CERTIFICATES

- International certificate of MATLAB
- International certificate of ICDL
- Certificate of technical supervision of medical equipment
- Training course in bioinformatics
- Certificate of project management: the basics for success

TECHNICAL SKILLS

Biomaterials Preparation and Characterization

- Natural and synthetic hydrogels preparation
- Tissue decellularization
- Fluorescent labelling of the proteins
- Mechanical testing
- DNA, Collagen and GAG content measurement
- Scanning electron microscopy(SEM) for measuring the porosity of the scaffolds
- Swelling and degradation measurement
- FTIR spectroscopy
- SDS-polyacrylamide gel electrophoresis
- Gas transmission rate (GTR) analysis

Biological Experiments

- 2D and 3D cell culture
- FLIPR
- Patch clamp
- Fluorescent microscopy
- Confocal microscopy
- MTT aasay
- Live/dead assay
- Flowcytometry (FC)
- Immunocytochemistry (ICC)
- Immunohistochemistry (IHC)
- PCR
- Cell culture and differentiation (ESCs, HUVECs, Cardiac Progenitor Cells, MEFs, Primary cardiac cells, Fibroblasts,…)

Microfabrication

- Photolitography
- Mask design
- Silicon etching
- PDMS chips fabrication
- Thin film deposition

Tools

- **Programming:** MATLAB & C++
- **Image Analysis Softwares:** ImageJ & Cell profiler
- **Statistical Data Analysis Tools:** SPSS & GraphPad
- **Mask Design Tool:** CleWin